# Development of Integrated Design Methodologies to Investigate the Effects of Control Factors and Uncertainties on Topologically Optimized Structures for Robust and Reliable Performances

## THESIS

Submitted in partial fulfillment of the requirements for the degree of

### DOCTOR OF PHILOSOPHY

by

### ARSHAD JAVED

(2008PHXF425P)

Under the Supervision of

### Prof. B.K. ROUT



**BITS** Pilani
Pilani | Dubai | Goa | Hyderabad

## BIRLA INSTITUTE OF TECHNOLOGY & SCIENCE

### PILANI – 333 031 (RAJASTHAN) INDIA

**2014**

**BIRLA INSTITUTE OF TECHNOLOGY & SCIENCE**

**PILANI – 333 031 (RAJASTHAN) INDIA**

# CERTIFICATE

This is to certify that the thesis entitled **"Development of Integrated Design Methodologies to Investigate the Effects of Control Factors and Uncertainties on Topologically Optimized Structures for Robust and Reliable Performances"** submitted by ARSHAD JAVED, ID. No. 2008PHXF425P for award of Ph.D. Degree of the institute embodies original work done by him under my supervision.

Signature in full of the Supervisor _____

Name          **:**     **Dr. B.K. ROUT**

Designation  **:**     **Associate Professor, Department of Mechanical Engineering**

                       **BITS-Pilani, Pilani Campus**

Date _____

*Dedicated to my beloved Parents*

# ACKNOWLEDGEMENTS

# ABSTRACT

Topology optimization is a powerful method of material minimization. This method comprises of the techniques of optimization using finite element method and has been primarily used for weight reduction problems for structural, automobile, aircraft components and for the design of micro-electro-mechanical systems. Therefore, based on the applications, several formulations of topology optimization have been developed by researchers in the recent past. For structural and machine components, the problems are formulated for the minimization of compliance value. Compliance is a performance measure for the structural problems, which is generally considered as the reverse of the stiffness. This performance measure depends on many factors such as the amount of material to be removed, the material property, applied load, dimensions of the material domain, and other boundary conditions. Apart from compliance, the maximum deflection is also one of the performance measures, for these components. These performance measures are sensitive to the aforesaid factors. In real life situations, these factors may not remain constant due to the presence of uncertainties. For example, assumed material properties may vary due to material uncertainty and manufacturing imperfections. Hence, the topology obtained during the theoretical design phase may not suffice the actual working condition. In order to capture the effects of these uncertainties, various methodologies of topology optimization have been proposed by the different researchers. Based on the available work, this thesis identifies the research gaps, which needs further investigation. The work presented here is motivated by the identified issues and the investigations are carried out by keeping designer's perspective. Incidentally, designers come across several challenges to design an optimal topology that is robust. The optimal topologies with less variations in performance measures are called robust. One of the requirements for this challenge is to have a thorough knowledge of the effects of each factor on the performance measure values while dealing with optimal topologies. Another requirement is to adjust the factor values and their tolerances to get targeted and robust performance while dealing with the effects of uncertainties. These requirements may be driven by aspects like cost, availability, manufacturing, etc.

In the present work, the behavior of performance measure of structural problems for optimal topologies with respect to the factor values and uncertainties are analyzed. Here the uncertainties/noises are considered in terms of direction and point of application of applied force, values of modulus of elasticity, and the variations in the values of selected factors such as applied force, volume fraction, and aspect ratio. The important point here is that the noises identified for the investigations are controllable in computer experiments rather than real life experiments.

Initially, a systematic approach is utilized to investigate the effect of different input factors on performances along with effects of uncertainties, for a topologically optimized structure. Here, applied force, volume fraction, and aspect ratio of the material domain are treated as input or controllable factors. The uncertainties of the material property and the point and angle of applied force are treated as the non-controllable factors. To obtain optimal topologies for a given problem several methods are available in the literature. The present thesis uses one of the widely used topology optimization method i.e. Solid Isotropic Microstructure with Penalization (SIMP) method for its computational simplicity. In order to investigate the identified research gaps, SIMP methods have been applied to simulate performances with the help of Design of Experiments (DOE) technique. To analyze the effect on performance at different controllable factors, a suitable range is decided for each of the factors. Based on these ranges, the levels of the factors are selected, and design combinations of identified factors are obtained using DOE technique. This analysis helps to analyze the performance, where level of each of the factors varies simultaneously. Each combination is then replicated to incorporate the effect of the non-controllable factors. To illustrate the concept, four-benchmark problems used in structural topology optimization research are selected. To maintain the consistency and efficacy of the proposed methods the same problems are used throughout the thesis. Thus, the designed combinations of factors and noises are used to simulate the performance values. The simulation results are then analyzed based on statistical techniques such as, analysis of mean (ANOM), analysis of variance (ANOVA), and signal to noise ratio (SNR). These techniques provide the statistical significance of each factor and their impact on the performance values. In addition, this investigation also provides the optimal factor values to produce the robust and targeted performance for the selected benchmark problems.

Based on identified research gaps, the need for a generalized and integrated method is felt and is achieved by considering the uncertainties of controllable factors. In this approach the variations of controllable factor (i.e. applied force, volume fraction, aspect ratio) with the uncertainties that was earlier considered are combined. In order to integrate the uncertainties with the reliability concept, the reliability based topology optimization (RBTO) method is utilized with DOE approach. The consideration of reliability enables the designer to design the component for a specific risk or targeted reliability that captures the effect of various uncertainties. At this stage, the combinations of the controllable factor and the noises are designed, which are similar to the previous discussion. The simulation for the optimal topology with its performance is carried out using the RBTO method. This method enables to simulate the performance measure in a desired design/controllable-factors space, including the effects of uncertainties, via a desired reliability index value. The simulation results are then analyzed using statistical techniques. The obtained results are also compared with scenarios and without the effects of uncertainties. With reliability based approach, the compliance and deflection values change from its initial desirable value. This issue has been dealt systematically with detailed analysis and explanation. In this analysis, the optimal value of factors, to produce the robust and targeted performance for the selected benchmark problems are provided.

After the selection of the optimal value of factors, it is also desired to analyze the effect of tolerance range of the factors on performance measures. The investigation on tolerance range provides closest performance values to robust and targeted performance. Thus, the tolerance of input factors like applied force, volume fraction, aspect ratio of material domain and modulus of elasticity are selected to investigate their effect on performance. For simulation, two tolerance ranges are defined for each factor, named as loose and tight tolerance. The objective of this investigation is to identify the tolerance range combination, which provides the targeted and robust performance. These combinations may contain the loose tolerance range of few factors and tight tolerance ranges of others. In this way, the designer's effort required to keep all tolerances of factors at tight range can be reduced. To incorporate the tolerance range in performance range simulation, a cross array design of experiment (CA-DOE) approach is utilized. Proposed approach provides a strategy to simulate the performance according to the tolerance values and analyze the obtained results using statistical techniques. By the

proposed tolerance range analysis method, the significant factors are identified. In addition, the different tolerance combinations are identified to achieve the targeted and robust performance. Similar methodology for tolerance range selection is developed to incorporate the effect of uncertainties of the controllable factors, based on RBTO method. The combinations are generated subject to the reliability index values, and analyzed in the similar way. Finally, the results obtained from both the methods are compared, to find out the effect of reliability index on the performances of different tolerance combinations.

The earlier investigations carried out in this thesis, included uncertainties in a very generalized way. In line with the earlier development, a particular method to incorporate the effect of manufacturing uncertainty is proposed. The rationale behind this development is to understand the impact of manufacturing uncertainties in a very specific way, so that the characteristic of uncertainties of a specific manufacturing process is captured accurately. The effects of manufacturing uncertainty are implemented by assuming probabilistic distribution of material. Here, the CA-DOE method is modified to suit the purpose and performances are simulated, including the effect of uncertainties. The simulated results are analyzed using similar approach as discussed in tolerance range selection method. To observe the effect of the uncertainties of controllable factors also, the RBTO method is used and the obtained results are compared with previous results.

Throughout the thesis, four benchmark problems have been utilized to illustrate the developed methodologies. To validate the developed methodologies, a real life problem is selected. For this purpose, a bell crank lever of a formula-one racing car is chosen. It was required to reduce the weight of the each component of the car. The design target was to reduce the crank lever weight by 13%, without sacrificing its performance. In addition to this, a detailed performance behavior was required to select the input factor values with their tolerances. The input factors are selected as, options for dimensional configurations, material property, and the values of weight reduction. The uncertainties due to applied force, angle of applied and output forces, thickness of the lever, material property, and weight reduction values are also included in the performance simulation. Here the performance values are selected as compliance, deflection and Von-Mises stress values. In earlier investigations, the stress values corresponding to benchmark problems

were not considered, because the stresses developed were always smaller than yield stress of the material. Hence, instead of stress, the deflection values were considered as more effective measure to characterize the performance. However, being a critical application, the stress values are considered here as one of the performance measures in case of bell crank lever. This problem is analyzed using the developed methodologies available in thesis. As a result, the performance behavior of bell crank lever is generated for the different level of the factors, uncertainties, tolerance, for different reliability values. Finally the optimal values of factors and their tolerances are also identified.

Present work proposes integrated methodologies to simulate the realistic performance with uncertain scenarios in design, manufacturing, and application phases for a topologically optimized component. Hence, these methodologies help to achieve robust, reliable, and targeted performance for the components. The proposed methodologies are found to be advantageous compared to the usual robust and reliable topology optimization methods by providing the performance at each possible point in the controllable factor space. Thus, present thesis provides an off-line design strategy to the designer/practitioner.

**Keywords:** *Topology optimization, Shape/Size Optimization, Computational mechanics, Finite element method, Discretization method, SIMP, Structural/beam analysis, Performance analysis, RBTO, Robust design, DOE, CA-DOE, Tolerance range selection, Manufacturing uncertainty.*

## CONTENTS

|  | CONTENTS | Page No. |
|---|---|---|

| | CONTENTS | Page No. |
|---|---|---|

# LIST OF TABLES

# LIST OF FIGURES

# LIST OF ABBREVIATIONS

| | |
|---|---|
| 2-D | Two Dimensional |
| 3-D | Three Dimensional |
| ANOM | Analysis of Mean |
| ANOVA | Analysis of Variance |
| BESO | Bidirectional Evolutionary Structural Optimization |
| CA-DOE | Cross-Array Design of Experiments |
| DOE | Design of Experiment |
| DTO | Deterministic Topology Optimization |
| ESO | Evolutionary Structural Optimization |
| FE | Finite Element |
| FORM | First Order Reliability Method |
| HL | Hasofer and Lind |
| MBB | Messerschmidt-Bolkow-Blohm |
| MEMS | Micro-Electro-Mechanical Systems |
| MMA | Method of Moving Asymptotes |
| MPP | Most Probable Point |
| OA | Orthogonal Arrays |
| OC | Optimality Criterion |
| PMA | Performance Measured Approach |
| RBDO | Reliability Based Design Optimization |
| RBTO | Reliability Based Topology Optimization |
| RIA | Reliability Index Approach |
| RTO | Robust Topology Optimization |
| SIMP | Structural Isometric Material with Penalization |
| SLP | Sequential Linear Programming |
| SNR | Signal to Noise ratio |
| SORM | Second Order Reliability Method |
| SQP | Sequential Quadratic Programming |

# LIST OF SYMBOLS

| | |
|---|---|
| $E_{ijkl}$ | Optimal elasticity tensor |
| $Enr$ | Energy Bilinear from |
| $\Omega$ | Material domain |
| $d_a$ | Arbitrary displacement |
| $d_v$ | Virtual displacement |
| $\varepsilon_{ij}$ | Strain value |
| $g$ | Body forces |
| $h$ | Boundary tractions |
| $\Gamma_T$ | Traction part on the boundaries |
| $E_a$ | The domain of allowable stiffness |
| $\tilde{U}$ | The domain of kinematically admissible displacement fields |
| C | Compliance |
| **F** | Applied force vector |
| **d** | Nodal displacement vector |
| $\mathbf{K_0}$ | Stiffness matrix of the element |
| **K** | Global stiffness matrix for the element |
| $x_i$ | Density parameter for element $i$ |
| $x_{min}$ | Minimum value of the density parameter |
| $V_f$ | Total volume of material domain |
| $V(x)$ | Volume of the matrial based on the density paramter $x$ |
| $f$ | Volume fraction value |
| $p$ | Penalization power |
| $n$ | Total number of elements |
| $\lambda_i$ | Lagrange Multiplier |
| $B_k^e$ | Heuristic parameter |
| $\eta$ | Numerical damping coefficient, |
| $\tilde{m}$ | Move limit |
| $P_{PE}$ | Complete potential energy for the plane stress |
| $\boldsymbol{\varepsilon}$ | Strain vector |
| $\boldsymbol{\sigma}$ | Stress vector |

| | |
|---|---|
| $\sigma_x, \sigma_y$ | Normal stresses corresponding to $X$ and $Y$-axes |
| $\tau_{xy}$ | Tangential stress in $XY$ plane |
| $\varepsilon_x, \varepsilon_y$ | Linear strains corresponding to $X$ and $Y$-axes |
| $\gamma_{xy}$ | Shear strains in $XY$ plane |
| $u$ | Linear displacements middle-point plane of plate corresponding to $X$-axis |
| $v$ | Linear displacements middle-point plane of plate corresponding to $Y$-axis |
| $p_x, p_y$ | Vector components of external loading corresponding to $X$ and $Y$-axis |
| $\mathbf{R}$ | Nodal reaction |
| $N_i$ | Nodal functions |
| $a_1, a_2, a_3,$ $a_4, a_5, a_6$ | Constant coefficients of the approximation functions |
| $a$ | Finite element dimension in $X$ direction |
| $b$ | Finite element dimension in $Y$ direction |
| $Th$ | The thickness of the plate |
| $E$ | Modulus of elasticity |
| $\upsilon$ | Poison's ratio |
| $S_t$ | Strain energy of the structure |
| $nc$ | Number of nodes in the circle of radius $r_{min}$, |
| $\mathbf{K^*}$ | Stiffness after removal of the element |
| $\alpha_i$ | Sensitivity number |
| $r_{min}$ | Minimum radius of circle |
| $r_{ij}$ | Distance of $i^{th}$ to $j^{th}$ element |
| $w(r_{ij})$ | Linear weight factor |
| $\hat{\alpha}$ | Modified sensitivity number |
| $S_{surf}$ | Surface function |
| $e$ | A point on space on the iso-surface $\Phi$ |
| $\Phi$ | Iso-surface function |
| $k_{iso}$ | Arbitrary iso-value |
| $D$ | Solid domain of the structure |
| $\partial D$ | Boundary of solid material domain |

| | |
|---|---|
| $u_0$ | Displacement at the boundary part |
| $\overline{D}$ | Fixed larger material domain |
| $V_{max}$ | The maximum amount of material that can present in the material domain $D$ |
| $\hat{G}$ | Specific physical or geometric type |
| $p_i$ | Performance function value |
| $Re$ | Response or performance value |
| $fc$ | Selected factor |
| $\hat{\beta}$ | Numerical constant |
| $\square r$ | Error value |
| $G$ | Limit-state function |
| $P_f$ | probability of failure |
| $\xi$ | Random or probabilistic variable |
| $\beta$ | Safety or reliability index, |
| $\sigma$ | Standard deviation |
| $\mathbf{U_g}$ | Gaussian variable vector |
| $U$ | Gaussian variables |
| $C_D, C_R, C_A$ | Compliance values for dense, rare, and exact conditions |
| $x_D, x_R, x_A$ | Density parameters for dense, rare, and exact conditions |
| $\overline{V}(x)$ | Random volume fraction |
| $x_S$ | Probabilistic density parameter |
| $\Pi_{(\cdot,\cdot)}$ | Boxcar function |
| $H$ | Heaviside step function, |
| $\Gamma(\cdot)$ | Gray scale suppression operator |
| $q$ | Powering factor in the gray scale suppression operator |
| $\mu$ | Nominal valued of the factor |
| $S$ | Spread of normal distribution |

# CHAPTER 1

## TOPOLOGY OPTIMIZATION METHOD

This chapter presents a short introduction to the topology optimization, along with basic methodologies. In this, the need for research is also discussed, including the motivation behind this research. The current chapter concludes with the developed framework and its contribution to the research community and industry.

## 1.1    INTRODUCTION

Use of material in an efficient way is an important task for designers' in all engineering fields. The aim of the designers is to achieve the desired performance that minimizes or maximizes selected responses like, cost, weight, stress, natural frequency, etc. Traditionally, design engineers rely on predictions and experience in developing designs for new problems. A specialized tool, i.e. structural optimization is used to optimize the performance of the structures. This technique is based on mathematical programming for optimizing the layout of an existing material domain (Bendsøe 1995, 1989; Bendsøe and Sigmund 2003). This tool is even extended to optimizing the material microstructure itself according to its intended use. Structural optimization is categorized into three main streams i.e., sizing optimization, shape optimization, and topology optimization (Herskovits 1995; Park 2010). In sizing optimization problems, the material distribution or the design domain is established and held fixed. In this case, finding out the optimal size or thickness of members or plate, becomes the objective function. In size optimization problem the optimal cross-section, length, or thickness of the structural member for weight minimization are obtained. In shape optimization problems, the optimal shape is found out. The examples can be, to obtain the optimal shape of a notch to reduce the stress concentration. With size and shape optimization, the prerequisite is the knowledge of the main features of the material domain distribution or topology. Strictly speaking, topology refers to the location of material continuity or connections, and the location of voids or

holes in the material design space (Bendsøe and Kikuchi 1988). Hence, topology optimization is considered as the most general technique because it allows the placement of material throughout the design, subject to design constraints (Sigmund 1994a & 1994b). The diagrammatic representations of differences of these optimization schemes are presented in Fig. 1.1.

| **Initial problem** | **Optimized solution** |
|---|---|
| (a) Size optimization | |
| (b) Shape optimization | |
| (c) Topology optimization | |
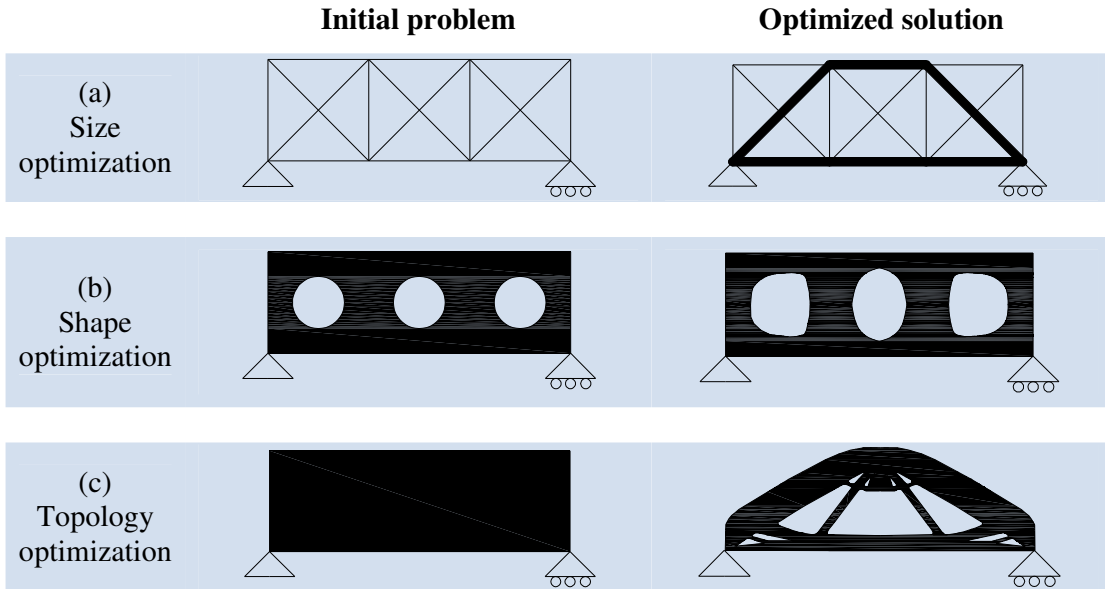


**Fig. 1.1: (a) - (c) Initial material domain and the respective optimum solution for different optimization schemes**

Fig. 1.1(a) demonstrates the example of size optimization of a truss system. As a result of the size optimization, the thickness of certain members is changed to satisfy the strength requirements. Fig. 1.1(b) shows the example of a shape optimization, where the shapes of the holes are optimized for weight reduction and strength requirements. In Fig. 1.1(c), material or weight minimization is shown subject to the strength requirement, using topology optimization method. It can be observed that the complete material distribution or the connection and voids are redefined to maximize the strength.

The topology optimization research area is vast because of its applicability. The major application areas include numerous design problems such as compliant mechanisms (Ananthasuresh et al. 1994), micro-electro-mechanical devices, nano-structures, off-shore structures, bone remodeling, robot path finding algorithms (Ryu et al. 2012), design of frame bracing (Mijar et al. 1998), tunnel supports (Yin and Yang 2000), biomechanical implants (Folgado and Rodrigues 1997), and structures subjected

to local stress constraints (Duysinx and Bendsøe 1998) and buckling constraints (Neves et al. 1995). It has also been used in designing of optimal vibration response of structures (Díaz and Kikuchi 1992, Tcherniak 2002), improving crashworthiness of vehicles (Mayer et al. 1996, Pedersen 2004), and optimizing structural support placement (Buhl 2002), design piezo-composites (Sigmund et al. 1998) and band-gap materials (Sigmund and Jensen 2003). Topology optimization is also used in the design of material microstructures. This implies that the material can be tailored to achieve desired or extreme properties. The idea here is to treat the microstructure of the material as a small structure. In this way, topology optimization methods can be used in the macroscopic design problems. For this type of problem, the microstructure cell is designed first and the overall material domain is assembled later. This process is opposite to the usual approach of homogenization, where the complete material domain is considered first and optimization process gives the necessary information for placement of microstructure cells. Hence, this approach is called as 'inverse homogenization' problem, which was proposed by Sigmund (1994a, 1995). Using this approach, the materials can be designed to meet prescribed or extreme elastic or thermal expansion properties (Sigmund and Torquato 1997). The famous example for such application is a material with negative Poisson's ratio by Sigmund (1994b). Thus, topology optimization technique has spread to many areas and gained widespread popularity in academia and industry. Along with the applications, there are many studies and approaches available, which are presented to enhance and improve the topology optimization methods. These methodologies are primarily classified into two groups and these are 'discrete topology optimization method' and 'continuum topology optimization method'.

**Discrete topology optimization method:** The approach here is to consider the material domain consist of all possible truss bar connections, as shown in Fig. 1.2. Here the objective is to optimize the weight of structure by eliminating the non-significant truss bars (Bendsøe and Sigmund 2003). Along with the truss frames, this method is widely used for the synthesis of the compliant mechanisms (Ananthasuresh et al.1994, Ananthasuresh & Kota, 1995, Frecker et al. 1997, Howell, 2001, Kota et al. 2001, Javed et al. 2007). In Fig. 1.2(a), the initial material domain can be observed, which is made of all possible truss bar connections. After the optimization, the possible topology can be seen in Fig. 1.2(b). This method is also known as 'ground structure parameterization' method (Howell, 2001).

(a)                                                          (b)
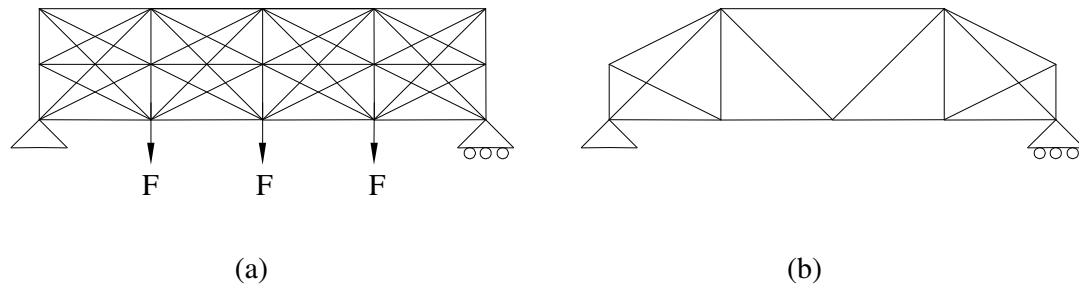
**Fig. 1.2: Topology optimization using discrete method, (a) ground structure,**
**(b) optimized topology for the structure (Fatma et al. 1999)**

**Continuum topology optimization method:** The second type of methodology refers to a continuum topology optimization method (Bendsøe 1995, 1989; Bendsøe and Sigmund 2003). In this method the material domain is continuum. Here, the whole domain is discretized into several small material cells. Each of these cells can be a solid material cell or a void. Based on this assumption, the optimization is performed to define the material cell and voids, in order to achieve the objectives within constraint conditions. Thus, an optimal topology is obtained. For illustration, Fig. 1.1(c) can be referred. In this problem, the complete material domain was defined with the boundary conditions. It can be seen that the obtained optimal topology has a smooth variation of material presence, unlike the discrete optimal topology (Fig. 1.2). This type of topology optimization is very popular because of its flexibility in assigning the martial cells. The latest developments in the field of topology optimization mainly utilizes the continuum topology optimization method. In the next section, the basic methodologies related to the continuum method of topology optimization are introduced, which are core to the latest developments and applications.

## 1.2     METHODOLOGIES FOR TOPOLOGY OPTIMIZATION

Topology optimization has roots in truss design dating back to the early 20th century (Michell 1904). Presently it is a very popular tool in the realm of design engineering for material optimization, in conceptual design phase. Thus, an overall optimized material distribution pattern in the material domain (or design domain) is obtained. The obtained material distribution can be utilized as the initial steps for next process i.e., size and shape optimization. Topology optimization method exploits the mathematical approach for assigning the material in an optimal pattern within the fixed design domain, and thus offers the overall topology of the component. This

optimal pattern is obtained by an objective function subject to few constraints. The objective function may be minimization of compliance, in the case of structures. Where, compliance is the property of a structure, and equivalent to the reciprocal of the global stiffness (Bendsøe and Sigmund 2003). Again, objective function can be maximization of compliance, if the aim is to design a compliant mechanism (Sigmund 1997). In general, the objective of the optimization process may be any desired quantity, which is dependent on material distribution. These optimizastion problems must be handled carefully because the numbers of variables are very large. There are several methods proposed by researchers for solving topology optimization problems. Still explorations are going on to upgrade the methods available (Rozvany 2009). In subsequent section the well-known methodologies for topology optimization i.e., Structural Isometric Material with Penalization (SIMP) method, Evolutionary Structural Optimization (ESO), Bidirectional ESO method, and Level Set method are introduced.

### 1.2.1 Structural isometric material with penalization method

Bendsøe and Kikuchi (1998) developed a homogenization approach using finite elements and homogenized materials consisting of solids and voids, which is the basis of the present state of art in topology optimization. They presented a technique for determining the optimal distribution of the material among elements in the design domain. The problem was worked out using a discretized approach, where the whole design domain was dealt in element wise manner. Each element was assigned a parameter, which decides the existence of "material" or "no material" case. Further, the "material" or "no material" case was determined by optimization algorithm, confirming the feasibility of the solution by various constraints posed. This design parameter, often labeled, as density parameter, which is binary valued. The value, one or zero is defined for "material" and "no material" case respectively. To solve the optimization problem for binary valued density parameter is quite difficult compared to continuous valued parameters (Sigmund and Petersson 1998). The optimization difficulty is resolved by considering the density parameters for intermediate values. In this way, the value was relaxed over a continuous interval from zero to one. Physically, this is equivalent to an intermediate state between solid or void. Strictly speaking, this design parameter is the material presence expressed in fractional values for each finite element cell. The value of this parameter (or density) is

constant within each element cell. Various attempts had been made to capture this problem but the results in most of the cases were microscopic holes rather than desired finite macroscopic voids. The assumed intermediate densities were purely mathematical and cannot be implemented at manufacturing level. To make this process feasible, density parameters were penalized using a power-law approach that produces an approximate discrete solution. A very high penalization makes the elements either filled or empty. Usually penalization power is taken as three. This technique is termed as Solid Isotropic Microstructure with Penalization (SIMP) (Rozvany and Zhou 1990; Rozvany et al. 1992; Bendsøe 1995, 1989; Bendsøe and Sigmund 2003). This method generates a large number of design parameters. Number of parameters depends on required smoothness of the solution. However, there was no theoretical proof for SIMP method until 2001(Bendsøe 1995). Rietz (2001) proved that the finite exponent penalized optimization problem would have same solution as a non-penalize discrete problem. There are some typical practical problems observed in numerical results. For example, the optimized topology may show the connectivity of elements in a peculiar manner, which may not be valid physically. The elements can be connected through corners only, called as checkerboard problem or isolated hinge. The other common problems, discussed by Sigmund and Petersson (1998) are the mesh dependency and local minima. These problems were well recognized from the time of development of topology optimization methods itself. There are many methods suggested to avoid these numerical instabilities in the final topology result. For example, perimeter control, employing filters and slope-constraints (Diaz and Sigmund 1995; Sigmund and Petersson 1998; Petersson 1999; Bendsøe and Sigmund 2003). Presently, various methods are developed that take care of the aforesaid problems in topology optimization (Bendsøe and Sigmund 2003). The well-known formulation of SIMP is based on finding out the optimal stiffness tensor, which is taken as a variable over entire domain $\Omega$ (Rozvany and Zhou 1990; Rozvany et al. 1992). A generalized formulation according to SIMP method is performed by considering a material design domain as shown in Fig. 1.3. In this figure, the topology is to be generated within the material domain $\Omega$. An external load acts on this material domain and the whole domain is fixed by the rigid supports. In the generalized material domain the possibilities of some desired solid space and void is also assumed.
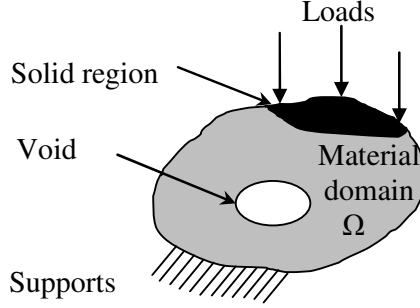
**Fig. 1.3: Material domain for general topology optimization problem**

For the posed problem, it is required to find out the optimal topology within the material domain. The approach finds out the optimal elasticity tensor $E_{ijkl}$, which is a variable within the material domain $\Omega$. Depending on the variable elasticity tensor the energy stored in the material domain will also vary. Thus, the energy bilinear form can be written based on the internal virtual work, considering $\Omega$ as an elastic body, at the equilibrium displacement $d_a$ and for an arbitrary virtual displacement $d_v$

$$Enr(d_a, d_v) = \int_\Omega E_{ijkl}(x) \varepsilon_{ij}(d_a) \varepsilon_{kl}(d_v) \, d\Omega \tag{1.1}$$

where, $\varepsilon_{ij}(d_a) = \dfrac{1}{2} \left( \dfrac{\partial d_{ai}}{\partial x_j} + \dfrac{\partial d_{aj}}{\partial x_i} \right)$ are the strain values

The load linear form is represented as

$$l(d_a) = \int_\Omega g \, d_a \, d\Omega + \int_{\Gamma_T} h \, d_a \, ds \tag{1.2}$$

where, $g$ is the body forces, and $h$ is the boundary tractions on the traction part $\Gamma_T$ on the boundaries. Based on above values, the minimization of compliance or maximization of global stiffness problem takes following form

$$\left. \begin{aligned} &\min_{d_a \in U, E_{ijkl}} \; l(d_a) \\ &subject \; to: \\ &Enr_{E_{ijkl}}(d_a, d_v) = l(d_a), \quad for \; all \;\; d_v \in \tilde{U} \\ &E_{ijkl} \in E_a \end{aligned} \right\} \tag{1.3}$$

where, $E_a$ is the domain for allowable stiffness in the design problem, $\tilde{U}$ is the domain for kinematically admissible displacement fields. In order to solve the above problem the complete material domain is discretized into finite elements. The basic equation for optimization can be written in the following discretized form.

The compliance value $C(x)$, is defined as

$$C(x) = \mathbf{F}^{\mathbf{T}}\mathbf{d} = \mathbf{d}^{\mathbf{T}}K\mathbf{d} \qquad (1.4)$$

where, $\mathbf{F}$ is applied force vector, $\mathbf{d}$ is the nodal displacement vector and $\mathbf{K}$ is the global stiffness matrix, $x$ is the density parameter. By coupling this equation for whole design domain (for n number of elements) and applying penalization by power-law approach, the objective function is converted to the following form

$$C(x) = \sum_{i}^{n} x_i^p d_i^T \mathbf{K_0} d_i \qquad (1.5)$$

where, element stiffness

$$\mathbf{K} = x_i^p \mathbf{K}_0 \qquad (1.6)$$

$\mathbf{K_0}$ is finite stiffness for the element, $x_i$ is the density parameter for element $i$, $p$ is the penalization power and $n$ is total number of elements. Finally, this SIMP based optimization is formulated as (Bendsøe and Sigmund 2003)

$$\left.\begin{aligned} &\min_{x} : C(x) = \sum_{i=1}^{n} x_i^p d_i^T \mathbf{K_0} d_i \\ &Subject \ \ to, \\ &\frac{V(x)}{V_f} \leq f \\ &\mathbf{Kd} = \mathbf{F} \\ &0 < x_{\min} \leq x_i \leq 1, \quad i = 1, \ 2, \ 3, \dots n \end{aligned}\right\} \qquad (1.7)$$

Here, $V(x)$ and $V_f$ is the material volume and design domain volume, respectively, and $f$ is the prescribed volume fraction. Conventionally above problem can be solved using optimization methods like, sequential linear programming (SLP), Sequential quadratic programming (SQP), optimality criterion (OC) (Zhou and Rozvany 1991) or method of moving asymptotes (MMA) (Svanberg 1987). In order to get the solution of this optimization problem, the optimization method is integrated with the finite element (FE) method. The other topology optimization methods are explained in the subsequent sections.

## 1.2.2 Evolutionary structural optimization and bidirectional evolutionary structural optimization method

Evolutionary Structural Optimization (ESO) is proposed by Xie and Steven (1993, 1994, 1997). The basic concept in ESO is the gradual removal of redundant elements from the design material domain, to achieve an optimal design. ESO can be

easilyimplemented in any generalized finite element analysis routine. Unlike SIMP, ESO involves minimum mathematical programming technique in optimization process. This approach initiates with the full material domain design and removes the non-significant material by considering the constraint of strain or stress energy level of the elements. The removal of element is done by assigning them the material property number of the removed elements to zero. For the removed elements, the material properties are eliminated from the global stiffness matrix. ESO works based on a key parameter, called as "Sensitivity number". This indicates the change in the overall stiffness or a specified displacement due to removal of an element, which is formulated using a finite element scheme. After the computation of sensitivity number of each element, the elements, which are having least sensitivity, are removed from the material design domain. This process is repetitive and continues until the desired stiffness or displacement of the structure is achieved. Based on this removal of material properties of elements, the number of equations solved in each iteration, reduces. Finally, this approach generates a clear topology.

The computation for sensitivity number is explained using the finite element analysis explained here. Using finite element method the nodal displacement vector $\mathbf{d}$ and load vector $\mathbf{F}$is related using the global stiffness matrix $\mathbf{K}$ as

$$\mathbf{F} = \mathbf{Kd} \tag{1.8}$$

The strain energy $S_t$, for the structure is defined as

$$S_t = \frac{1}{2}\mathbf{F}^T\mathbf{d} \tag{1.9}$$

The minimization of this term implies the maximization of stiffness of structure. Now by considering the removal of the $'i'$ th element from a structure having $'n'$ numbers of finite elements. The change in stiffness matrix can be computed as,

$$\Delta\mathbf{K} = \mathbf{K}^* - \mathbf{K} \tag{1.10}$$

where,$\mathbf{K}^*$ is the stiffness after removal of the element. It can be assumed that the removal of the element has no effect on the load vector $\mathbf{F}$. The change of the displacement vector from equation (1.8) can be found out as

$$\Delta\mathbf{d} = -\mathbf{K}^{-1}\Delta\mathbf{Kd} \tag{1.11}$$

From equations (1.9) and (1.10),

$$\alpha_i = \frac{1}{2}d_i^{-1}\mathbf{K}d_i \tag{1.12}$$

The quantity shown in equation (1.12) is termed as "Sensitivity number", $\alpha_i$. The term is the elemental strain energy. In order to remove the element, the sensitivity number of each element is computed and the lowest value is chosen for removal. The overall process can be summarized in following steps.

Step1: Discretization of overall design material domain

Step2: Performing load analysis using finite element procedure

Step3: Computation of the sensitivity number for each element

Step4: Removal of elements, which have the lowest sensitivity numbers and refreshing the overall stiffness matrix

Step5: Repetition of Steps 3-4 until the constraint limits on strain energy or displacement limit is reached.

ESO is a simple material removal process. However, material elements removed in the early stage may be required in the later iterations. The recovery of the removed element cell is not possible in basic ESO method. For these complexities, there are possibilities of geting a non-optimal topology in the end result. The conventional ESO method has few other difficulties such as checkerboard pattern, local minima, mesh dependency, etc. To overcome these numerical difficulties, an improved version of ESO is developed, known as Bidirectional Evolutional Structural Optimization (BESO) (Querin et al. 1998, Yang et al. 1999, Young 1999, Huang and Xie 2007). The BESO method uses a filtration scheme to compute the improved sensitivity number. For an element sensitivity number, computation is carried out by considering the sensitivity of the neighboring elements within a circle of radius $r_{min}$. The modified formulation for the sensitivity, $\hat{\alpha}$, is given as

$$\hat{\alpha}_i = \frac{\sum_{j=1}^{nc} w(r_{ij})\alpha_j^n}{\sum_{j=1}^{nc} w(r_{ij})} \tag{1.13}$$

where, $nc$ is the number of nodes in the circle of radius $r_{min}$, and $w(r_{ij})$ is the linear weight factor defined as

$$w(r_{ij}) = r_{min} - r_{ij} \qquad (j = 1, 2,...nc) \tag{1.14}$$

Above modified scheme is purely heuristic, and by employing this scheme the problem such as checkerboard pattern, local minima, mesh dependency can be solved.

The SIMP, ESO, and BESO methods discussed earlier were FE based methods, where the complete material domain of the structure was treated in elements. Unlike this approach, there is another method of topology optimization named as level set method. This mrthod is based on the scalar surface interaction. A short discussion on this method is given in the next section.

### 1.2.3   Level set method

Levelset method was developed by Osher and Sethian (1988). This method was initially applied to topology optimization problem by Sethian and Wiegmann (2000), Osher and Fedkiw (2001), Wang et al. (2003), and Allaire et al. (2004). Level set method is based on the level set models that optimize linear elastic structures. In this method, the structure is implicitly represented by a scalar function i.e. the level set function. These level sets of higher dimensionality represent the structure in a moving boundary. The level sets have the property of remaining to be simple in its topology, while the shape and topology of the structure may undergo major changes. Hence, the changes in the shape and topology of the structure can be simulated using the movement of the design boundaries. Based on this property, this is also referred as implicit moving boundary models. These models can easily enable the actions required to simulate various topologies such as forming holes, splitting into multiple pieces, or merging. To satisfy the required constraint values in the optimization, the change in the topology is generated by implementing a mathematical programming for the optimization. Mathematically, a surface boundary in an implicit form, can be represented as,

$$S_{surf} = \left\{ e : \Phi(e) = k_{iso} \right\} \tag{1.15}$$

where, $e$ is a point on the iso-surface $\Phi$ , and $k_{iso}$ is an arbitrary iso-value. Using this relation, a model is created, which enables the level set function to change dynamically. The model expressed as

$$S_{surf}(t) = \left\{ e(t) : \Phi(e(t), t) = k_{iso} \right\} \tag{1.16}$$

Using above dynamic surface, the topology optimization problem is remodeled as,

$$
\left.
\begin{aligned}
&\underset{\Phi}{Minimize} \quad J(d_a,\Phi) = \int_{\bar{D}} \hat{G}(d_a)H(\Phi)d\Omega \\
&subject\ to: \ \ Enr(d_a,d_v,\Phi) = l(d_v,\Phi) \\
&\qquad\qquad d_a\big|_{\partial D_u} = d_{a0}, \forall d_v \in U \\
&\qquad\qquad V(\Phi) \le V_{max}
\end{aligned}
\right\}
\qquad (1.17)
$$

In this model, the solid domain for the structure is represented by $D$ with its boundary $\partial D$. The displacement at the boundary part $\partial D_u$ is given as $d_{u0}$. In order to model the problem using the level set functions, a fixed larger material domain is defined and denoted as $\bar{D}$, such that the domain fully contains the current material domain $D$. The maximum amount of material that is present in the material domain $D$ is $V_{max}$. Thus, the optimization problem is defined to find the optimal boundary $\partial D$ such that the function $J(d_u,\Phi)$ is minimized, which considers a specific physical or geometric type described by $\hat{G}$. Here, $H$ is the Heaviside function. The key feature for this scheme is to move the design boundary until the objective can be improved further. The optimization problem formulated in equation (1.17) can be implemented as a mathematical programming problem and the optimal topologies can be generated.

With emerging requirements and multiphysics applications, new research goals are being set in the field of topology optimization. The next section focuses on need for research in topology optimization area, and the motivation to pursue research in this area.

## 1.3    NEED FOR RESEARCH

In recent years, extensive efforts have been put in the development and expansion of topology optimization procedures to various domains of application. As a result, several strategies are developed and a few of them are generalized while many are highly problem dependent. The motivation behind the accelerated research in topology optimization is its significant practical importance (Bendsøe and Sigmund 2003), which can attain greater design improvements and saving, than mere sizing or shape optimization. Hence, development took place with increased pace by the help of comprehensive software developments in branches of technology and interdisciplinary fields. Another reason is, being a complex and intellectually challenging field, topology optimization involves basic research, with rather unusual problems in mathematics, mechanics, computer technology, and material sciences like, microstructure optimization of composites. Special and multidisciplinary applications include design-dependent

loads, acoustic coupling, acoustic meta-materials, compliant mechanism mostly used in micro-tooling, fluid-solid interaction, bio-mechanics, bone reconstruction, bone adaption, micro-thermo-electro-mechanical systems, etc.(Bendsøe and Sigmund 2003). In addition, the traditional design and applications are also improved. Namely, design of material unit cells for "high frequency" responses, modeling of topology optimization framework to nonlinear transient systems, tailoring of stress wave that allows noise control, earthquake mitigation, etc. These advancements in topology optimization applications resulted in a number of successful algorithms. Also, the extensions of topology optimization method reveal other complications, i.e. implementation details, numerical instabilities or computational inefficiencies, grey scale control, local stress control, and keeping the computational time to a tractable level, which are still under exploration. This, being a well-established research fields, various aspects are still open for the development and improvement, and a few important ones' are discussed below.

➤ One of the important needs of the research in this field is the development of accurate and efficient method to manufacture topologically optimized component. For example, micro-structural fields are highly heterogeneous and therefore may be difficult or costly to manufacture. Hence, manufacturing constraints can be implemented to improve the manufacturability of the designs. One can probably tailor the manufacturing constraints for the specific manufacturing method.

➤ During development and manufacturing of the products, the need for measure is arise that improve the quality and reliability in a systematic manner without exceeding the manufacturing efforts. By looking at the increasing designs and applications based on topology optimization method, the rise in demand on the reliability, efficiency, and shortened development cycle of a topologically optimized product is predictable. Thus, it becomes inevitable to enhance the topology optimization method towards new goals.

➤ In recent years, reliability and robust design related approaches in the topology optimization has been receiving increased attention. These approaches primarily deal with uncertainties in the realistic environment. The uncertainties may involve in various factors of a topologically optimized components, right from the beginning to end of the life cycle, which includes design, manufacturing, and application phase. In past, various methods are developed using reliable and

robust topology optimization methods. These optimization methods provide greater benefits to the designer; however, certain aspects of performance analysis are still unexplored.

The research presented in this thesis is motivated by above shortcomings in the current state of the art. In this work, the aforementioned aspects of reliability and robust design of the topologically optimized components are incorporated to provide flexibility to designer.

## 1.4    THESIS OUTLINE

This thesis presents the work carried out in identified research gaps. Here, a few methodologies are proposed and their applications are discussed with the help of its practical and theoretical background. The chapters of thesis are organized in following manner,

In Chapter 2, detailed literature review is presented. Here, review is divided into two parts. The first part discusses about the robust design methodologies of topology optimization problems, and the second part discusses about the reliability based topology optimization methods. In this chapter the development of the different design methodology over the years to improve the performance of topologically optimized components are chronicled. Finally, important research gaps in the state of the art are highlighted.

Chapter 3, discusses and analyzes the performance of topologically optimized structures in a realistic environment. For this purpose, design of experiments based method is used. To explore the effect of real life scenario, the noises or uncertainties are included in the analysis. Based on this methodology, four benchmark problems are analyzed and the optimum factor values for robust and targeted performance are obtained.

Chapter 4, uses the similar design methodology by incorporating the effects of uncertainties of design/controllablefactors. Here, the performances of the topologically optimized structures are analyzed by combining reliability and design of experiments methods. To maintain consistency, same benchmark problems are used for reliability based methodology and the optimum factor values are obtained for robust and targeted performance.

To reduce performance variations further, the tolerance range of controllable factors is required to be selected for topologically optimized structures. Chapter 5 aims to identify the combinations of the tolerance of factor to achieve the robust and targeted performance. For this, cross array design of experiment method for topology optimization problems are devised. Tolerance range for controllable factors is also obtained by incorporating reliability index values.

In Chapter 5, the effect of manufacturing uncertainties was included in a generic way. To explore the same in a specific manufacturing process, a simulation technique is introduced in Chapter 6.This chapter discusses the simulation approach employed for tolerance range selection of controllable factors. Like in the earlier case, tolerance range for controllable factors is also obtained by incorporating reliability index values.

To emphasize the significance of the developed methodologies, a case study of bell crank lever is taken. The real life project is executed using the developed methods and obtained results are analyzed in Chapter 7. As a result of this investigation, complete performances range of the bell crank lever is available for robust and targeted performance requirements.

In Chapter 8, the conclusions made in all the chapters are summarized and the future perspective of the research is highlighted.

## 1.5    CONTRIBUTIONS OF THE THESIS

As discussed earlier, present research is performed to analyze the effects of uncertainties of the various factors involved in the topology optimization problem. In this regard, the main contribution of the thesis is the development of design methodologies to achieve the robust, reliable, and targeted performance of a structural or machine element. This aim is pursued by the integration of design of experiments methods and topology optimization techniques. Developed methodologies will enable the simulation of the performance of topologically optimized components and determine the optimum factor values and their tolerancesranges, considering the various effects of uncertainties. The implementations of developed methodologies are illustrated using four benchmark problems. These methodologies are an offline tool for the designer to achieve the targeted values and the robustness of the performances in the realistic environment.

# CHAPTER 2

# LITERATURE REVIEW

In the previous chapter, foundation of topology optimization is elaborated with various aspects of its applications. The need for reliability and robust design approaches in topology optimization problem was also emphasized looking at overall developments and applications in this area. The necessity of the reliable and robust design approaches are felt to design structures for realistic scenarios. This chapter discusses latest developments and attempts of researchers to incorporate effect of uncertainties in topology optimization problems. After reviewing literature regarding the uncertainties consideration in topology optimization problems, a few research gaps are identified, which are the source of motivation for this thesis.

In last decade or so, there has been renewed focus on the impact of uncertainties on topologically optimized structures. The main objective of these studies and developments are to ensure robust and reliable performance. In recent years, research has been growing on the uncertainties issues of different factors in topology optimization. These studies resulted in reliability based topology optimization (RBTO) and robust topology optimization (RTO) method. This chapter reviews these developments in the area of topology optimization. The chapter presents the review in two parts; first section deals with the literatures related to reliability based methods in topology optimization problems and second section deals with robust design methods in topology optimization problems. As discussed earlier, basic topology optimization method for a structural component and compliant mechanisms is similar. Therefore, in literature, the RBTO and RTO methods are applied to structure and compliant mechanisms simultaneously. Thus, the reliability and robust design methods applied to topologically optimized structures and the compliant mechanisms are considered in the review.

## 2.1 RELIABILITY BASED TOPOLOGY OPTIMIZATION METHOD

In past the reliability concept, together with the optimization, received a lot of attention from researchers working in design optimization area. The reliability consideration in design optimization resulted as reliability based design optimization (RBDO) methods. The various methods in RBDO are based on stochastic methods. These methods enable the designer to design the component for a specific risk or targeted reliability that contains the effect of various uncertainties. Here the main idea is to combine the design optimization with the probabilistic constraints. In a usual RBTO problem, extra constraint is included, which state the probability of failure (Tu et al. 1999; Youn and Choi 2004). When this constraint is deployed in topology optimization problem, the deterministic optimization problem (equation (1.7)) is modified as,

$$
\left.
\begin{aligned}
&\min_{x} : C(x) = \sum_{i=1}^{n} x_i^p d_i^T K_0 d_i \\
&\text{Subject to} : \frac{V(x)}{V_f} \leq f \\
&\qquad P(G(\mathbf{x},\xi) \geq 0) > P_f \\
&\qquad 0 < x_{\min} \leq x_i \leq 1, \quad i = 1,\ 2,\ 3,\ ....n
\end{aligned}
\right\}
\tag{2.1}
$$

where, $C$ is the compliance value, $K_0$ is the stiffness matrix for an element, $x_i$ is the density parameter for element $i$, and $p$ is the penalization power. $V_f$ is the total volume of material domain, $V(x)$ is the material volume, and $f$ is the volume fraction. The extra constraint $P(G(\mathbf{x},\xi) \geq 0) > P_f$, denotes the design safety probability based on the limit state function $G(\mathbf{x},\xi)$. Where $P_f$ is the probability of failure, $\mathbf{x}$ is the density matrix, and $\xi$ is the probabilistic variable accounting the uncertainties. A limit state function for topology optimization problem can be defined for the compliance, deflection, or stress values. For example, a limit state function for deflection is shown in equation (2.2).

$$
G(\mathbf{x}, \xi) = d(\mathbf{x}, \xi) - d^* \tag{2.2}
$$

where, $d(\mathbf{x},\xi)$ is the maximum deflection, which is dependent on the material distribution (density matrix $\mathbf{x}$) and the probabilistic variable $\xi$. For a safe design, the maximum deflection should not exceed a set value $d^*$. For topology optimization problems, the number of parameters in $\mathbf{x}$ and $\xi$ are very large and complex. Usually a Taylor series based approximation method is employed to simplify the limit-state

function $G(\mathbf{x}, \xi) = 0$. Based on the order of Taylor series, the simplification method is called as First Order Reliability Method (FORM) and Second Order Reliability Method (SORM). FORM is largely applied in topology optimization problems compared to SORM. The reason being, SORM improves marginal amount of accuracy by offering high computation costs (Maute and Frangopol 2003; Youn and Choi 2004). There are two approaches available in FORM to approximate the limit state function, namely, Reliability index approach (RIA) and Performance measured approach (PMA).

*Reliability index approach (RIA):* The idea for the reliability index approach is to find out the minimum distance from the structural response surface i.e. limit-state approximation from the origin to the surface in the standard Gaussian space. Hasofer and Lind (1974) presented a transformation technique to simplify FORM based reliability index method, named as HL transformation (Maute and Frangopol 2003; Kharmanda et al. 2004,). In this transformation, the physical random variables are transformed into the normalized and independent Gaussian variable. For a limit-state function, $G(\mathbf{x}, \xi) = 0$ the variables where $\xi = [\xi_1, \xi_2, \xi_3 .... \xi_n]^T$ are transformed as,

$$U_i = \frac{\xi_i - \mu_i}{\sigma_i} \qquad (2.3)$$

where, $\mu_i$ and $\sigma_i$ are the mean and standard deviation of physical variable $\xi_i$ respectively. $U_i$, are the elements of Gaussian variable, $\mathbf{U}_g = [U_1, U_2, U_3 .... U_n]^T$. Here, the mean and standard deviation of variable $u_i$, are zero and unity, respectively. This transformation is presented in Fig. 2.1. The nearest point of failure is termed as Most Probable Point (MPP) of failure. The minimum distance from the mean values of variables to the MPP is termed as reliability index β.

For a given value of reliability index, the normalized variable can be estimated based on equation (2.4). This optimization problem can be solved using a suitable scheme.

$$\left. \begin{aligned} &\min : \beta = \sqrt{\mathbf{U}_g{}^T \mathbf{U}_g} \\ &\text{subject to} : G(\mathbf{x}, \mathbf{U}_g) = 0 \end{aligned} \right\} \qquad (2.4)$$
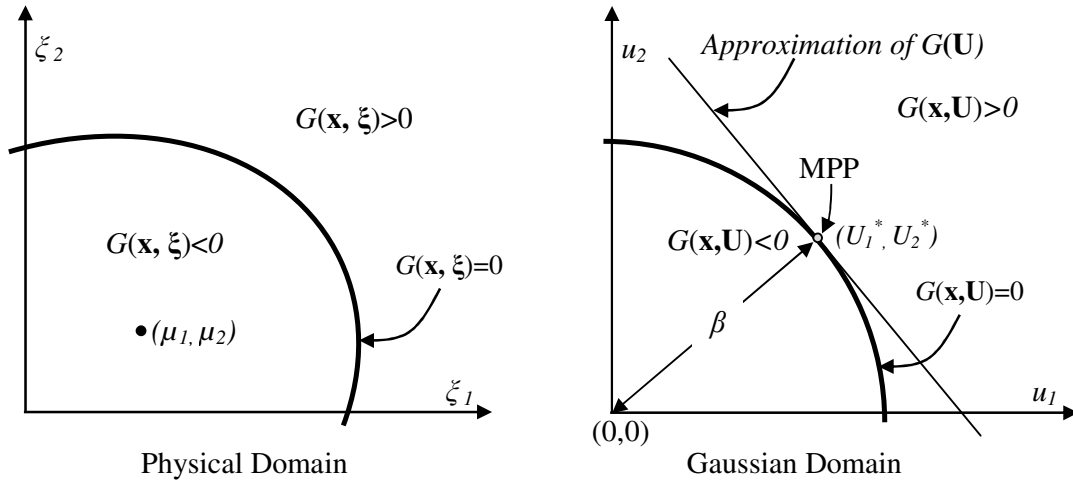
**Fig. 2.1: HL transformation from physical to Gaussian domain and reliability index**

Using RIA, the optimization is carried out with respect to a desired value of reliability index, $\beta^*$. Hence, the topology optimization problem using RIA is expressed as,

$$\left.\begin{aligned}
\min_{x} : C(x) &= \sum_{i=1}^{n} x_i^p d_i^T K_0 d_i \\
\text{Subject to} : &\frac{V(x)}{V_f} \leq f \\
&\beta \geq \beta^* \\
&0 < x_{\min} \leq x_i \leq 1, \quad i = 1, 2, 3, \ldots n
\end{aligned}\right\} \tag{2.5}$$

In this approach, the reliability index is estimated using the optimization routine for equation (2.4). For each iteration step for equation (2.5), the optimization problem given in equation (2.4) is solved.

*Performance measured approach (PMA):* According to PMA the reliability index problem is modified as,

$$\left.\begin{aligned}
\min : &\quad G(\mathbf{x}, \mathbf{U}_g) \\
\text{subject to} : &\sqrt{\mathbf{U}_g^{\mathbf{T}} \mathbf{U}_g} - \beta^* = 0
\end{aligned}\right\} \tag{2.6}$$

By doing so, the reliability requirement is included in the limit-state function. Further, topology optimization is carried out as,

$$\left.\begin{array}{l} \min_{x} : C(x) = \sum_{i=1}^{n} x_i^p d_i^T K_0 d_i \\ \text{Subject to} : V(x) \leq V_f \\ \qquad G(\mathbf{x}, \boldsymbol{\xi}) \geq 0 \\ \qquad 0 < x_{\min} \leq x_i \leq 1, \quad i = 1, \ 2, \ 3, \dots n \end{array}\right\} \qquad (2.7)$$

There are a few advantages of PMA over RIA. PMA gives more robust results compared to RIA as the variations in parameter are lesser (Maute and Frangopol 2003). The convergence property of PMA is good compared to RIA, when constraint function has non-Gaussian probability distribution. In order to apply reliability concepts in topology optimization problems these approaches can be employed. In this section, the methodologies developed for RBTO are reviewed and presented below.

**Review on RBTO:**

RBTO is an approach to generate optimal topology subject to uncertainties of the factors. The reliability concepts in topology optimization problems were initially applied by Bae et al. (2002). They presented a combined model of probabilistic optimal design with finite elements method. The topology optimization problem was modified and reliability constraint equation was incorporated into optimization problem using FORM. The reliability constraint in their work was handled using PMA. Uncertainties of Young's modulus, structure thickness, and loading conditions were considered as uncertain variables. After this, a landmark work was reported by Maute and Frangopol (2003). This work focused on design of MEMS mechanisms or compliant mechanism by considering stochastic loading and boundary conditions as well as material properties. They modified topology optimization scheme also, because MEMS mechanisms undergo large deformation unlike a usual structural problems. To model these mechanisms, co-rotational finite element formulation were incorporated into topology optimization problem. In their work, reliability formulation was carried out using FORM and PMA.

Later, Kang et al. (2004) presented a RBTO method for electromagnetic systems. These systems are a particular type of compliant mechanisms. For these problems, a 2-D magnetostatic finite element model was constructed. Permeability, coercive force, and applied current density were considered as uncertain variables. Computation of reliability constraint was done using PMA and limit state function was approximated using FORM. At the same time, reliability consideration on geometrically non-linear structures was

incorporated by Jung and Cho (2004). Here the problem was reformulated by keeping minimization of volume fraction as objective function. In this model, uncertainty of material property, i.e. elasticity value and external loads were considered and limit-state function was modeled using a predefined deflection value and reliability constraint.

The approaches discussed above required large computations to generate a reliable topology. Focusing on computation issue, a different RBTO was proposed by Khramanda et al. (2004). They employed Hasofer and Lind transformation technique to map uncertain factors from physical to normal Gaussian domain (Hasofer and Lind 1974). Then, based on the desired reliability index values, the MPP is searched in the Gaussian domain and corresponding to the MPP, the factor values are computed. Using values of these factors, a reliable topology was generated. This procedure reduced computation time to a large extent. Considering issue of computation time, Kim et al. (2005) proposed a parallel computing RBTO based on response surface method. The methodology was applied to design the components of MEMS. The uncertainties of dimensions were considered, reliability constraint was incorporated using PMA, and limit state function was developed using a predefined deflection value.

As discussed earlier, a usual RBTO couples topology optimization scheme with reliability consideration. Patel et al. (2005) proposed a decoupled approach to separate topology optimization and reliability problem. For this purpose, a hybrid cellular automata method was utilized. In this methodology, a deterministic topology optimization (DTO) followed by reliability assessment was carried out. To accommodate a global constraint for maximum displacement, a mechanism in RBTO was developed. In addition, they discussed methodology for the six-sigma design of structures using topology optimization. Another hybrid approach for RBTO was proposed by Mohsine et al. (2006). They improved classical RBTO, which has high computation time and weak convergence. The efficiency of hybrid method was demonstrated on static and dynamic cases with extension to the variability of probabilistic model. Unlike usual RBTO, this method allowed to handle increased number of uncertain variables by introducing their standard deviations.

On the issue of practical application of RBTO model, Kim et al. (2006) presented a reliability based design process for Laser scanned models. They mainly discussed process of rapid product development from reverse engineering to create reliable optimal design. In their work, response surface methodology was used to characterize uncertainty

of dimensions. The reliability constraint in the model was included using PMA and the limit state function used maximum allowable deflection and natural frequency. They implemented this model on the upper part of a cellular phone. Similarly, Wang et al. (2006) dealt with practical issues and presented the applications of RBTO in various fields e.g., structures, electromagnetic, heat transfer, and coupled systems. For reliability consideration, PMA was utilized and the limit state function was based on allowable deflection. Similar to these applications of RBTO, Kim et al. (2007) presented a generalized approach for MEMS. In this work, they used topology optimization software to generate topology. They were the first to introduce geometric uncertainty due to the manufacturing processes. In their implementation, the reliability constraint was handled using PMA and limit state function was based on maximum allowable deflection.

The RBTO scheme is successfully employed on other methods of topology optimization apart from SIMP. Kim et al. (2007, 2008) developed RBTO using ESO method, where the uncertainties in material property, load, and dimensions were considered. The implementation of reliability was performed using RIA and limit state function was prepared based on maximum deflection. The limit state function was approximated using Monte Carlo simulation and central composite design approach. Another work on RBTO was reported by Ouyang et al. (2008), in which topology optimization was carried out using level set method. In this work, they proposed a level set method for continuous structures. The uncertainties of load, dimensions, and volume fraction were included in this model and RIA was used to include the reliability constraint.

In continuation to RBTO developments, few methods are proposed, which consider the non-probabilistic reliability approach. Luo et al. (2009) discussed a non-probabilistic RBTO methodology using a mathematical definition of non-probabilistic reliability index, based on the multi-ellipsoid convex model. This method was proposed for design of continuum structures with uncertain-but-bounded parameters in material properties i.e. elasticity value, geometrical dimensions and loading conditions. The problem was formulated in double loop where inner loop handled evaluation of non-probabilistic reliability index based on RIA, and outer loop treated optimum material distribution using SIMP. In continuation to non-probabilistic reliability approach, Kang and Luo (2009) proposed a non-probabilistic RBTO optimization method for design of continuum structures undergoing large deformations. In this model, variation of structural system was treated with multi-ellipsoid convex model. Proposed method gave a realistic

description of parameters being inherently uncertain-but-bounded or lacking sufficient probabilistic data.

Recently, a single-loop system RBTO was proposed by Nguyen et al. (2011), in which statistical dependence between multiple limit-states were considered. This approach used matrix based system reliability method to compute the system failure probability and its parameter sensitivities. In order to improve the accuracy of reliability calculations with high nonlinearity, proposed method incorporated SORM, unlike traditional RBTO methods. To reduce computation costs, multi-resolution topology optimization method was used in this work. One more study was reported by Eom et al. (2010) recently, which combine BESO and response surface method for 3-D structures. Similar to past research on RBTO, this method also uses PMA and limit state function using maximum allowable deflection. Similarly, Yoo et al. (2011) developed a RBTO method based on BESO and used response surface method and successive response surface method to generate limit state function. Another scheme for RBTO was proposed by Wang et al. (2011), where they incorporated the uncertainties of loading in the structural system by considering the magnitude, angle of direction, and the location of applied load. In this model, PMA was utilized and limit state function was developed using deflection value. In a very recent work, Li et al. (2014) proposed a RBTO method based on interval parameter approach. They modified the equivalent static loads for non linear static response structural optimization and solved this problem for dynamic reliability.

This section, presents recent development of methods to use uncertainties for RBTO method. In next section, a comparative summary of above review is presented.

### 2.1.1   Summary of reliability based topology optimization methods

RBTO methods developed so far use some of the commonly available techniques and approaches. In this section, a summary of developed RBTO methods is given to observe the commonalities and differences between techniques and approaches. This summary is prepared based on the literature survey presented in the previous section, consist of 21 papers. Figures 2.2-2.6 show the comparison of common techniques available in the aforementioned research on RBTO.

Figure 2.shows that SIMP and software based method are highly used in RBTO. The remaining optimization methods i.e. BESO, SLP, SQP, and level set method are used in 34% of the cases.
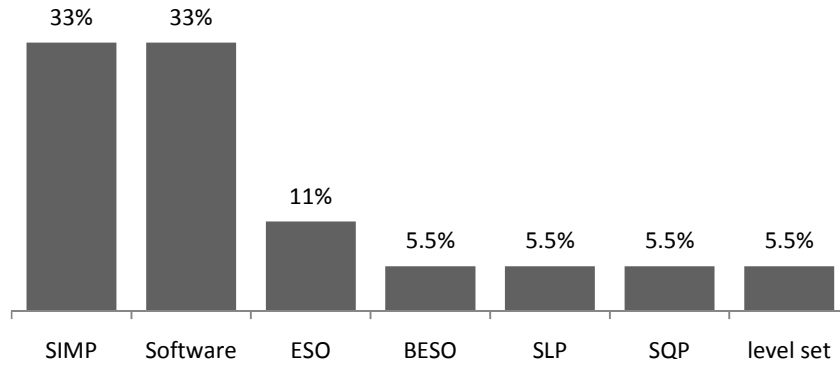
**Fig. 2.2: Comparison on types of topology optimization scheme**
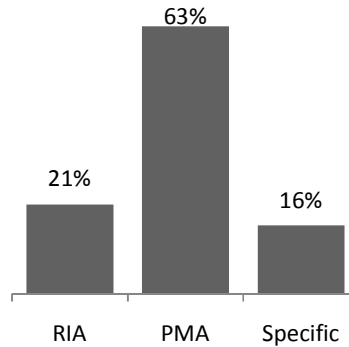


**Fig. 2.3: Comparison of techniques used for reliability constraint**

Figure 2.3 shows the types of approach used to incorporate reliability constraint in the RBTO. It can be observed that PMA is utilized to most of the cases compared to other approaches.
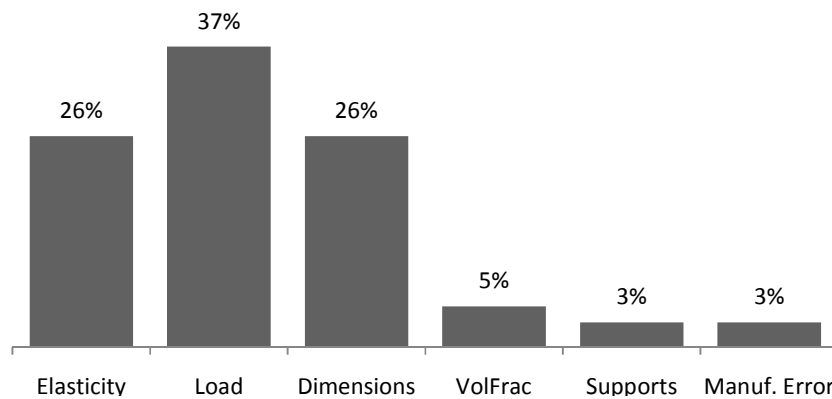


**Fig. 2.4: Comparison of various parameters considered in RBTO method**

Similarly, Fig. 2.4 shows the percentage of the various uncertainties considered in different RBTO methods. Here, the uncertainties of load is considered in most of the cases, while other uncertainties such as rigidity of supports and geometrical manufacturing error due to manufacturing process are considered in smaller number of cases.
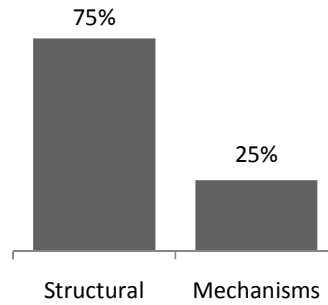
**Fig. 2.5: Comparison of types of problem**

From Fig. 2.5, it can be seen that the structural problems are dealt in most of the cases compared to MEMS or compliant mechanisms.
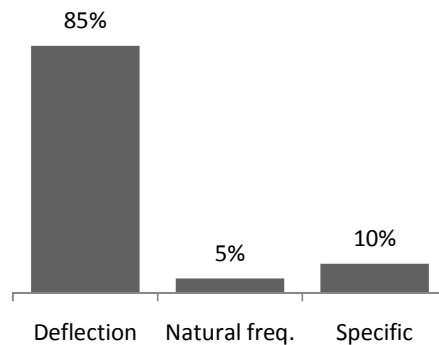


**Fig. 2.6: Comparison of the parameters used in limit state function in RBTO methods**

Figure 2.6 represents the percentage of parameters, which are used to define limit state function. Majority of RBTO method uses the maximum allowable deflection/displacement as limit state function to incorporate reliability constraint in RBTO method. As discussed earlier, the consideration of effect of uncertainties in topology optimization leads to reliable and robust methods. A review of robust topology optimization method is presented in next section.

## 2.2    ROBUST DESIGN BASED TOPOLOGY OPTIMIZATION METHODS

In recent years, extensive research has been carried out to incorporate the effects of uncertainty of various factors in topology optimization. Result of such method is termed as RTO method, which is based on robust design optimization (Beyer and Sendhoff 2007). The theoretical foundations of robust design were laid by Genichi Taguchi, a Japanese engineer. According to Taguchi's view, the traditional definitions of quality, etc. were inadequate. He developed his own definitions of these concepts and coined the definition of a robust design as: "a product or process whose performance is insensitive

to the uncertainty of factors, at the lowest possible cost" (Sung 1998; Montgomery 2007; Mitra 2008). The concept of robust design and performance is currently applied to numerous application and design problems. A general overview of various formulations to obtain robust solution for an optimization problem is available in Beyer and Sendhoff (2007).

Recently, the concept of robust design is implemented for topologically optimized components. In this case, design is made robust against uncertainty of factors such as applied load, material properties, dimensions, manufacturing error, etc. In general, robust topology optimization problem is expressed as (Dunning et al. 2011),

$$
\left.\begin{aligned}
&\min_{x} : C = \mathrm{E}[C]\\
&\text{Subject to}:\\
&\mathbf{F} = \mathbf{Kd}\\
&\frac{V(x)}{V_f} \le f\\
&\mathrm{STD}[C] \le \hat{S}\\
&0 < x_{\min} \le x_i \le 1, \quad i = 1,\ 2,\ 3,....n
\end{aligned}\right\}
\tag{2.8}
$$

The equation (2.8) shown above, is obtained by modifying the DTO equation (1.7). Here, E[$C$] is the expected value of compliance. The variation of compliance is limited to by its standard deviation, STD[$C$]. Here, $\hat{S}$ is the limiting value of standard deviation of compliance. Other terms of equation (2.8) are similar to equation (1.7). Alternatively, optimal robust design can be obtained by,

$$
\left.\begin{aligned}
&\min_{x} : C = \mathrm{E}[C] + \kappa \times \mathrm{STD}[C]\\
&\text{Subject to}:\\
&\mathbf{F} = \mathbf{Kd}\\
&\frac{V(x)}{V_f} \le f\\
&0 < x_{\min} \le x_i \le 1, \quad i = 1,\ 2,\ 3,....n
\end{aligned}\right\}
\tag{2.9}
$$

Equation (2.9) is an alternate to equation (2.8) (Lazarov et al. 2011;, 2012a; Richardson et al. 2013). Here the effects of uncertainties are incorporated in the objective function itself. The term $\kappa$ controls the contribution of the standard deviation in the objective function. Other terms of the equation (2.9) are similar to the DTO equation (1.7). There are many methods available to evaluate the effect of uncertainties

parameters on compliance values, such as, stochastical method, Monte Carlo method, generation random process/field, interval analysis, etc. The methodologies developed in the field of robust topology optimization are focused on types of uncertainties, parameters and the methods to model the uncertainties. A detailed discussion on developed methods and approaches are presented next.

**Review on RTO:**

Use of robust design methods in topology optimization problems is initiated by Logo (2007). He added a deterministic constraint in topology optimization scheme to include allowable variations of compliance. The variations of compliance are observed due to random loading. Proposed method was applied using SIMP and OC method. Similarly, loading uncertainty was analyzed by Kogiso et al. (2008). They considered uncertainty of direction and values of applied load for compliant mechanisms. A sensitivity based robust topology optimization method for synthesis of compliance mechanisms was proposed by them. Gournay et al. (2008) investigated uncertainties of applied load using the worst-case criteria. This methodology was applied using level set method and it was supported by examples of 2-D and 3-D structural problems. Similar to load uncertainty, there can be uncertainties in other factors also. Lee et al. (2002) analyzed effects of uncertainties in material property, i.e. elasticity value and Poisson's ratio, on dynamic behavior of topology optimization problems. They used interval analysis method to analyze effect of uncertainties. Chen et al. (2010) modeled loading and material uncertainties using random fields. The randomness of factors was generated using Karhunen-Loeve (KL) expansion. A robust shape and topology optimization method was developed, which offered very low computation cost compared to available techniques. Dunning et al. (2011) also proposed a robust topology optimization problem based on level set method. In their work, uncertainties in load magnitude and its directions were considered. These uncertainties were incorporated similar to multiple loadings using their weights. The uncertainties in load values were also considered by Takezawa et al. (2011) by minimizing robust compliance that is defined as the maximum compliance induced by the worst load case. Tootkaboni et al. (2012) proposed a method that combined spectral stochastic approach for representation and propagation of uncertainties with DTO technique. In this method, extra dimension is added e.g random dimension, where the stochastic variability of input parameters and outputs of interest can be modeled.

Apart from the uncertainties of different factors, uncertainties of manufacturing process plays a greater role in the performance of topologically optimized component. Manufacturing errors in topologically optimized structures mainly affect the predefined geometry of the component, called as geometrical uncertainties. The effect of uncertainties due to manufacturing processes was analyzed by Sigmund (2007, 2009) and his coworkers. The team implemented uncertainties as either too thin or thick distribution of material, and used the morphological operators available in image processing literature. Later, a generalized modification for DTO scheme was proposed by Schevenels et al. (2011). They proposed a robust topology optimization method by incorporating the mean and the standard deviations of uncertain factors. The effects of manufacturing uncertainties are simulated as the too thin or too thick distribution of material. In this work, the simulations of uncertainties were carried out using a random field based projection method. Similar problem on geometric uncertainties was addressed by Chen and Chen (2011), using partial differential equation based level set method. Here, geometric uncertainties were modeled using random normal boundary velocity field. Lazarov et al. (2011) explored issues on projection method that suppresses gray scales in topology for compliant mechanisms at micro scale. Use of this method reduced robustness against the geometrical errors. To handle this problem, a model was proposed with the help of random variables, which used stochastic formulation. The method was robust with respect to the uncertainties of production process, i.e. without any hinges or small details that create manufacturing difficulties. Wang et al. (2011a) also discussed similar issues of mesh convergence and gray scale removal methods. A modified robust topology optimization formulation based on the types of projection method i.e. erosion, intermediate and dilation is proposed, that ensures both global and local mesh-convergence. They applied the proposed method with slight modification on the photonic crystal waveguides, with consideration of manufacturing uncertainties (Wang et al. 2011b). Amir et al. (2012) focused on issues of computation cost involved in robust topology optimization methods. The effect of uncertainties of manufacturing process is captured in their work using worst-case formulation and stochastic formulation approach. Lazarov et al. (2012a) considered material and geometric uncertainties. To model these uncertainties, stochastic collocation method was utilized. In this paper a memory-less spatially varying Gaussian random fields were employed to represent random variations. Later, Lazarov et al. (2012b) proposed a methodology that captured the manufacturing uncertainty using perturbation techniques. This technique offered lesser computation cost

compared to the previous one proposed by them. Connected to manufacturing uncertainties, the under and over-etching uncertainties involved in the MEMS was handled by Jang et al. (2012). A robust design methodology was proposed by Jansen et al. (2013) taking account of deformation of topologically optimized structure. They considered the slenderness in optimized structures that creates geometric imperfections i.e. misplacement and misalignment of material. In this work, geometric imperfections were incorporated in robust optimization scheme using stochastic random fields. Recently, Richardson et al. (2013) proposed a robust topology optimization method, which uses stochastic finite element method, with a polynomial chaos expansion to propagate uncertainties. The uncertain parameters were modeled using a spatially correlated random field, which was discretized using the KL expansion. Several examples are dealt to demonstrate method on both 2-D and 3-D continuum and truss structures. Logo et al. (2013) proposed a numerical method for uncertain loading positions. The optimization problem was formulated and solved using volume minimization subject to probabilistic compliance constraint. Guo et al. (2013) considered the uncertainty of boundary variations via level set approach in topology optimization problems. They choose the compliance and fundamental frequency of structure including the worst case perturbation as the objective function for ensuring the robustness of the optimal solution.

The presented section elaborates the attempts to consider the effect of uncertainties on the topology optimization problem through the robust design methods. In next section, a comparative summary of this review is presented.

### 2.2.1   Summary of robust design based topology optimization methods

The developed methods for robust topology optimization utilize some of the available techniques and the approaches. Although there are major differences among the available RTO methods, but literature are compared based on methods, types of problem and types of uncertainties. This summary is prepared based on the literature survey presented in the previous section, consist of 23 papers.

From Fig. 2.7, it is seen that the majority of these literature focus on SIMP approach. The reason being compatibility of SIMP with different approaches.
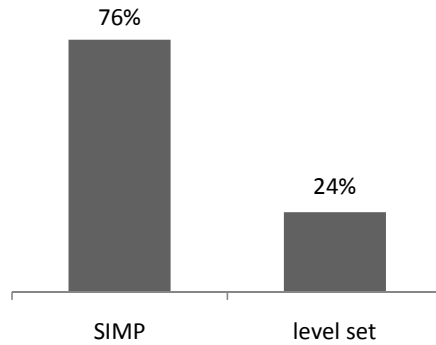
**Fig. 2.7: Comparison on types of topology optimization methods**
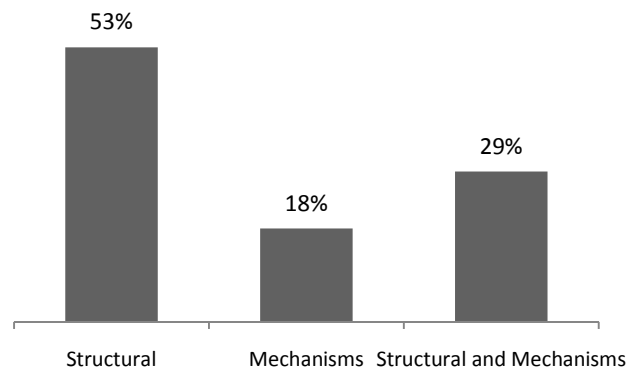


**Fig. 2.8: Comparison on types of problems handled in RTO methods**

In Fig. 2.8, type of problems dealt in RTO method is presented. Majority of the research is carried out using structural problems. A good percentage of the research can also be seen that utilized structural as well as compliant mechanism problems.
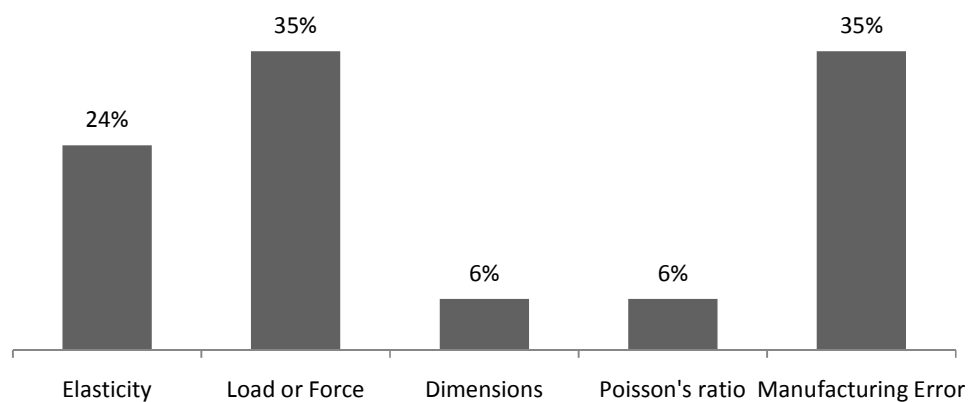


**Fig. 2.9: Comparison based on factors for which uncertainties are considered**

Figure 2.9, presents the percentage of the literature that considers effect of uncertainties. Most of the research is focused on effect of uncertainties due to load or force, manufacturing error and elasticity value. The literature reviews for reliable and robust

methodology in topology optimization highlights recent developments. In addition, a few research gaps can also be observed from the research so far, which is presented in the next section.

## 2.3    GAPS IN THE EXISTING RESEARCH

Based on the literature survey, gaps in the existing research are identified and discussed below

- **Need for a generalized method to incorporate the effect of uncertainties:** The work carried out in literature related to reliability and robust design methods in topology optimization area is found out to very problem dependent. Thus, a generalized approach to handle different problem become a necessity. It can be seen that in most of the work, uncertainties of a few factors are considered. In most of the papers, number of factors considered for uncertainties are not more than three. Hence, a generic methodology should be developed, which can include effects of uncertainties of large number of important factor simultaneously.

- **Analysis of performance:** By applying reliable or robust method, one can obtain optimal topology with effects of the uncertainties. Optimal topology generated by such method is the end result. These methods do not include the intermediate results, which may be designer's alternative. In other words, a methodology is required that provide performance map at different values of uncertainties of factors, to offer greater flexibility to designer.

- **Targeted performance problem:** The effort in the available reliable and robust topology optimization method is to bring compliance, volume fraction, or deflection to its minimum values, especially for structural problems. However, there are certain conditions in which the designer requires a particular value of these outputs even in uncertain scenario. For example, optimization of a component of mechanism, where the deflections have to match with other mating part. In addition, it is also observed that, usually by application of RBTO or RTO the performance change from that of deterministic values. But, this is undesirable from designer/customer perspective. These issues are very important during optimization of a mechanical or structural system consisting of several components. Therefore, a methodology should be developed, which can address

the issues of targeted performance value problem considering designer/customer perspective.

- **Manufacturing issues:** The concepts to handle manufacturing of the topologically optimized structures as well as the 'Design for Manufacturing' are still in its infancy. Therefore, specialized methods are required, which can generate the optimal topology considering capabilities of manufacturing process. Few methodologies are recently available for micro and nano fabrication domain. However, there are no methods available for components in macro domain. Hence, consideration of effects of uncertainties in macro manufacturing process is required to be developed.

- **Computational cost:** The computational cost is one of the major concerns in topology optimization problems. This cost should be considered while developing a method to handle effects of uncertainties. For example, to model the effects of various parameters help of Monte Carlo method is usually taken. However, implementations of such methods involve huge computation cost. Hence, an integrated method is required that reduces computational cost.

## 2.4    CONCLUSIONS

Present chapter discusses fundamentals of reliability and robust topology optimization problems, with its developments. There are different methodologies proposed in literature and emphasis is given to the effects of manufacturing uncertainties of micro and nano scale components. The gaps in the available research are also identified in this chapter. As a whole, the work presented in this area is limited to some specific applications. From this survey, the need for further research has emerged, i.e. development of generalized method, use of statistical method for performance analysis to obtain targeted and robust design, manufacturing issues, reducing the computational cost, etc. The work presented in this thesis is motivated by these outcomes. The presented work takes the whole analysis one step ahead by incorporating designer and manufacturer's perspective.

# CHAPTER 3

# ANALYSIS OF THE PERFORMANCE OF TOPOLOGICALLY OPTIMIZED STRUCTURES

## 3.1 INTRODUCTION

At conceptual stage, designers/practitioners often face a challenging situation to select the various input factors for a targeted performance and topology. In some problems, the loading condition and few boundary conditions may be offered to design a component. The complete material domain and the amount of material, which is to be removed, are decided by the designer based on the compliance and deflection value. This kind of problem may be termed as "*targeted performance value problem*", where input factors are decided by the targeted performance values. In such situations, it is important to know the overall impact of input factors on the performances. Again, in real life situations, these input factors may vary at manufacturing and application phases. Hence, it is essential to investigate the behavior of performances for various factor values. Nevertheless, the simulated result should be applicable to the variety of problems, considering the different range of factors and uncertainties involved. These results provide insight to designers regarding performance behavior within the identified factor values. To explore further, the objectives are,

- To develop a method that explores performance behavior over the possible range of the factors in the realistic environment,
- To observe the sensitivity of each factor,
- To obtain the values of the factors for a robust design and targeted performance value.

For this analysis, the level values of a few input factors are defined referring to the published literature. The experimental design combinations of input factors are generated using full factorial Design of Experiments (DOE) approach. The effects of uncertainties are also incorporated in design combinations. The generated combinations are taken as

the treatment combinations to topology optimization method that generates topologies with performance values. Here, the compliance and deflection values act as performance values. Effect of each factor on performance value will help to in identifying the factor, which has dominating nature within specified range, and interactions among them. This analysis is helpful to define the allowable range of input factor for a given range of performance values. Present chapter will become an aid to select the input factor values subject to a robust and targeted performance. The description of the methodology and analysis is given in subsequent sections.

## 3.2    METHODOLOGY

In order to achieve the objectives of this chapter, a methodology based on the DOE approach is developed. DOE is a systematic process to design efficient experiments. The objective of the experiments is to analyze the effects of several factors on the response or performance of a product or a process. Factors are the parameters that affect the performance of the process or product (Montgomery 2007). Using the normal experimental process, more number of experiments is required to generate the relation between responses and factors in a generalized way. Here, the DOE approach offers a scientific way to choose the number and type of experiment to reduce the cost of experiment without losing efficiency. This is achieved by merging the several design factors in one investigation instead of conducting separate investigation for each factor. In such way, the number of experiments decrease and detailed understating of the product or performance is achieved. Therefore, the statistical significance of factors can easily be identified, and the treatment combinations that have reduced variations in the performance can be found out. The steps for the methodology are given as,

Step 1.   **Selection of problem and performance measures:** In this step, problem is selected for analysis, or a given problem is well defined for its boundary conditions, etc. The performance measures are defined based on application requirements.

Step 2.   **Input factors and their level values:** Main input factors in the problem are identified and their level values are decided based on analysis requirement.

Step 3.   **Noise or uncertainties**: The noise/uncertainties are identified in this step. In normal experimental scenario these noise are difficult to control.

Step 4.    **Experimental combination set:** Based on the number of input factors and their levels, experimental combination set is generated.

Step 5.    **Selection of topology optimization method**: A proper method for topology optimization is selected to generate optimal topology with performance values. Necessary changes are also incorporated in the selected method to accommodate uncertainties / noises of factors.

Step 6.    **Simulation of performance values:** Corresponding to experimental combination set with effect of noise, topologies and performance values are generated based on topology optimization method.

Step 7.    **Analysis of simulated results:** Using various statistical techniques the simulated results are analyzed.

For illustration, the above methodology is applied to a few benchmark problems, which are available in topology optimization literature. For implementation, the above said steps are discussed in next section.

## 3.3    IMPLEMENTATION OF PROPOSED METHODOLOGY

A detailed description of the proposed methodology is presented in this section.

### 3.3.1    Selection of problem and performance measures

#### 3.3.1.1    *Description of the chosen benchmark problems*

In order to investigate the effect of input factors on performance value, various theoretical experiments are conducted. These experiments are performed on four specific types of problems that are usually analyzed by the different researchers (Bendsøe 1995; Rozvany 1998; Bendsøe and Sigmund 2003; Kharmanda and Olhoff 2002; Kharmanda et al. 2004; Patel et al. 2005; Mozumder et al. 2006; Ouyang et al. 2008; Rozvany 2009; Luo et al. 2009, Sigmund 2009; Tootkaboni et al. 2012). The physics of these problems are given below,

**Problem-1:** MBB-beam with a point load, as shown in Fig. 3.1(a). This problem is a reduced form of a simply supported plate and is well analyzed for different formulation and fundamental changes, by the various researchers. The problem is named based on a German aircraft company "Messerschmidt-Bolkow-Blohm", and famous as "MBB beam" in the literature (Rozvany 1998).
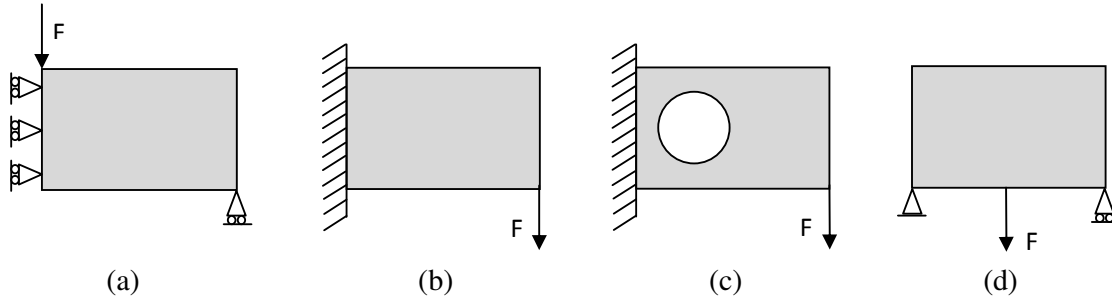
(a)                    (b)                    (c)                    (d)

**Fig. 3.1: Selected benchmark problems (a) MBB-Beam (b) cantilever plate (c) cantilever plate with a hole (d) simply supported plate**

**Problem-2:** The second problem is chosen as a simple cantilever plate, shown in Fig. 3.1(b). The lower right end of the plate is subject to a point load. This problem is analyzed by the various researchers. Hence, the values of the various factors and uncertainties can be directly referred from the available literature.

**Problem-3:** The third problem is a variation of a simple cantilever plate and shown in Fig. 3.1(c). This problem has a predefine hole in the material domain. Thus, high performance values, i.e. compliance and deflections are obtained compared to problem-2. In other words, the comparative results of problem-2 and 3 will help to analyze the effect of a slight change in the shape of the structure for same boundary conditions.

**Problem-4:** The fourth problem is a simply supported plate with a point load acting at the lower mid part, in downward direction and shown in Fig. 3.1(d). Like cantilever plate, this problem is also analyzed by the various researchers.

These problems are the basic building blocks of any structural system, which provide the basic guideline for analysis of structural system.

### 3.3.1.2   *Performance measures*
In order to analyze the performance of structural problems, maximum deflection and minimum compliance values of optimal topology are selected as the performance measures. These two measures are frequently used in the available literature as discussed in section 2.1.1 and 2.2.1. Since structural problem selected are optimized for the minimum compliance, its values can be directly computed from objective function (equation 1.7). Similarly, value of maximum deflection is computed using the finite element routine in-built in topology optimization scheme. These performance measures are obtained as output of simulation, as shown in process diagram Fig. 3.2.
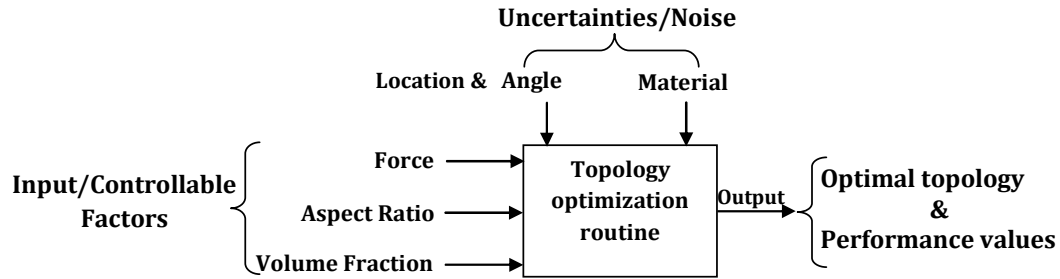
**Fig. 3.2: Process diagram for generation of performance and optimal topology**

### 3.3.2   Input factors and their level values

For the selected benchmark problems, applied force, volume fraction, and aspect ratio are identified as the input factors. The input factors are selected based on the discussion in section 2.1.1 and 2.2.1. Applied force and volume fraction are very sensitive for optimal topology and its performance values. Dimensions of the initial material domain also play an important role in the generation of optimal topology. In case of 2-D problems, the domain is usually kept as rectangular (Bendsøe 1995; Rozvany 1998; Bendsøe and Sigmund 2003). Here, the dimensions are considered in terms of aspect ratio. For problem-1, material domain with aspect ratio is shown in Fig. 3.3. Similarly, material domains are defined for other problems. Different levels of factors values are utilized to generate input factor combinations using DOE. The factor combinations are input for simulation process, as shown in Fig. 3.1.
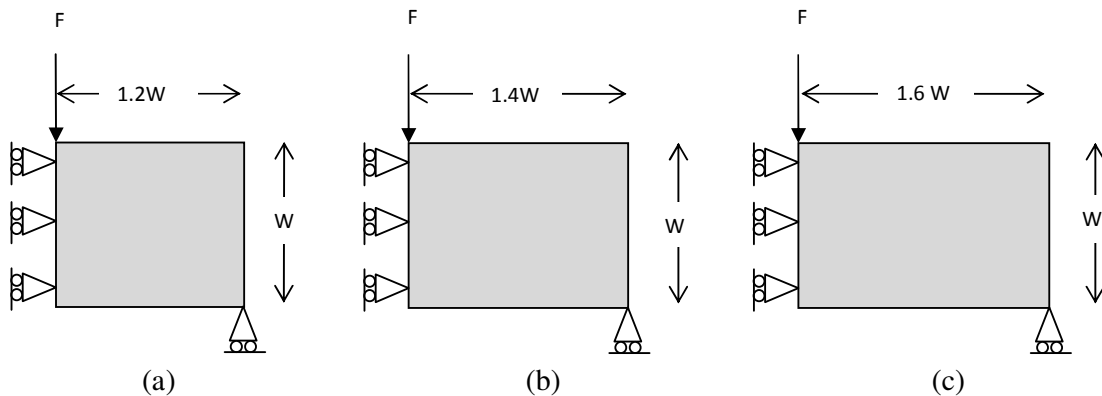


**Fig. 3.3: MBB beam with aspect ratio (a) 1.2 (b) 1.4 & (c) 1.6**

### 3.3.3   Uncertainties due to non-controllable factors

For a particular problem, conditions of applied force and material property are considered as non-controllable factors. The details are presented below.

### 3.3.3.1    *Uncertainties due to applied force*

In deterministic condition, the load vector is fixed with respect to point of action on the body. However, due to the involvement of different imperfections and errors, though minor, the location of point of action may change from its desired position. These loads may deviate by some small angle or some linear distance or combination of both as summarized in Table 3.1.
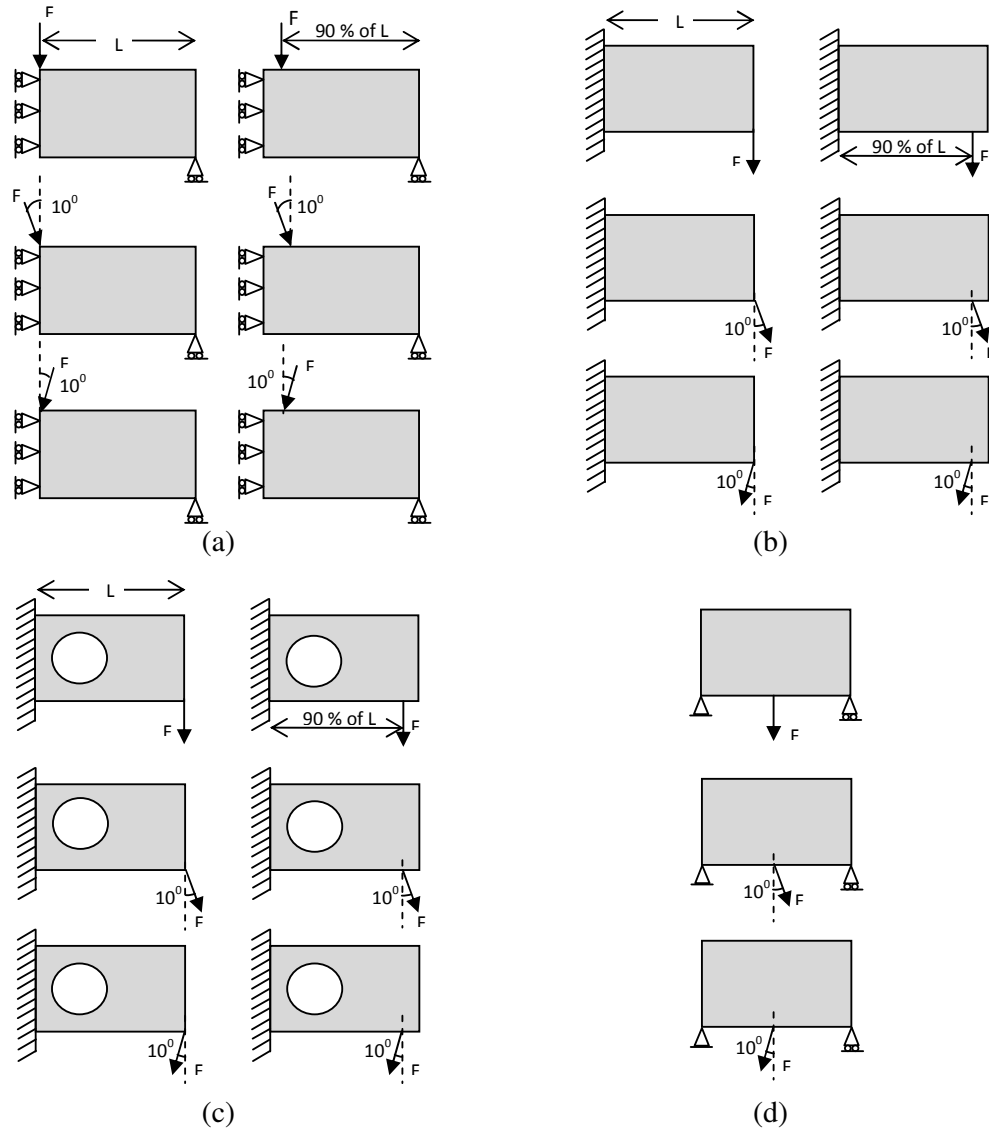


**Fig. 3.4: Loading conditions for (a) problem-1, (b) problem-2, (c) problem-3, (d) problem-4**

To incorporate these effects in applied force, different cases are assumed, which are shown in Fig. 3.4. In case of simply supported plate, only angular deviations are taken whereas linear deviations are not considered because this condition will lead to unsymmetrical loading.

**Table 3.1: Different loading cases for the bench mark problems**

| Case | Deviation from exact position |
| --- | --- |
| 1 | Load at the exact position |
| 2 | $+10^0$ angular deviation from the case 1 |
| 3 | $-10^0$ angular deviation from the case 1 |
| 4 | Linear deviation of 10% of the beam length |
| 5 | $+10^0$ angular deviation from the case 4 |
| 6 | $-10^0$ angular deviation from the case 4 |

### 3.3.3.2   *Material uncertainty*

Variations in material property are other noises/uncertainties, which are considered in present work. It is incorporated by the manipulation of material property i.e. modulus of elasticity. To enable perturbation in modulus of elasticity, Gaussian distribution is chosen. The range of variation is decided based on the previous work which deals with material uncertainty issues (Maute and Frangopol 2003; Jung and Cho 2004; Kharmanda et al. 2004). The values of modulus of elasticity are randomized for each finite element cell with a mean value and standard deviation of 200 GPa and 6.667 GPa respectively. The poison's ratio is taken as 0.3. The process shown in Fig. 3.2 is followed to incorporate the effect of material uncertainty in simulation.

### 3.3.4   **Experimental combination set**

Here, experimental combination set are formed using DOE approach. In order to create a space of chosen input factors, technique of full factorial design is adopted. A full factorial design is used to evaluate more than one factor simultaneously. It requires the selection of performance values and factors with their level values. To generate experimental combinations $3^k$ full factorial design approach is utilized, where $k$ is the number of input factors and 3 is the number of levels considered for input factors (Mitra 2008; Montgomery 2007). The rationale behind this selection is to observe the non-linear

relationship between the input factors and output (i.e. performance values). For example, if there are three factors A, B and C and their levels are $a$, $b$, and $c$ respectively, then each replicate contains all $a \times b \times c$ experimental combinations. One of the special cases is that of $k$ factors, each at three levels. A complete replicate of such design requires $3 \times 3 \times 3 \times .... = 3^k$ combinations and called as $3^k$ factorial design. For example, experimental combination for two factors (i.e. $k = 2$) with three levels is shown in Table 3.2. The levels of each factor is represented as +1, 0 and −1, which denotes high, middle, and lower level values, respectively.

**Table 3.2: Example of a $3^2$ factorial design**

| Combination Number | Factors | |
|---|---|---|
| | A | B |
| 1 | +1 | +1 |
| 2 | 0 | +1 |
| 3 | −1 | +1 |
| 4 | +1 | 0 |
| 5 | 0 | 0 |
| 6 | −1 | 0 |
| 7 | +1 | −1 |
| 8 | 0 | −1 |
| 9 | −1 | −1 |

If more than three level values are selected, then the number of experimental combinations and computational burden will increase substantially, to observe the same non-linear behavior. For the present investigation, the level values of selected input factors are chosen and provided in Table 3.3.

**Table 3.3: The level values of selected input factors**

| Level | Force (N) | Volume fraction | Aspect ratio |
|---|---|---|---|
| 1 | 100 | 0.4 | 1.2 |
| 2 | 120 | 0.5 | 1.4 |
| 3 | 140 | 0.6 | 1.6 |

The aim of the presented investigation is to analyze the performance for predefined factor levels. This is purely based on the choice of designer. The result of this investigation will be valid for the selected levels. In present case, all factor levels are uniformly spaced. For, selected problems $3^3$ design is chosen which lead to 27 combinations of input factors as shown in Appendix A1. It is notable that based on the values of forces, stress generated for all problems are in safe region. Thus, stress values induced in structures are not used as one of the performance measures.

### 3.3.5 Application of SIMP to generate optimal topology

Out of available methodologies, discussed in Chapter 1, SIMP method is chosen for the work presented in this thesis. SIMP is generally accepted by topology optimization groups and a plenty of research is carried out on different issues, using this method. As a result, many filtering techniques are available for the different complexities such as, local minima, gray scale (or intermediate density) removal, mesh-independency, checkerboard pattern, one node connected hinges, etc. (Sigmund and Petersson 1998; Blaise 2001, Bendsøe and Sigmund 2003; Svanberg and Svard 2013). The usage of these techniques is confirmed on different problems by researchers. In addition, SIMP based solutions show closeness to analytical optimal truss structures of benchmark problems (Rozvany 2009). Due to these characteristics of SIMP, almost all industrial applications of topology optimization use this method (Rozvany 2009).

The discretized topology optimization equation (1.7) was presented in section 1.2.1. This equation can be solved by a suitable optimization technique such as SLP, SQP, OC, MMA, etc. These optimization techniques require nodal deflections subject to boundary conditions. Thus, a FE method based routine is also needed to complete the optimization process. For the selected benchmark problems, OC method is chosen for the optimization. OC is widely used by the researchers because of its simplicity in application and suitability in single constraint problems. In the next section, application of OC is explained along with FE procedure.

### 3.3.5.1 Optimality criterion method

OC method aims to prepare an iterative procedure to update the design variables. The generalized problem is given in equation (1.7). Here the upper and lower bounds of the density parameters are one and $x_{min}$, instead of one and zero. The lower bound is assigned

a finite minimum value to avoid any possibility of the singularity in the equilibrium equation. With Lagrange multipliers, equation (1.7) can be written as,

$$L = C + \lambda_0(V - fV_0) + \lambda_1^T(Ku - F) + \sum_{i=1}^{n}\lambda_2^i(x_{min} - x_i) + \sum_{i=1}^{n}\lambda_3^i(x_i - x_{max}) \quad (3.1)$$

where, $\lambda's$ are the Lagrange multipliers. For the condition of optimality the $\frac{\partial L}{\partial x_i} = 0$,

$i = 1, 2, ... n$.

The values of $\frac{\partial L}{\partial x_i}$ is found out as,

$$\frac{\partial L}{\partial x_i} = \frac{\partial C}{\partial x_i} + \lambda_0\frac{\partial V}{\partial x_i} + \lambda_1^T\frac{\partial(Ku)}{\partial x_i} - \lambda_2^i + \lambda_3^i \quad (3.2)$$

Assuming that, the upper and lower bounds constraints are not active, i.e. $\lambda_2^i = \lambda_3^i = 0$, and the loads are independent of design, i.e. $\frac{\partial F}{\partial x_i} = 0$.

By incorporating these assumptions and putting the values of $C$ from equation (1.5), equation (3.2) is written as,

$$\frac{\partial L}{\partial x_i} = u^T\frac{\partial K}{\partial x_i}u + \lambda_0\frac{\partial V}{\partial x_i} + \lambda_1^T\frac{\partial K}{\partial x_i}u - \frac{\partial u}{\partial x_i}(2u^T K + \lambda_1^T K) \quad (3.3)$$

The sensitivity of volume fraction with respect to design variable is defined as, $\frac{\partial V}{\partial x_i} = V_i$.

Since the values of $\lambda_1^T$ is arbitrary, it is chosen as $-2u^T$ so that $\frac{\partial u}{\partial x_i}$ can be eliminated.

with these, the derivative of Lagrangian is written as,

$$\frac{\partial L}{\partial x_i} = -u^T\frac{\partial K}{\partial x_i}u + \lambda_0 V_i \quad (3.4)$$

or,

$$\frac{\partial L}{\partial x_i} = -p(x_i)^{p-1}(x_i)^T K^0 u_i + \lambda_0 V_i \quad (3.5)$$

By putting the optimality condition in equation (3.5), the design variables can be updated as,

$$\frac{-p(x_i)^{p-1}(u_i)^T K^0 u_i}{\lambda_0 V_i} = \frac{-\frac{\partial C}{\partial x_i}}{\lambda_0 V_i} = 1 \quad (3.6)$$

This quantity is defined as a heuristic parameter $B_k^e$,

$$B_i^k = \frac{-\dfrac{\partial c}{\partial x_i}}{\lambda_0 V_i} \tag{3.7}$$

The updating of the design parameter will be carried out as,

$$x_i^{k+1} = B_i^k x_i^{k+1} \tag{3.8}$$

In order to avoid the abrupt change in design variable a moving limit, $\tilde{m}$ is introduced. Finally, the heuristic scheme (Bendsøe 1995) is formulated as,

$$x_i^{k+1} = \begin{cases} \max(x_{\min}, x_i^k - \tilde{m}) & \text{if } x_i^k (B_i^k)^\eta \leq \max(x_{\min}, x_i^k - \tilde{m}), \\ x_i^k (B_i^k)^\eta & \text{if } \max(x_{\min}, x_i^k - \tilde{m}) < x_i^k (B_i^k)^\eta < \min(1, x_i^k + \tilde{m}), \\ \min(1, x_i^k + \tilde{m}) & \text{if } x_i^k (B_i^k)^\eta \geq \min(1, x_i^k + \tilde{m}) \end{cases} \tag{3.9}$$

where, $\eta = 1/2$ is a numerical damping coefficient, $\tilde{m}$ is the move limit set as 0.2. Presented OC method is applied to compute the density parameter $x$, iteratively. In order to solve force-displacement equation in the topology optimization process, FE method is applied, which is explained next.

*3.3.5.2 Finite Element Method*

The chosen benchmark problems are example of plates. Hence, these problems are handled using plane stress condition. For these plates the functional of complete potential energy is written in following form,

$$P_{PE} = \frac{1}{2} \int_\Omega \boldsymbol{\varepsilon}^T \boldsymbol{\sigma} d\Omega - \int_L \mathbf{F}^T \mathbf{d} dL \tag{3.10}$$

where, $\boldsymbol{\varepsilon}, \boldsymbol{\sigma}, \mathbf{F}$, and $\mathbf{d}$ are the vectors of strain, stress, applied load and displacements, as given below. $d\Omega, dL$ are the infinitely small element of two-dimensional area and outline.

$$\boldsymbol{\varepsilon} = \begin{bmatrix} \varepsilon_x & \varepsilon_y & \gamma_{xy} \end{bmatrix}^T \tag{3.11}$$

$$\boldsymbol{\sigma} = \begin{bmatrix} \sigma_x & \sigma_y & \tau_{xy} \end{bmatrix}^T \tag{3.12}$$

$$\mathbf{F} = \begin{bmatrix} p_x & p_y \end{bmatrix}^T \tag{3.13}$$

$$\mathbf{d} = \begin{bmatrix} u & v \end{bmatrix}^T \tag{3.14}$$

where, $\sigma_x, \sigma_y, \tau_{xy}$ are normal and tangential stresses, $\varepsilon_x, \varepsilon_y, \gamma_{xy}$ are linear and angular strains, $u, v$ are linear displacements of the points on the middle plane of plate corresponding to axes $X$ and $Y$. $p_x, p_y$ are the vector components of external loading corresponding to axes $X$ and $Y$ respectively. For isotropic material, the relation of stress and strain is written as,

$$\boldsymbol{\sigma} = \begin{bmatrix} \sigma_x \\ \sigma_y \\ \tau_{xy} \end{bmatrix} = \begin{bmatrix} \dfrac{E}{1-\upsilon^2} & \dfrac{\upsilon E}{1-\upsilon^2} & 0 \\ \dfrac{\upsilon E}{1-\upsilon^2} & \dfrac{E}{1-\upsilon^2} & 0 \\ 0 & 0 & \dfrac{E}{2(1+\upsilon)} \end{bmatrix} \begin{bmatrix} \varepsilon_x \\ \varepsilon_y \\ \gamma_{xy} \end{bmatrix} \tag{3.15}$$

or,
$$\boldsymbol{\sigma} = \mathbf{E}\boldsymbol{\varepsilon} \tag{3.16}$$

where, $E$ is the modulus of elasticity and $\upsilon$ is the Poison's ratio

$$\boldsymbol{\varepsilon} = \begin{bmatrix} \varepsilon_x \\ \varepsilon_y \\ \gamma_{xy} \end{bmatrix} = \begin{bmatrix} \dfrac{\partial}{\partial x} & 0 \\ 0 & \dfrac{\partial}{\partial y} \\ \dfrac{\partial}{\partial y} & \dfrac{\partial}{\partial x} \end{bmatrix} \begin{bmatrix} u \\ v \end{bmatrix} \tag{3.17}$$

or,
$$\boldsymbol{\varepsilon} = \mathbf{Dd} \tag{3.18}$$

In order to form the stiffness matrix, displacement approximation is required for finite element, which relates stiffness matrix with the degrees of freedom. In order to select an element type, its applicability in topology optimization is considered. The various filtering techniques developed for topology optimization are based on 4-node quadrilateral elements (Q4) (Sigmund and Petersson 1998; Blaise 2001, Bendsøe and Sigmund 2003; Svanberg and Svard 2013). Thus, it becomes the necessary to choose Q4 elements (Fig. 3.5) for FE analysis. Following form of polynomials are chosen to connect four nodes of Q4 element with necessary quantity of constant coefficients of the approximation functions.

$$u(X,Y) = a_1 + a_2 X + a_3 Y + a_4 XY \tag{3.19}$$

$$v(Y,Y) = a_5 + a_6 X + a_7 Y + a_8 XY \tag{3.20}$$

The nodal displacements and nodal reactions are given as,

$$\mathbf{d} = \begin{bmatrix} u_1 & v_1 & u_2 & v_2 & u_3 & v_3 & u_4 & v_4 \end{bmatrix}^T \tag{3.21}$$

$$\mathbf{R} = \begin{bmatrix} R_{x1} & R_{y1} & R_{x2} & R_{y2} & R_{x3} & R_{y3} & R_{x4} & R_{y4} \end{bmatrix}^T \tag{3.22}$$

The stiffness matrix **K** of dimension 8×8 connects these vectors as,

$$\mathbf{R} = \mathbf{Kd} \tag{3.23}$$
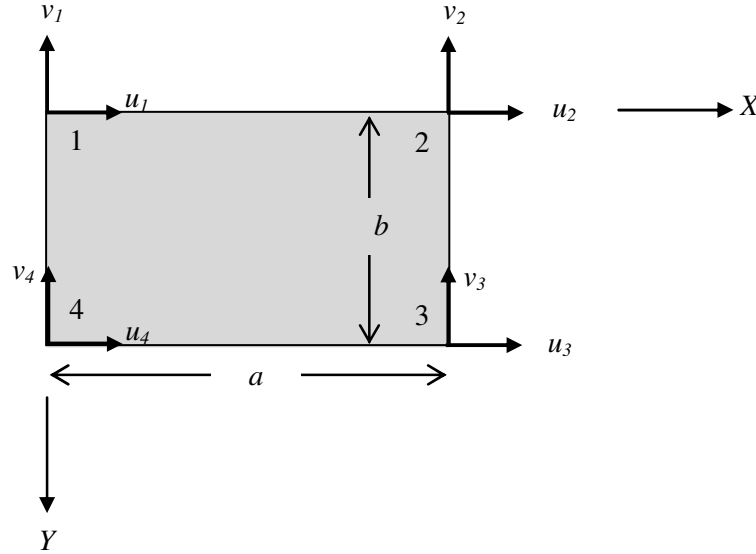


**Fig. 3.5: Quadrilateral finite element**

The approximation functions for four nodes is represented in a form of matrix using equations (3.19) & (3.20)

$$\begin{bmatrix} u_1 \\ u_2 \\ u_3 \\ u_4 \end{bmatrix} = \begin{bmatrix} 1 & x_1 & y_1 & x_1 y_1 \\ 1 & x_2 & y_2 & x_2 y_2 \\ 1 & x_3 & y_3 & x_3 y_3 \\ 1 & x_4 & y_4 & x_4 y_4 \end{bmatrix} \begin{bmatrix} a_1 \\ a_2 \\ a_3 \\ a_4 \end{bmatrix} \tag{3.24}$$

$$\begin{bmatrix} v_1 \\ v_2 \\ v_3 \\ v_4 \end{bmatrix} = \begin{bmatrix} 1 & x_1 & y_1 & x_1 y_1 \\ 1 & x_2 & y_2 & x_2 y_2 \\ 1 & x_3 & y_3 & x_3 y_3 \\ 1 & x_4 & y_4 & x_4 y_4 \end{bmatrix} \begin{bmatrix} a_5 \\ a_6 \\ a_7 \\ a_8 \end{bmatrix} \tag{3.25}$$

Equations (3.24) & (3.25) is represented as

$$\mathbf{d} = \mathbf{Ca} \tag{3.26}$$

The coefficients are computed as,

$$\mathbf{a} = \mathbf{C}^{-1}\mathbf{d} \tag{3.27}$$

For a Q4 element, approximation functions are given as,

$$u(x, y) = \sum_{i=1}^{4} d_i N_i \tag{3.28}$$

$$v(x, y) = \sum_{i=5}^{8} d_i N_i \tag{3.29}$$

where $d_i (i = 1, 2, ...8)$ are degrees of freedom of element, and $N_i (i = 1, 2, ...8)$ are nodal functions. The approximation function is expanded as,

$$u(x, y) = \frac{1}{ab}(a - x)(b - y)u_1 + \frac{1}{ab}x(b - y)u_2 + \frac{1}{ab}xyu_3 + \frac{1}{ab}(a - x)yu_4 \tag{3.30}$$

$$v(x, y) = \frac{1}{ab}(a - x)(b - y)v_1 + \frac{1}{ab}x(b - y)v_2 + \frac{1}{ab}xyv_3 + \frac{1}{ab}(a - x)yv_4 \tag{3.31}$$

Now, the stiffness matrix is computed based on following relation,

$$(k_{ij})_r = \int_{\Omega} \sigma_j \varepsilon_i d\Omega_r \tag{3.32}$$

where, $\sigma_j$ and $\varepsilon_i$ are stress and strain, respectively. The expression for stiffness is obtained using plane stress condition (equations (3.16) & (3.18))

$$k_{ij} = Th \int_0^a \int_0^b (\mathbf{E}\boldsymbol{\varepsilon}_i)^T \boldsymbol{\varepsilon}_j dx dy \tag{3.33}$$

where *Th* is thickness of the plate. The overall stiffness matrix takes following form,

$$\mathbf{K} = \begin{bmatrix} k_{11} & k_{12} & . & . & . & . & . & k_{18} \\ k_{21} & k_{22} & . & . & . & . & . & k_{28} \\ . & . & . & . & . & . & . & . \\ . & . & . & . & . & . & . & . \\ . & . & . & . & . & . & . & . \\ . & . & . & . & . & . & . & . \\ . & . & . & . & . & . & . & . \\ k_{81} & k_{82} & . & . & . & . & . & k_{88} \end{bmatrix} \tag{3.34}$$

Based on the relation given in equation (3.33) stiffness matrix is computed as,

$$\left(\frac{Eh}{1-v^2}\right)\times$$

$$\begin{bmatrix}
\left(\frac{m}{3}+\frac{1-v}{6m}\right) & \left(\frac{1+v}{8}\right) & \left(\frac{m}{3}-\frac{1-v}{12m}\right) & \left(-\frac{1}{8}+\frac{3v}{8}\right) & \left(-\frac{m}{6}-\frac{1-v}{12m}\right) & \left(-\frac{1+v}{8}\right) & \left(\frac{m}{6}-\frac{1-v}{8}\right) & \left(\frac{1}{8}-\frac{3v}{8}\right) \\
. & \left(\frac{1}{3m}+\frac{1-v}{6}m\right) & \left(\frac{1}{8}-\frac{3v}{8}\right) & \left(\frac{1}{6m}-\frac{1-v}{6}m\right) & \left(-\frac{1+v}{8}\right) & \left(-\frac{1}{6m}-\frac{1-v}{12}m\right) & \left(-\frac{1}{8}-\frac{3v}{8}\right) & \left(-\frac{1}{3m}+\frac{1-v}{12}m\right) \\
. & . & \left(\frac{m}{3}+\frac{1-v}{6m}\right) & \left(-\frac{1+v}{8}\right) & \left(\frac{m}{6}-\frac{1-v}{6m}\right) & \left(-\frac{1}{8}+\frac{3v}{8}\right) & \left(-\frac{m}{6}-\frac{1-v}{12m}\right) & \left(\frac{1+v}{8}\right) \\
. & . & . & \left(\frac{1}{3m}+\frac{1-v}{6}m\right) & \left(\frac{1}{8}-\frac{3v}{8}\right) & \left(-\frac{1}{3m}+\frac{1-v}{12}m\right) & \left(\frac{1+v}{8}\right) & \left(-\frac{1}{6m}-\frac{1-v}{12}m\right) \\
. & . & . & . & \left(\frac{m}{3}+\frac{1-v}{6m}\right) & \left(\frac{1+v}{8}\right) & \left(-\frac{m}{3}+\frac{1-v}{12m}\right) & \left(-\frac{1}{8}+\frac{3v}{8}\right) \\
. & . & . & . & . & \left(\frac{1}{3m}+\frac{1-v}{6}m\right) & \left(\frac{1}{8}-\frac{3v}{8}\right) & \left(\frac{1}{6m}-\frac{1-v}{6}m\right) \\
. & . & . & . & . & . & \left(\frac{m}{3}+\frac{1-v}{6m}\right) & \left(-\frac{1+v}{8}\right) \\
. & . & . & . & . & . & . & \left(-\frac{1}{3m}+\frac{1-v}{6}m\right)
\end{bmatrix}$$

$$(3.35)$$

where, $m=\dfrac{b}{a}$ (as shown in Fig. 3.5).

The obtained stiffness matrix is used in the equation (3.23). According to the problem domain, elemental equations are assembled and nodal deflections corresponding to the boundary condition can be computed. The nodal deflections are then utilized by OC method to compute objective function and constraints values iteratively. An algorithm is developed to generate optimal topology with performance values using OC and FE routine. The steps used for this algorithm are given below,

Step 1. The objective function and constraints for the problem are defined. Then, domain of material, desired volume fraction, force value, material properties i.e. Young's modulus and Poisson's ratio, mesh size of domain, and penalization power are chosen

Step 2. First iteration is started with initial guess of density parameter $x$

Step 3. Stiffness matrix of material domain based on density matrix is computed

Step 4. The deflection at each node is calculated by finite element formulation, incorporating random field of elasticity value to simulate material uncertainty

Step 5. Objective function is computed and sensitivity analysis is carried out based on density matrix. Then, deflection values of each node are computed

Step 6. Mesh independency and optimality criterion formulations are applied to update the density parameter values

Step 7. The convergence is checked for the result, based on change in density value before and after iteration

Step 8. If convergence is not achieved, steps 3-7 are repeated. If convergence is achieved, then iteration is terminated and the performance values are obtained

To simulate the results, experimental combinations are generated using DOE approach, which is explained in next section.

### 3.3.6 Simulation of performance values

A code is written in MATLAB that uses experimental combinations to simulate the performance values. This code is prepared using the optimization and FEM routine provided by Sigmund (2001) and Andreassen et al. (2011). To maintain the consistency in the results, the same code is utilized throughout the thesis for the generation of optimal topology and performance values. The penalization power is chosen as three. For detailed discussion on penalization-power work by Bendsøe and Sigmund is referred (Bendsøe 1995; Bendsøe and Sigmund 2003). Each combination of input factor is used to simulate the performance value, in the environment of loading and material uncertainties. Since the loading uncertainties (loading cases 1-6, Table 3.2) were not incorporated inside SIMP routine, each combination is repeated for specified loading conditions. Thus, for problems-1, 2, and 3, six different performance values are obtained, and for problem-4, three performance values are obtained for each combination. The simulated results are analyzed using statistical methods.

### 3.3.7 Analysis of simulated results

As mention earlier, for each combination of factors, there are set of performance values corresponding to the noise or uncertainty conditions. Analysis of these performance values are utilized to generate necessary information regarding the combination. These informations are, impact of each factor on the performance, mutual interactions of factors, significance of factors, and the most and least sensitive factors in terms of performance variation. Along with this information, an important analysis is performed which addresses robust and targeted performance for different combinations. In order to perform this analysis statistical techniques such as Analysis of Mean (ANOM), Analysis of Variance (ANOVA) are used (Mitra 2008; Montgomery 2007). Description of these techniques with analysis of simulated result is given in next section.

## 3.4    ANALYSIS AND DISCUSSION

In this section, optimal topologies of the benchmark problem are presented. Subsequently description of techniques such as ANOM, and ANOVA are presented with their applications. Analysis of robust and targeted performance and parametric sensitivity is described later.
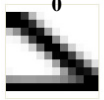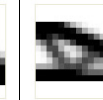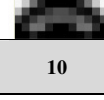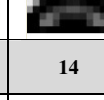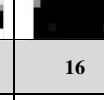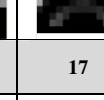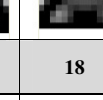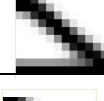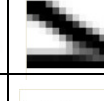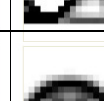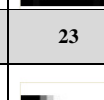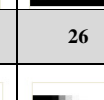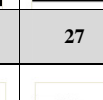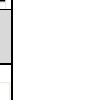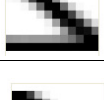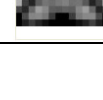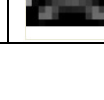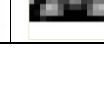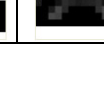
### 3.4.1   Optimal topologies of bench mark problems

In order to generate optimal topology, experimental combinations set with uncertainties are utilized in SIMP. The generated optimal topologies are shown in Table 3.4. These results are shown only for loading case 1 (Table 3.2) because total number of topologies generated for all loading cases are very large (i.e. 567). From this table, differences in topologies for various combinations of input factors are easily observed. There are variations in optimal topologies because of the factor values and material uncertainties. It has been observed that aspect ratio and volume fraction are the factors, which change the topology. Effect of force on optimal topology is minimum compared to these factors. In present work, compliance and deflection values are comprehensibly analyzed keeping optimal topologies in mind. Reason being, optimal topology is nothing but function of density parameters, and same density parameter is utilized to compute compliance and deflection. The changes in compliance and deflection values indicate either marginal change in shape/size of the topology or change in the topology.

### 3.4.2   Analysis of mean

The analysis of obtained results is carried out using analysis of mean (ANOM). ANOM is a statistical technique to analyze interaction among the factors, their significance, and sensitivity on the performance values (Mitra 2008; Montgomery 2007). In present case, ANOM is performed for three factors with three levels of each. In this section ANOM of compliance and deflection are presented for all problems. The simulated compliance values are used to compute mean for each combinations. Thus, 27 such mean compliance values are generated for a single problem. These mean compliance values for four benchmark problems are summarized in Appendix A2-A3. Now, these mean compliance values are consolidated further to identify the effect of each factor level on compliance. Since, three input factors are considered in this work, so three curves are plotted for each problem, as shown in Fig. 3.6. Considering problem-1, the combined effect of variation of factors is shown in Fig. 3.6(a).

**Table 3.4: Optimal topologies for loading case 1 for different combination of factor**

| Combination→ | 1 | 2 | 3 | 4 | 5 | 6 | 7 | 8 | 9 |
|---|---|---|---|---|---|---|---|---|---|
| Problem-1 | | | | | | | | | |
| Problem-2 | | | | | | | | | |
| Problem-3 | | | | | | | | | |
| Problem-4 | | | | | | | | | |
| Combination→ | 10 | 11 | 12 | 13 | 14 | 15 | 16 | 17 | 18 |
| Problem-1 | | | | | | | | | |
| Problem-2 | | | | | | | | | |
| Problem-3 | | | | | | | | | |
| Problem-4 | | | | | | | | | |
| Combination→ | 19 | 20 | 21 | 22 | 23 | 24 | 25 | 26 | 27 |
| Problem-1 | | | | | | | | | |
| Problem-2 | | | | | | | | | |
| Problem-3 | | | | | | | | | |
| Problem-4 | | | | | | | | | |

It is observed that all three factors have strong interaction with each other. Meaning that effect of a factor on compliance is linked with other factors. And the change of all factors affect the compliance value. As the material domain understudy is rectangular, obtained results validate obvious relationship of length to width ratio on compliance value. Figs. 3.6(b) & (c) show factor effect in the case of problem-2 and problem-3, respectively.

The behavior is almost same in both cases. However, compliance value in Fig. 3.6(c) is high because of the hole in plate. Three factors are have good interaction with each other, and almost equally influential. In Fig. 3.6(d), effect of factors can be observed for problem-4. Compliance value in this case is lesser than all other problems. This difference in compliance value is supported by theory of beams also. For problem-4, all the factors have similar behavior compare to other cases. The behavior of three factors is similar to other cases. In all these observations impact of factors are more or less same because of similar physics of problems.
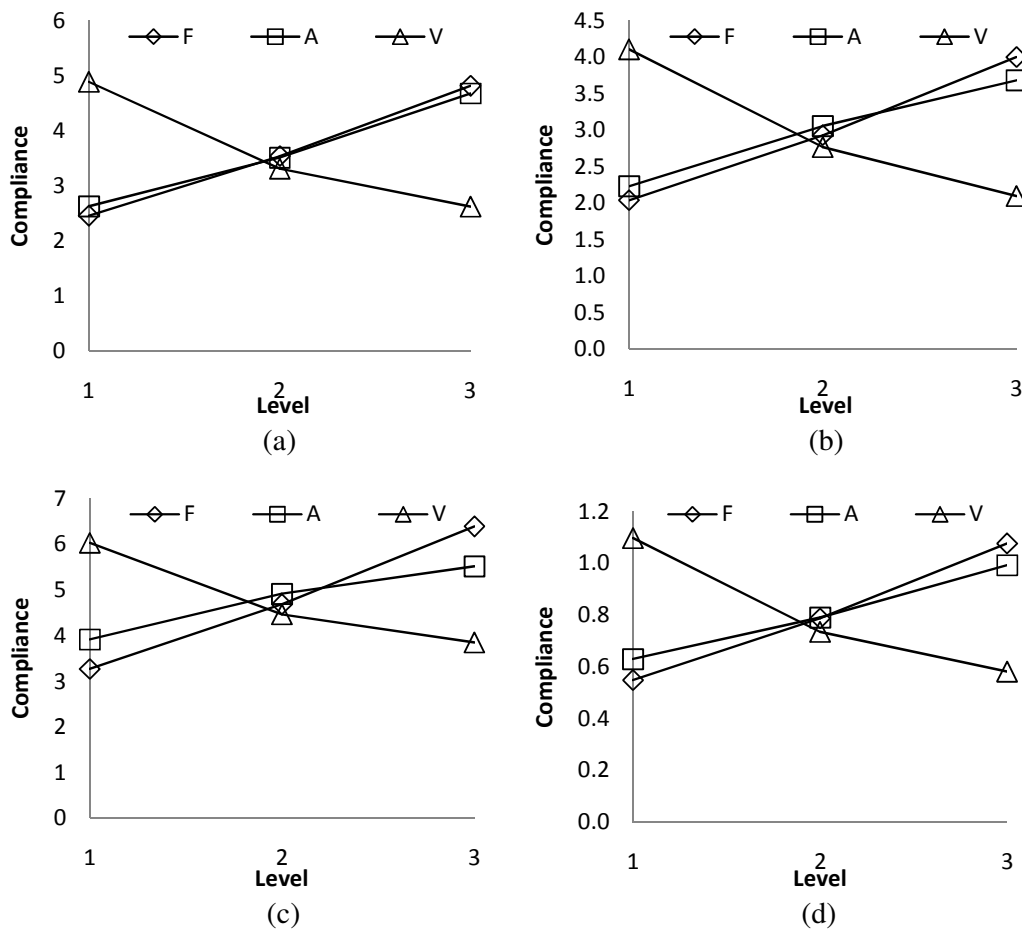


**Fig. 3.6: Effect of input factors on the compliance value for (a) problem-1, (b) problem-2, (c) problem-3, (d) problem-4**

Similar to compliance, another performance value i.e. maximum deflection of each problem is also simulated using SIMP method. ANOM is performed for mean deflection and results are presented in Fig. 3.7. It can be observed from Fig. 3.7 that all the factors have good interactions. Volume fraction is found to be influential factor and force appears to be least influential. Also, volume fraction shows highest nonlinearity, while aspect ratio shows a linear behavior. The results shown in Figs. 3.6 & 3.7 can be utilized to generate topology for a required value of compliance. For example, to design a MBB-beam with a low compliance value, force should be at 'level 1'; volume fraction should be at 'level 3' and aspect ratio should be at 'level 1'.



(a)

(b)

(c)

(d)
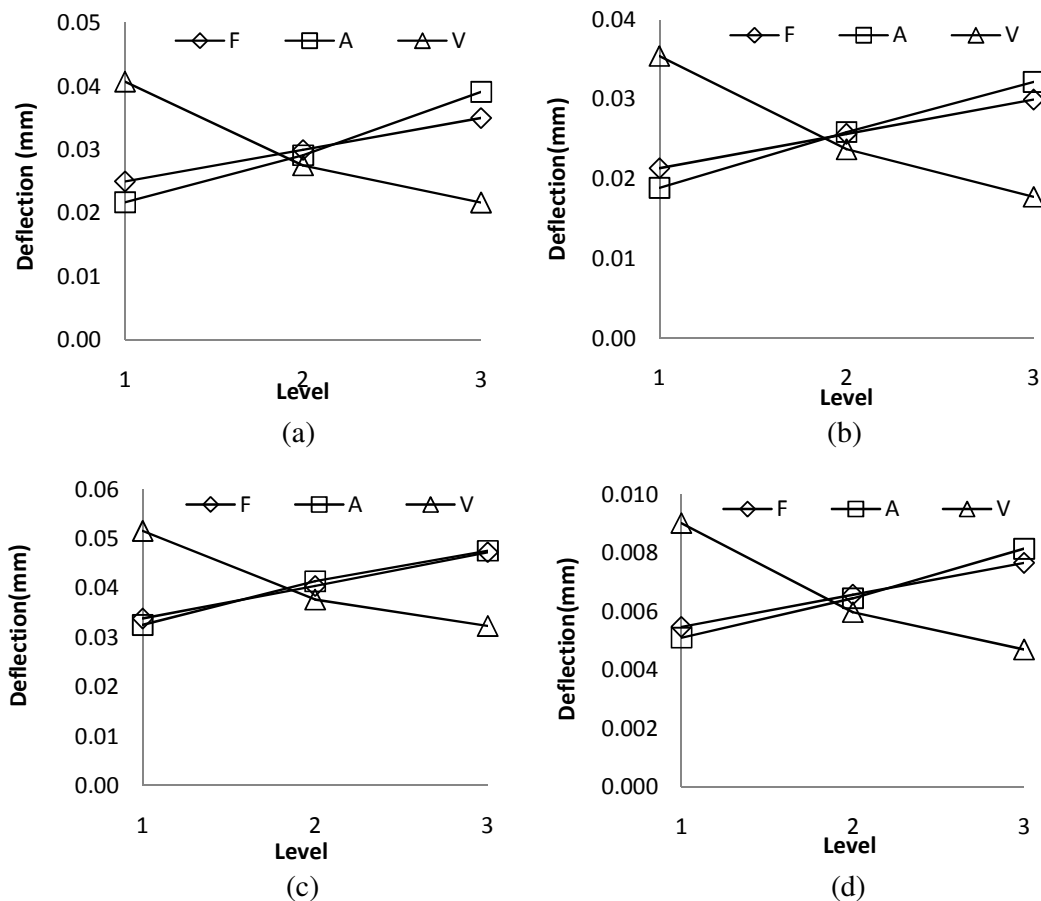
**Fig. 3.7: Effect of input factors on the deflection values for (a) problem-1, (b) problem-2, (c) problem-3, (d) problem-4**

### 3.4.3   Signal to noise ratio

In order to capture the variations in performance value for different combinations, a statistical measure SNR proposed by Taguchi, is employed (Sung 1998; Mitra 2008; Montgomery 2007). The variation in performance value is representation of degree of

robustness of design. Hence, based on SNR, robustness of each combination can be obtained. In present case, signal refers to performance value i.e. compliance and deflection and noise refers to its variation about mean performance values. For chosen structural problems, both performance values should be minimum. Hence, SNR with "smaller the better" criterion is chosen, and accordingly its computation is carried out. Mathematically, SNR is a negative log of mean of squared deviation, as shown in equation (3.36),

$$SNR_C = -10\log_{10}\frac{1}{n}\sum_{i=1}^{n}p_i^2 \tag{3.36}$$

where, $p_i$ is the performance value for each simulation. In present case, performance value is computed corresponding to each loading condition. Hence, for problem-1, 2 & 3, $i$ =1 to 6, and for problem-4, $i$ =1 to 3 is used in equation (3.36). In this way, using equation (3.36), SNR is computed for each combination. The computed SNR for each problem are specified in Appendix A2 & A3, for compliance and deflection respectively. It is observed that 7th combination has the highest SNR value. It indicates that combination 7 is robust compared to others. Also, standard deviation is observed to be lowest for the same combination in all considered problems. The lowest SNR is observed for 21st combination. Hence, this factor combination produces the poor design, which implies a high variation compared to other combinations. Similarly, all the combinations can be compared for their robustness of design. Thus, SNR analysis can be utilized to select combinations based on required robustness of design.

### 3.4.4   Analysis of variance

To investigate the impact of change of factor levels on simulated performance values, analysis of variance (ANOVA) technique is used. ANOVA is a statistical technique to analyze variation of different group of input factors. Thus, ANOVA helps in identifying statistical significance of factors. The procedural details are available in Mitra (2008) and Montgomery (2007). In present case, ANOVA is performed using Design Expert software (2011) at 5% level of significance. The symbols A, B, and C are used in ANOVA to denote aspect ratio, volume fraction and force respectively. Results of ANOVA are summarized in Tables 3.5 and 3.6 for compliance and deflection respectively.

**Table 3.5: Statistically significant factors from ANOVA, for compliance**

| Bench Mark Problems | Statistically Significant Input factors |
|---|---|
| Problem-1 | A, B, C, AB, AC, BC |
| Problem-2 | A, B, C |
| Problem-3 | A, B, C, AB |
| Problem-4 | A, B, C |

**Table 3.6: Statistically significant factors from ANOVA, for deflection**

| Bench Mark Problems | Statistically Significant Input factors |
|---|---|
| Problem-1 | A, B, C, AB, AC, BC |
| Problem-2 | A, B, C, AB |
| Problem-3 | A, B, C, AB |
| Problem-4 | A, B, C, AB, AC, BC |

Apart from above analysis, half-normal plots (HNP) are also used for these problems. HNP, as a part of ANOVA have been provided here to highlight the influence of change in level values of input factors on simulated results (Montgomery 2007). In this method, responses that are negligible are normally distributed with zero mean and variance, and these tend to fall along a straight line for this plot. Whereas statistically significant effects will have nonzero means and will not lie along the straight line. Thus, the preliminary model will be specified to contain those effects that are apparently nonzero means, based on normal probability plot. To plot HNP, help of Design Expert (2011) software has been taken. Figs. 3.8 & 3.9 show HNP for compliance and deflection respectively. These results are similar to the result available in Tables 3.5 & 3.6.

While performing ANOVA, a regressive relation among factors and performance value is also derived. This relation may be linear or nonlinear based on number of levels selected for factors. The linear and nonlinear relations are presented in equations (3.37) and (3.38) respectively.

$$Re = \hat{\beta}_0 + \hat{\beta}_1 fc_1 + \cdots + \hat{\beta}_k fc_k + \varepsilon r \tag{3.37}$$

$$Re = \hat{\beta}_0 + \sum_{i=1}^{N} \hat{\beta}_i fc_i + \sum_{i=1}^{N} \hat{\beta}_{ii} fc_i^2 + \sum_{i<j}^{N} \hat{\beta}_{ij} fc_i fc_j + \varepsilon r \tag{3.38}$$

where, $Re$ is response or performance value, $fc$'s are the selected factor. $\hat{\beta}$'s are the numerical constants, and $\square r$ is error. The functional relationships for all the problems are presented in Tables 3.7 and 3.8 for compliance and deflection respectively.
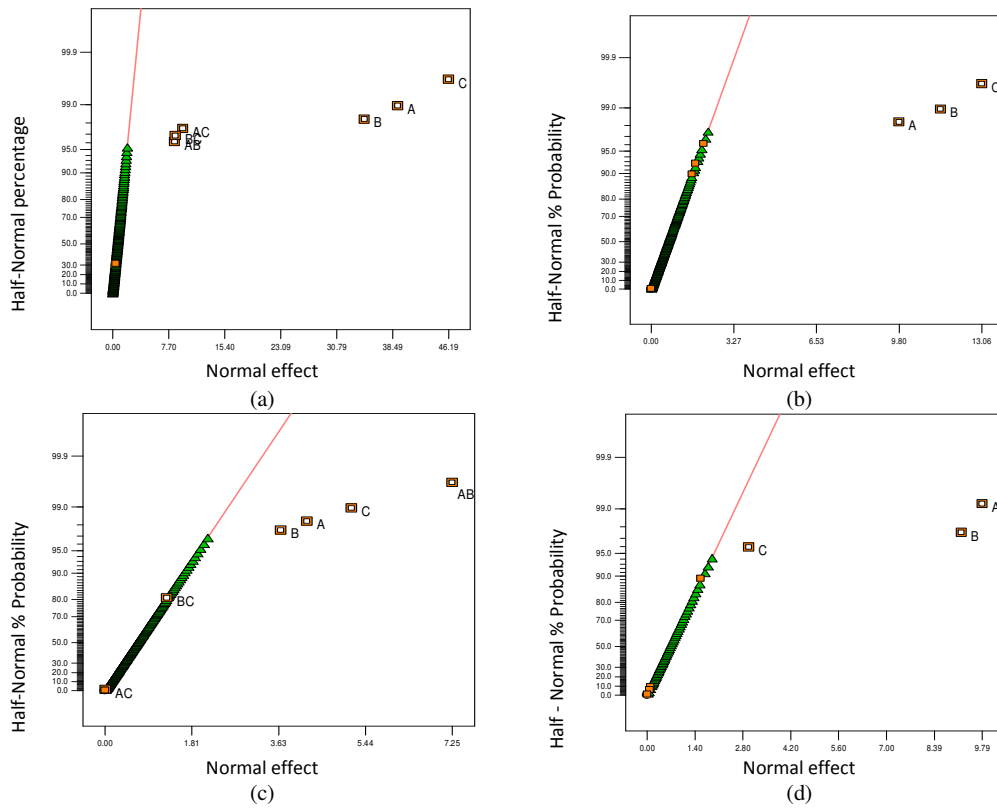
**Fig. 3.8: Half -Normal plot for (a) problem-1, (b) problem-2, (c) problem-3, (d) problem-4, considering compliance values**
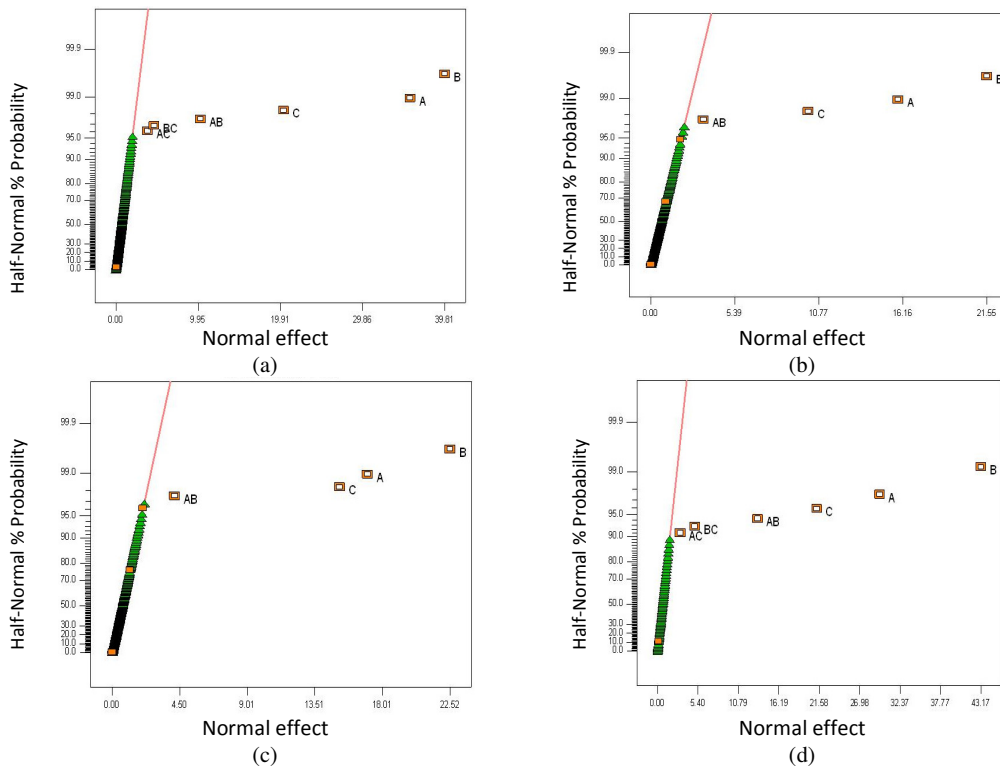


**Fig. 3.9: Half -Normal plot for (a) problem-1, (b) problem-2, (c) problem-3, (d) problem-4, considering deflection values**

**Table 3.7: Functional relationship between compliance values and the input factors**

| Benchmark Problems | Functional relationship in coded values* |
|---|---|
| Problem-1 | Compliance = 3.214934 -0.87828 × A -0.02643 ×$A^2$ + 0.850433 × B - 0.14788 × $B^2$ -1.01993 × C - 0.05881 × $C^2$ - 0.28209 × AB - 0.00467 × $A^2$B + 0.070908 × $AB^2$ + 0.006984 × $A^2B^2$ + 0.274867 × AC + 0.006549 × $A^2$C + 0.016647 × $AC^2$ - 0.0031 × $A^2C^2$ - 0.27009 × BC + 0.045336 × $B^2$C - 0.0168 × $BC^2$ + 0.005115 × $B^2C^2$ |
| Problem-2 | Compliance = 2.70664-0.69583 × A + 0.049082 × $A^2$ + 0.844208 × B - 0.14823 × $B^2$ - 0.86214 × C - 0.05074 × $C^2$ |
| Problem-3 | Compliance = 3.886914 + 0.482457 × A + 0.141772 × $A^2$ - 0.53836 × B + 0.082959 × $B^2$ + 0.761738 × C - 0.22716 × $C^2$ - 0.7823 × AB + 0.151402 × $A^2$B + 1.537121 × $AB^2$ - 0.36245 × $A^2B^2$ + 0.022964 × AC + 0.059304 × $A^2$C - 0.03548 × $AC^2$ + 0.019475 × $A^2C^2$ - 0.35736 × BC - 0.08214 × $B^2$C + 0.077162 × $BC^2$ + 0.011577× $B^2C^2$ |
| Problem-4 | Compliance =0.80723+0.3123 × A - 0.08274 × $A^2$ - 0.25596 × B - 0.01466 × $B^2$ + 0.006663 × C - 0.09836 × $C^2$ |
| *The coded values are: A=[-1, 0, +1], B=[-1, 0, +1] and C=[-1, 0, +1] where -1, 0, +1 refers to the level values 1, 2 and 3 respectively of Table 1. | |

**Table 3.8 Functional relationship between deflection values and the input factors**

| Benchmark Problems | Functional relationship in coded values* |
|---|---|
| Problem-1 | Deflection=0.03-0.008287 × A-0.000848 × $A^2$+0.010762 × B-0.002457 × $B^2$-0.005007 × C-0.003155 × AB-0.000661×$A^2$B +0.000637 × $AB^2$+0.001375 × AC+0.000137 × $A^2$C-0.001790 × BC+0.000418 × $B^2$C |
| Problem-2 | Deflection=0.025651 -0.006762 × A +0.000245 × $A^2$+0.009785 × B - 0.001919 × $B^2$-0.004279 × C -0.002469 × A B +0.000156 × $A^2$B +0.000447 × A $B^2$ |
| Problem-3 | Deflection=0.040492 -0.007938 × A +0.000883 × $A^2$+0.011037 × B - 0.002831 × $B^2$-0.006681 × C -0.003501 × A +0.001392 × $A^2$B +0.000922 × A $B^2$-0.000416 × $A^2B^2$ |
| Problem-4 | Deflection=0.006567 -0.001460 × A -0.000116 × $A^2$+0.002450 × B - 0.000586 × $B^2$-0.001097 × C -0.000935 × A B +0.000234 × A $B^2$+0.000234 × A C -0.000398 × B C |
| *The coded values are: A=[-1, 0, +1], B=[-1, 0, +1] and C=[-1, 0, +1] where -1, 0, +1 refers to the level values 1, 2 and 3 respectively of Table 1. | |

### 3.4.5 Targeted performance values

One of the important outcomes of presented work is to select the input factor combination based on the targeted compliance and deflection value. This investigation opens up a very interesting option for designer at conceptual design phase. The targeted performances are mean performance values corresponding to each combination. The

values of mean compliance and deflection are given in Figs. 3.10 & 3.11 respectively, for all the problems.
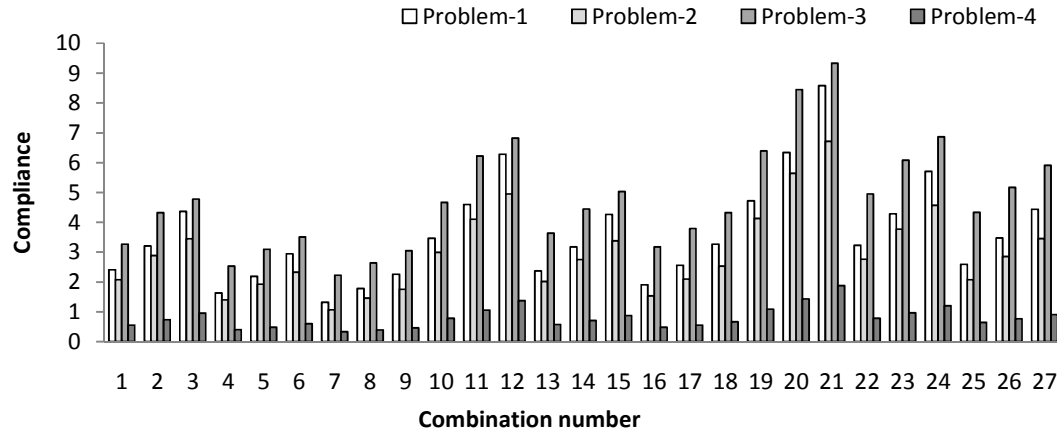


**Fig. 3.10: Comparison of mean compliance against combination numbers**
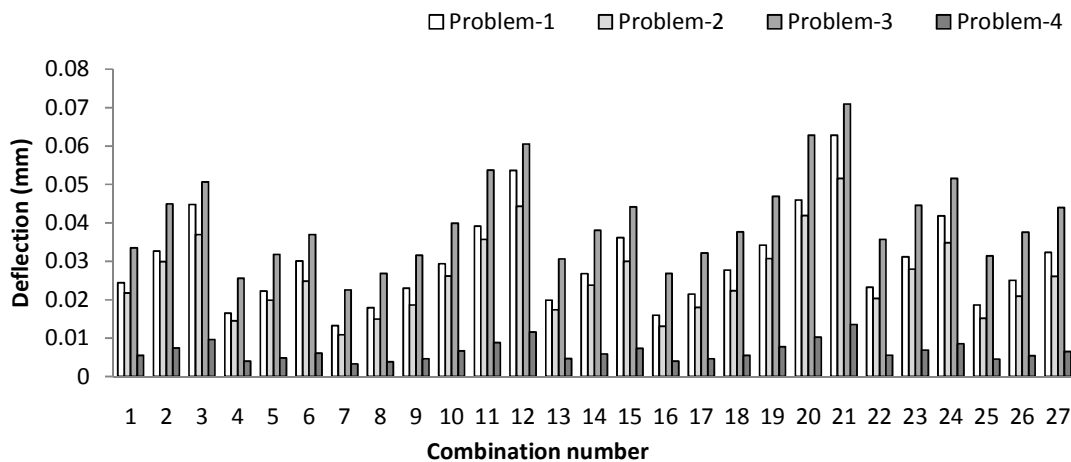


**Fig. 3.11: Comparison of mean deflection against combination numbers**

These figures show mean performance value against the combination number. It is observed that for each problem, many values of compliance and deflection are close to each other. From these values, alternative factor combination can be chosen for a targeted performance. Thus, this activity provides flexibility to the designer for selection of favorable combinations.

### 3.4.6 Parametric sensitivity

To investigate further, performance values are simulated by incrementing input factors individually. While doing so, other factors are held constant. For this purpose, another code is written in MATLAB. The range of applied force is selected from 90 N to 150 N having increment of 5 N. Volume fraction ranges from 0.1 to 0.8 having increment of

0.1. Similarly, range of aspect ratio is selected from 1.0 to 2.0 having increment of 0.2. During simulation, value of a factor is incremented whereas the other two factors are kept constant at level 2 (Table 3.3). At the same time, effect of force and material uncertainties are not used in simulation. The simulated results are presented in Figs. 3.12 & 3.13, for compliance and deflection respectively.



(a)

(b)

(c)
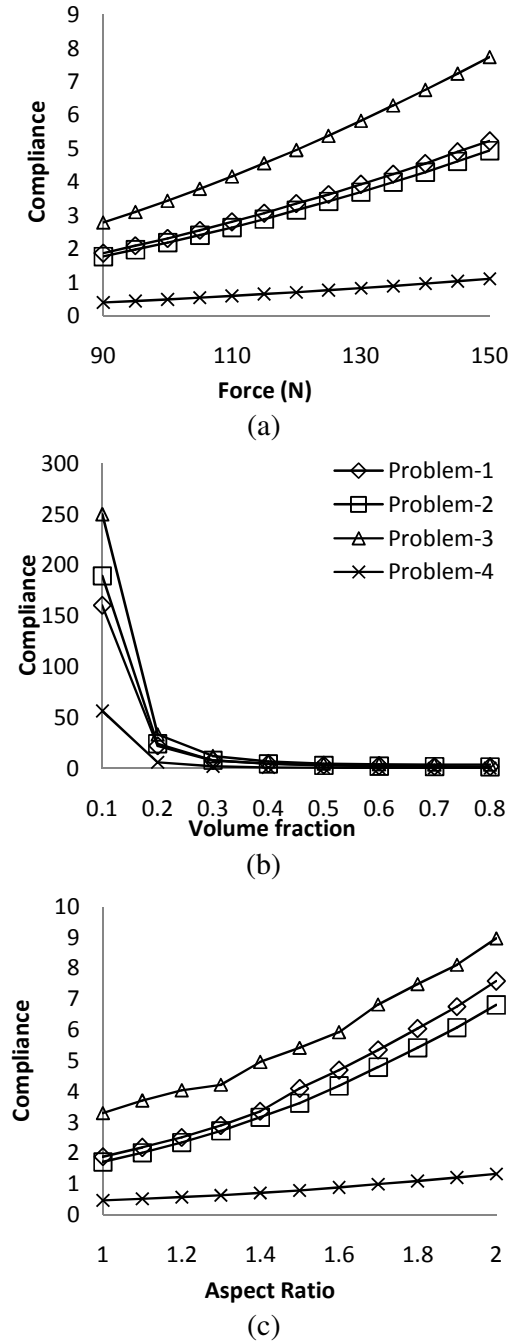
**Fig. 3.12: Variation of compliance for four problems, (a) force, (b) volume fraction and, (c) aspect ratio**

From Fig. 3.12, it is observed that factors are having non-linear relationship with compliance value. Force vs compliance variation (Fig. 3.12(a)) is nonlinear and has an increasing trend. Compliance value is highest for problem-3 and lowest for problem-4, as expected. Effect of volume fraction is observed in Fig. 3.12(b).



(a)

(b)

(c)
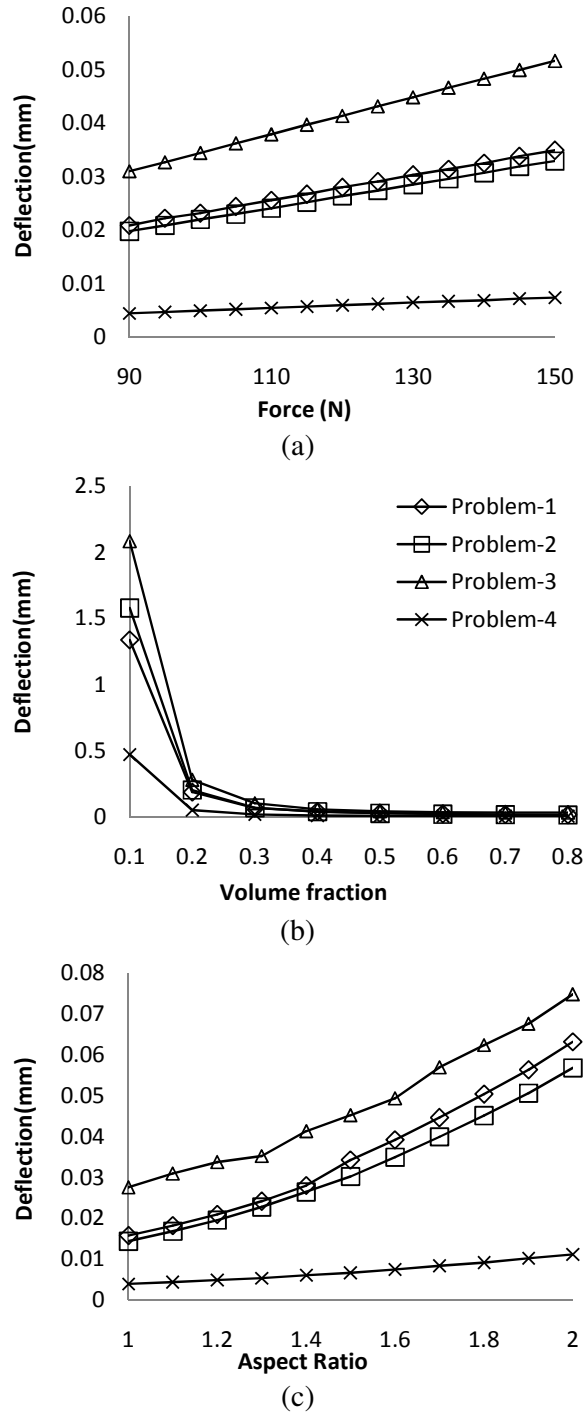
**Fig. 3.13: Variation of deflection for four problems, (a) force, (b) volume fraction and, (c) aspect ratio**

The curve is very steep for initial values (0.1-0.3). However, small volume fractions values are not usually selected for structural problems. The high value of compliance is obtained for problem-3 and small value for problem-4. Fig. 3.12(c) shows effect of aspect ratio variation on compliance. The observations are similar to that of previous factors.

From Fig. 3.13, it is observed that applied force has linear relation, whereas volume fraction and aspect ratio have non-linear relation with deflection value. These variations are supported by theory of deflection of beams. The relationship of factor with compliance and deflection are found to be similar

The analysis presented here using individual factor helps to emphasize the significance of DOE based analysis, performed in earlier sections. The various inferences regarding factor vs performance were obtained using DOE approach. These inferences would be very difficult to derive from the individual factor analysis. Reason being, DOE method facilitates a systematic incorporation of factor levels including uncertainties/noise. Thus, it enables various statistical techniques to analyze obtained results efficiently.

## 3.5    CONCLUSIONS

This chapter focuses on the behavior of performance value of topologically optimized structure with respect to selected factors. Current analysis helps in identifying the optimum values of these factors subject to robust and targeted performance. To achieve these objectives, a methodology based on DOE approach is proposed. For this purpose, applied force, volume fraction, and aspect ratio of material domain were the selected factors. This methodology was applied to four benchmark problems and optimum factor values were obtained, which will be utilized further for different investigations. For problem-1, 2, and 3, the most and least significant factors are force and aspect ratio, respectively when compliance is the performance measure. For same performance measure, aspect ratio and force are the most and least significant factor in problem-4. For all the problems, the most and least significant factors are volume fraction and force, respectively, when deflection is the performance measure. From the analysis of SNR and targeted performance values, it is found that 7th combination has highest SNR, with minimum compliance and deflection values. Whereas, 21st combination has smaller SNR with highest compliance and deflection values. It can also be observed that the combination having low performance values show high SNR. To differentiate between deterministic and realistic scenario, individual factor analysis was also presented in this chapter. The proposed methodology of

performance analysis is one-step ahead of simple deterministic method, because of the consideration of noises. These noises are embodiment of realistic scenario of material uncertainty and loading conditions, which were modeled based on worst-case scenario. The presented analysis of performance can be made more comprehensive by including the uncertainty of the design/controllable factors.

# CHAPTER 4

# ANALYSIS OF PERFORMANCE FOR RELIABLE AND OPTIMAL TOPOLOGIES OF STRUCTURES

## 4.1    INTRODUCTION

The practical design and applications of structures require specialized and accurate approaches to evaluate the effect of uncertainties in applied force, material property, geometry, manufacturing processes, and operating conditions. In such scenario, the reliability-based methods are applied to improve the safety and performances of the structures. As discussed in sections 2.1 and 2.3, the RBTO methods developed so far are not generalized for different factors and uncertainties, which can evaluate impact of uncertainties on the performance behavior. Present chapter proposes a generic methodology that explores the impact of uncertainties of the factors and focuses on the issue of analysis of the performance considering reliability aspect.

Analysis of performance of topologically optimized structures, in a realistic environment was already attempted in Chapter 3. In that chapter, applied force, volume fraction, and aspect ratio were considered as controllable factors. The effect of noises/uncertainties was considered in terms of elasticity values, and angle and point of applied force. However, uncertainties of controllable factors were not considered earlier. This investigation helped in analyzing impact of each factor in the environment where each factor level varies. The analysis carried out by this approach was more realistic compared to "one factor at a time" case. In addition, the optimal value of factors for targeted and robust performance was also obtained. Hence, looking at the usefulness of proposed methodology in previous chapter, it is desired to include the uncertainties of controllable factors, to make analysis more realistic and robust.

In the present chapter, same controllable factors are used to analyze further. There are many methods available to incorporate effect of uncertainties of controllable factors, such as Monte-Carlo, RBTO, or DOE based method. Monte-Carlo method is computationally expensive, more specifically in the topology optimization problems (Javed et al. 2011). Hence, this method is avoided. The alternate choice is to use a suitable RBTO method, which offers lesser computations, or to use DOE approach that can include both types of uncertainties. The background of RBTO and its various aspects of applications are reviewed in Chapter 2. RBTO is evolved from a broad field of Reliability Based Design Optimization (RBDO) (Tu and Choi 1999). The main idea of RBDO is to combine design optimization with probabilistic constraints. RBTO schemes easily accommodate uncertainties of controllable factors and generate performance values subject to a desired reliability. Looking at an additional consideration of reliability aspect, RBTO method is chosen here. However, RBTO is inefficient in considering uncertainties of point and angle of applied force and elasticity. Also, with RBTO, it is difficult to conduct analysis of performance of structural component at each point of a desired design space. To overcome these problems, DOE approach is combined with RBTO. Hence, present work proposes a methodology that combines advantages of DOE and RBTO. Here, DOE is utilized to include uncertainty of point and angle of applied force and elasticity and RBTO is utilized to include effect of uncertainties of controllable factors. The performance values are simulated based on this methodology and analyzed using statistical techniques such as ANOM and ANOVA. In order to emphasize effects of uncertainties, the results from this analysis are compared with deterministic results.

## 4.2    METHODOLOGY

As discussed earlier, current work explores impact of both types of noise/uncertainties on topologically optimized structures. The process diagram of the proposed method is shown in Fig. 4.1. In this figure, the input to the simulation process is factor levels, and noises, simulation is performed using RBTO. The output from this simulation process is reliable optimal topology with performance values. The steps of the proposed methodology are given as,
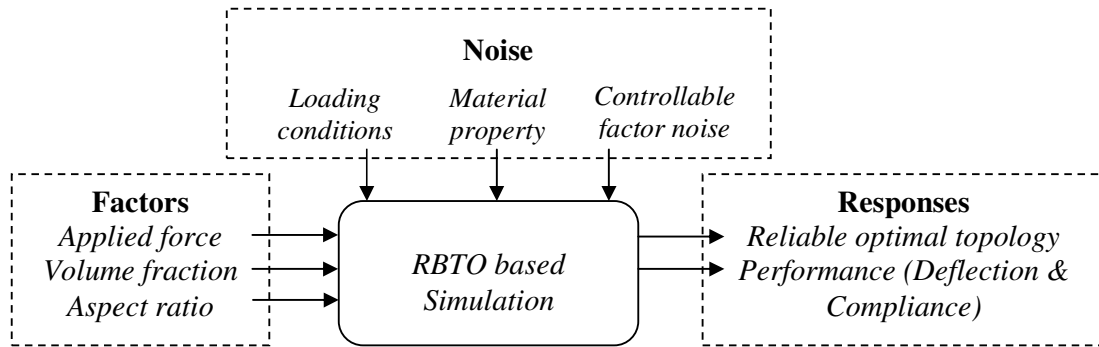
**Fig. 4.1: Process diagram of the proposed methodology**

Step 1.    Selection of the problem and performance measures

Step 2.    Selection of factors and their level values

Step 3.    Identification of noise or uncertainties

Step 4.    Generation of experimental combination set

Step 5.    Simulation of performance values using RBTO

Step 6.    Analysis of results

Above steps are used to simulate the performance and reliable optimal topology of structure. The implementation of these step are described in the next section.

## 4.3    IMPLEMENTATION OF PROPOSED METHODOLOGY

In the present work, following steps are employed to analyze the performance of reliable optimal topology of components.

Step 1.    **Selection of the problem and performance measures:** For illustration, four benchmark problems are chosen as described in section 3.3.1.1. The performance measures are selected as compliance and deflection values, described in section 3.3.1.2.

Step 2.    **Selection of the factors and their level values:** The factors selected for analysis are, applied force, volume fraction, and aspect ratio. Their level values are available in Table 3.3 and the detailed discussion on this selection is available in section 3.3.2.

Step 3.    **Identification of noise or uncertainties:** Effect of noise is incorporated by loading conditions and material uncertainties as described in sections 3.3.3.1

and 3.3.3.2. The noise of controllable factors i.e. applied force, volume fraction, and aspect ratio, are incorporated using their nominal and standard deviation (SD) values. Their nominal values are equal to their level values. The SD's of factors are selected in terms of variation around nominal values. These variations are assumed as Gaussian distribution (Maute and Frangopol 2003; Kang et al. 2004; Jung and Cho 2004; Khramanda et al. 2004). From Fig. 4.2 the nominal values ($\mu$) can be observed with the spread (S) of Gaussian distribution. The spread for each factors are assumed as 10%, 20%, and 30% of their nominal values (Maute and Frangopol 2003; Jung and Cho 2004; Khramanda et al. 2004). Hence, the SD's are computed for each factor based on chosen spread.
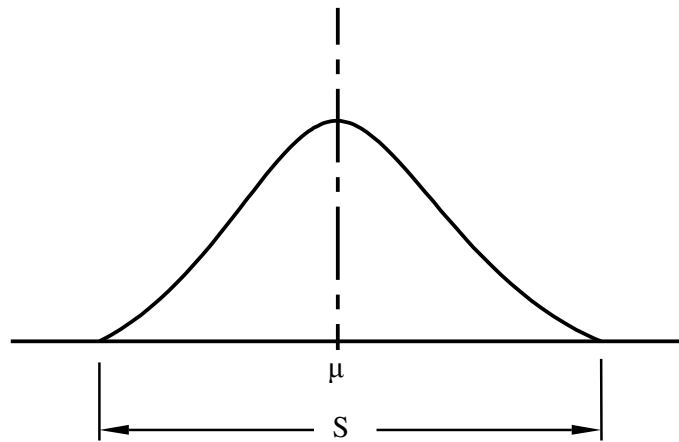


**Fig. 4.2: Nominal and spread values of a factor**

Step 4. **Generation of experimental combination set:** Based on number of factors and their levels, experimental combination set is designed. As described in section 3.3.4, total 27 combinations are generated for this experiment. The design combinations are available in Appendix A1. To incorporate the effect of noise, corresponding to each loading condition the experiment is replicated.

Step 5. **Simulation of performance values:** For each replication and problem, reliable optimal topologies with performances are simulated. This simulation is carried out using a selected RBTO scheme. Many methods for RBTO are available, as discussed in section 2.1. A RBTO method proposed by Kharnmada and Olhoff (2002) is selected (Kharmanda and Olhoff 2002; Kharmanda et al. 2004)

because of ease of implementation and lower computational cost. The steps for the selected RBTO method is given as,

1.  Define the problem

2.  Select the nominal values of controllable factor. The uncertainties of these factors are given in terms of spread (S) values

3.  Select a required reliability index ($\beta$) value

4.  Use HL-transformation to map the variables from physical to the standard Gaussian domain as explained in section 2.1 and equation (2.3)

5.  Compute the Gaussian variable, $\mathbf{U_g}$ for a required reliability index value as,

$$\begin{aligned} \text{min}: \quad & \beta = (\mathbf{U_g}^T \mathbf{U_g})^{1/2} \\ \text{subject to}: \quad & G(\mathbf{U_g}) = 0 \\ & \beta \geq \beta^* \end{aligned} \tag{4.1}$$

6.  Using the normalized variable $\mathbf{U_g}$, compute physical variables $\xi$, by the help of equation (2.3). These physical variables are the *reliable-controllable factor* values subject to chosen reliability index ($\beta$).

7.  Use the revised-controllable factor values to generate the optimal topology and performance values. For this simulation, the steps of SIMP method, available in section 3.3.5, are utilized.

The above steps are implemented in MATLAB, where "Trust-region-dogleg" algorithm (Matlab Optimization toolbox 2013) is used to compute the normalized parameters based on a given reliability index value, shown in equation (4.1). The usual SIMP routine is also modified to incorporate,

- Fractional changes in aspect ratio by the non-square finite elements

- Selection of loading conditions, based on different cases

- Randomization of elasticity value for each finite element cell

- Computation for the maximum deflection and compliance

The developed code is called in the main DOE routine, where the combination and the replications for different loading conditions are used with the reliability scheme. The computation process of this simulation is presented in Fig. 4.3. DOE approach is used to create experimental combinations. The generated set of combinations use spread (S) of controllable factor and reliability index value ($\beta$), to apply RBTO. Optimal topology and performances are simulated incorporating loading, material, and uncertainties of

controllable factors. These performances are analyzed using DOE and statistical techniques.

It is important to note that the selected RBTO method provide the reliable optimal topology and performances without increasing the volume fraction value. The RBTO applied here, mainly search the MPP of the performance with respect to the chosen reliability index and spread. Then the actual values of the factors are found out at that MPP. Therefore, the volume fraction value actually decreases in proportion to the reliability index and spread to simulate a realistic scenario of uncertainties because volume fraction is considered as one of the input controllable factor. As a result, the obtained reliable performances, i.e. compliance and deflection increase compared to deterministic case. This discussion can be summarized by stating that, the present RBTO scheme increases the reliability of the design by sacrificing a little bit of performance. It is advantageous from the designer's point of view, as the value of input factor remains same for this analysis.
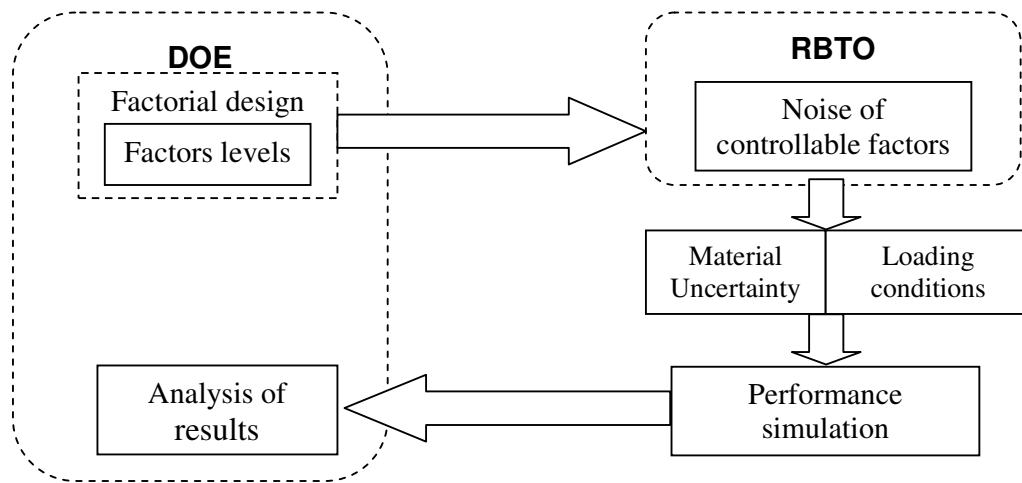


**Fig. 4.3: Framework for integrated DOE and RBTO approach**

The presented methodology gives the reliable optimal topology with performance values based on the selected reliability index and spread values of factors. Hence, in the interest of the designer it becomes vital to observe the effect of these two parameters on the outcome. To do so, reliability index and spread values are considered in distinct level values. Using the level values, an experimental combination set is generated for their combinations. The whole procedure of topology and performance simulation is illustrated in Fig. 4.4.

| Combination No. | 1 | 2 | … | 27 |
|---|---|---|---|---|
| Aspect Ratio | 1.2 | 1.4 | … | 1.6 |
| Volume fraction | 0.4 | 0.4 | … | 0.6 |
| AppliedForce | 100 | 100 | … | 140 |

| Combination No. | β | S(%) | RBTO | Loading cases | | | | | | Mean $P_{M(\beta/S)}$ | SNR $P_{S(\beta/S)}$ |
|---|---|---|---|---|---|---|---|---|---|---|---|
| | | | | 1 | 2 | 3 | 4 | 5 | 6 | | |
| 1 | 2 | 10 | | $P_{1(2/10)}$ | $P_{2(2/10)}$ | $P_{3(2/10)}$ | $P_{4(2/10)}$ | $P_{5(2/10)}$ | $P_{6(2/10)}$ | $P_{M\,(2/10)}$ | $P_{S\,(2/10)}$ |
| 2 | 2 | 20 | | $P_{1(2/20)}$ | $P_{2(2/20)}$ | $P_{3(2/20)}$ | $P_{4(2/20)}$ | $P5_{(2/20)}$ | $P_{6(2/20)}$ | $P_{M(2/20)}$ | $P_{S\,(2/20)}$ |
| 3 | 2 | 30 | | … | … | … | … | … | … | … | … |
| 4 | 2.5 | 10 | | … | … | … | … | … | … | … | … |
| 5 | 2.5 | 20 | RBTO | … | … | … | … | … | … | … | … |
| 6 | 2.5 | 30 | | … | … | … | … | … | … | … | … |
| 7 | 3 | 10 | | … | … | … | … | … | … | … | … |
| 8 | 3 | 20 | | … | … | … | … | … | … | … | … |
| 9 | 3 | 30 | | … | … | … | … | … | … | … | … |
| 10 | 3.8 | 10 | | … | … | … | … | … | … | … | … |
| 11 | 3.8 | 20 | | … | … | … | … | … | … | … | … |
| 12 | 3.8 | 30 | | $P_{1(3.8/30)}$ | $P_{2(3.8/30)}$ | $P_{3(3.8/30)}$ | $P_{4(3.8/30)}$ | $P_{5(3.8/30)}$ | $P_{6(3.8/30)}$ | $P_{M(3.8/30)}$ | $P_{S\,(3.8/30)}$ |

**Fig. 4.4: Methodology for the simulation of performance values through combined DOE and RBTO method**

In this figure, two tables are shown. The table shown at top is for factor combination (same as Appendix A1), and table shown below is for reliability index (β) and spread (S). In the table below, RBTO methodology is used. Each combination is treated for the all combinations of β & S. As stated earlier, input to RBTO process are input factor combination, and the β and S values, i.e. a combination of reliability factor. Hence, the output of RBTO generates *reliable-controllable factor* values to produce reliable topology and its performance. Each *reliable-controllable factor* value is then replicated for the loading uncertainty conditions. Using the replications of experiments, mean and SNR of performances are computed, i.e. $P_M$ and $P_S$. In the table, simulated performances are shown with the corresponding pair of β and S values as $P_{(\beta/S)}$. Thus, for each factor combination, reliable topology and performance values are simulated corresponding to all pair of β and S values.

## 4.4    ANALYSIS AND DISCUSSION

The proposed methodology is used for the selected benchmark problems. The performance values in terms of compliance and maximum deflection are simulated for reliable optimal topology. For simulation, FE mesh size is varied from coarse to fine i.e. 12×10, 24×20, 36×30, and 60×50. It is observed that comparative results remain same for the considered mesh sizes. The reason for this observation is mesh independency filter used in simulation routine (Bendsøe and Sigmund 2003). Hence, it is decided to use a coarse mesh can also be used for the analysis, as the physics of the problem do not change. The reliable optimal topologies obtained from simulation are shown in Table 4.1. This table shows the topologies of each problem for DTO and RBTO based methods. For illustration, RBTO based topologies are generated by keeping the reliability index β=3.0, with spread S=10%, and the next set of topologies are generated by keeping, β=3.8 with S=20%. It is observed that the topologies change slightly when the simulation process is changed from DTO to RBTO. This is the reason for the change in the performance values. The performance values are analyzed by ANOM and ANOVA. The analysis for robust and targeted performances is presented in the next sections.

**Table 4.1: Optimal topologies for the corresponding combination numbers,**

**reliability index (β), and spread (S)**

| C. No. | Problem-1 | | | Problem-2 | | | Problem-3 | | | Problem-4 | | |
|---|---|---|---|---|---|---|---|---|---|---|---|---|
| | DTO | β=2.0 S=10% | β=3.8 S=30% | DTO | β=2.0 S=10% | β=3.8 S=30% | DTO | β=2.0 S=10% | β=3.8 S=30% | DTO | β=2.0 S=10% | β=3.8 S=30% |
| 1 | | | | | | | | | | | | |
| 2 | | | | | | | | | | | | |
| 3 | | | | | | | | | | | | |
| 4 | | | | | | | | | | | | |
| 5 | | | | | | | | | | | | |
| 6 | | | | | | | | | | | | |
| 7 | | | | | | | | | | | | |
| 8 | | | | | | | | | | | | |
| 9 | | | | | | | | | | | | |
| 10 | | | | | | | | | | | | |
| 11 | | | | | | | | | | | | |
| 12 | | | | | | | | | | | | |
| 13 | | | | | | | | | | | | |
| 14 | | | | | | | | | | | | |
| 15 | | | | | | | | | | | | |
| 16 | | | | | | | | | | | | |
| 17 | | | | | | | | | | | | |
| 18 | | | | | | | | | | | | |
| 19 | | | | | | | | | | | | |
| 20 | | | | | | | | | | | | |
| 21 | | | | | | | | | | | | |
| 22 | | | | | | | | | | | | |
| 23 | | | | | | | | | | | | |
| 24 | | | | | | | | | | | | |
| 25 | | | | | | | | | | | | |
| 26 | | | | | | | | | | | | |
| 27 | | | | | | | | | | | | |

### 4.4.1  Analysis of mean

Analysis of the mean (ANOM) is performed using simulated performance values of the problems. The objective of this analysis is to investigate the sensitivity and the significance of factors in benchmark problems with RBTO method. Hence, it is desirable to compare the ANOM of results obtained from DTO and RBTO based simulation. As discussed in methodology, for each combination, all possible simulations are performed corresponding to specified $\beta$ and S values. From these simulations, the extreme cases are identified. This identification is based on the maximum and minimum variation of performances. The maximum variation of the performance is obtained when $\beta=3.8$ with S=30%, and minimum variation is obtained when $\beta=2$ with S=10%. Hence, ANOM of these two extremes are compared with that of deterministic case. The ANOM of performances are shown in Figs. 4.5 to 4.8, for all the considered problems. In these figures, the ANOM of compliance and deflection are presented column wise.

Fig. 4.5 shows the ANOM for problem-1. It is observed that three factors are interacting. When performance measure is compliance, volume fraction is the most significant factor and aspect ratio is the least significant factor. However, in Fig. 4.5(c) when $\beta=3.8$ and S=30%, effect of aspect ratio is slightly higher than force. The reason for this change is the increased variation of the factor in presence of uncertainties. When performance measure is deflection, volume fraction is the most significant factor and force is the least significant factor. For both performances, volume fraction shows the nonlinear effect, while force shows linear effect. It is also observed that with the increasing value of $\beta$ and S the performance values increase.

Fig. 4.6 shows the ANOM for problem-2. All three factors are in good interaction. When performance measure is compliance, volume fraction is the most significant factor and aspect ratio is the least significant factor. When performance measure is deflection, volume fraction is the most significant factor and force is the least significant factor. For both performances, among all factors, volume fraction shows the most nonlinear, while

force shows linear effect. In addition, withincreasing value of β and S, performance values also increased, as expected.



(a) deterministic

(d) deterministic

(b) β=2, S=10%

(e) β=2, S=10%

(c) β=3.8, S=30%

(f) β=3.8, S=30%
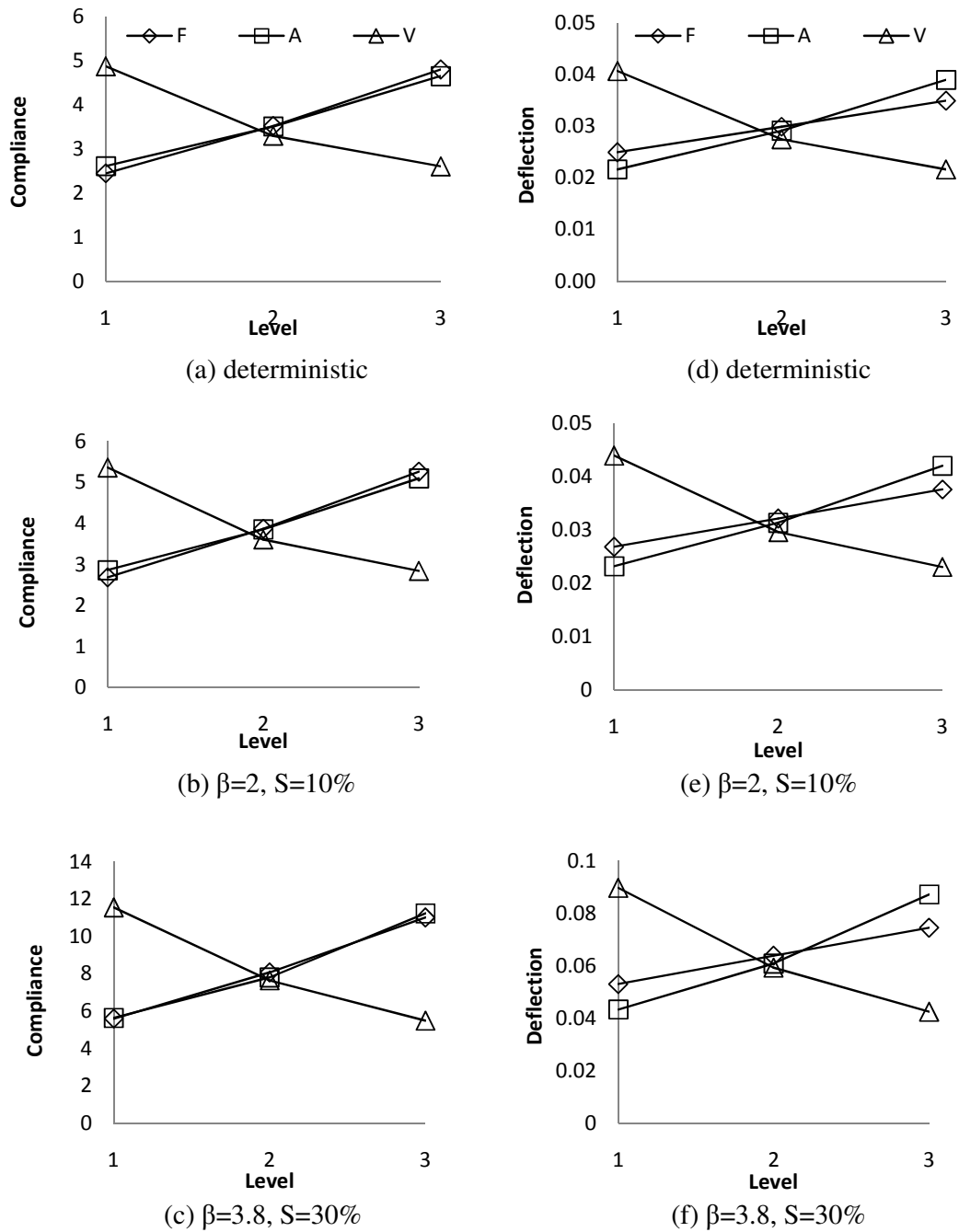
**Fig. 4.5: ANOM of compliance (a), (b), & (c), and ANOM of deflection (in mm) (d), (e), & (f) for problem-1**
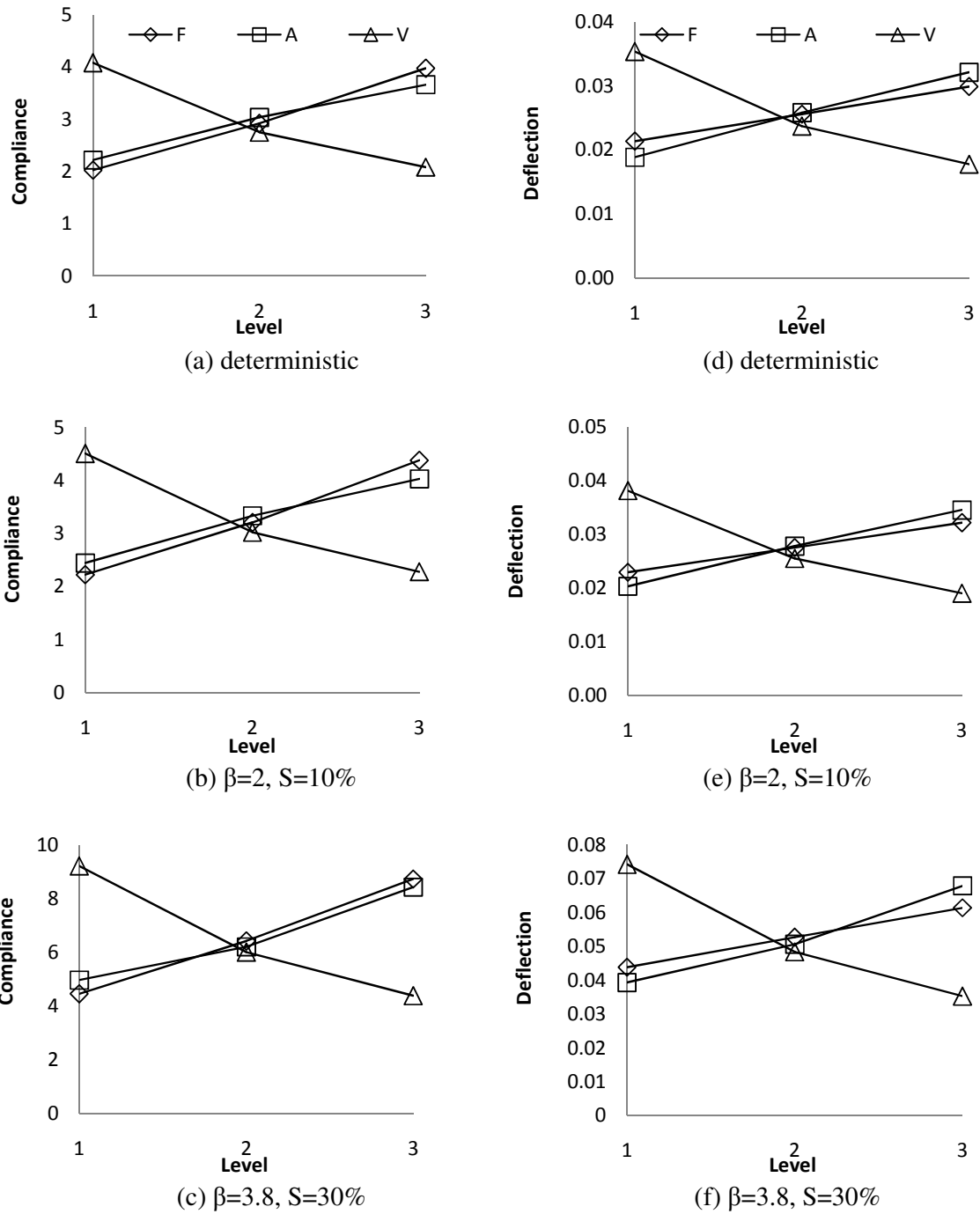
Fig. 4.6: ANOM of compliance (a), (b), & (c), and ANOM of deflection (in mm) (d), (e), & (f) for problem-2
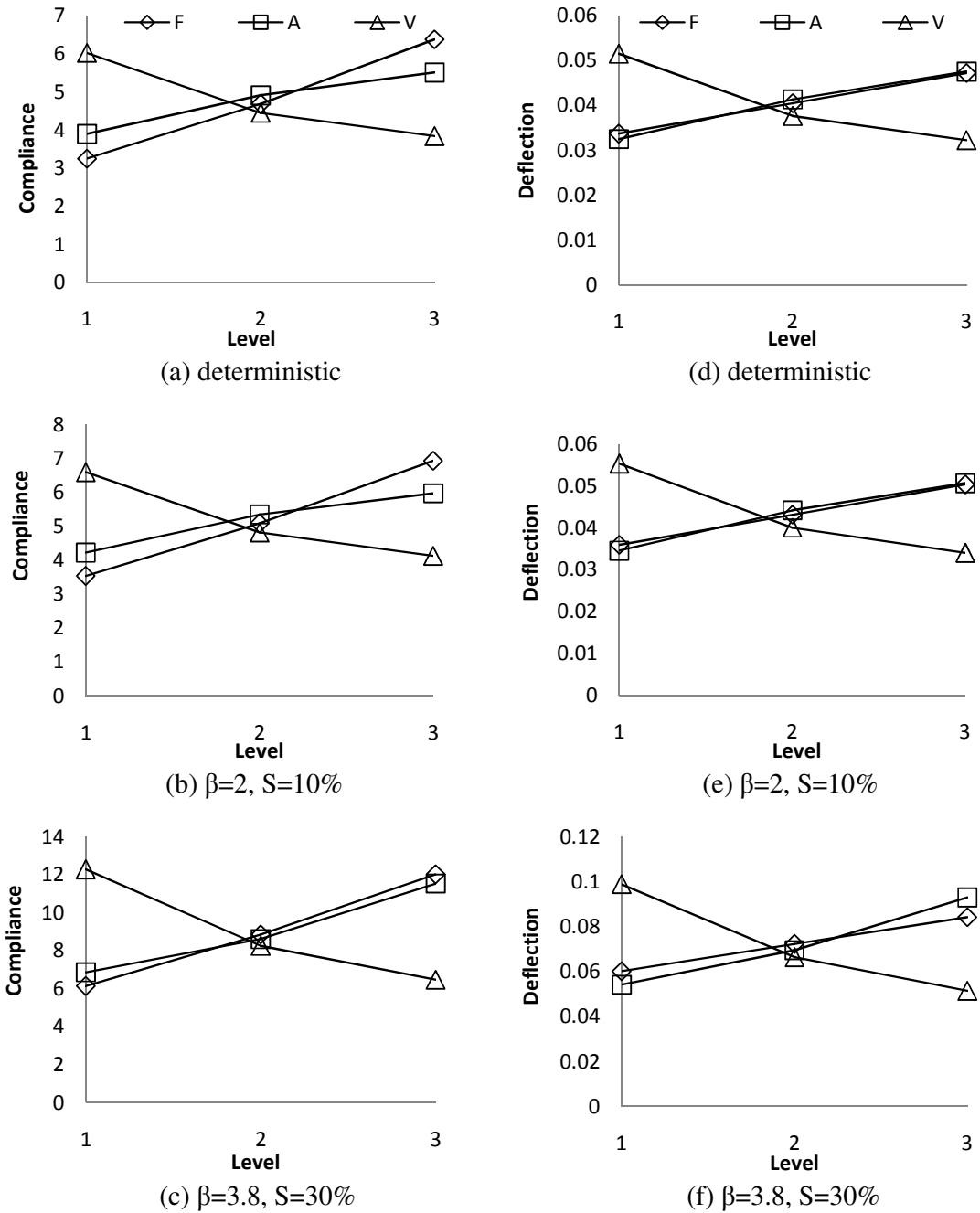
**Fig. 4.7: ANOM of compliance (a), (b), & (c), and ANOM of deflection (in mm) (d), (e), & (f) for problem-3**

Fig. 4.7 shows the ANOM for problem-3. Since this problem is similar to the problem-2, the inferences are almost similar to that. All the factors show good interaction. When performance measure is compliance, force is the most significant and aspect ratio is the least significant factor, except for the last case (Fig. 4.7(c)), where volume fraction is the most significant factor. When performance measure is deflection,

volume fraction is the most significant factor and force is the least significant factor. For both performances, volume fraction shows the nonlinear effect, while force shows linear effect.



(a) deterministic



(d) deterministic

(b) β=2, S=10%

(e) β=2, S=10%

(c) β=3.8, S=30%

(f) β=3.8, S=30%
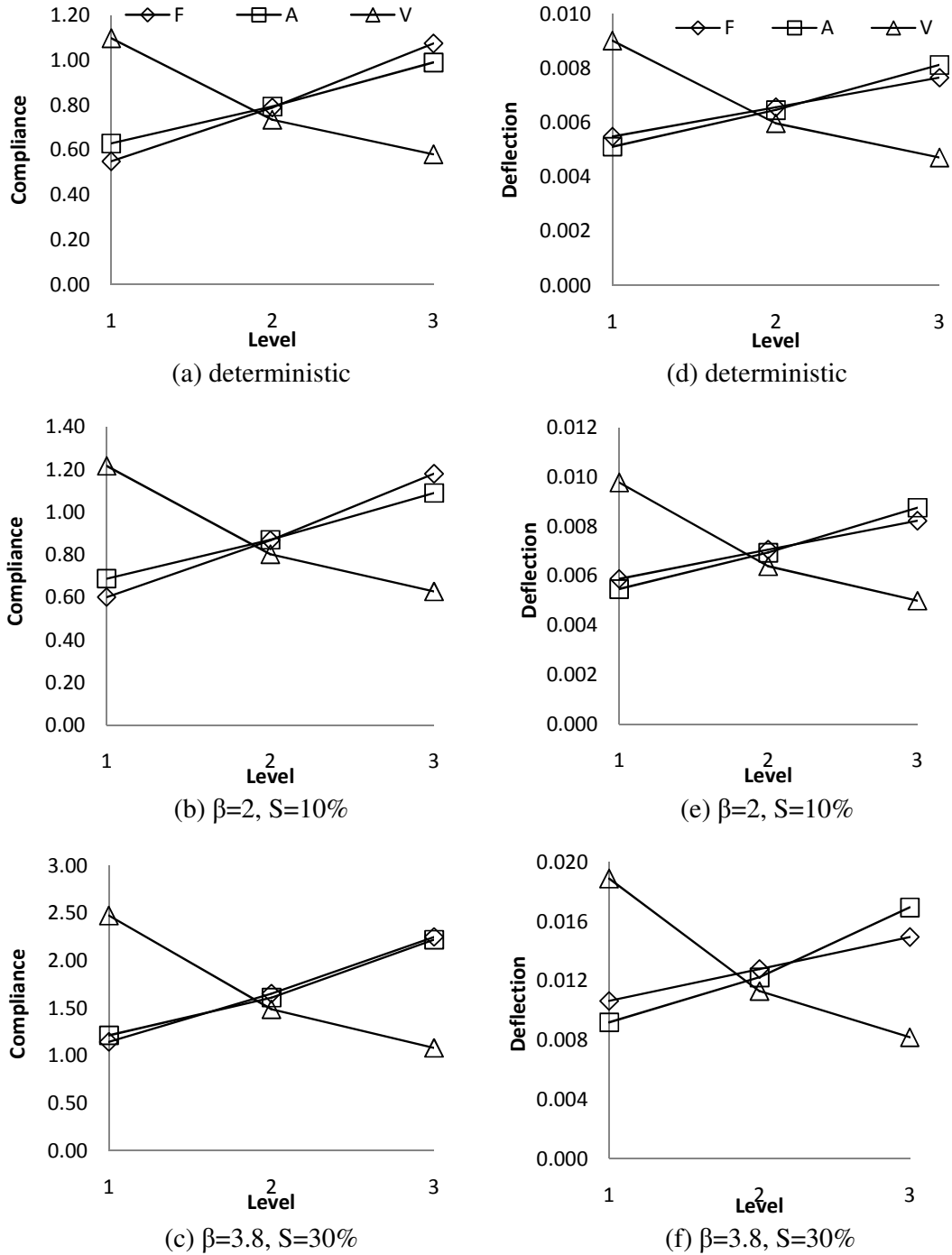
**Fig. 4.8: ANOM of compliance (a), (b), & (c). and ANOM of deflection (in mm) (d), (e), & (f) for problem-4**

Fig. 4.8 shows the ANOM for problem-4. All the factors are in good interaction. When performance measure is compliance, volume fraction and force are equally significant and aspect ratio is the least significant factor, except for the last case (Fig. 4.7(c)), where only volume fraction is the most significant factor. When performance measure is deflection, volume fraction is the most significant factor and force is the least significant factor. For both performances, among all factors, volume fraction shows nonlinear effect, while force shows linear effect. Similarly, for all the problems, performance values show increased trend when $\beta$ & S are increases.

From these figures, it is seen that all the factors have good interaction. Volume fraction appears as the significant factor in the ANOM of both performances. Whereas, aspect ratio and force are the least significant factor in the ANOM of compliance and deflection, respectively. The linear and non-linear effect of the factors is explainable by theory of beams. It can also be seen that by increasing the reliability index and the spread of the factors, the values of compliance and deflection also increase. In addition to this observation, the increased values of $\beta$ and S bring the effects of aspect ratio and force closer, when compliance is the performance measure. For deflection, the effect of aspect ratio and force are distinct. This is because of the variations of the factor values that are introduced by the $\beta$ and S values. The observations available here provide the guidelines to design a reliable optimal topology.

### 4.4.2  Signal to noise ratio

As discussed earlier in section 3.4.3, SNR is computed based on equation (3.36). In Fig. 4.9, SNR of compliance is shown for different reliability index and spread values. For engineering applications the preferred values reliability index are taken 3.8 or 3. At the same time, the spread of the factors are not more the 20%. Hence, SNR corresponding to $\beta$ value equal to 2.5 and 2, and S value equal to 30% are dropped here to present the realistic values. The legends are given in terms of $\beta$/Svalue. As for example, 3.8/10 represent, $\beta$=3.8 and S=10% around the nominal values for the factors.
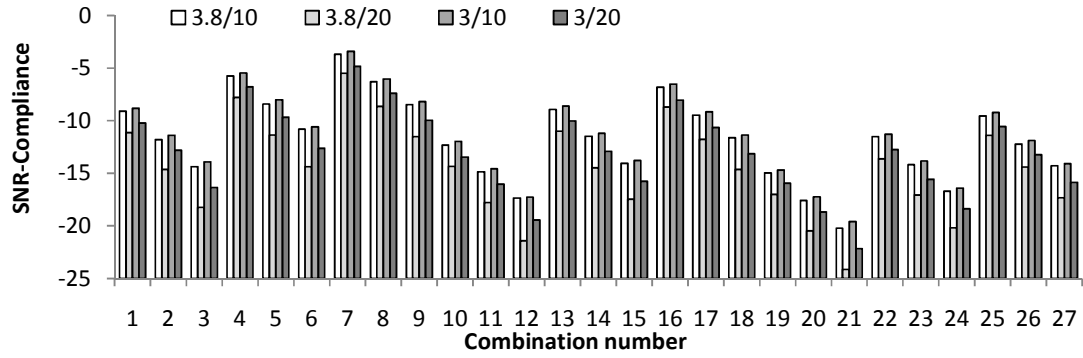
**Fig. 4.9(a): SNR of compliance for problem-1**
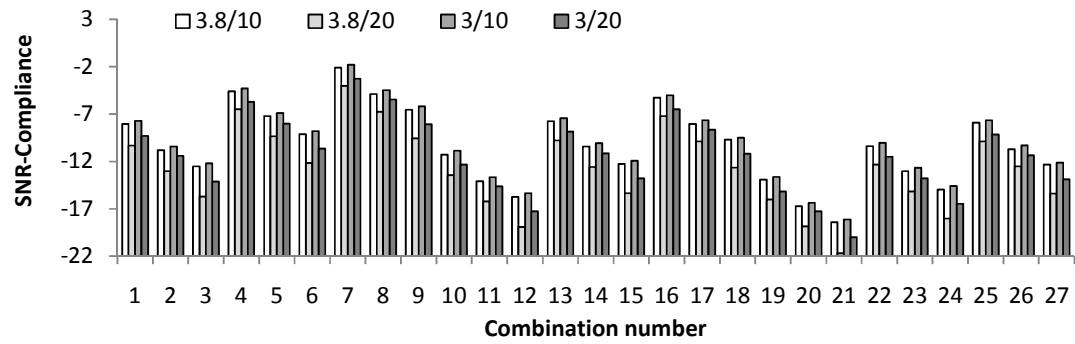


**Fig. 4.9(b): SNR of compliance for problem-2**
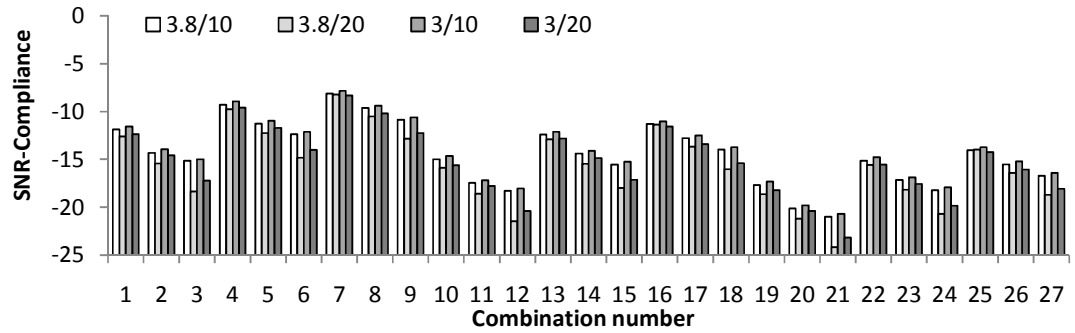


**Fig. 4.9(c): SNR of compliance for problem-3**
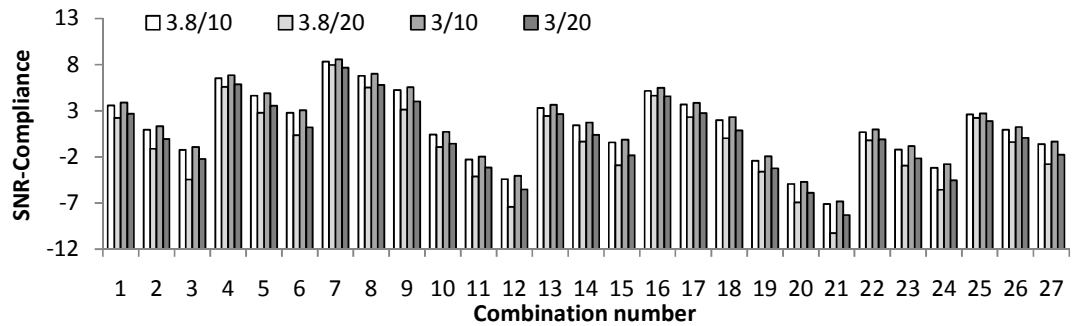


**Fig. 4.9(d): SNR of compliance for problem-4**

Fig. 4.9 shows the SNR of all problems for compliance. It is observed that SNR decreases with the increased values ofβ and S. This change in SNR with respect to S is more than that of β. The performance variation for β and S implies that there is a tradeoff between the reliability and robustness value. The SNR value is highest for the 7th combination and lowest for the 21st combination. Hence, the 7th combination offers the high and 21st offers the lowest robustness. It is similar to the analysis carried out in previous chapter. Hence, the inclusion of the uncertainties of controllable factor does not have significant effect on the comparative robustness of the combinations. Similar to the SNR of compliance, SNR of deflection is presented for all problems in Fig. 4.10.
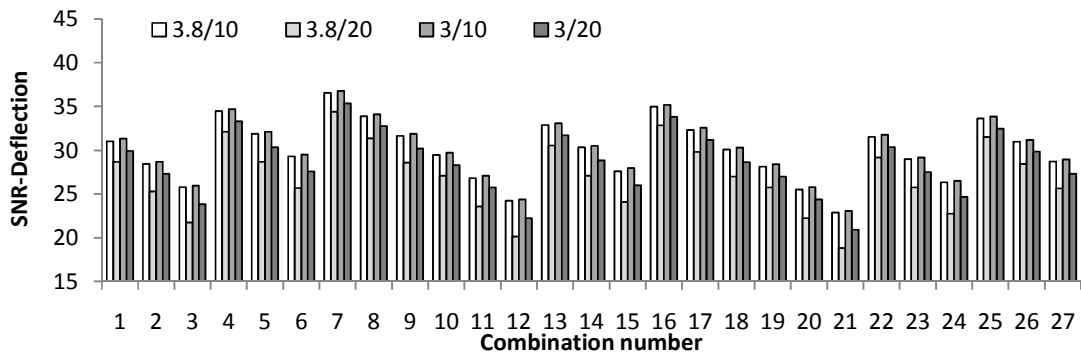


**Fig. 4.10(a): SNR of deflection for problem-1**
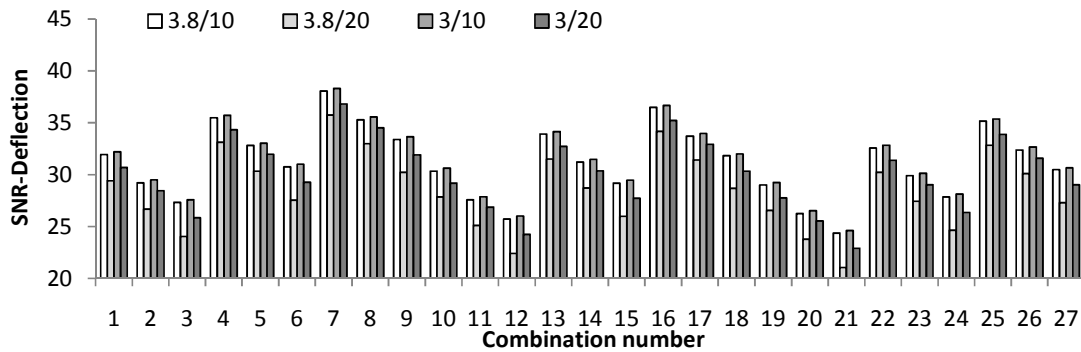


**Fig. 4.10(b): SNR of deflection for problem-2**
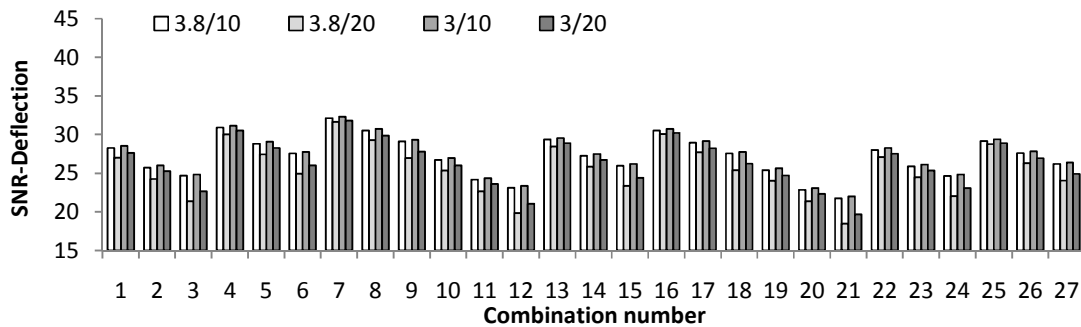


**Fig. 4.10(c): SNR of deflection for problem-3**
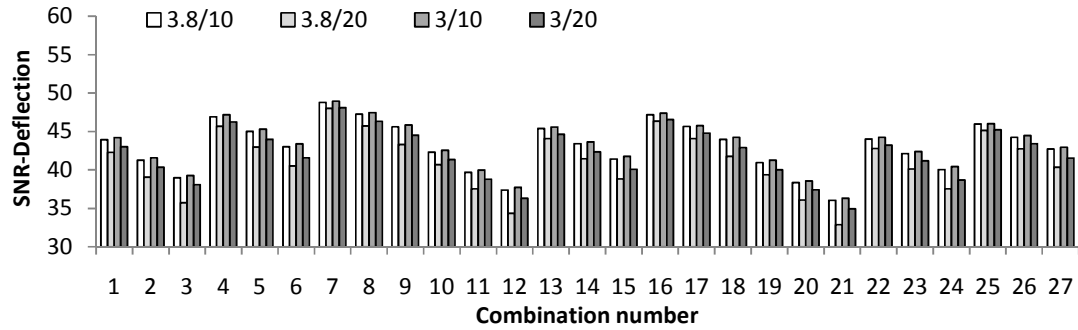
**Fig. 4.10(d): SNR of deflection for problem-4**

From Fig. 4.10, the SNR of all problems for deflection as performance can be observed. All observations are similar to that of SNR of compliance. The SNR value decreases with increased value of reliability index and spread. It is highest for the 7th combination and lowest for the 21st combination. The presented curves for SNR of performance can be used to select the factor value and reliability index to achieve a desired value of robustness. It is also observed that for 7th combination, variations in the performance values are least, while it is highest for 21st combination. The changes in performance values are lesser with respect to the $\beta$ variation, compare to that of with respect to S variation. In addition, the effect of change of S value is high when $\beta=3.8$ compared to that of $\beta=3$. Using these results, a targeted robust design can also be formulated by selecting a proper value of factors, reliability index, and spread of factors. This selection will be purely based on the choice and affordability. Thus, the SNR analysis provides flexibility to designers' by providing alternate options for robust performance.

### 4.4.3  Analysis of variance

As discussed earlier, ANOVA helps to identify the statistically significant factor of a design. In the present work, ANOVA is carried out by employing Design Expert software, version 8.0.6 (2011). The functional relationship between the performance value and the factors are given in Tables 4.2 & 4.3, in terms of the coded values of the factors. The symbols A, B and C denote aspect ratio, volume fraction and force respectively. The equations are given for the deterministic condition and the extreme conditions of reliability based performances for the comparison.

**Table 4.2: Performance equations for compliance, subject to extreme and deterministic conditions**

| | | |
|---|---|---|
| Problem 1 | Deterministic | $3.593-0.979\times A-0.08\times A^2 +1.28\times B-0.293\times B^2-1.142\times C-0.067\times C^2-0.37\times AB-0.068\times A^2B +0.079\times AB^2 +0.002\times A^2B^2 +0.31\times AC +0.023\times A^2C +0.02\times AC^2 +0.009\times A^2C^2-0.406\times BC +0.093\times B^2C-0.026\times BC^2 +0.006\times B^2C^2$ |
| | $\beta=2$ S=10% | $3.935-1.077\times A-0.084\times A^2 +1.426\times B-0.328\times B^2-1.253\times C-0.071\times C^2-0.42\times AB-0.072\times A^2B +0.094\times AB^2 +0.004\times A^2B^2 +0.34\times AC +0.026\times A^2C +0.022\times AC^2 +0.005\times A^2C^2-0.462\times BC +0.105\times B^2C-0.028\times BC^2-0.001\times B^2C^2$ |
| | $\beta=3.8$ S=30% | $8.233-2.587\times A-0.419\times A^2+3.316\times B-0.577\times B^2-2.625\times C-0.157\times C^2-1.206\times AB-0.362\times A^2B+0.208\times AB^2+0.111\times A^2B^2+0.834\times AC+0.124\times A^2C+0.034\times AC^2+-0.018\times A^2C^2-1.059\times BC+0.188\times B^2C-0.059\times BC^2+0.017\times B^2C^2$ |
| Problem 2 | Deterministic | $2.975 +0.469\times A-0.223\times A^2 +0.096\times B +0.025\times B^2-0.128\times C +0.271\times C^2 +0.372\times AB-0.315\times A^2B-0.043\times AB^2-0.149\times A^2B^2 +0.06\times AC +0.344\times A^2C +0.371\times AC^2-0.508\times A^2C^2-0.456\times BC +0.047\times B^2C +0.494\times BC^2-0.177\times B^2C^2-0.091\times ABC-0.176\times A^2BC-0.088\times AB^2C +0.127\times A^2B^2C +1.139\times ABC^2-0.234\times A^2BC^2-0.869\times AB^2C^2 +0.244\times A^2B^2C^2$ |
| | $\beta=2$ S=10% | $3.271-0.828\times A +0.067\times A^2 +1.238\times B-0.248\times B^2-1.048\times C-0.061\times C^2$ |
| | $\beta=3.8$ S=30% | $6.537-1.568\times A-0.327\times A^2+2.681\times B-0.528\times B^2-2.083\times C-0.117\times C^2$ |
| Problem 3 | Deterministic | $4.774 -0.57\times A-0.245\times A^2 +0.092\times B +0.013\times B^2-0.124\times C +0.252\times C^2 +0.335\times AB-0.347\times A^2B-0.043\times AB^2-0.146\times A^2B^2 +0.079\times AC +0.4\times A^2C +0.438\times AC^2-0.651\times A^2C^2-0.515\times BC +0.104\times B^2C +0.445\times BC^2-0.195\times B^2C^2-0.197\times ABC-0.137\times A^2BC +0.038\times AB^2C +0.042\times A^2B^2C +1.423\times ABC^2-0.273\times A^2BC^2-1.205\times AB^2C^2 +0.333\times A^2B^2C^2$ |
| | $\beta=2$ S=10% | $5.184-0.958\times A +0.166\times A^2 +1.414\times B-0.363\times B^2-1.646\times C-0.099\times C^2-0.452\times BC +0.124\times B^2C-0.031\times BC^2 +0.004\times B^2C^2$ |
| | $\beta=3.8$ S=30% | $9.011-2.140\times A-0.392\times A^2+3.276\times B-0.748\times B^2-2.868\times C-0.150\times C^2-0.885\times AB-0.290\times A^2B+0.190\times AB^2+0.054\times A^2B^2-1.07\times BC+0.243\times B^2C-0.052\times BC^2+0.016\times B^2C^2$ |
| Problem 4 | Deterministic | $0.804-0.175\times A-0.01\times A^2 +0.294\times B-0.07\times B^2-0.256\times C-0.015\times C^2-0.109\times AB-0.002\times A^2B +0.027\times AB^2-0.001\times A^2B^2-0.093\times BC +0.022\times B^2C-0.007\times BC^2 +0.002\times B^2C^2$ |
| | $\beta=2$ S=10% | $0.883-0.195\times A-0.012\times A^2 +0.335\times B-0.08\times B^2-0.282\times C-0.015\times C^2-0.125\times AB +0.033\times AB^2-0.005\times A^2B^2-0.105\times BC +0.023\times B^2C-0.004\times BC^2 +0.001\times B^2C^2$ |
| | $\beta=3.8$ S=30% | $1.683-0.468\times A-0.071\times A^2+0.793\times B-0.193\times B^2-0.538\times C-0.029\times C^2-0.296\times AB-0.060\times A^2B+0.086\times AB^2+0.021\times A^2B^2+0.155\times AC+0.019\times A^2C+.008\times AC^2+0.000\times A^2C^2+-0.256\times BC+0.060\times B^2C-0.005\times BC^2+0.001\times B^2C^2$ |

From Tables 4.2 & 4.3, it is observed that the equation corresponding to β=2, S=10%, is near to that of deterministic case, while equation corresponding toβ=3.8, S=30% is far, which confirms the previous analysis. It is because of the characteristics of the selected RBTO method. The linear and quadratic effect of each factor can also be seen using the coefficients of the equation. In most of the problems, it is found that the volume fraction is the most significant factor. Apart from the relative performance of factors, these equations are useful to generate the performance values within the range of factor levels. Hence, this equation provides the necessary mathematical relation to estimate the approximate performance values.

**Table 4.3: Performance equations for deflection (in mm), subject to extreme and deterministic conditions**

| | | |
|---|---|---|
| **Problem 1** | Deterministic | $0.03-0.008\times A-0.001\times A^2 +0.011\times B-0.002\times B^2-0.005\times C -0.003\times AB-0.001\times A^2B +0.001\times AB^2 +0.001\times AC$ |
| | β=2 S=10% | $0.032-0.009\times A-0.001\times A^2 +0.012\times B-0.003\times B^2-0.005\times C-0.003\times AB-0.001\times A^2B +0.001\times AB^2 +0.001\times AC-0.002\times BC$ |
| | β=3.8 S=30% | $0.064-0.020\times A-0.003\times A^2+0.026\times B-0.005\times B^2-0.011\times C-0.010\times AB-0.002\times A^2B+0.002\times AB^2+0.001\times A^2B^2+0.003\times AC-0.004\times BC+0.001\times B^2C$ |
| **Problem 2** | Deterministic | $0.026 +0.003\times A-0.002\times A^2 +0.001\times B-0.001\times C +0.002\times C^2 +0.002\times AB-0.002\times A^2B-0.002\times A^2B^2 +0.001\times AC +0.002\times A^2C +0.002\times AC^2-0.003\times A^2C^2-0.003\times BC +0.004\times BC^2-0.001\times B^2C^2$ |
| | β=2 S=10% | $0.028-0.007\times A +0.011\times B-0.002\times B^2-0.005\times C-0.003\times AB$ |
| | β=3.8 S=30% | $0.053-0.013\times A-0.002\times A^20.022\times B+-0.004\times B^2-0.009\times C-0.005\times AB-0.001\times A^2B+0.001\times AB^2$ |
| **Problem 3** | Deterministic | $0.04 +0.004\times A-0.002\times A^2-0.001\times C +0.002\times C^2 +0.001\times AC +0.003\times A^2C +0.002\times AC^2-0.003\times A^2C^2$ |
| | β=2 S=10% | $0.043-0.009\times A +0.001\times A^2 +0.012\times B-0.003\times B^2-0.007\times C-0.004\times AB +0.002\times A^2B +0.001\times AB^2$ |
| | β=3.8 S=30% | $0.072-0.018\times A-0.003\times A^2+0.027\times B+-0.006\times B^2-0.012\times C-0.007\times AB-0.002\times A^2B+0.001\times AB^2$ |
| **Problem 4** | Deterministic | $0.007-0.001\times A +\mathbf{0}\times A^2 +0.002\times B-0.001\times B^2-0.001\times C-0.001\times AB$ |
| | β=2 S=10% | $0.007-0.002\times A +0.003\times B-0.001\times B^2-0.001\times C-0.001\times AB$ |
| | β=3.8 S=30% | $0.013-0.004\times A-0.001\times A2+0.006\times B-0.001\times B2-0.002\times C-0.002\times AB+0.001\times AB2+0.001\times AC-0.001\times BC$ |

For the detailed observation of significance of factor, the ANOVA results are presented in Table 4.4. The significant factors are identified for the deterministic as well as the extreme cases of the performance values. In this table, there is a change of significant factors, while moving from the deterministic to the reliable scenario. Also, with the change of reliability index and spread value, the significant factor remain same in almost all cases.

**Table 4.4: Significantfactor for the extreme values of performances**

| Bench Mark Problems | Statistically Significant Input factors for compliance | | |
|---|---|---|---|
| | Deterministic | β=3.8, S=30% | β=2, S=10% |
| Problem-1 | A, B, C, AB, BC, AC | A, B, C, AB, BC, AC | A, B, C, AB, BC, AC |
| Problem-2 | A, ABC | A, B, C, | A, B, C, |
| Problem-3 | A, ABC | A, B, C, AB, BC, | A, B, C, BC |
| Problem-4 | A, B, C, AB, BC | A, B, C, AB, BC, AC | A, B, C, AB, BC |
| **Bench Mark Problems** | **Statistically Significant Input factors for deflection** | | |
| | Deterministic | β=3.8, S=30% | β=2, S=10% |
| Problem-1 | A, B, C, AB, BC, AC | A, B, C, AB, BC, AC | A, B, C, AB, BC, AC |
| Problem-2 | A | A, B, C, AB | A, B, C, AB |
| Problem-3 | A | A, B, C, AB | A, B, C, AB |
| Problem-4 | A, B, C, AB, BC, AC | A, B, C, AB, BC, AC | A, B, C, AB, BC, AC |

As discussed earlier, the values of compliance and deflection are altered by applying RBTO method. In such scenario, finding desired or targeted performance value is an issue, and the procedure adopted is discussed in the next section.

### 4.4.4 Targeted performance values

From a designer's perspective, it is desired to achieve a targeted value of performance subject to high reliability index. However, when the selected RBTO scheme is applied to topology optimization problem, the value of performances gets altered. In such scenario, the intended performance cannot be achieved with desired reliability. To achieve a targeted performance with specified reliability, the design factor must be selected properly. This selection is carried out using mean performance value analysis. The mean values of performances are computed for each factor combination. In Fig. 4.11, the mean compliance values with respect to the different combinations are shown. The mean compliance values are computed corresponding to the different pair of $\beta$ and S values. The legends indicate $\beta$/S% values in figures.
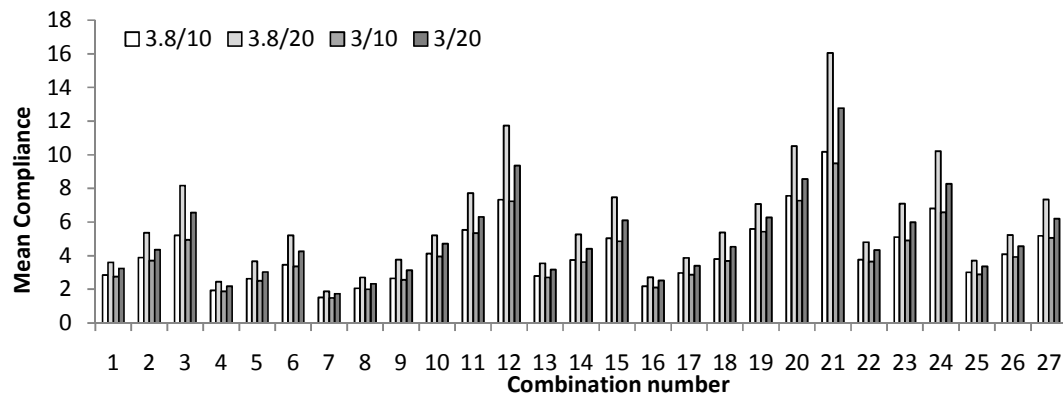


**Fig. 4.11(a): Mean values of compliance for problem-1**
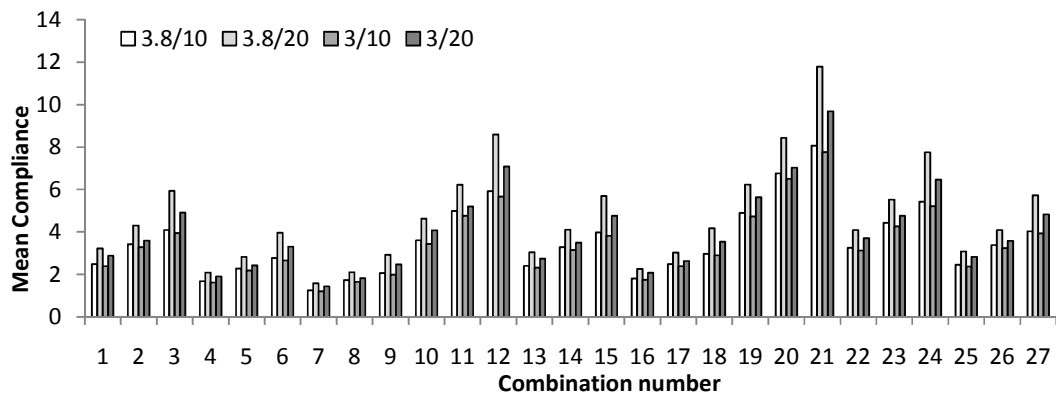


**Fig. 4.11(b): Mean values of compliance for problem-2**
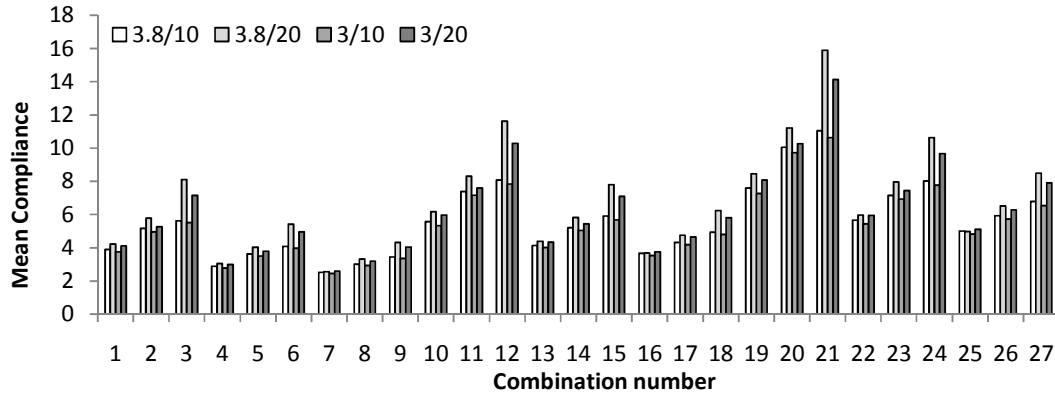
**Fig. 4.11(c): Mean values of compliance for problem-3**
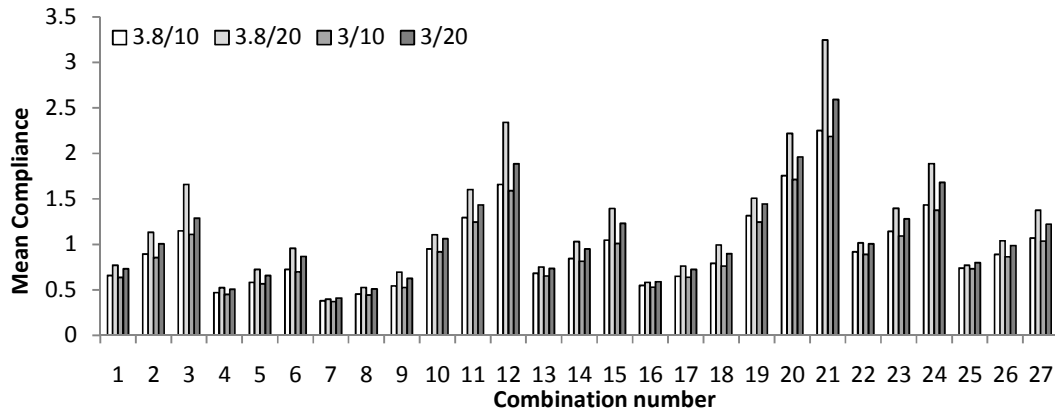


**Fig. 4.11(d): Mean values of compliance for problem-4**

From Fig. 4.11, it is observed that with increased $\beta$ and S values the mean compliance increases. The compliance value is highest for 21st combination and lowest for 7th combination. It can be observed that for a desired value of compliance or deflection, there are different combinations of factors available. A targeted performance value can be achieved by selecting the available combinations of controllable factors, reliability index, and spread value. To illustrate, the compliance values are presented in Appendix A4 for problem-1. The values are given corresponding to the combination of the factors created by factorial design. From this table it is seen that a desired value of compliance and deflection is available at different combinations, $\beta$, and S values.

Similar to mean compliance, the mean deflection is also plotted for all four problems, as shown in Fig. 4.12. The legends are shown for $\beta/S\%$value.
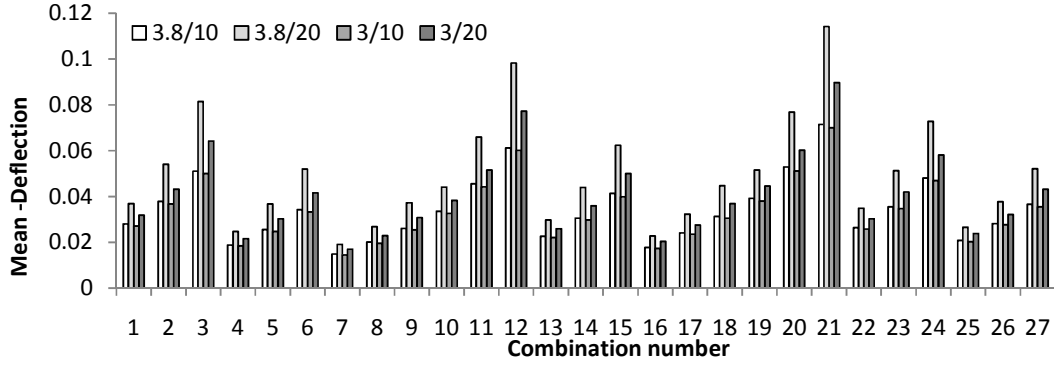
**Fig. 4.12(a): Mean values of deflection (in mm) for problem-1**
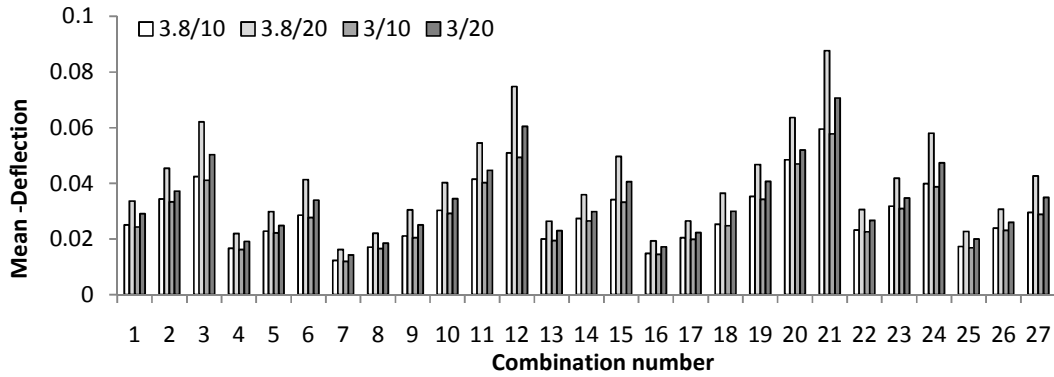


**Fig. 4.12(b): Mean values of deflection (in mm) for problem-2**
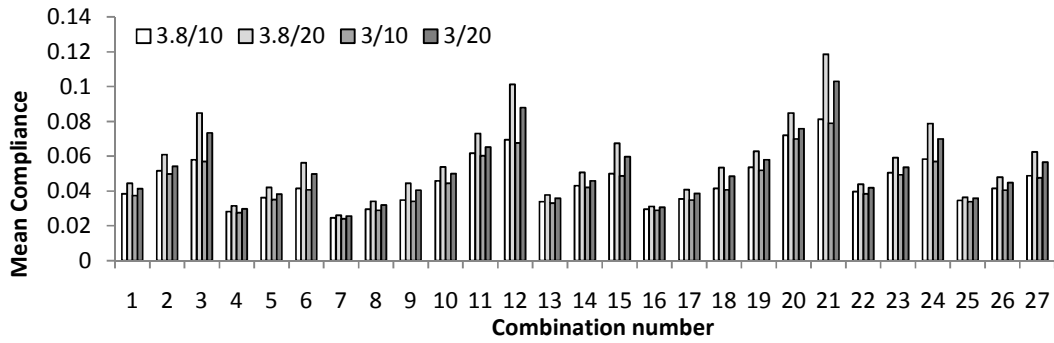


**Fig. 4.12(c): Mean values of deflection (in mm) for problem-3**
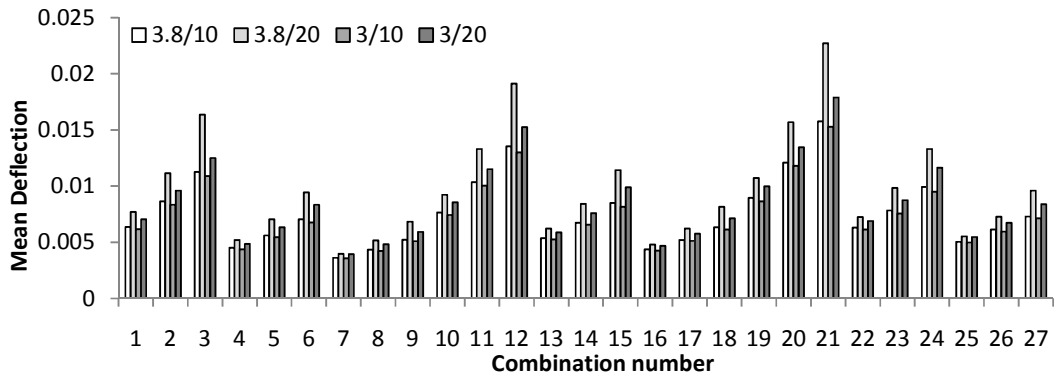


**Fig. 4.12(d): Mean values of deflection (in mm) for problem-4**

In Fig. 4.12, all observations are similar to that of compliance. It is observed that with increased β and S values, the mean deflection also increases. The deflection value is highest for 21st combination and lowest for 7th combination. Here also, a targeted performance value can be achieved by selecting the available combinations of controllable factors, β, and S values. To illustrate, the values of mean deflection are presented in Appendix A5 for problem-1. This analysis provides flexibility to the designer to select an optimal topology for desired value of performances at specified reliability.

Similar to the previous performance measure, a few observations are made here. For 7th combination, the variation in the performance values are less when β and S change, and it is high for 21st combination. The changes in performance values are lesser with respect to the β, compared to that of S. In addition, the effect of change of S value is high, when β=3.8 compared to β=3. The observation regarding the performance verses β and S are because of their level values and the specific characteristic of RBTO method.

## 4.5    COMPARISON OF RESULTS

To highlight the significance of the results obtained by including the noises/uncertainties of the controllable factors in the simulation, a comparison is shown here. As discussed earlier the results of Chapter 3 are obtained with the noise of point and angle of applied force and elasticity only. Hence, the simulation results are compared between Chapter 3 and 4 for mean and SNR of compliance. For problem-1, these values are presented in Fig. 4.13.

From this comparison, it is observed that the mean values increases and the SNR decreases when the noise of controllable factors is included in the simulation. This scenario is closer to the realistic situation. However, the comparative performances of the combinations are same. For the other problems and performance measure also, the similar observation are obtained. Hence, the results obtained in this chapter are realistic compared to that of previous chapter.

(a)



(b)
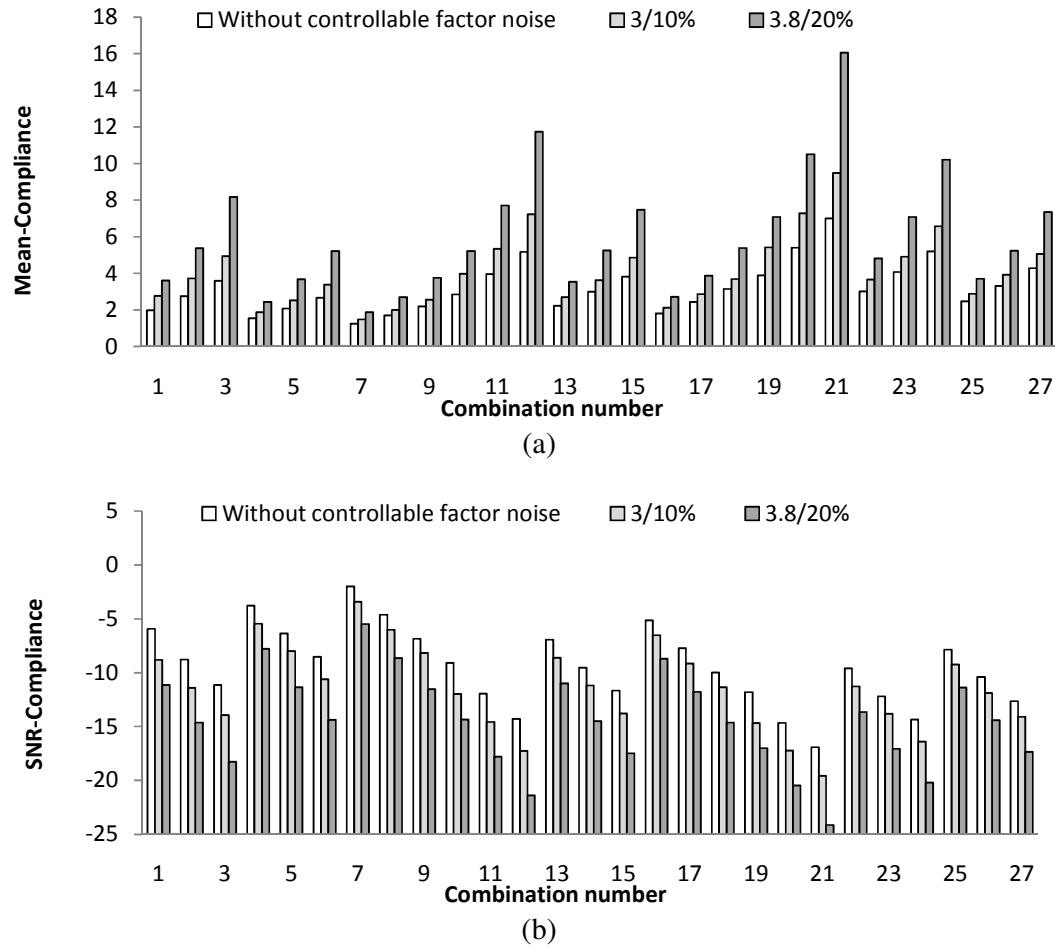
**Fig. 4.13: Comparison of (a) mean compliance and (b) SNR of compliance for problem-1**

## 4.6    CONCLUSIONS

In this chapter, a DOE based methodology was proposed to analyze the performance of a topologically optimized structure with RBTO in the realistic scenario. The methodology was illustrated using four benchmark problems. The realistic scenario was created by incorporating the uncertainties in the deterministic model. In addition to the performance analysis, a method of identifying the optimum values of design factor is developed to ensure the robust and targeted performance. It is found that volume fraction is the significant factor in almost all cases. It is also observed that the change of reliability and spread values change the sensitivity of the factor slightly. The 7th combination performed best for robust design and generated the minimum compliance and deflection values. Whereas, 21st combination gave maximum values of compliance and deflection, and showed minimum robustness.

# CHAPTER 5

# SELECTION OF TOLERANCE RANGE OF CONTROLLABLE FACTORS FOR TOPOLOGICALLY OPTIMIZED STRUCTURES

## 5.1    INTRODUCTION

The analysis of the various factors and their uncertainties on the performance values of a topologically optimized structure was described in the previous chapters. The controllable factors considered were, force, volume fraction, and aspect ratio. The noise or uncertainties such as, elasticity value, angle, and application point of applied force were also included in that analysis. A combined approach using DOE and RBTO was proposed to analyze the performance. In addition, the optimal values of the factors were identified to achieve a targeted and robust performance. Now, to investigate the performance around the nominal values, the impact of tolerance ranges of factors on performance should be investigated.

In real life scenario, each factor will have some tolerance range, because of process variability. These tolerances affect the performance values. Ideally, the tight or narrow tolerance for every factor provides minimum performance variation. However, to maintain a very tight tolerance for each factor needs high investment and effort. In such situation, the tolerance of only a few factors should be tightened. These factors are the ones, which requires lesser effort for tightening the tolerance, or the one, which has the statistically significant effect on the performance values. Thus, the selection of such key factors becomes an important issue. This issue is dealt in this chapter using a cross array design of experiments (CA-DOE) approach. This approach helps to simulate the performances by incorporating the factor values along with their tolerance ranges. This method provides a simple way to design an efficient and cost effective experiment. For illustration, CA-DOE approach is applied to the chosen benchmark problems and the

simulated results are analyzed using statistical techniques. This analysis efficiently provides the evaluation of performance value at each point of the design space of factor-tolerance, which is not possible by traditional robust topology optimization methods.

The importantcontribution of this work is to develop a method, which is used to obtain targeted performance for various topology optimization problems. Present analysis is helpful for the robust design of topologically optimized components.

## 5.2 TOLERANCE RANGE SELECTION USING CA-DOE METHOD

As described in the previous chapters, DOE refers to a process of systematic design and analysis of the experiment, which enables to reach the conclusions efficiently.In order to use DOE approach for tolerance range selection, the uncertainties due the tolerances of factors are required to be incorporated in the experiments. For such condition, a usual DOE technique requires high computation costs. To reduce expensive computation, a cross array based DOE approach proposed by Taguchi is utilized (Sung 1998; Mitra 2008; Montgomery 2007). In this method, two different orthogonal arrays (OA) are designed or selected, termed as inner and outer OA. Here, inner and outer OA accommodate the levels of control factors and noise factors respectively. The product of these two arrays forms a cross array. Initially, the factors, their levels, and interactions need to be determined to design an experiment. For the tolerance range selection, each selected factor is considered as statistically independent variable. In addition, the random error generated, within a given tolerance range of each of these factors is also considered as statistically independent variable. This error is treated as noise. Specifically, noises indicate the deviation of the tolerance from the nominal value. Thus, the selected variables are assigned a limited set of discrete levels. In this method, normally two levels (i.e. loose and tight) are recommended to investigate linear variation in the system. Here, the OA'sare employed to investigate the controllable factors and their noise in one experiment. The role of inner and outer OA's are specifically mentioned here,

*Inner OA*: For controllable factors, an inner OA is used. It consists of the all combinations of tolerance levels of the controllable factors. If there are 'n' control factors with two levels, the total number of combinations will be $2^p$, as shown in Fig. 5.1.

*Outer OA*: For noise of above controllable factors, outer OA is used. The number of controllable factors, their levels, and the number of selected interactions is required to

identify the correct OA that suits the scenario (Sung 1998; Mitra 2008; Montgomery 2007). Based on this criterion, an OA is selected. This array represents the worst case of tolerance deviations in terms of maximum limits of Gaussian distribution, i.e. $+3\sigma$ and $-3\sigma$.

| Noise factors | Orthogonal Array | | |
|---|---|---|---|
| $A_1$ | 1  1 . . . 1 | | |
| $A_2$ | 1  2 . . . 2 | Outer OA | |
| ... | . . . . . . . | | |
| ... | . . . . . . . | | |
| $A_n$ | 2  2 . . . 2 | | |

| Combination No. | Controllable Factors $F_1$  $F_2$  .....$F_p$ | Response Values | Mean Response | $\overline{\text{Signal}}$ / Noise |
|---|---|---|---|---|
| 1 | 1  1 . . . 1 | $S_{11}\,S_{12}...\,S_{1T}$ | $M_1$ | $SNR_1$ |
| 2 | 1  1 . . . 2 | $S_{21}\,S_{21}....S_{2T}$ | $M_2$ | $SNR_2$ |
| ... | . . . . . . . | . . . . . . . | ... | ... |
| ... | . . . . . . . | . . . . . . . | ... | ... |
| $2^p = Q$ | 2  2 . . . 2 | $S_{C1}\,S_{C1}....S_{CT}$ | $M_Q$ | $SNR_Q$ |

Inner OA
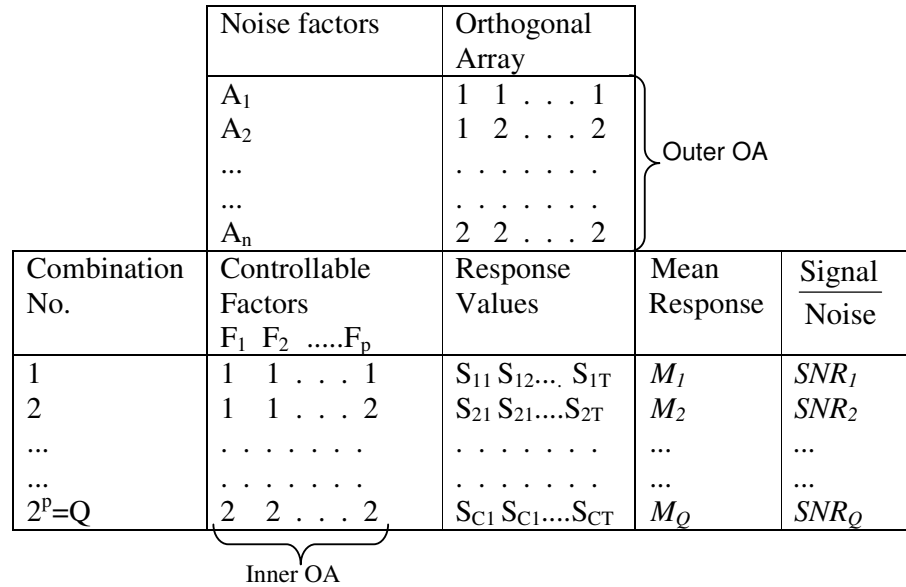
**Fig. 5.1: Structure of a CA-DOE technique**

The framework for CA-DOE is shown in Fig. 5.1. Here, there are '$p$' numbers of controllable factors, which may have a few levels of noise. Based on number of factors and their number of levels of noise, the outer OA are selected form the Taguchi's OA. Taguchi's OA helps to reduce the number of replication required to simulate the performance, whereas any other OA will increase the number of replication (Sung 1998; Mitra 2008; Montgomery 2007). In the selected outer OA, 1 and 2 represents the extreme limits of random variable, which have Gaussian distribution. For each combination in inner OA, the data for each outer OA noise combination are treated as replication. By doing so, the effect of noise is incorporated in each combination of inner OA. Thus, a cross array consists of all combinations of levels of control and noise factors. Finally, experiments or simulations are conducted for each combination of cross array. The obtained results of experiments are analyzed using various statistical techniques. The outcome of the experiment is robust because it incorporates the effect of noise factors. From this experiment, a response function for the performance can also be generated.

The CA-DOE method is beneficial in many aspects. It is faster, as the use of OAs simplifies the experimental design procedure compared to normal DOE approach. It

simulates the worst-case scenarios and uses lesser computation compared to the Monte Carlo simulation. Besides the robust design optimization method, CA-DOE method gives the fine resolution of results for the each incremental change of tolerance of factor. Since the increments are generated in terms of the each possible combination of controllable factor-tolerance, it provides much flexibility to the designer. The details of the proposed methodology are given in next section.

## 5.3    METHODOLOGY

In the tolerance range selection problems, it is required to find out the acceptable range of variation around the nominal settings of selected factors, based on the performance values. The strategy here is to replace the noise factor by the tolerance deviation of the controllable factors. Here, the tolerances can be tight or loose based on tradeoff between the effort applied in tolerance setting, and performance variations. The steps of the methodology are given below,

Step 1. **Selection of problem and performance measures:** In this step, problem is selected for analysis, or a given problem is well defined for its boundary conditions, etc. The performance measures are defined based on application requirements.

Step 2. **Input factor and their tolerance range:** Main input factors are identified and their tolerance values are decided based on the realistic values. While applying CA-DOE approach, these factors are considered as controllable factors.

Step 3. **Design of orthogonal array for tolerance of factors:** In order to apply CA-DOE approach, inner and outer arrays are to be designed or selected. This selection is made based on the number of factors and their levels (Sung 1998; Mitra 2008; Montgomery 2007).

Step 4. **Simulation of performance values:** To simulate the performance values and optimal topology a topology optimization method is chosen and the simulations are performed based on the cross array.

Step 5. **Analysis of simulated results:** The simulated performance values are analyzed using different statistical measures. In addition, the targeted and robust performances are also analyzed.

This method attempts to determine optimum tolerance of the chosen structural problems. The implementation details of CA-DOE approach has been provided in next section.

## 5.4    IMPLEMENTATION OF PROPOSED METHODOLOGY

The tolerance design of a topologically optimized structure is carried out using CA-DOE approach. The details of each step of this approach are given in this section.

### 5.4.1    Selection of problem and performance measures

To implement the CA-DOE approach, four-benchmark problems discussed in Chapter 3 are selected. The rationale behind selecting these four benchmark problems is to provide generic prescriptions to designers regarding the impact of the tolerance of input factor on topologically optimized structure, and not problem dependent solutions. To analyze the impact of the tolerances of input factor on the outcome of simulation, compliance and deflection values are selected as performance measures.

### 5.4.2    Input factor and their tolerance range

The tolerance values of applied force, volume fraction, aspect ratio, and elasticity are selected to analyze their effects on performance value. The selection of nominal values for these factors is based on the results of performance analysis, carried out in Chapter 3 & 4. The nominal values for each of these factors are provided in Table 5.1. Different realistic tolerance ranges are defined for each of these factors, based on literature. The tolerances are grouped into two ranges, loose and tight tolerance. The values of these tolerances are also available in Table 5.1. The values of these tolerances are generated by considering its variation/spread around the nominal value. Hence, this variation will be equal to the spread of the normal distribution i.e. within the ±3σ limits. The standard deviation σ can be determined from this consideration. A Separate discussion on each of these factor tolerances is given in following sections,

#### 5.4.2.1    Tolerance of applied force

Applied force is a factor, which is considered at the initial design phase of topology optimization. Force has very less effect on the topology but it changes the value of compliance and deflection by a large amount, as observed in Chapter 3. To ensure the desired performance value, applied force value should not change. However, variations

in its value of applied force is always possible in realistic situations, and generally, 10%-20% variation is considered in the available literature (Jung and Cho 2004; Kim et al. 2007; Eom et al. 2010). In the present work, a 10% variation from the nominal value of force is considered to generate the loose tolerance limit and 5% of that is considered to generate the tight tolerance limit.

### 5.4.2.2    *Tolerance of aspect ratio*

The tolerance of aspect ratio for the considered material domain is chosen as another factor. To proceed with this analysis, two different tolerance values are assumed for the aspect ratio, named as tight and loose tolerance. Their values are dependent on manufacturing process and different for macro and micro domain. A suitable range of aspect ratio is selected here, which are given in Table 1. In the present work, a 5% variation from the nominal value of aspect ratio is considered to generate the loose tolerance limit and 1% of that, is considered for generating the tight tolerance limit.

### 5.4.2.3    *Tolerance of volume fraction*

Volume fraction is an important factor, which affects the topology and performance value. It is directly linked to the topology and the uncertainty in the manufacturing process (Kharmanda et al. 2004, Sigmund 2009). Like aspect ratio, a suitable range of volume fraction is selected and given in Table 5.1. In the present work, a 10% variation from the nominal value of volume fraction is considered to generate the loose tolerance limit and 5% of that, is considered for generating the tight tolerance limit.

### 5.4.2.4    *Tolerance of elasticity value*

The tolerance of material property is considered in terms of the modulus of elasticity value. Similar to applied force, the value of modulus of elasticity does not change the topology but effects compliance value and deflection value. In the available literature, 10%-20% variation  of modulus of elasticity is considered for topology optimization problems (Jung and Cho 2004; Kim et al. 2007; Eom et al. 2010). In the present work, a 10% variation from the nominal value of elasticity is considered to generate the loose tolerance limit and 5% variation for generating the tight tolerance limit.

**Table 5.1: Nominal values and loose and tight tolerance range for the selected factors**

| S. No. | Factor | Nominal Value | Loose tolerance | Tight tolerance |
|--------|--------|---------------|-----------------|-----------------|
| 1 | Force (N) | 100 | ±5 | ±2.5 |
| 2 | Aspect Ratio | 1.2 | ±0.03 | ±0.006 |
| 3 | Elasticity (GPa) | 200 | ±10 | ±5 |
| 4 | Volume fraction | 0.60 | ±0.03 | ± 0.015 |

It is important to note that, the presented work also focuses on the manufacturing uncertainty in the form of tolerances of aspect ratio and volume fraction. This approach is also useful where a secondary process like shape, size optimization, or manual modification on the optimal topology is performed before the manufacturing. Hence, the approach presented in this chapter is a generalized one, where manufacturing uncertainties or a secondary modification processes are considered.

### 5.4.3  Design of orthogonal array of tolerance

As stated earlier, based on the number of factors and their tolerance level, the inner and outer OA are designed. In the present case, there are four controllable factors and their noises are treated at two levels i.e. loose and tight tolerances. Hence, experimental combinations are generated based on these values. This combination set is the inner OA, as shown in Appendix A5. To select the outer OA, the number of controllable factors and their noise levels are required to be identified. The outer OA represents the worst case of tolerance deviations in terms of maximum limits of Gaussian distribution, i.e. $+3\sigma$ and $-3\sigma$. Hence, each factor tolerance is defined with two levels. Thus, for four factors with two level of noise, Taguchi's $L_8$ outer OA is selected as shown in Appendix A7 (Mitra 2008; Sung 1998; Montgomery 2007). The product of the Inner and outer OA is shown in Table 5.2. The table at the top shows the outer OA, while the table at bottom shows inner OA. It can be seen that the outer OA consist the values of each factor by incorporating its maximum variation with the nominal values. Here the notation A, E, F, and V, indicates the nominal values of aspect ratio, elasticity, force, and volume fraction respectively. In the outer OA, the combination of loose and tight tolerance can be seen. The notation L and T represents the loose and tight tolerance respectively. The simulations are carried out by considering a combination of the inner OA, replicated by

each run of outer OA. The corresponding simulations are shown as $R_{i,j}$, where, $'i'$ is the combination of inner OA, and $'j'$ is the run of outer OA. Finally the mean and SNR of each combination of inner OA is obtained, using $R_{i,j}$'s. The process use to obtain the optimal topology with the performance is described in the next section.

**Table 5.2:CA-DOE approach**

| Run No. | 1 | 2 | … | 8 |
|---|---|---|---|---|
| Aspect ratio | A-3 $\sigma_A$ | A-3 $\sigma_A$ | … | A+3 $\sigma_A$ |
| Elasticity | E-3 $\sigma_E$ | E+3 $\sigma_E$ | … | E+3 $\sigma_E$ |
| Volume fraction | V-3$\sigma_V$ | V-3$\sigma_V$ | … | V-3$\sigma_V$ |
| Force | F-3 $\sigma_E$ | F+3 $\sigma_E$ | … | F+3 $\sigma_E$ |

| Combination No. | Aspect ratio $\sigma_A$ | Elasticity $\sigma_E$ | Volume fraction $\sigma_V$ | Force $\sigma_F$ | | | | | Mean | SNR |
|---|---|---|---|---|---|---|---|---|---|---|
| 1 | L | L | L | L | $R_{1,1}$ | $R_{1,2}$ | … | $R_{1,8}$ | $M_1$ | $S_1$ |
| 2 | L | L | L | T | $R_{2,1}$ | $R_{2,1}$ | … | $R_{2,8}$ | $M_2$ | $S_2$ |
| ... | … | … | … | … | … | … | … | … | | |
| ... | … | … | … | … | … | … | … | … | | |
| 16 | T | T | T | T | $R_{16,1}$ | $R_{16,2}$ | … | $R_{16,8}$ | $M_{16}$ | $S_{16}$ |

### 5.4.4 Simulation of compliance and deflection using SIMP

To simulate the performance values and optimal topology, a MATLAB code is written. In this code, the finite element routine is made flexible to handle non-square elements, as the aspect ratio varies in a small range. The problem of local minima is handled by applying an oscillation filter. Here, the filter detects the oscillations in the compliance value, which prolongs infinitely and results do not converge. In such scenario, the value of minimum compliance from a repetitive oscillation is selected and other values (deflection, volume fraction) corresponding to this is recorded. The steps used in code for implementation is given below,

Step 1. The initial data, i.e. mesh size, length and width of material domain, nominal values of the factors and their loose and tight tolerances are defined

Step 2. Inner and outer OAs are selected and their combinations are generated

Step 3. Values of each factor are determined using the proposed cross array approach

Step 4. The topology optimization problem is defined according to SIMP approach. Penalty value is set as three

Step 5. The first iteration is started with initial guess of density parameter '*x'*. The stiffness matrix of material domain based on density matrix is found out. Using this, the deflection at each node is calculated by finite element formulation, incorporating non-square elements

Step 6. The objective function is evaluated

Step 7. Optimality criterion is applied with mesh independency filter to update the density parameter

Step 8. If convergence is achieved, then iteration is terminated and the compliance, deflection value, and topology are recorded.

Step 9. If convergence is not achieved then the process is repeated from step 5 to 8.

Step 10.  Along with steps 8 and 9, a routine on oscillation filter is implemented to check the oscillation in the simulated objective function. If repetition in oscillation is observed then, the optimization routine is terminated and the minimum value of objective function, topology, and deflection values are stored.

Based on above steps, topology with the performance values is simulated for the considered problems. The methods used to analyze the results are discussed in next section.

### 5.4.5   Analysis of simulated results

By the application of CA-DOE and SIMP, the values of performance are obtained. The mean and SNR values of compliance and deflections are computed for each combination of inner OA. In addition, ANOVA is used and its results are provided for the significant factors and the functional relation between performance and tolerance values is obtained. The analysis is carried out based on obtained results, which is detailed in next section.

### 5.5   ANALYSIS AND DISCUSSION

In this section, the simulated compliance and deflection values for chosen benchmark problems are analyzed using different statistical measures. For simulation, FE mesh size

is varied i.e. 12×10, 24×20, 36×30, & 60×50, and observed that the trend of performances remain same for the different mesh sizes (Javed and Rout 2012). This is due to mesh independency filter used in the simulation (Bendsøe and Sigmund 2003). For illustration, the topologies at different mesh sizes are shown in Fig. 5.2. In present chapter, the mesh size 60×50 is used for analysis. The effect of small changes in the tolerances of factors can be captures with such fine mesh size.

| | Mesh size 12 x 10 | Mesh size 24 x 20 | Mesh size 36 x 30 | Mesh size 48 x 40 | Mesh size 60 x 50 |
|---|---|---|---|---|---|
| Problem 1 | | | | | |
| Problem 2 | | | | | |
| Problem 3 | | | | | |
| Problem 4 | | | | | |
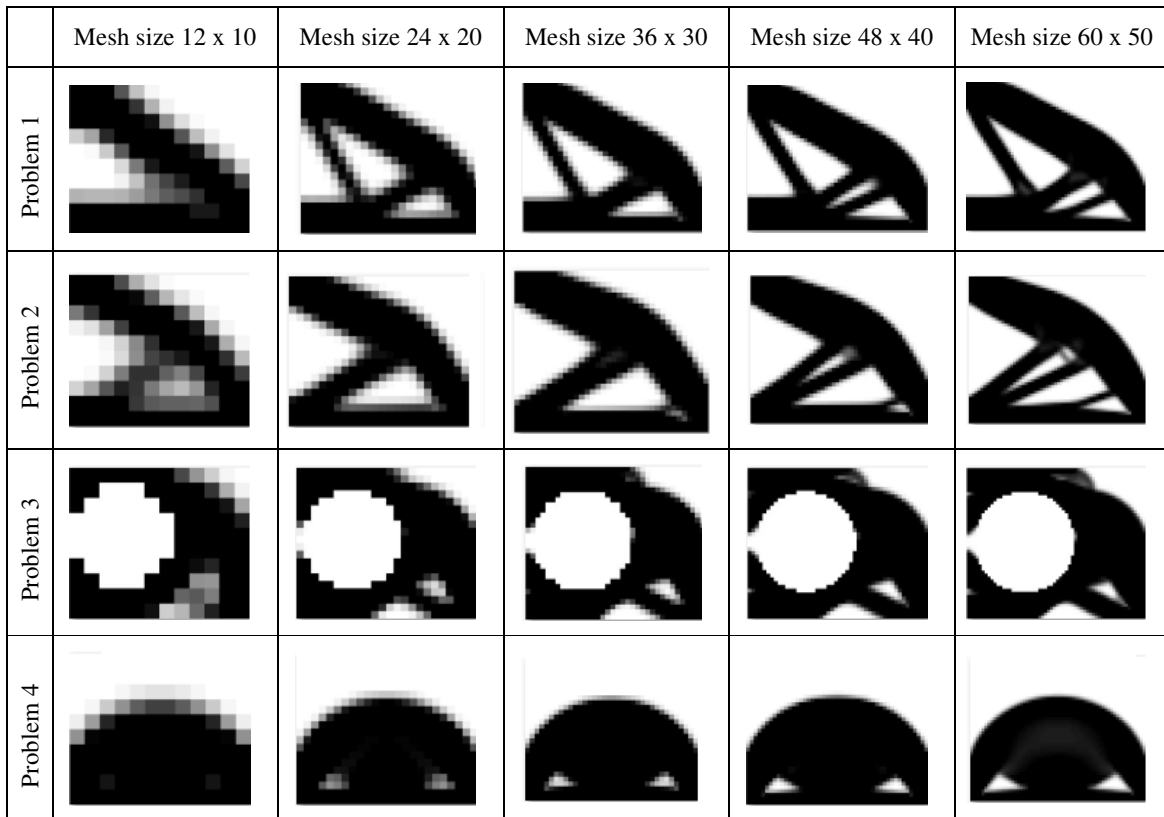


**Fig. 5.2: Optimal topologies with different mesh sizes**

By applying CA-DOE, for each problem and each mesh size, results are observed corresponding to the each combination in inner OA. For illustration, one set of the results of problem-1, for mesh size 60×50 is provided in Table 5.3. The topologies look alike, but the compliance and deflection values differ in each case. This is observed because the tolerance values introduce very small change in factor values. The discussion regarding performance analysis is given in next section.

**Table 5.3: Optimal topologies for 60×50 mesh size**

| Inner OA (C. No.)† | Outer OA (Run No.) ‡ | | | | | | | |
|---|---|---|---|---|---|---|---|---|
| | 1 | 2 | 3 | 4 | 5 | 6 | 7 | 8 |
| 1 | | | | | | | | |
| 2 | | | | | | | | |
| 3 | | | | | | | | |
| 4 | | | | | | | | |
| 5 | | | | | | | | |
| 6 | | | | | | | | |
| 7 | | | | | | | | |
| 8 | | | | | | | | |
| 9 | | | | | | | | |
| 10 | | | | | | | | |
| 12 | | | | | | | | |
| 13 | | | | | | | | |
| 14 | | | | | | | | |
| 15 | | | | | | | | |
| 16 | | | | | | | | |
| | † Refer Appendix Table A6, ‡Refer Appendix Table A7 | | | | | | | |

### 5.5.1 Signal to noise ratio

As detailed in section 3.4.3, the SNR of compliance is computed from the simulated values and shown in Fig. 5.3.
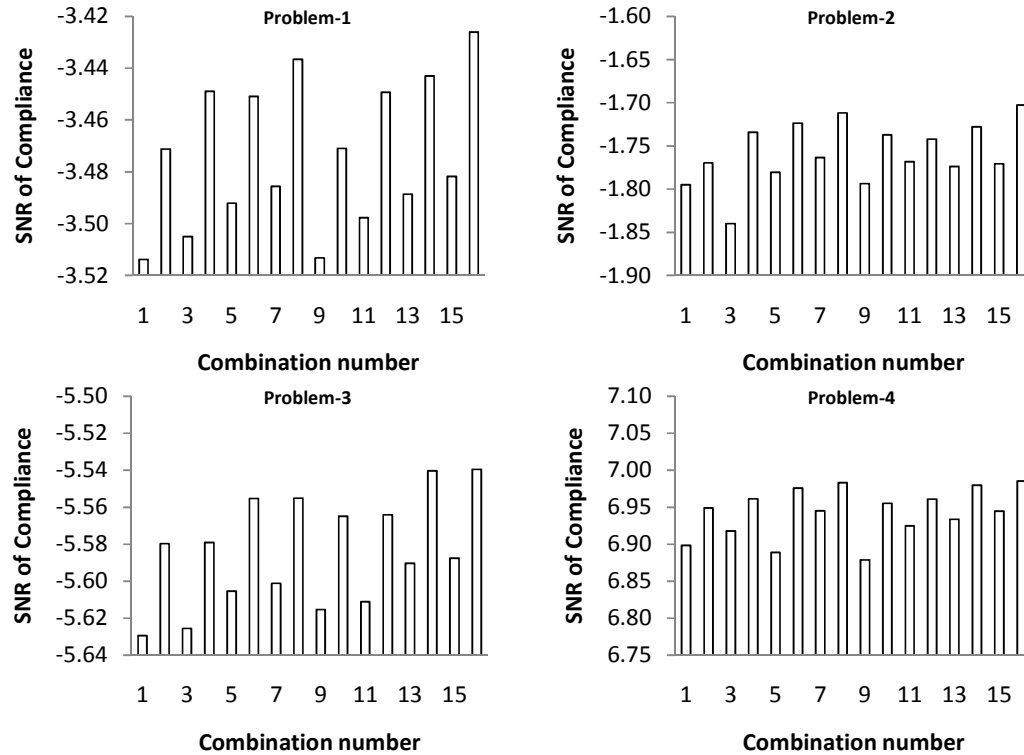


**Fig. 5.3: SNR of compliance for chosen problems**

The SNR values are shown for each combination in inner OA, for the four benchmark problems. It can be observed from the obtained SNR values that the last combination in each problem gives the maximum SNR. Hence, the $16^{th}$ combination of tolerance is the robust design for the corresponding problems. This is an obvious result for all the problems as all factors are in its tight tolerance range. It also represents the ideal situation where the designer desires to keep all factors very close to the nominal values. In other words, the noise of each factor around its nominal value is very limited. To achieve this condition practically, lot of effort is required in terms of cost and time. Hence, to reduce the effort in minimizing the effect of noise factors the next highest SNR value should be selected which will be another choice for robust design. In the same way, depending upon the degree of robustness other combinations can be chosen and analyzed. The tolerance combinations, which provide same result, are grouped together. Hence, three groups are formed for each problem. Based on the suitability of keeping loose tolerance, any combination of a group can be selected, without sacrificing the performance. The combinations of tolerance, which give the best results for

problem-1 are, 16, 14, 12, 8, 6, and 4. The group of combination number 2, 10, and 15 provide satisfactory result. Group of combination number 1, 3, 5, 7, 9, 11, and13, show the worst result. For problem 2, group of combination number 16, 14, 12, 10, 8, 6, and 4 shows best result and group of combination number 1 and 3 show worst result. For problem 3, group of combination number 16, 14, 12, 10, 8, and 6 show best result and group of combination number 11, 9, 7, 5, 3, and 1 shows worst result. For problem 4, group of combination number 16, 14, 12, 10, 8, 6, and 4 shows best result. Group of combination number 9, 5, and 1 shows worst result. These observations for SNR of the compliance value are summarized in Table 5.4.

In similar way, SNR for maximum deflection of each problem is plotted using bar chart and shown in Fig. 5.4. Using this bar chart, the selection of tolerance combination with high SNR for deflection should be selected. This selection is purely based on reduced effort to keep a tolerance limit in tight range. It is seen that for problem-4 the trend is different from the other problems. It is because of the effect of tolerance values for specific physics of the problem. The remaining observation and analysis are similar to the case of compliance value. The observations for SNR of the deflection are summarized in Table 5.4.
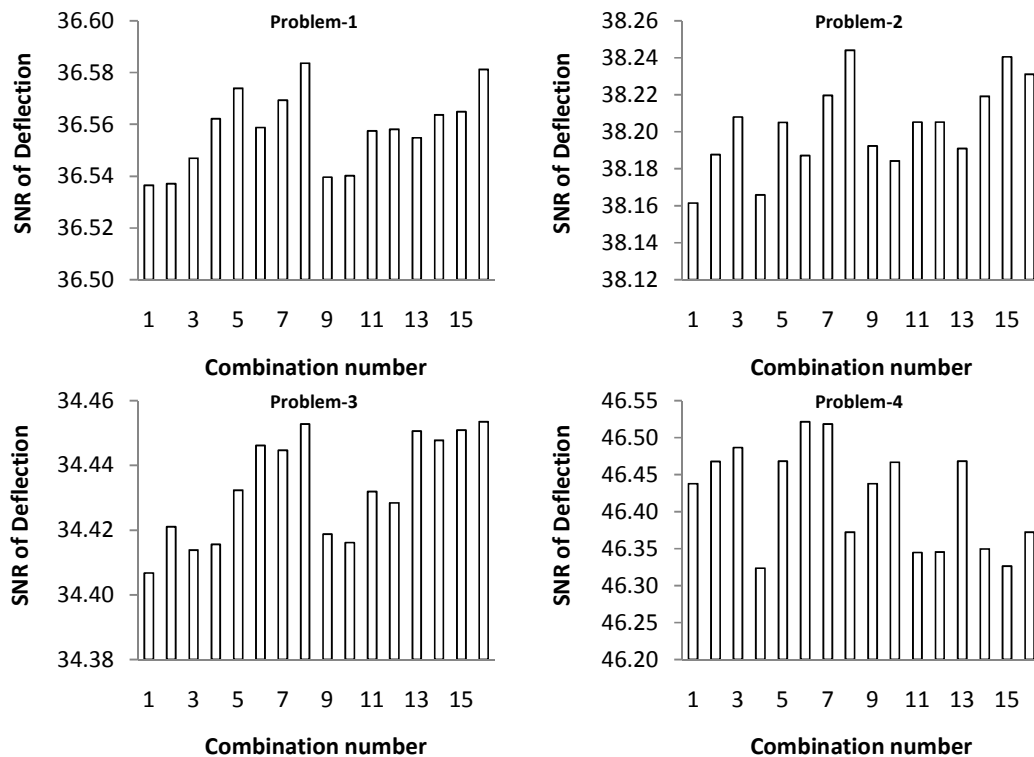


**Fig. 5.4: SNR of deflection for chosen problems**

**Table 5.4: Tolerance combination group for SNR of performance functions**

| | SNR of Compliance | | |
|---|---|---|---|
| | Group 1 | Group 2 | Group 3 |
| Problem 1 | 16, 14, 12, 8, 6, 4 | 15, 10, 2 | 13, 11, 9, 7, 5, 3, 1 |
| Problem 2 | 16, 14, 12, 10, 8, 6, 4 | 15, 13, 11, 9, 7, 5, 2 | 1, 3 |
| Problem 3 | 16, 14, 12, 10, 8, 6 | 15, 13, 4, 2 | 11, 9, 7, 5, 3, 1 |
| Problem 4 | 16, 14, 12, 10, 8, 6, 4 | 15, 13, 11, 7, 3, 2 | 9, 5, 1 |
| | SNR of deflection | | |
| | Group 1 | Group 2 | Group 3 |
| Problem 1 | 16, 15, 14, 12, 8, 7, 6, 5, 4 | 13, 11 | 10, 9, 3, 2, 1 |
| Problem 2 | 16, 15, 14, 8, 7 | 13, 12, 11, 9, 5, 3, 2 | 10, 6, 4, 1 |
| Problem 3 | 16, 15, 14, 13, 8, 7, 6 | 12, 11, 5 | 10, 9, 4, 3, 2, 1 |
| Problem 4 | 13, 10, 7, 6, 5, 3, 2 | 9, 1 | 16, 15, 14, 11, 12, 8, 4 |

The change in the combination numbers can be seen by comparing the compliance and deflection results. It can be concluded that the deflection and compliance values change differently for the same values of factors and tolerances. It can be intuitively predicted that the trend of SNR of deflection value will be same as SNR of compliance value. Logically, with the increasing compliance, the maximum deflection should also increase. However, this is not observed from the obtained values. To get an insight, all the obtained compliance values are plotted along with its corresponding maximum deflection values. In Fig. 5.5(a) the obtained compliance values are arranged in ascending order and the corresponding maximum deflections are plotted in Fig. 5.5(b). Curve, C1, C2, C3, and C4 represents the compliance values for problem-1, 2, 3 & 4 respectively, and curve D1, D2, D3 & D4 represents the maximum deflections obtained for problem-1, 2, 3 & 4 respectively. It can be observed that the corresponding maximum deflections do not increase smoothly, and has small variations, with increasing trend. Due to this variation, the intuitive prediction goes wrong and mismatch in the combination number is observed.

(a)



(b)
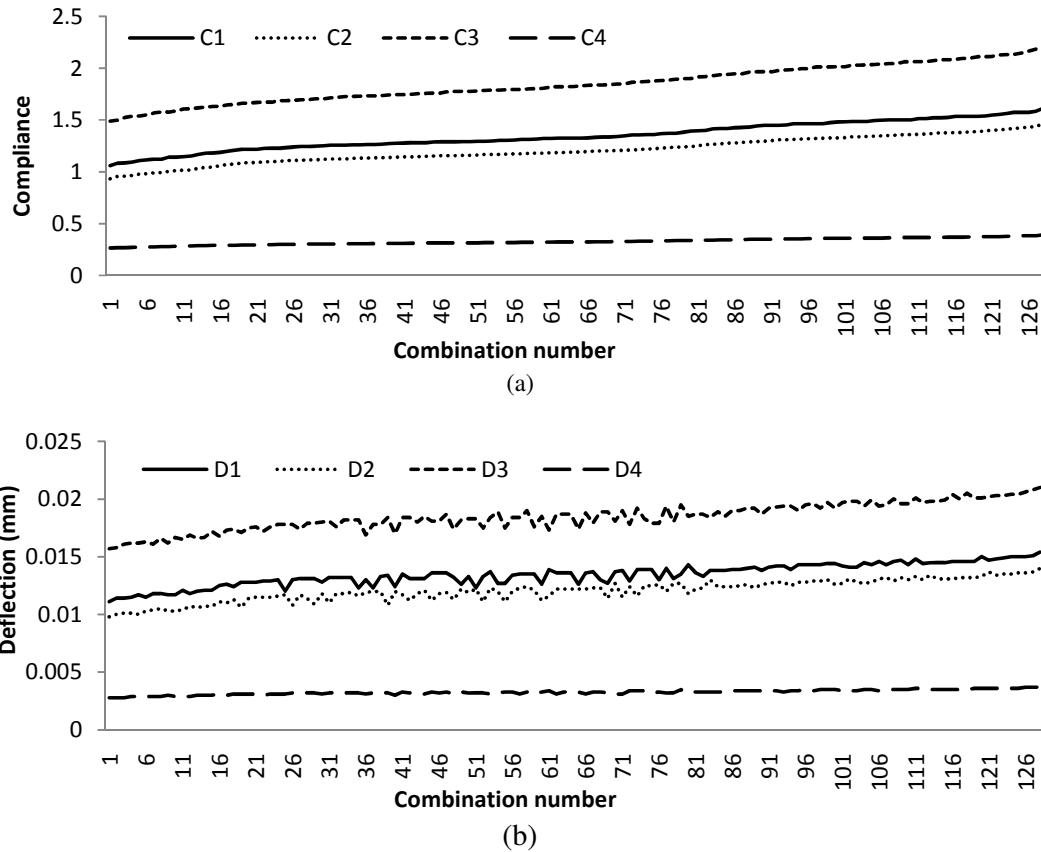
**Fig. 5.5: Variation of (a) compliance and (b) deflection values**

A smooth increasing curve for maximum deflection would have been observed, if only one input factor, or many factors of similar sensitivity had been incremented. Hence, in case of combined variation of factors, the compliance value behaves differently. From above discussion, it can be also said that a targeted compliance value can be the obtained by the set of different combination of input factor-tolerances.

### 5.5.2 Targeted performance value

Due to the variation of the tolerances, the performance value is altered from its desired value. In order to achieve the desired value of performance, the identification of the tolerance combination is needed, which produces at par performance. In this way, the cost and effort required to tighten all factor tolerance can be reduced. To do so, the mean values of the performances are analyzed here.

From the results obtained by the CA-DOE approach, the mean value of the compliance is computed for each run of inner OA. The bar chart for the four problems containing the mean compliance value for each combination is shown in Fig. 5.6.
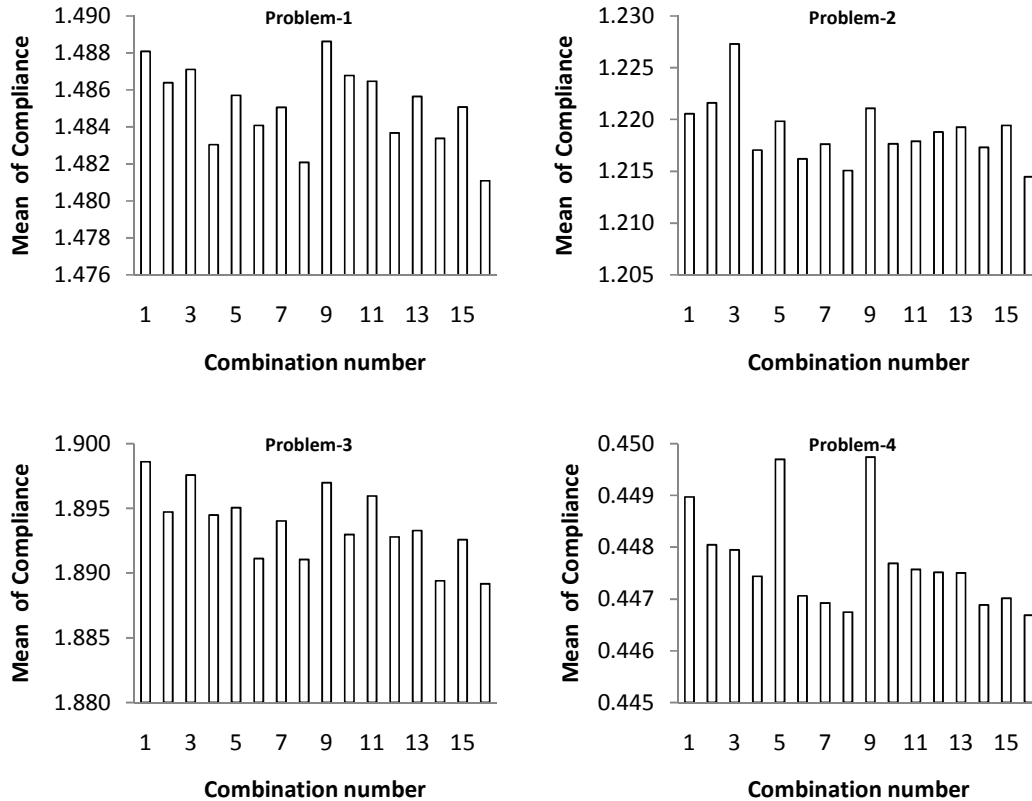


**Fig. 5.6: Mean of compliance for chosen problems**

From Fig. 5.6, the combination of tolerance can be selected which show the lowest value. These results are more or less similar to the SNR value of compliance, leaving a few combinations. In Table 5.5, the observations on mean values of compliance are summarized in form of combination groups. Further analysis on mean deflection will open the other aspect of selection of combination based on maximum deflection in the beam/plates.

Similar to the mean compliance values, the mean deflection values are presented in Fig. 5.7.From these results, the combination that gives a minimum deflection can be identified. Similar to SNR of deflection of problem-4 the irregular trend is observed for mean deflection of the same problem. As discussed earlier, it is because of the specific physics of the problem. For other problems also, the best combinations are different from that of the SNR of maximum deflections. The earlier discussion on reasons applies here.
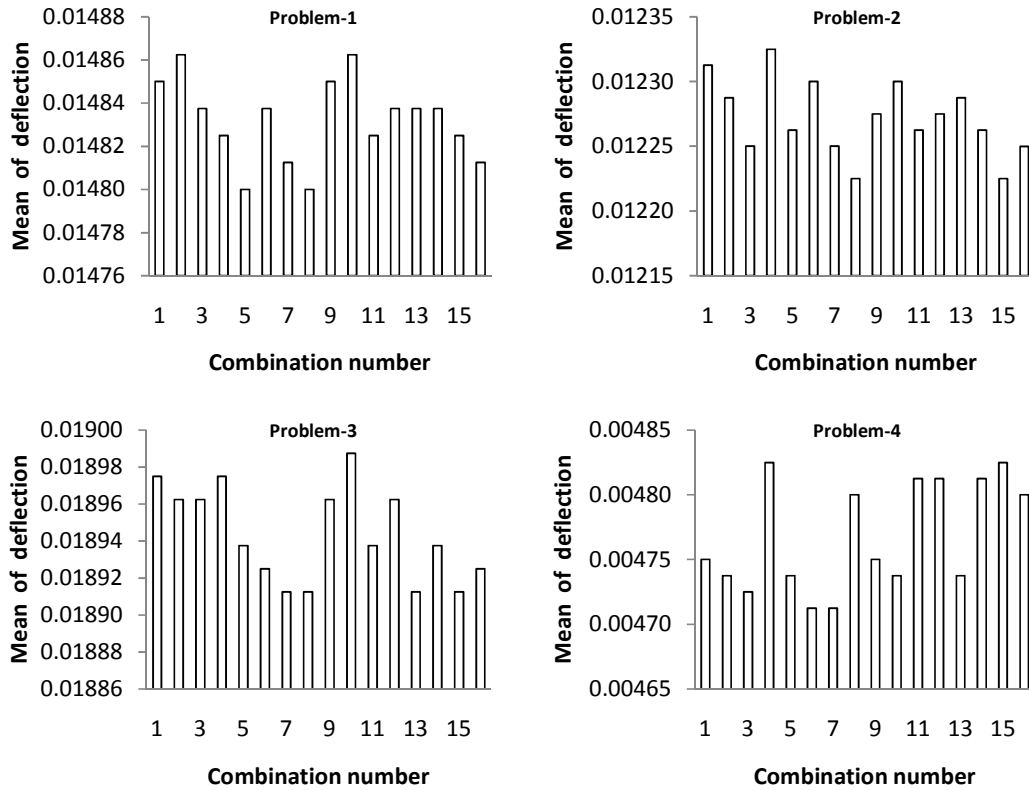
**Fig. 5.7: Mean of deflection for chosen problems**

The summary of tolerance combination for mean values of deflections is provided in Table 5.5. The variations present in results of fourth problem is very minute, hence the combinations can be divided into two groups only. In this table, Group 1 is the best performance and the subsequent groups are arranged for descending order of performances.

**Table 5.5: Tolerance combination groups for mean of performance**

| | Group 1 | Group 2 | Group 3 |
|---|---|---|---|
| **Mean of Compliance** | | | |
| | Group 1 | Group 2 | Group 3 |
| Problem 1 | 16, 14, 12, 8, 4 | 15, 13, 7, 6, 5 | 11, 10, 9, 3, 2, 1 |
| Problem 2 | 16, 14, 12, 11, 10, 8, 7, 6, 4 | 15, 13, 9, 5, 2, 1 | 3 |
| Problem 3 | 16, 14, 8, 6 | 15, 13, 12, 10, 7, 5, 4, 2 | 11, 9, 3, 1 |
| Problem 4 | 16, 15, 14, 13, 12, 11, 10, 8, 7, 6, 4 | 3, 2 | 9, 5, 1 |
| **Mean of Deflection** | | | |
| | Group 1 | Group 2 | Group 3 |
| Problem 1 | 16, 8, 7, 5 | 15, 14, 13, 12, 11, 6, 4, 3 | 10, 9, 2, 1 |
| Problem 2 | 16, 15, 14, 11, 8, 7, 5, 3 | 13, 12, 10, 9, 6, 2 | 4, 1 |
| Problem 3 | 16, 15, 14, 13, 11, 8, 7, 6, 5 | 12, 9, 3, 2 | 10, 4, 1 |
| Problem 4 | 13, 10, 9, 7, 6, 5, 3, 2, 1 | 16, 15, 14, 12, 11, 8, 4 | --- |

From above, it can be concluded that combination number 16 and 8 are best suited for all problems. The significance of factor tolerance will provide more insight about these observations, given in next section.

### 5.5.3 Analysis of variance

The obtained values of mean compliance and deflection for four problems are analyzed using ANOVA with the help of Design expert software 8.0.7.1 (2011), and the results are presented in Table 5.6. In this table, the statistically significant factor, and the regressive relationship between the factor-tolerance and performance measure is provided. Similarly, statistically significant factors are provided in Table 5.7. From mean compliance analysis of all the four problems, it can be observed that all factors are statistically significant. By observing the response equation, the effect of each factor can also be analyzed separately. For the problems 1-3, volume fraction is statistically significant followed by, force, elasticity, and aspect ratio has least effective on performance. For problem 4, force is statistically significant followed by, elasticity, volume fraction, and aspect ratio has least effective on performance. Hence, for all the four problems, the designer can consider a loose tolerance for aspect ratio only.

**Table 5.6: Response equation for different problems**

| Analysis type - Mean compliance | |
|---|---|
| | Response equation |
| Problem 1 | $C1 = 1.484144 - 1.29 \times 10^{-3} \times F - 1.43 \times 10^{-3} \times V - 1.28 \times 10^{-3} E + 5.78 \times 10^{-4} \times A$ |
| Problem 2 | $C2 = 1.218823 - 1.15 \times 10^{-3} \times F - 1.6 \times 10^{-3} \times V - 1.07 \times 10^{-3} E + 5.19 \times 10^{-4} \times A$ |
| Problem 3 | $C3 = 1.893741 - 1.73 \times 10^{-3} \times F - 3.8 \times 10^{-3} \times V - 1.69 \times 10^{-3} E + 6.59 \times 10^{-4} \times A$ |
| Problem 4 | $C4 = 0.447716 - 2.8 \times 10^{-4} \times F - 1.3 \times 10^{-4} \times V - 2.7 \times 10^{-4} E + 8.44 \times 10^{-5} \times A$ |
| Analysis type - Mean deflection | |
| | Response equation |
| Problem 1 | $D1 = 0.01483 - 1.17 \times 10^{-5} \times V - 1.17 \times 10^{-5} \times E + 5.5 \times 10^{-6} \times A$ |
| Problem 2 | $D2 = 0.01227 - 9.38 \times 10^{-6} \times V - 1.25 \times 10^{-5} \times E + 1.6 \times 10^{-6} \times A - 1.56 \times 10^{-6} \times FV$ $+ 1.6 \times 10^{-6} \times FE + 4.7 \times 10^{-6} \times VE - 3.13 \times 10^{-6} \times VA$ |
| Problem 3 | $D3 = 0.01894 - 3.67 \times 10^{-5} \times V - 1.33 \times 10^{-5} \times E + 1.2 \times 10^{-5} \times A$ |
| Problem 4 | $D4 = 0.00477 - 5.47 \times 10^{-6} \times FE - 3.91 \times 10^{-6} \times VA + 2.3 \times 10^{-6} \times EA$ |
| C1,…,C4=Compliance, D1,…,D4=Deflection, F=Applied force, V=Volume fraction, E= Elasticity value, A=Aspect ratio | |

**Table 5.7: Statistically significant factors for different problems**

| Bench mark problems | Statistically significant input factors for compliance |
|---|---|
| Problem 1 | V, F, E, A |
| Problem 2 | V, F, E, A |
| Problem 3 | V, F, E, A |
| Problem 4 | F, E, F, A |
| **Bench mark problems** | **Statistically significant input factors for deflection** |
| Problem 1 | V, E, A |
| Problem 2 | V, E |
| Problem 3 | V, E, A |
| Problem 4 | FE, VA |
| F:Applied force, V:Volume fraction, E: Elasticity value, A:Aspect ratio ||

The response equation for problems 1-3, indicate volume fraction is the most significant factor and aspect ratio is the least significant factor. For problem 4, the interaction of force-elasticity and volume fraction-aspect ratio is statistically significant. It is seen that the targeted values of performance and, the combination with minimum variations in performance value can be achieved by relaxing the tolerance of few factors. It is advantageous, because the efforts required to keep tight tolerance are less. Needless to say, that the identification of such factors is valid for a particular range.

## 5.6 RELIABILITY BASED TOLERANCE RANGE SELECTION OF TOPOLOGICALLY OPTIMIZED STRUCTURES

Similar to Chapter 4, the reliability concept is applied in the present investigation to derive the suitable combinations of tolerances for the chosen problems. This will help to incorporate the noise of controllable factors. In the present work, the noise of controllable factors is treated as their tolerance values. The methodology used to generate the tolerance combinations is described below,

### 5.6.1 Methodology

The detail of the RBTO scheme is already discussed in section 4.3. The tolerance combinations are used in RBTO methodology to simulate the performances, subject to a given reliability index. The simulation method is presented in Table 5.8.

**Table 5.8: Methodology for reliability based tolerance analysis**

| Combination No. | Aspect ratio $\sigma_A$ | Elasticity $\sigma_E$ | Volume fraction $\sigma_V$ | Force $\sigma_F$ | | Compliance | Deflection |
|---|---|---|---|---|---|---|---|
| 1 | L | L | L | L | | $C_1$ | $D_1$ |
| 2 | L | L | L | T | **RBTO** | $C_2$ | $D_2$ |
| … | … | … | … | … | | | |
| … | … | … | … | … | | | |
| 16 | T | T | T | T | | $C_{16}$ | $D_{16}$ |

From Table 5.8, the application of RBTO in the simulation of tolerance values can be observed. Each combination of loose (L) and tight (T) tolerance of the factors is fed to the RBTO scheme. As discussed earlier in section 4.3 (Step 5), the RBTO method requires the nominal values of factors, their spread or tolerance values and the desired reliability index values to simulate the performance. In the present case, the nominal values and their tolerance are already defined (section 5.4.2). Using these values and a desired reliability index i.e. 3.8 and 3, the performances are simulated. The simulated results are provided and implications are discussed in next section.

### 5.6.2 Results and discussion

The simulated result for compliance and deflection at different reliability index are given in Figs. 5.8 & 5.9.
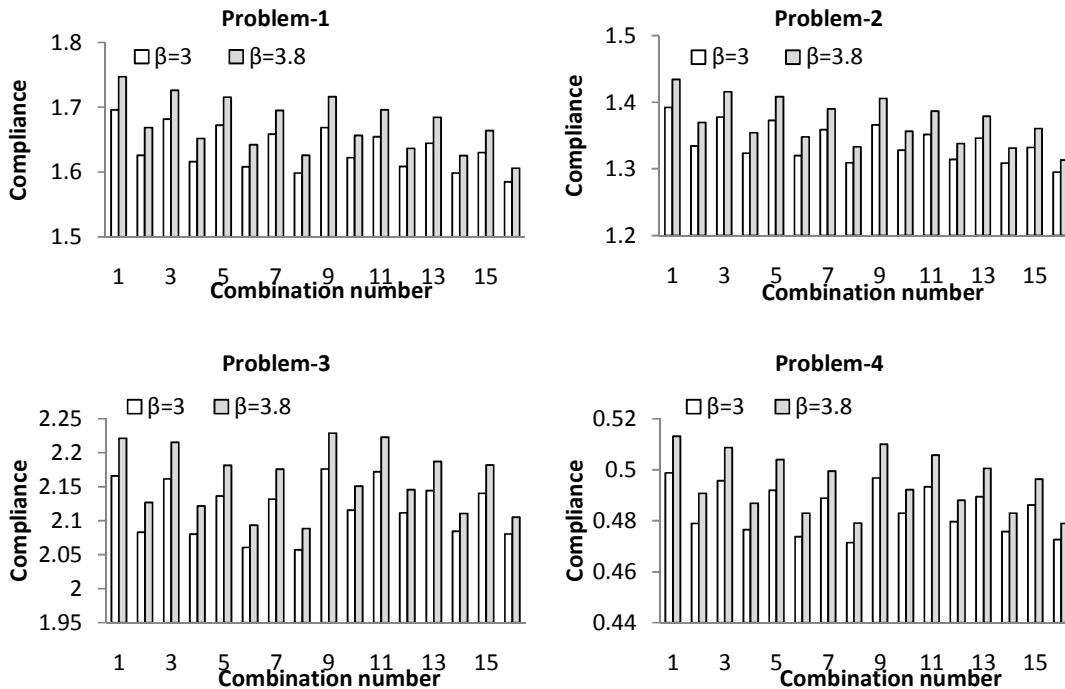


**Fig. 5.8: Compliance values using RBTO approach**

From Fig. 5.8 it is seen that, by introducing reliability index value, the compliance values increase. Also, with increase in reliability index β, the variation of the compliance values increases. These changes in the compliance values are because of the specific characteristics of the RBTO method, as discussed in section 4.3. The relative performance of the each combination is slightly changed compared to a CA-DOE based simulation. Therefore, present analysis is helpful to realize the targeted values of the performances in the new scenario.
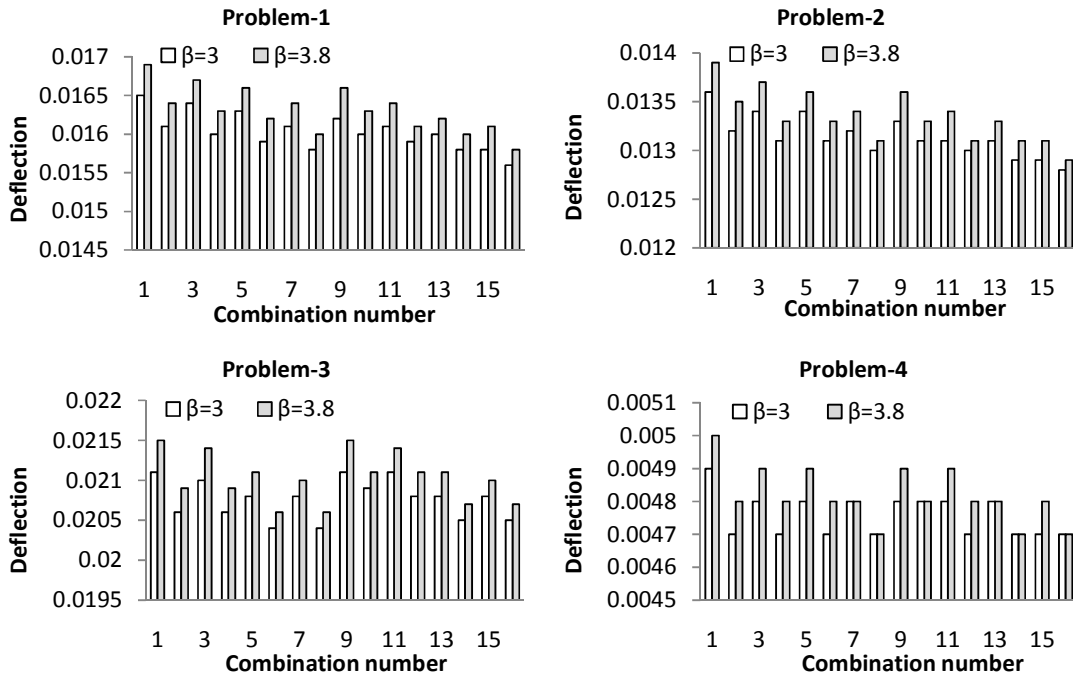


**Fig. 5.9: Deflection values using RBTO approach**

From Fig. 5.9 it is seen that, by introducing the reliability, the deflection values increase. Similar to the compliance, the deflection values also increase because of the RBTO method. However, for the fourth problem the observation is different. In this problem, for combinations 7, 8, 10, 13, 14, and 16 the deflection values remain same with increased values of reliability index. This happens because of the specific physics of problem-4, which produces less deflection compared to other problems at same factor tolerance values.

The results shown above can be utilized in the scenarios where reliability aspect is considered for the tolerance range selection. The different tolerance combinations are shown here with the corresponding performance values. Based on the performance and reliability requirement a suitable tolerance combination can be selected from the shown result.

## 5.7    CONCLUSIONS

In this chapter, a method to select optimum tolerance of input factors for topologically optimized structural problem is described. For the tolerance range selection, the tolerance of factor are identified and classified as loose and tight range. Using CA-DOE approach, the combination of tolerance was generated and the performance of the structure are simulated and analyzed in worst cases scenarios. As a result of this analysis, a selection process of the tolerance range is developed subject to robust and targeted performance. This selection method provides and aid to the designer, which considers the choice and affordability of the factor-tolerances. This method is illustrated with the use of benchmark problems. For most of the problems, it is found that the tolerance of aspect ratio is not significant and tolerance of force is highly significant. In order to include the uncertainty of the design factors a reliability based tolerance range selection procedure is also developed. The presented methodology can be applied for robust performance of realistic applications like, various structural elements; components of MEMS, i.e. micro cantilever, micro levers, force amplifier, etc. This methodology is applicable in the cases where obtained optimal topology can be reshaped further before manufacturing. There are other processes where the optimal topology is forwarded to the manufacturing department without any modifications. For such processes, an approach for tolerance range selection is presented in the next chapter.

# CHAPTER 6

## TOLERANCE RANGE SELECTION FOR TOPOLOGICALLY OPTIMIZED STRUCTURES WITH EFFECTS OF UNCERTAINTIES IN MANUFACTURING PROCESS

### 6.1 INTRODUCTION

The investigations on effects of input factors on optimal topologies were carried out in the Chapters 3 and 4. In Chapter 5, the effect of tolerance of same factor tolerances investigated further to generate the design, which is robust and provides targeted performance. In this work, the tolerances of the factors are treated as the uncertainty range. Proposed methodology offers flexibility to incorporate any numbers and type of the factors, which influence the performance. In addition, the tolerance of aspect ratio and volume fraction were included to consider the uncertainties caused by manufacturing or any other secondary process of topology modification. Thus, the methodology developed in Chapter 5 addressed the manufacturing uncertainties in a very generic way. From the literature, it is observed that a stream of current research (2009-2013) moves in the direction of uncertainties caused by the manufacturing processes. Various methods have been proposed by researchers to deal with the manufacturing uncertainties. In course of this investigation, the manufacturing uncertainties, and geometric uncertainties caused by the manufacturing processes are considered. Here, basic assumption is that the optimal topology should be replicated in the manufacturing process, without any further modification i.e. shape/size optimization. This assumption is valid for many of the topology-optimized components like, structures in MEMS, compliance mechanisms, etc. For such cases, the uncertainties of the manufacturing process have to be dealt corresponding to the specific manufacturing process. To address this, a simulation technique is required that simulates the uncertainties cause by a specific manufacturing process. Thus, a simulation method is proposed here, which is based on the modeling of

random placement of the material within the worst-case ranges. The methodology is very much similar to what is proposed in Chapter 5. The important difference here is the simulation of geometric uncertainty or imperfection due to manufacturing processes. For this purpose, the tolerance of volume fraction is utilized in the simulation of part and its impact on remaining controllable and non-controllable factors are incorporated in the same way, as discussed in Chapter 5. The simulation for uncertainties of manufacturing process uncertainty will provide better result compared to the generic approach developed.

## 6.2    SIMULATION FOR MANUFACTURING UNCERTAINTIES

In the present work, geometric uncertainty of the processes such as etching, e-beam lithography, laser micro-machining and milling processes is considered. The uncertainties involved in these processes lead to inaccurate deposition/doping/etching/cutting of the material. These inaccuracies are critical for topologically optimized components because the intended performance is dependent on proper material distribution. In order to simulate these uncertainties, a method based on random selection of density parameter is introduced. Usually, an extreme case on manufacturing uncertainties produces either too thin or thick members, as investigated by Sigmund (2009). This variation in the density parameter provide random volume fraction $\overline{V}(x)$. Thus, the compliance of the generated topology is also random. Mathematically this relation is expressed in equation (6.1).

$$\underset{x_D, x_R, x_A}{\text{Min}} : \begin{cases} C_D(x) = \sum_{i=1}^{n} [x_D]_i^p u_i^T K_0 u_i \\[2mm] C_R(x) = \sum_{i=1}^{n} [x_R]_i^p u_i^T K_0 u_i \\[2mm] C_A(x) = \sum_{i=1}^{n} [x_A]_i^p u_i^T K_0 u_i \end{cases}$$

$$\text{subject to :}$$
$$\overline{V}(x) \leq V_f \tag{6.1}$$
$$0 < x_{\min} \leq [x_D]_i, [x_R]_i, [x_A]_i \leq 1$$
$$i = 1, 2, 3, \ldots n$$

where, $C_D$, $C_R$, and $C_A$ are the compliance values corresponding to the dense, rare and accurate volume fractions and $x_D$, $x_R$, and $x_A$ are the density parameters. In actual scenario, the inaccuracy may lie within the domain of dense to rare material deposition.

Thus, the random density parameter can take any values from this domain. It is assumed that each density parameter independently attains a random value. In order to simulate the worst-case scenario, the random domain is discretized into three segments i.e. dense, rare and the accurate density parameter value. Thus, the simulated density matrix '$x_S$' can be expressed as a probabilistic function of the extreme values.

$$(x_s)_i = \Pi_{0,A}(\xi_i) \times (x_D) + \Pi_{A+\varepsilon,B}(\xi_i) \times (x_R) + \Pi_{B+\varepsilon,1}(\xi_i) \times (x_A) \qquad (6.2)$$

where, $\xi_i$ is a random variable, $\Pi_{(\cdot,\cdot)}$ is Boxcar function (David 2006) that is the function on Heaviside step function, $H$

$$\Pi_{a,b}(\xi) = H(\xi - A) - H(\xi - B) \qquad (6.3)$$

$$H(x) = \lim_{t \to 0}\left[\frac{1}{2} + \frac{1}{\pi}\tan^{-1}\left(\frac{x}{t}\right)\right] \qquad (6.4)$$

The Boxcar function acts as a coefficient and its values can be either zero or one, which is dependent on random variable $\xi_i$. Thus, it randomly selects any one of the density parameter in equation (6.2). The Boxcar function, $\Pi_{A,B}$ is equal to zero except in the interval [$A,B$] as shown in Fig. 6.1
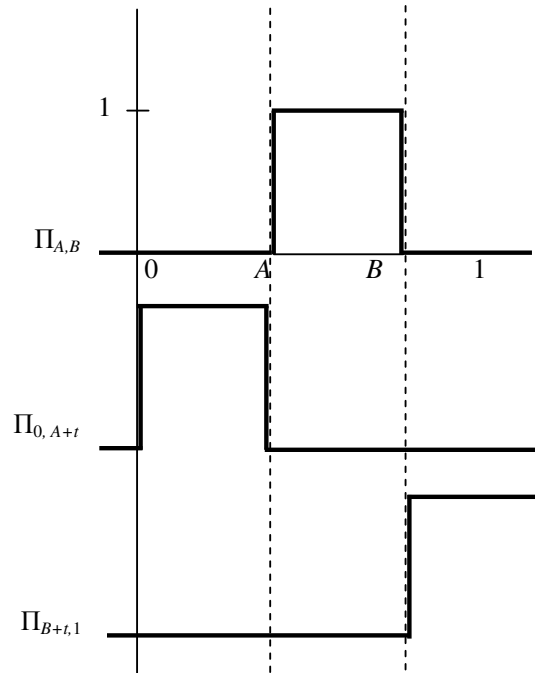


**Fig. 6.1: Boxcar function, $\Pi_{A,B}$**

In order to eliminate the overlapping values at the limits of Boxcar function, the adjacent interval limit is incremented by a small value *'t'*. In this interval, it is uniformly distributed and its probability is equal to one. In equations (6.2) & (6.3), $\xi$ is a random probabilistic variable, which lies in the interval [0, 1]. Thus, equation (6.2) represents a random selection of density parameter for each element. The selection is made using range of extreme manufacturing uncertainties including the accurate values also. To enable equal probability of the selection of density parameters for simulated density matrix $x_s$, the intervals [a, b], [b+$t$, c] and [c+$t$, d] are set as a=0, b=1/3, c=2/3 and d=1, where $t$ is small increment within the random field.

To illustrate the simulation, an example for such manufacturing process is shown in Fig. 6.2. The widely used MBB beam is selected and the optimal topologies are shown. The exact value of volume fraction is kept as 0.5. Due to the uncertainties in manufacturing process, the extreme cases of volume fraction may become 0.4 and 0.6 (Sigmund 2009). For this case, the randomized material distribution will be in the form of a function of the extreme and exact volume fraction cases, described by equation (6.1). Corresponding to the exact volume fraction, the optimal topology is shown in Fig. 6.2(c). The topologies for extreme cases of volume fraction, i.e. 0.4 and 0.5 are shown in Fig 6.2(a) and (b) respectively. Using proposed method, the topology is simulated and shown in Fig 6.2(d).



(a)                                        (b)

(c)                                        (d)
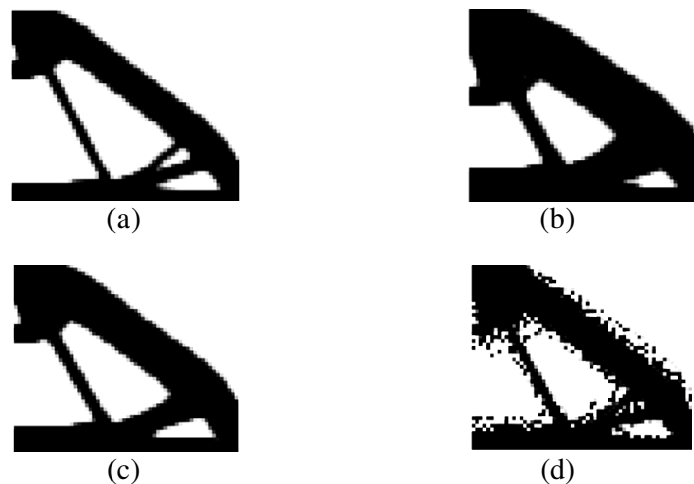
**Fig. 6.2: Extreme cases of manufacturing uncertainties, equivalent to (a) volume fraction 0.4, and (b) 0.6. (c) The accurate topology with volume fraction 0.5, (d) Example of simulation of manufacturing uncertainty**

The amount of uncertainties can be regulated by controlling the intervals of Boxcar function. For example, considering small value of uncertainties in manufacturing process, the simulation will be close to the accurate volume fraction (or accurate manufacturing) compared to the results for upper and lower extremes. Hence for such simulation the interval [b+$t$, c] will be broad compared to [a, b], and [c+ $t$, d]. Similarly, for a highly uncertain manufacturing process the interval [b+ $t$, c] will be very narrow or zero, compared to [a, b], and [c+ $t$, d].

It can be observed from this simulation process that the mesh size plays an important role. If the amount of geometric imperfection cause by manufacturing uncertainty is smaller than the element size, then it cannot be simulated, as the density parameters have constant values for the respective mesh elements. Hence, to simulate it correctly, the chosen mesh size should be smaller than or equal to the smallest unit of geometric imperfection. In such case, the above procedure is applied by combining the elements on the computation space, which forms the smallest unit of geometric imperfection as shown in Fig. 6.3. Here, the smallest unit for geometric imperfection is accommodated in a sub mesh. Based on the type and quantity of the imperfection, the elements can be arranged and, provides flexibility to the designer to simulate the desired manufacturing process.
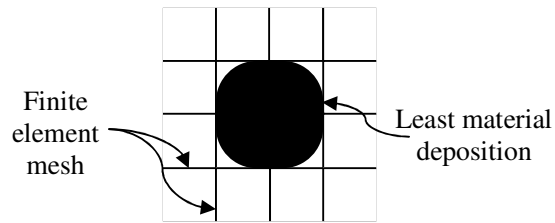


**Fig. 6.3: Approximation of smallest unit of manufacturing error on finite element cells**

In order to apply the suggested approximation, the density parameters in equation (6.2) are replaced by a group of elements, which accommodates the smallest unit for geometric imperfection. Equation (6.5) shows the generalized approach to capture these uncertainties, where the geometric imperfection is accommodated in $m{\times}n$ mesh size.

$$(x_S)_{m\times n} = \Pi_{0,A}(\xi_i)\times(x_D)_{m\times n} + \Pi_{A+\varepsilon,B}(\xi_i)\times(x_R)_{m\times n} + \Pi_{B+\varepsilon,0}(\xi_i)\times(x_A)_{m\times n} \quad (6.5)$$

The type of geometric imperfection of material can also modeled in the proposed simulation method. For illustration, two cases of manufacturing errors and their simulations are shown in Fig. 6.4. Figure 6.4 (a) and (c) show the manufacturing error approximation in finite element cells, for milling and coarse doping process, respectively. The corresponding simulation of manufacturing error of these processes are represented in Fig. 6.4 (b) and (d). In these simulations, the freely suspended material can be removed after the simulation. While in Fig 6.2 (d) the freely suspended material is retained after simulation. It can be generalized by the use of a filtering algorithm incorporated in post processing of the simulation. The decision to remove these suspended materials depends on the type manufacturing process.



|     (a)     |     (b)     |     (c)     |     (d)     |
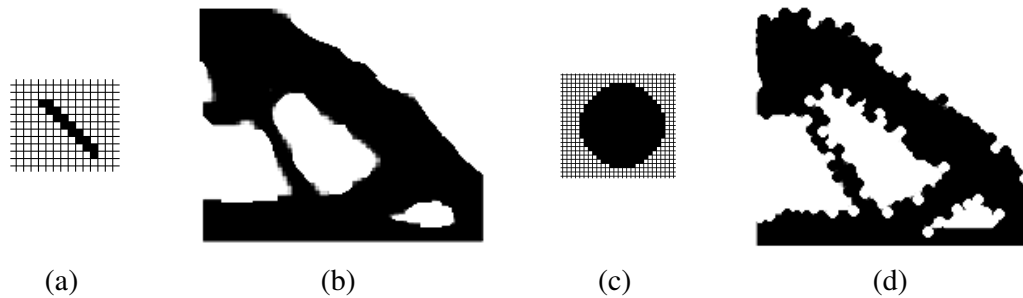
**Fig. 6.4: The approximation of manufacturing errors (a) & (c) and their corresponding simulations (b) & (d) respectively**

The proposed geometric uncertainties or material misplacement simulation is suitable for user customization. This method offers the customization for, the manufacturing process, type, and amount of least material misplacement, degree of smoothness of simulation by the change of the mesh size, retention of removal of suspended material, and incorporation of correlated or non-correlated density parameters. In addition, the procedure offers the control on the proportion of the uncertainties, contributed by the worst and exact (or accurate) cases, in the final simulation. By proper control of the intervals of Boxcar-functions, the obtained simulation can be shifted to either too thin or thick conditions, shown by Sigmund (2009). Apart from these two extremes of too thick and thin, any other extremes can also be chosen based on the specific manufacturing process. In the current work, the proposed simulation method is used along with CA-DOE based method. Proposed method can also be used for other formulations of robust design. The formulation of geometric uncertainties caused by manufacturing process is independent of the

method used for topology optimization. This method can be applied to any method for topology optimization, as long as the whole material domain is discretized.

In the current work, the proposed simulation approach is incorporated in the tolerance range selection approach for topologically optimized structures. For illustration, proposed methodology is applied to four benchmark problems and results are discussed in subsequent section.

## 6.3    IMPLEMENTATION OF PROPOSED METHODOLOGY

The presented methodology for selection of tolerance range of the factors is based on the CA-DOE approach, which was applied earlier. The implementation of each step is discussed below.

Step 1. **Selection of problem and performance measures:**

To apply the CA-DOE approach with the geometric uncertainties, four-benchmark problems, as discussed in section 3.3, are selected. The responses or the main performance values are the outcomes, based on which the effects of tolerance ranges of factors are examined. For this work, performance measures are taken as the compliance and deflection similar to the earlier chapters.

Step 2. **Selection of input factor and their tolerance limits:**

In the present work, the input factors selected are same as in Chapter 5. Their nominal values and the loose and tight tolerance limits of these factors are selected based on information available in literature (Kharmanda et al. 2004, Jung and Cho 2004; Maute and Frangopol 2003; Sigmund 2009). In this case, the assumed values are given in Table 6.1.

**Table 6.1: Selected factors with their nominal and tolerance values**

| S. No. | Factor | Nominal Value | Loose tolerance | Tight tolerance |
|--------|--------|---------------|-----------------|-----------------|
| 1 | Force (N) | 100 | ±5 | ±2.5 |
| 2 | Aspect Ratio | 1.2 | ±0.03 | ±0.006 |
| 3 | Elasticity(GPa) | 200 | ±10 | ±5 |
| 4 | Volume fraction | 0.60 | ±0.075 | ±0.045 |

Step 3. **Design and selection of orthogonal arrays:**

Based on the number of factors and their tolerance level, the inner and outer OAs are designed or selected. In this work, the tolerance of volume fraction is considered separately for the simulation of manufacturing uncertainties. Thus, to apply CA-DOE method inner OA three factors. For three factors with their two levels of tolerances, an inner OA is generated and the design matrix is shown in Appendix A8. Similarly, based on the numbers of factor and their tolerances level Taguchi's $L_4$ outer OA is selected and the matrix is shown in Appendix A9 (Mitra 2008; Sung 1998; Montgomery 2007). As stated earlier, the tolerance of volume fraction is utilized to perform the simulation of geometric uncertainties. Hence, for the loose and tight tolerance range of volume fraction, two set of manufacturing uncertainties are realized. For each set of, the inner OA is Appendix A10.

Step 4. **Simulation of performances:**

In the presented problem, the well-known optimization scheme discussed in earlier chapters i.e. SIMP is applied with optimality criterion approach. The optimization problem is given in equation (1.7). Since this work focuses on the issue of manufacturing the exact topology for the selected components, hence, it is necessary to eliminate the intermediate densities from the optimal topologies. There are few methodologies available to suppress the intermediate density (Albert and Etman 2009; Sigmund 2007; Svanberg and Werme 2005; Bruns 2005; Lau et al. 2001). The method suggested by Albert and Etman (2009) is adopted here for simplicity and reduced computation time. In this method, they proposed a simple heuristic method to eliminate the gray scale of intermediate density from the optimal topology by modifying the OC method (Equation (1.12)). The modified OC for removing the gray scales is given as,

$$
x_{k+1}^e = \begin{cases} \max(x_{\min}, x_k^e - \tilde{m}) & \textit{if } \Gamma(x_k^e(B_k^e)^\eta) \leq \max(x_{\min}, x_k^e - \tilde{m}), \\ \Gamma(x_k^e(B_k^e)^\eta) & \textit{if } \max(x_{\min}, x_k^e - \tilde{m}) < \Gamma(x_k^e(B_k^e)^\eta) < \min(1, x_k^e + \tilde{m}) \\ \min(1, x_k^e + \tilde{m}) & \textit{if } \Gamma(x_k^e(B_k^e)^\eta) \geq \min(1, x_k^e + \tilde{m}) \end{cases} \quad (6.17)
$$

where, the operator $\Gamma(\cdot)$ biases individual gray scale variables towards void densities during iterations. Finally, the volume constraint is also satisfied in each iteration. The values of gray scale suppression operator is given as,

$$\Gamma(x_k^e (B_k^e)^\eta) = (x_k^e (B_k^e)^\eta)^q \tag{6.18}$$

The value of power $q$ in equation (6.18) is suggested as 2 or 3 in order to obtain a topology without any other numerical instability. In the present work, the value of $q$ is taken as 3.

The effect of manufacturing uncertainties is simulated out using the process detailed in section 6.2. These simulations are carried out for each set of input factor values incorporating the randomness of the factors by CA-DOE method. In order to obtain the overall behavior, a Monte Carlo based technique is applied.

Step 5. **Analysis of simulated results:**

> The obtained results provide compliance and deflection values for the selected benchmark problems. There can be two objectives of this analysis, through the selection of tolerance combinations. The first one is to achieve the targeted values of compliance and deflection. The second objective is to achieve the minimum variation of the main performance values i.e. robustness. For targeted values of main performance value, the ANOM is performed. For the minimum variations of performance value or robust design, SNR is utilized (Mitra 2008; Sung 1998**;** Montgomery 2007).

Above steps are performed in order to analyze the effect of tolerance ranges of the factors. For better illustration, the whole methodology is presented in Fig. 6.5. The CA-DOE based experiment is performed by considering the inner OA of four factors with two levels loose (L) and tight (T) tolerances, and the outer OA for three factors with two levels. In order to enable the simulation, the whole CA-DOE based experiment is replicated three times based on the tolerance range of volume fraction ($V_R$, $V_A$, and $V_D$). The simulated density parameters ($x_R$'s, $x_A$'s, and $x_D$'s) of the corresponding combination and run numbers are utilized to simulate the effect of manufacturing uncertainties. The result is obtained as the randomized density parameter, $x_S$. Since the density parameter represents a topology, the performance values of the topology can be computed by incorporating the boundary conditions to the randomized density parameter, $x_S$. In this way corresponding to the each combination and run of inner and outer OA respectively, the compliance and deflection values are obtained. Finally, the mean and SNR is computed for each combination of the inner OA, as the response of the whole experiment.

Three replications of the experiment, for volume fraction tolerances

Outer OA

| | | | | | Rare : $V_R$ | | | | Accurate: $V_A$ | | | | Dense: $V_D$ | | | |
|---|---|---|---|---|---|---|---|---|---|---|---|---|---|---|---|---|
| | | | | | V-3$\sigma_V$ | V-3$\sigma_V$ | V-3$\sigma_V$ | V-3$\sigma_V$ | V | V | V | V | V+3$\sigma_V$ | V+3$\sigma_V$ | V+3$\sigma_V$ | V+3$\sigma_V$ |
| | | | | Run No. | 1 | 2 | 3 | 4 | 1 | 2 | 3 | 4 | 1 | 2 | 3 | 4 |
| | | | | Aspect ratio | A-3 $\sigma_A$ | A-3 $\sigma_A$ | A+3 $\sigma_A$ | A+3 $\sigma_A$ | A-3 $\sigma_A$ | A-3 $\sigma_A$ | A+3 $\sigma_A$ | A+3 $\sigma_A$ | A-3 $\sigma_A$ | A-3 $\sigma_A$ | A+3 $\sigma_A$ | A+3 $\sigma_A$ |
| | | | | Elasticity (Pa) | E-3 $\sigma_E$ | E+3 $\sigma_E$ | E-3 $\sigma_E$ | E+3 $\sigma_E$ | E-3 $\sigma_E$ | E+3 $\sigma_E$ | E-3 $\sigma_E$ | E+3 $\sigma_E$ | E-3 $\sigma_E$ | E+3 $\sigma_E$ | E-3 $\sigma_E$ | E+3 $\sigma_E$ |
| | | | | Force (N) | F-3 $\sigma_E$ | F+3 $\sigma_E$ | F+3 $\sigma_E$ | F-3 $\sigma_E$ | F-3 $\sigma_E$ | F+3 $\sigma_E$ | F+3 $\sigma_E$ | F-3 $\sigma_E$ | F-3 $\sigma_E$ | F+3 $\sigma_E$ | F+3 $\sigma_E$ | F-3 $\sigma_E$ |
| Combination No. | Volume fraction $\sigma_V$ | Aspect ratio $\sigma_A$ | Elasticity (Pa) $\sigma_E$ | Force (N) $\sigma_F$ | | | | | | | | | | | | |
| 1 | L | L | L | L | $x_{R11}$ | … | … | … | $x_{A11}$ | … | … | … | $x_{D11}$ | … | … | … |
| 2 | L | L | L | T | $x_{R21}$ | … | … | … | $x_{A21}$ | … | … | … | $x_{D21}$ | … | … | … |
| … | … | … | … | … | … | … | … | … | … | … | … | … | … | … | … | … |
| … | … | … | … | … | … | … | … | … | … | … | … | … | … | … | … | … |
| 16 | T | T | T | T | … | … | … | $x_{R164}$ | … | … | … | $x_{A164}$ | … | … | … | $x_{D164}$ |

Inner OA

Simulation for effect of manufacturing uncertainty

| $x_{S11}$ | … | … | … |
|---|---|---|---|
| $x_{S21}$ | … | … | … |
| … | … | … | … |
| … | … | … | … |
| … | … | … | $x_{S164}$ |

Computation of the compliance & deflection corresponding to the density parameter

| CS$_{11}$, DS$_{11}$ | … | … | … |
|---|---|---|---|
| CS$_{21}$, DS$_{21}$ | … | … | … |
| … | … | … | … |
| … | … | … | … |
| … | … | … | CS$_{164}$, DS$_{164}$ |

Response computation

| Responses | |
|---|---|
| Mean | S/N |
| CM$_{11}$, DM$_{11}$ | CSNR$_{11}$, DSNR$_{11}$ |
| CM$_{21}$, DM$_{21}$ | CSNR$_{21}$, DSNR$_{21}$ |
| … | … |
| … | … |
| CM$_{164}$, DM$_{164}$ | CSNR$_{164}$, DSNR$_{164}$ |

**Fig. 6.5: Flowchart for simulation method**

The important differences between the present methodology and the methodology described in Chapter 5, are made clear in Fig. 6.5. In Chapter 5, the volume fraction was also included as factor while generating the outer OA. However here, the volume fraction tolerances in not included within the CA-DOE experiment and is applied over the cross arrays. The levels of volume fraction are chosen as three different values, whereas in Chapter 5 it had two values i.e. loose and tight. These changes were necessary to incorporate the effect of manufacturing uncertainties. Thus, the final responses are the performance of the randomized topologies. The detailed analyses of the responses are presented in next section.

## 6.4     ANALYSIS AND DISCUSSION

The simulations are performed based on proposed method for the four different benchmark problems. As stated earlier, a technique proposed by Albert and Etman (2009) is employed to suppress the gray scales and to compare the results the simulations are carried out with and without intermediate density. For simulation, FE mesh size for the problems are varied as, 12×10, 24×20, 36×30, and 60×50. The comparative results remain same for the considered mesh sizes, due to mesh independency filter used in the simulation (Javed and Rout 2014). For different mesh sizes the topologies are shown in Fig. 6.6. In this chapter, the result of mesh size 60×50 is used for simulation and analysis.
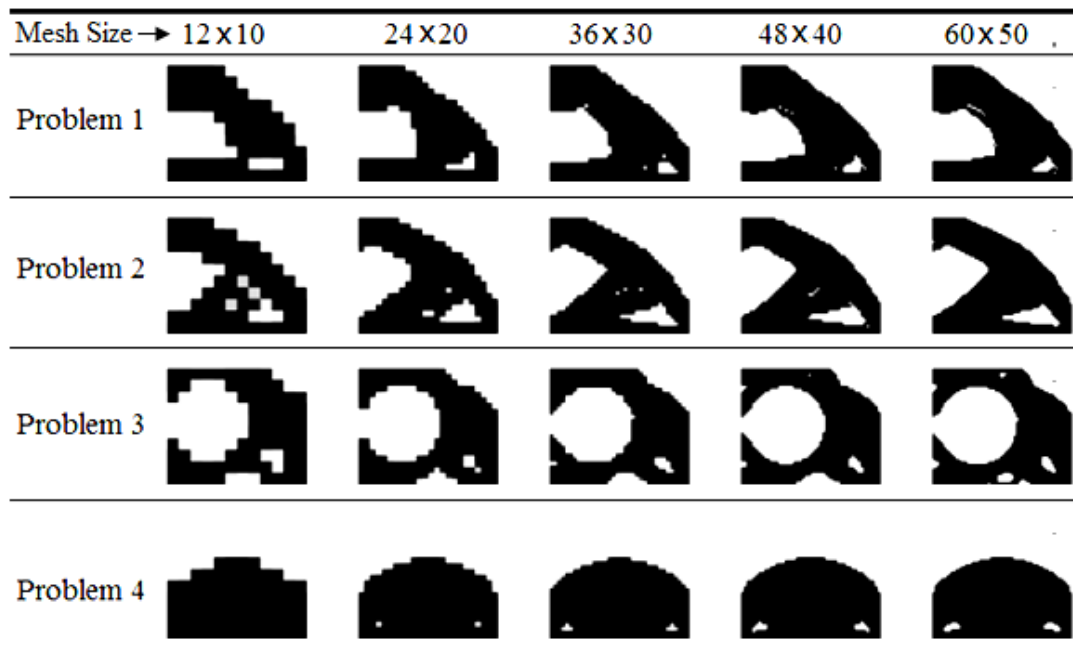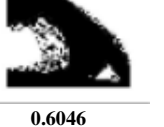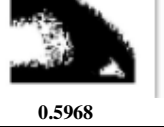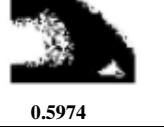


**Fig. 6.6: Optimal topologies for different mesh size at the nominal values of the factors**

### 6.4.1 Signal to noise ratio

The proposed CA-DOE based methodology is applied and the results are discussed in this section. For illustration, the topologies for problem-1, corresponding to 60×50 mesh is shown in Table 6.2. The SNR of compliance and deflection is computed using equation (3.35). Here, the replications are obtained by outer OA i.e. Taguchi's $L_4$ OA.

**Table 6.2: Simulated topologies for problem-1, with corresponding volume fraction**

| Inner OA (Combination No.)* | Outer OA (Run No.)** | | | |
|---|---|---|---|---|
| | 1 | 2 | 3 | 4 |
| 1 | 0.6043 | 0.6010 | 0.5976 | 0.6035 |
| 2 | 0.5974 | 0.5999 | 0.5977 | 0.6004 |
| 3 | 0.6020 | 0.6027 | 0.5979 | 0.6022 |
| 4 | 0.5972 | 0.5989 | 0.6091 | 0.6009 |
| 5 | 0.5981 | 0.5954 | 0.6079 | 0.6049 |
| 6 | 0.6005 | 0.6004 | 0.6055 | 0.6046 |
| 7 | 0.6008 | 0.5921 | 0.5968 | 0.5974 |
| | | | * Refer Appendix A9, **Refer Appendix A10 | |

| Inner OA (Combination No.)* | Outer OA (Run No.)** | | | |
|---|---|---|---|---|
| | 1 | 2 | 3 | 4 |
| 8 | 0.6034 | 0.6010 | 0.5980 | 0.5970 |
| 9 | 0.5999 | 0.6008 | 0.6058 | 0.5987 |
| 10 | 0.5977 | 0.6047 | 0.6007 | 0.5966 |
| 11 | 0.6026 | 0.6008 | 0.6046 | 0.5942 |
| 12 | 0.6052 | 0.6016 | 0.6033 | 0.5965 |
| 13 | 0.5929 | 0.6000 | 0.5984 | 0.5980 |
| 14 | 0.5996 | 0.6028 | 0.6041 | 0.6044 |
| 15 | 0.6008 | 0.6008 | 0.5992 | 0.5976 |
| 16 | 0.5993 | 0.5935 | 0.5948 | 0.6022 |
| | | | * Refer Appendix A9, **Refer Appendix A10 | |

Hence, for each set of tolerance combinations (Appendix A10), four replications are obtained. The SNR value is the consolidated value of replications by using *i=1, 2, 3 & 4* in equation (3.35). The simulated values of SNR for compliance are shown in Fig. 6.7. In this figure, value of SNR corresponding to each combination number of inner OA is shown in bar chart.
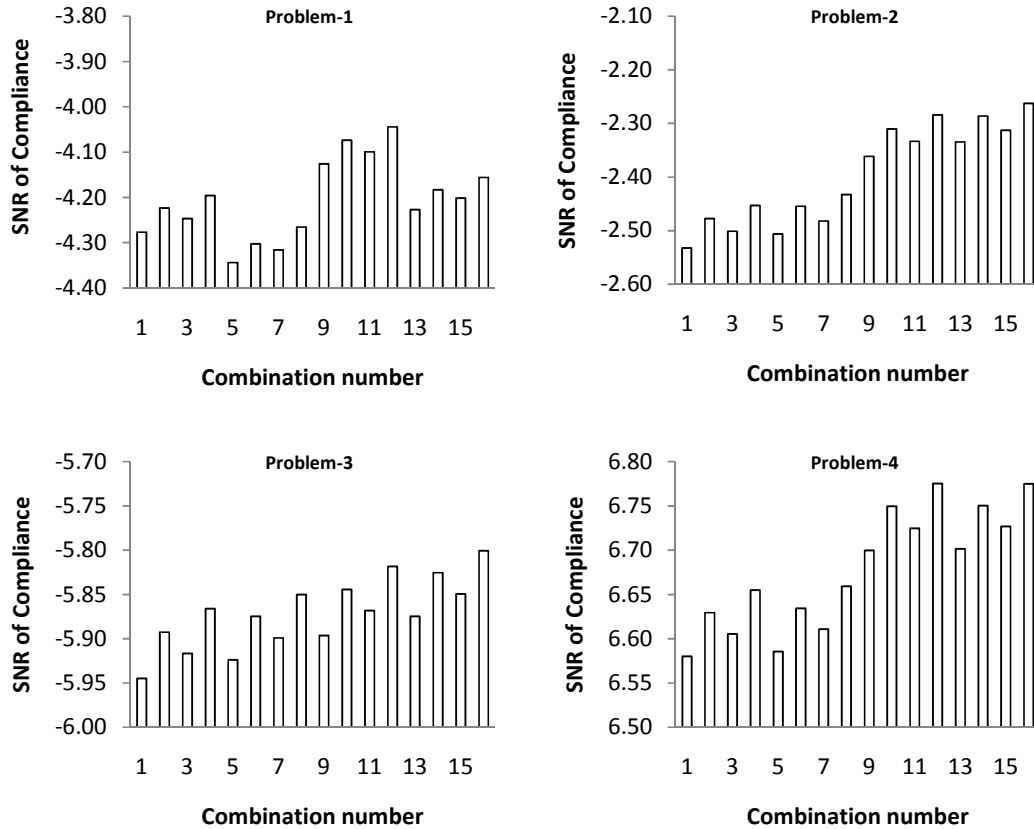


**Fig. 6.7: SNR of compliance values for different tolerance combinations**

From Fig. 6.7, the variations of SNR corresponding to different combinations of the tolerances is shown. For problem-1, the highest SNR is observed for 12th combination. This observation is different from that of results in Chapter 5 (Fig. 5.3), and it is due to the effect of specific manufacturing uncertainties. For other problems, the highest SNR value is achieved by the 16th combination. The highest value for SNR represents the combination with robust design. Referring to Appendix A10, it can be seen that the 16th combination, have factors with tight tolerance range. This is an ideal situation, where the designer chooses narrow range for tolerance to minimize the variation in the

performance. However, this activity requires a lot of cost and effort. The alternate to this situation is to select the combination numbers, which have high SNR value. Based on the affordability of tolerance range, the designer should select a suitable tolerance combination.

From these results, it is observed that there are different combination numbers, which have high SNR value corresponding to each problem. It can also be identified that the gap between nearest SNR values are small. Hence, the tolerance combinations can be grouped together based on the similar values of SNR, as it was presented in Chapter 5. In this way, a group can represent similar performance variations and provide the alternatives to the designer. The grouping based on the SNR value is shown in Table 6.3. The SNR values decrease while moving from group one to three.

**Table 6.3 Tolerance combination groups for SNR values**

| SNR of Compliance | | | |
|---|---|---|---|
| | Group 1 | Group 2 | Group 3 |
| Problem 1 | 12, 11, 10, 9 | 16, 15, 14, 13, 4, 2 | 8, 7, 6, 5, 3, 1 |
| Problem 2 | 16, 15, 14, 13, 12, 11, 10 | 9, 8, | 7, 6, 5, 4, 3, 2, 1 |
| Problem 3 | 16, 14, 12, 10 | 15, 13, 11, 9, 8, 6, 4, 2 | 7, 5, 3, 2, 1 |
| Problem 4 | 16, 15, 14, 12, 11, 10 | 13, 9, 8, 4 | 7, 6, 5, 3, 2, 1 |
| SNR of deflection | | | |
| | Group 1 | Group 2 | Group 3 |
| Problem 1 | 12, 11, 10, 9 | 16, 15, 14, 13, 4, 3, 2 | 8, 7, 6, 5, 1 |
| Problem 2 | 16, 15, 14, 12, 11, 10, 9,8 | | 8, 7, 6, 5, 3, 4, 2, 1 |
| Problem 3 | 16, 15, 14, 12, 11 | 13, 10, 9, 8, 7 | 6, 5, 4, 3, 2, 1 |
| Problem 4 | 16, 15, 14,13, 12, 11, 10, 9 | 8, 7, 6, 5 | 4, 3, 2, 1 |

Similar to compliance value, the SNR of maximum deflection is also shown in Fig. 6.8, for selected problems. The important observations in Fig 6.8, are similar to that of compliance. For problem-1, the highest SNR is observed for 12th combination. For problem-4, highest SNR is observed for 15th combination. This observation is different from results available in Chapter 5 (Fig. 5.4).
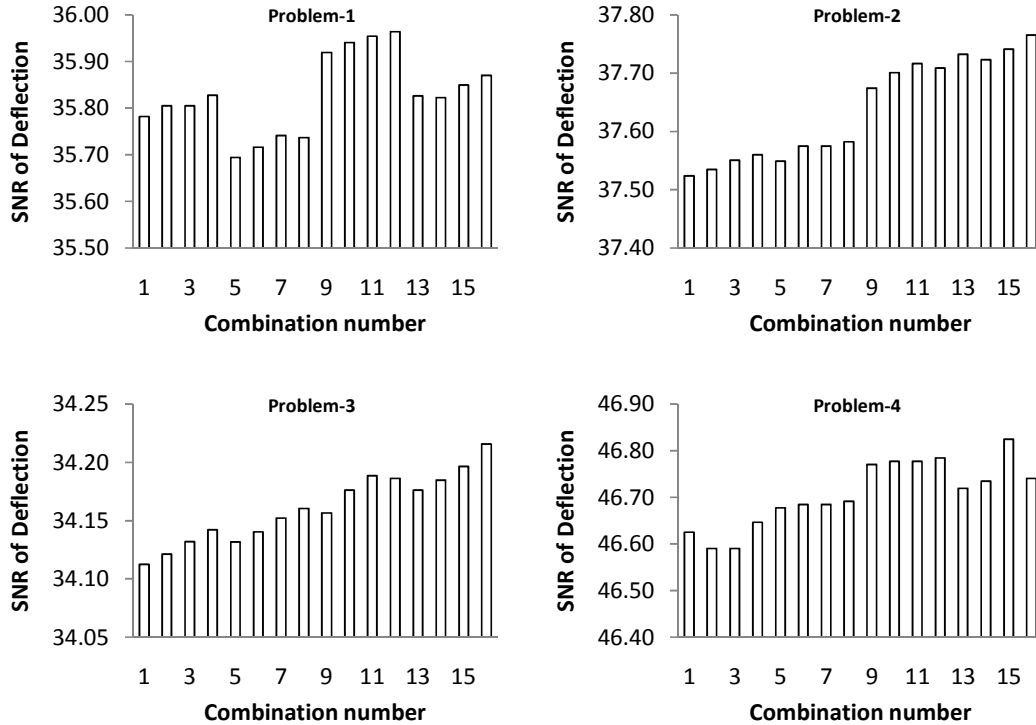
**Fig. 6.8: SNR of deflection values for different tolerance combinations**

The consolidated grouping based on SNR values of deflection is shown in Table 6.3. These groups represent the comparative robustness offered by the different combinations. The SNR values decrease while moving from group one to three. Hence, the combinations of group one is desirable to achieve the high level of robustness. Similar to the SNR of performance the mean values of the performances are also analyzed, which are detailed in the next section.

### 6.4.2   Targeted performance value

The mean values of compliance and deflection help to solve the targeted value problem. In these problems, it is required to achieve desired values of the performance. Due to changes in tolerance and noise of the factors, the targeted values change from the intended one. As discussed earlier, present work provides the variations of performance over individual factor tolerance value, to achieve the intended performance by selecting the tolerances of factors. For structural problems, the performance is represented by the mean values of compliance and deflection. The variation in the mean values of compliance and deflection is discussed in this section. Based on the CA-DOE approach, the compliance and deflections are consolidated for each combination of inner OA

(Appendix A10). The bar charts for the four problems are plotted in Fig. 6.9. The mean compliance is shown against combination numbers. These value of compliance and deflections are generated using the topologies without gray scale similar to that of SNR.
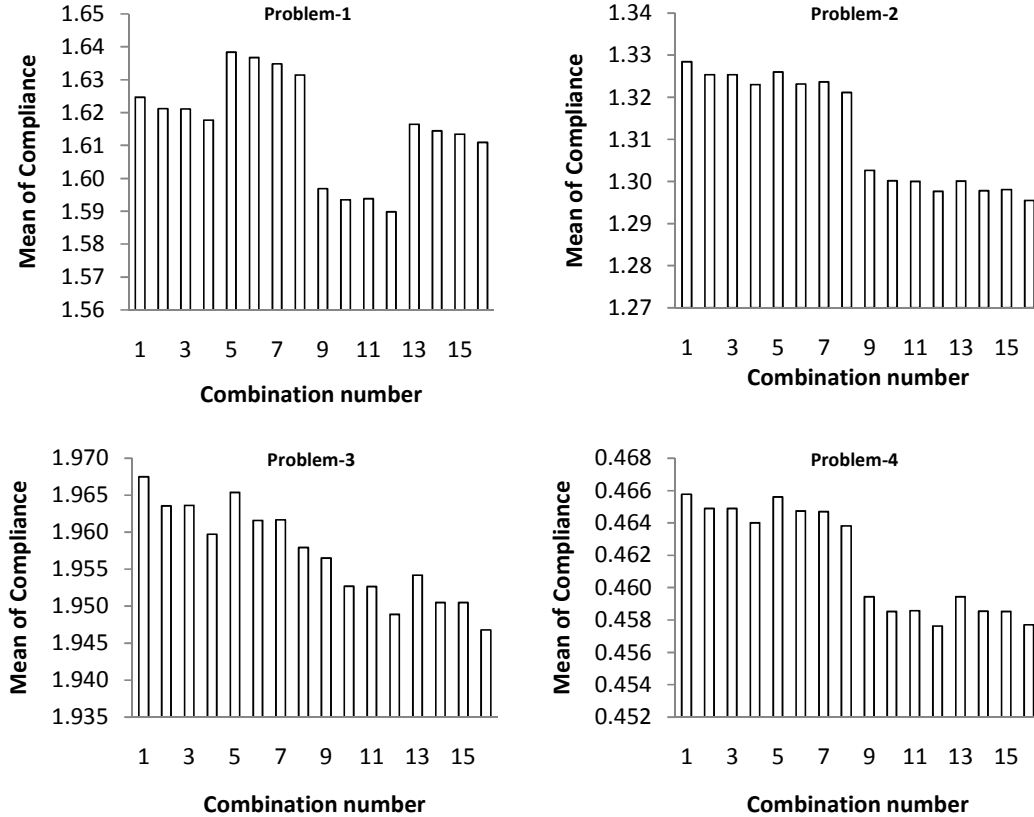


**Fig. 6.9: Mean of compliance values for different tolerance combinations**

For problem-1, the lowest compliance value is observed for 12th combination. This observation is different from that of the results available in Chapter 5 (Fig. 5.6). For other problems, the lowest compliance value is achieved by the 16th combination. In order to reduce the effort spent in tightening the tolerance of all factors, the combinations that gives the compliance closer to the minimum value, can be selected. Similar to previous cases the grouping of the combination is done here. These groups show the similar performance in compliance, and shown in Table 6.4. The mean values of performances increase while moving from group one to three.

The results for mean values of defection are shown in Fig 6.10. The observations for mean deflection are similar to mean compliance.
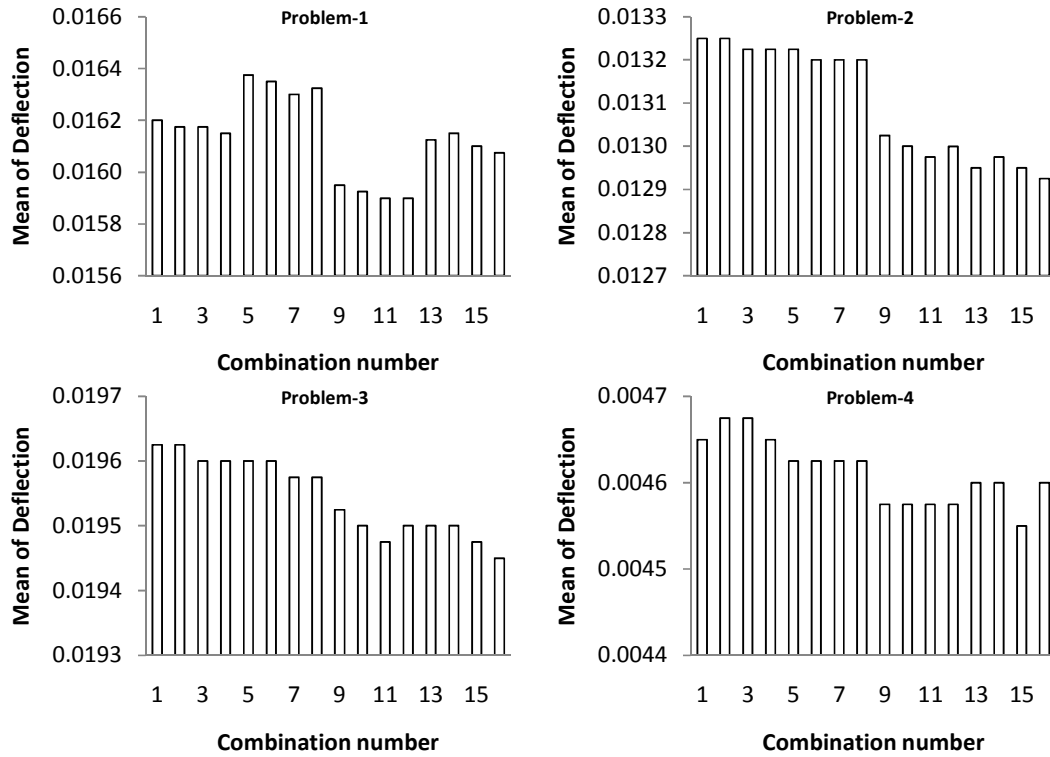
**Fig. 6.10: Mean of deflection values for different tolerance combinations**

**Table 6.4: Tolerance combination groups for mean values**

| Mean of Compliance | | | |
|---|---|---|---|
| | Group 1 | Group 2 | Group 3 |
| Problem 1 | 12, 11, 10, 9 | 16, 15, 14, 13, 4, 3, 2, 1 | 8, 7, 6, 5 |
| Problem 2 | 16, 15, 14, 12, 11, 10, 9 | | 8, 7, 6, 5, 3, 4, 2, 1 |
| Problem 3 | 16, 15, 14, 12, 11, 10 | 13, 9, 8, 4 | 7, 6, 5, 4, 3, 2, 1 |
| Problem 4 | 16, 15, 14, 12, 11, 10, 9 | | 8, 7, 6, 5, 3, 4, 2, 1 |
| Mean of Deflection | | | |
| | Group 1 | Group 2 | Group 3 |
| Problem 1 | 12, 11, 10, 9 | 16, 15, 14, 13, 4, 3, 2 | 8, 7, 6, 5, 1 |
| Problem 2 | 16, 15, 14, 12, 11, 10, 9 | | 8, 7, 6, 5, 4, 3, 2, 1 |
| Problem 3 | 16, 15, 14, 12, 11, 10 | 9 | 8, 7, 6, 5, 4, 3, 2, 1 |
| Problem 4 | 15, 12, 11, 10, 9 | 16, 14, 13, 8, 7, 6, 5 | 4, 3, 2, 1 |

For problem-1, the lowest deflection value is observed for 12th combination, and for problem-4, the lowest deflection value is observed for 15th combination. This observation is different from that the results in Chapter 5 (Fig. 5.7). For problems-2 and 3, the lowest deflection value is achieved by the 16th combination. The results for mean compliance and deflections are found to be similar. The effect of tolerance on the performance value can be observed from the presented analysis. From the grouping of the tolerance combination, it can be concluded that the adjustment in tolerances values of factors should be carried out to get desired/intended performance or robustness.

## 6.5    COMPARISON OF RESULTS

In order to analyze the significance of the proposed simulation method specific to uncertainties due to manufacturing process, the obtained results are compared with the results obtained from a generalized approach. As mentioned earlier, Chapter 5 uses a generalized method to capture the effect of uncertainties due to manufacturing or secondary shaping/sizing process in terms of the tolerance of volume fraction and aspect ratio.  The results shown above is based on the values available Table 6.1. To compare the results of both approaches, the chosen problems are simulated on the same nominal and tolerance values of factors already given in Table 5.1. The differences in mean and SNR of compliance and deflection are shown in Tables 6.5 & 6.6 for each combination number.

It is observed from Tables 6.5 & 6.6 that for all problems, the mean compliance and deflection values increase, and SNR decrease, when the specific simulation approach is employed. However, for problem 4, the mean deflection value decrease and SNR of deflection increase when specific simulation approach is employed. These changes point towards the sensitivity of factor and its effect on compliance and deflection. Thus to observe the sensitivities, ANOM is used. In the present case, there are four factors with two levels of tolerance (loose and tight) each. Therefore, for each factor ANOM is performed at two levels. The comparison is shown in Figs. 6.11 and 6.12 for compliance and deflection values respectively.

**Table 6.5: Comparison of mean and SNR of compliance for generalized and specific approach**

| C. No. | Problem 1 | | | | Problem 2 | | | | Problem 3 | | | | Problem 4 | | | |
|---|---|---|---|---|---|---|---|---|---|---|---|---|---|---|---|---|
| | Generalized | | Specific | | Generalized | | Specific | | Generalized | | Specific | | Generalized | | Specific | |
| | Mean | SNR | Mean | SNR | Mean | SNR | Mean | SNR | Mean | SNR | Mean | SNR | Mean | SNR | Mean | SNR |
| 1 | 1.4881 | -3.5139 | 1.5844 | -4.0581 | 1.2206 | -1.7950 | 1.2897 | -2.2754 | 1.8986 | -5.6295 | 1.9520 | -5.8761 | 0.4490 | 6.8982 | 0.4560 | 6.7652 |
| 2 | 1.4864 | -3.4713 | 1.5808 | -4.0045 | 1.2216 | -1.7698 | 1.2872 | -2.2236 | 1.8947 | -5.5797 | 1.9481 | -5.8241 | 0.4481 | 6.9490 | 0.4551 | 6.8148 |
| 3 | 1.4871 | -3.5051 | 1.5813 | -4.0314 | 1.2273 | -1.8401 | 1.2871 | -2.2471 | 1.8976 | -5.6256 | 1.9481 | -5.8481 | 0.4480 | 6.9180 | 0.4551 | 6.7913 |
| 4 | 1.4830 | -3.4489 | 1.5777 | -3.9779 | 1.2171 | -1.7342 | 1.2847 | -2.1977 | 1.8945 | -5.5790 | 1.9444 | -5.7980 | 0.4474 | 6.9614 | 0.4542 | 6.8405 |
| 5 | 1.4857 | -3.4921 | 1.6040 | -4.1597 | 1.2198 | -1.7806 | 1.2894 | -2.2625 | 1.8951 | -5.6053 | 1.9497 | -5.8543 | 0.4497 | 6.8890 | 0.4559 | 6.7685 |
| 6 | 1.4841 | -3.4510 | 1.6019 | -4.1156 | 1.2162 | -1.7237 | 1.2869 | -2.2133 | 1.8911 | -5.5553 | 1.9460 | -5.8054 | 0.4471 | 6.9761 | 0.4550 | 6.8174 |
| 7 | 1.4851 | -3.4857 | 1.6012 | -4.1359 | 1.2176 | -1.7633 | 1.2874 | -2.2412 | 1.8940 | -5.6012 | 1.9459 | -5.8291 | 0.4469 | 6.9452 | 0.4550 | 6.7934 |
| 8 | 1.4821 | -3.4367 | 1.5986 | -4.0890 | 1.2151 | -1.7120 | 1.2847 | -2.1899 | 1.8911 | -5.5551 | 1.9423 | -5.7805 | 0.4468 | 6.9834 | 0.4542 | 6.8419 |
| 9 | 1.4886 | -3.5133 | 1.5609 | -3.9260 | 1.2211 | -1.7936 | 1.2797 | -2.2077 | 1.8970 | -5.6153 | 1.9488 | -5.8620 | 0.4497 | 6.8789 | 0.4532 | 6.8180 |
| 10 | 1.4868 | -3.4709 | 1.5578 | -3.8753 | 1.2177 | -1.7374 | 1.2771 | -2.1554 | 1.8930 | -5.5649 | 1.9450 | -5.8101 | 0.4477 | 6.9553 | 0.4524 | 6.8676 |
| 11 | 1.4865 | -3.4977 | 1.5581 | -3.9015 | 1.2179 | -1.7682 | 1.2771 | -2.1792 | 1.8960 | -5.6110 | 1.9450 | -5.8343 | 0.4476 | 6.9246 | 0.4524 | 6.8432 |
| 12 | 1.4837 | -3.4493 | 1.5541 | -3.8460 | 1.2188 | -1.7423 | 1.2746 | -2.1292 | 1.8928 | -5.5641 | 1.9413 | -5.7840 | 0.4475 | 6.9608 | 0.4515 | 6.8920 |
| 13 | 1.4856 | -3.4886 | 1.5899 | -4.0831 | 1.2193 | -1.7739 | 1.2778 | -2.1843 | 1.8933 | -5.5902 | 1.9468 | -5.8417 | 0.4475 | 6.9336 | 0.4530 | 6.8249 |
| 14 | 1.4834 | -3.4430 | 1.5868 | -4.0334 | 1.2173 | -1.7279 | 1.2755 | -2.1358 | 1.8894 | -5.5404 | 1.9432 | -5.7926 | 0.4469 | 6.9795 | 0.4521 | 6.8735 |
| 15 | 1.4851 | -3.4818 | 1.5868 | -4.0579 | 1.2194 | -1.7706 | 1.2757 | -2.1615 | 1.8926 | -5.5875 | 1.9431 | -5.8166 | 0.4470 | 6.9445 | 0.4521 | 6.8494 |
| 16 | 1.4811 | -3.4260 | 1.5839 | -4.0091 | 1.2145 | -1.7028 | 1.2731 | -2.1115 | 1.8892 | -5.5395 | 1.9395 | -5.7677 | 0.4467 | 6.9853 | 0.4512 | 6.8990 |

**Table 6.6: Comparison of mean and SNR of deflection for generalized and specific approach**

| C. No. | Problem 1 | | | | Problem 2 | | | | Problem 3 | | | | Problem 4 | | | |
|---|---|---|---|---|---|---|---|---|---|---|---|---|---|---|---|---|
| | Generalized | | Specific | | Generalized | | Specific | | Generalized | | Specific | | Generalized | | Specific | |
| | Mean | SNR | Mean | SNR | Mean | SNR | Mean | SNR | Mean | SNR | Mean | SNR | Mean | SNR | Mean | SNR |
| 1 | 0.01485 | 36.537 | 0.01580 | 36.000 | 0.01231 | 38.162 | 0.01285 | 37.792 | 0.01898 | 34.407 | 0.01948 | 34.178 | 0.00475 | 46.438 | 0.00458 | 46.770 |
| 2 | 0.01486 | 36.537 | 0.01578 | 36.022 | 0.01229 | 38.188 | 0.01288 | 37.783 | 0.01896 | 34.421 | 0.01948 | 34.189 | 0.00474 | 46.468 | 0.00458 | 46.777 |
| 3 | 0.01484 | 36.547 | 0.01578 | 36.022 | 0.01225 | 38.208 | 0.01285 | 37.800 | 0.01896 | 34.414 | 0.01943 | 34.210 | 0.00473 | 46.486 | 0.00455 | 46.829 |
| 4 | 0.01483 | 36.562 | 0.01575 | 36.045 | 0.01233 | 38.166 | 0.01283 | 37.826 | 0.01898 | 34.416 | 0.01943 | 34.219 | 0.00483 | 46.324 | 0.00455 | 46.835 |
| 5 | 0.01480 | 36.574 | 0.01600 | 35.895 | 0.01226 | 38.205 | 0.01285 | 37.799 | 0.01894 | 34.432 | 0.01943 | 34.210 | 0.00474 | 46.468 | 0.00453 | 46.866 |
| 6 | 0.01484 | 36.559 | 0.01600 | 35.903 | 0.01230 | 38.187 | 0.01285 | 37.808 | 0.01893 | 34.446 | 0.01945 | 34.208 | 0.00471 | 46.522 | 0.00453 | 46.873 |
| 7 | 0.01481 | 36.569 | 0.01598 | 35.916 | 0.01225 | 38.220 | 0.01283 | 37.825 | 0.01891 | 34.445 | 0.01940 | 34.229 | 0.00471 | 46.518 | 0.00453 | 46.873 |
| 8 | 0.01480 | 36.584 | 0.01598 | 35.925 | 0.01223 | 38.244 | 0.01283 | 37.833 | 0.01891 | 34.453 | 0.01940 | 34.238 | 0.00480 | 46.372 | 0.00453 | 46.881 |
| 9 | 0.01485 | 36.540 | 0.01558 | 36.127 | 0.01228 | 38.192 | 0.01275 | 37.859 | 0.01896 | 34.419 | 0.01945 | 34.190 | 0.00475 | 46.438 | 0.00453 | 46.866 |
| 10 | 0.01486 | 36.540 | 0.01555 | 36.149 | 0.01230 | 38.184 | 0.01278 | 37.851 | 0.01899 | 34.416 | 0.01945 | 34.199 | 0.00474 | 46.467 | 0.00453 | 46.873 |
| 11 | 0.01483 | 36.558 | 0.01553 | 36.163 | 0.01226 | 38.205 | 0.01273 | 37.886 | 0.01894 | 34.432 | 0.01938 | 34.233 | 0.00481 | 46.345 | 0.00450 | 46.920 |
| 12 | 0.01484 | 36.558 | 0.01555 | 36.157 | 0.01228 | 38.205 | 0.01273 | 37.894 | 0.01896 | 34.428 | 0.01940 | 34.231 | 0.00481 | 46.345 | 0.00453 | 46.881 |
| 13 | 0.01484 | 36.555 | 0.01585 | 35.976 | 0.01229 | 38.191 | 0.01275 | 37.867 | 0.01891 | 34.451 | 0.01943 | 34.210 | 0.00474 | 46.468 | 0.00453 | 46.866 |
| 14 | 0.01484 | 36.564 | 0.01588 | 35.971 | 0.01226 | 38.219 | 0.01275 | 37.876 | 0.01894 | 34.448 | 0.01943 | 34.218 | 0.00481 | 46.350 | 0.00453 | 46.873 |
| 15 | 0.01483 | 36.565 | 0.01580 | 36.012 | 0.01223 | 38.241 | 0.01273 | 37.893 | 0.01891 | 34.451 | 0.01938 | 34.241 | 0.00483 | 46.326 | 0.00453 | 46.873 |
| 16 | 0.01481 | 36.581 | 0.01580 | 36.021 | 0.01225 | 38.231 | 0.01273 | 37.901 | 0.01893 | 34.454 | 0.01938 | 34.250 | 0.00480 | 46.372 | 0.00450 | 46.931 |
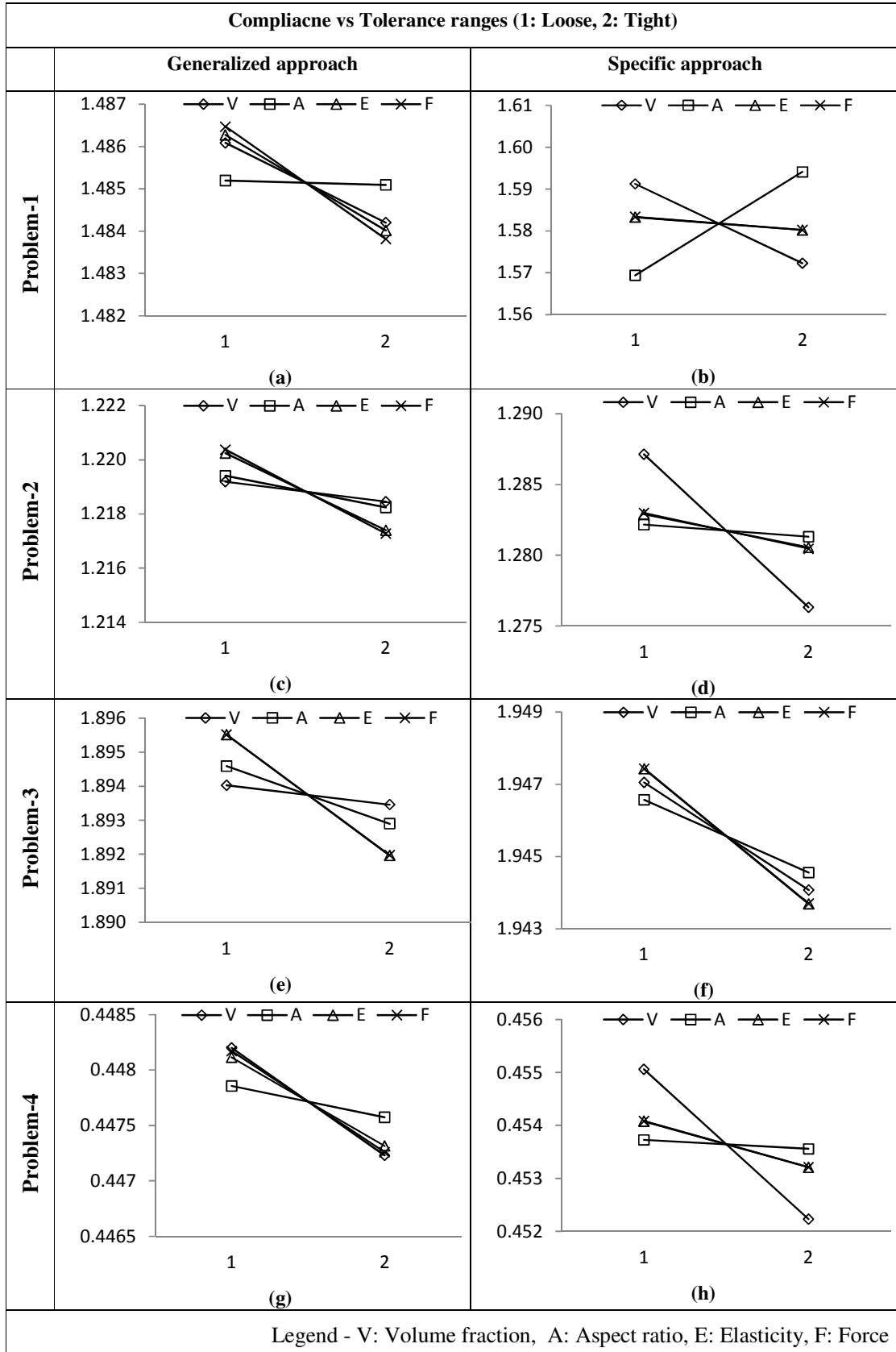
**Fig. 6.11: ANOM of compliance for each problem and approaches**

Fig. 6.11 shows the ANOM for compliance verses tolerance levels for the four problems using both approaches. It is observed that the sensitivities of each factor in both cases are different. Also, the most and least influential factors are different for each problem and approach. The summary of observations is presented in Table 6.7.

**Table 6.7: Comparison of sensitivities between two approaches with compliance value**

| Problem No. | Generalized approach | | Specific approach | |
|:---:|:---:|:---:|:---:|:---:|
| | Most influential factor | Least influential factor | Most influential factor | Least influential factor |
| 1 | F | A | A | E & F |
| 2 | F | V | V | E & F |
| 3 | E | V | E | A |
| 4 | V | A | V | A |
| Legend - V: Volume fraction,  A: Aspect ratio, E: Elasticity, F: Force | | | | |

Similar to the ANOM of compliance values, the ANOM of deflection values is used to compare both approaches. The comparison is presented in Fig. 6.12. It is observed that the sensitivities of each factor in both cases are different. Also, the most and least influential factors are different for each problem and approach. The summary of observation for ANOM of deflection value is presented in Table 6.8.

The reason for this change is the randomized simulation of density matrix, which was not considered in the generalized approach. In specific process approach, the material distribution within the topology is altered from the deterministic one (Table 6.2) while in the generalized approach, the topology change uniformly (Table 5.6). Hence, significant differences in the sensitivity is observed here. Thus, the specific approach discussed in the present chapter captures true characteristic of the manufacturing process more accurately compared to the generalized approach. Therefore, the accuracy of the obtained analysis for tolerance range is useful for specific manufacturing process.

| Deflection(mm) vs Tolerance ranges (1:Loose, 2: Tight) | |
|---|---|
| **Generalized approach** | **Specific approach** |
| (a) | (b) |
| (c) | (d) |
| (e) | (f) |
| (g) | (h) |
| V: Volume fraction, A: Aspect ratio, E: Elasticity, F: Force | |
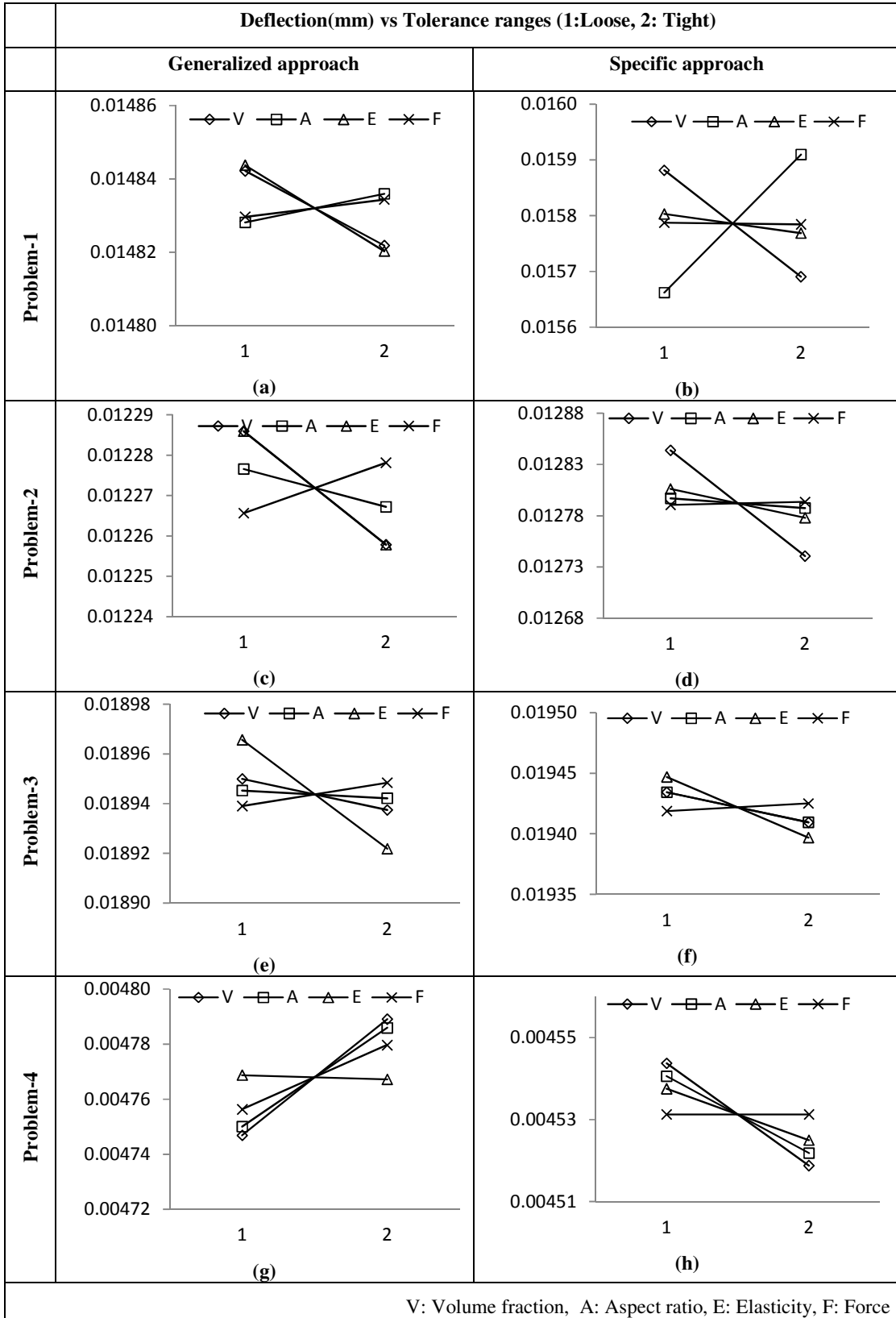
**Fig. 6.12: ANOM of deflection for each problem and approaches**

**Table 6.8: Comparison of sensitivities between two approaches with deflection value**

| Problem No. | Generalized approach | | Specific approach | |
|:---:|:---:|:---:|:---:|:---:|
| | Most influential factor | Least influential factor | Most influential factor | Least influential factor |
| 1 | F | E | A | F |
| 2 | E & V | A & F | V | F |
| 3 | E | F | E | F |
| 4 | V | F | V | E |
| | Legend - V: Volume fraction, A: Aspect ratio, E: Elasticity, F: Force | | | |

## 6.6 RELIABILITY BASED TOLERANCE RANGE SELECTION WITH EFFECTS OF UNCERTAINTIES IN MANUFACTURING PROCESS

Like earlier discussion in section 5.5, the reliability concept is also applied in the present chapter to derive the suitable combinations of tolerances for the chosen problems. The reliability method helps to simulate the performances including the uncertainties or noise of controllable factors. In present case, these uncertainties are treated as the tolerances. Hence, the RBTO method described in Chapter 4 is suitable to simulate the performances for the tolerance range election of the controllable factors. The methodology for generating the tolerance combinations is described below,

### 6.6.1 Methodology

In order to perform the tolerance range analysis based on reliability concept; the outer OA is replaced and the tolerance values are simulated using RBTO method. The illustration of the methodology is provided in Fig. 6.13. Figure 6.13, represents methodology for reliability based tolerance range selection. The method initiates from the inner OA similar to the CA-DOE based method. Each combination is simulated for the performance values using RBTO method, with the nominal and tolerance values of the factor and a desired reliability index value, as described in section 4.3. In order to incorporate the effect of uncertainties of specific manufacturing process, the tolerance of volume fraction is utilized. The replication of inner OA is performed for the rare accurate and dense volume fractions and the density matrixes are simulated as $x_R$'s, $x_A$'s, and $x_D$'s respectively.

| Combination No. | Aspect ratio $\sigma_A$ | Elasticity $\sigma_E$ | Force $\sigma_F$ | | Three replications of the experiment, for volume fraction tolerance | | | Volume fraction $\sigma_V$ |
| | | | | | Rare : $V_R$ | Accurate: $V_A$ | Dense: $V_D$ | |
| | | | | | $V-3\sigma_V$ | $V$ | $V+3\sigma_V$ | |
| 1 | L | L | L | RBTO | $x_{R1}$ | $x_{A1}$ | $x_{D1}$ | L |
| 2 | L | L | T | | $x_{R2}$ | $x_{A2}$ | $x_{D2}$ | L |
| ... | ... | ... | ... | | ... | ... | ... | |
| | | | | | | | | |
| ... | ... | ... | ... | | ... | | ... | |
| 16 | T | T | T | | $x_{R16}$ | $x_{A16}$ | $x_{D16}$ | T |

Simulation for effect of manufacturing uncertainty

| $x_{S1}$ |
| $x_{S2}$ |
| ... |
| ... |
| $x_{S16}$ |

Computation of the compliance & deflection corresponding to density parameter

| $C_1$ | $D_1$ |
| $C_2$ | $D_2$ |
| ... | ... |
| ... | ... |
| $C_{16}$ | $D_{16}$ |

**Fig. 6.13: Methodology for reliability based tolerance range selection**

Using these density matrixes, the simulation of manufacturing uncertainties are preformed, as explained in section 6.2. The simulated density matrix ($x_S$'s) are then further processed to generate the compliance and deflection values using the boundary conditions. The obtained compliance and deflection values are the performance measures for the tolerance range analysis. The results and discussion of the simulated results are given in next section.

### 6.6.2 Results and discussion

The simulated results for compliance and deflection values are given in Fig. 6.14 and 6.15 respectively, for different values of reliability index. From Fig. 6.14 the compliance values for the reliability index equal to 3 and 3.8 is observed. The values of compliance increase with increase in reliability index. This is because of the specific characteristic of the RBTO method, discussed in section 4.3.
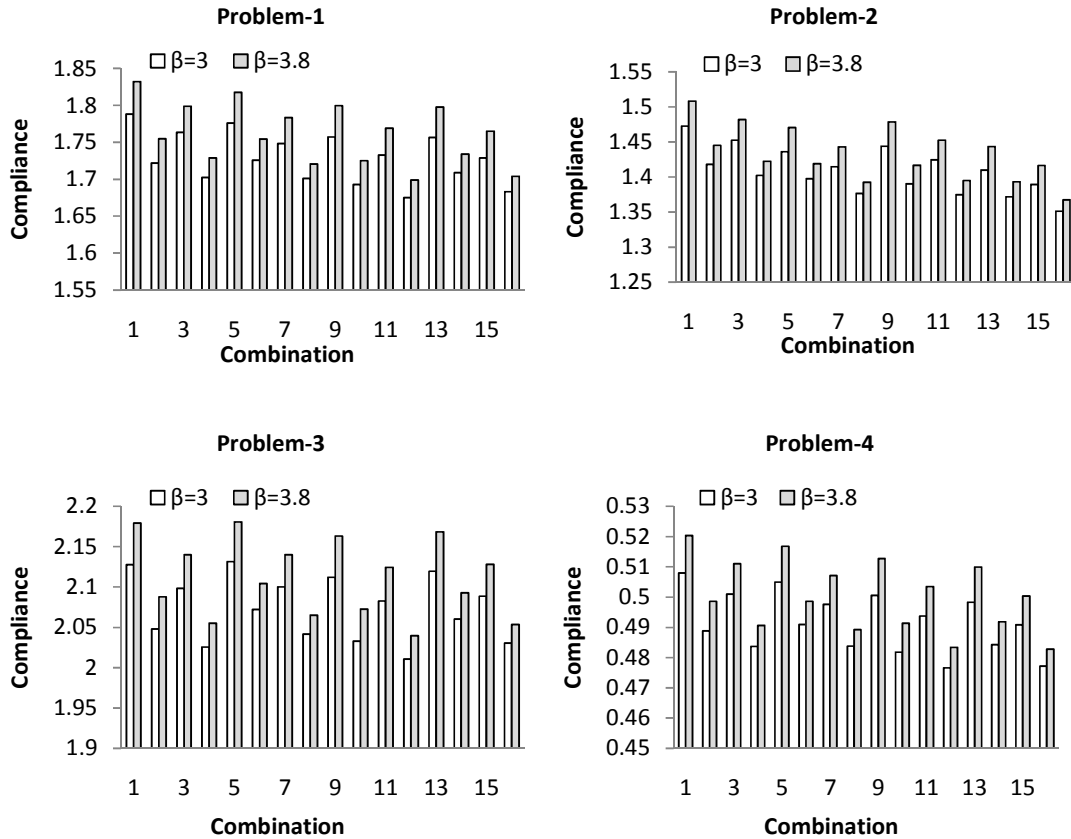
**Fig. 6.14: Compliance values for tolerance combinations**

The variations in compliance values for the different combination are also observed, similar to that of CA-DOE method (Fig. 6.9). However, the range of compliance variations is higher compared to earlier case. This is because of incorporation of the spread and reliability index value used in the RBTO simulation. Due to these parameters, the factor values become distinct. Hence, high variation in compliance values is observed. It is also observed that the minimum compliance value is obtained for 16th combination, and a maximum values is obtained for 1st combination. The compliance values for different combinations differ from what of obtained from CA-DOE method. Hence, the characteristics of the combinations are slightly different with application of reliability index. Similar to compliance values, the results are obtained for the deflection values as shown in Fig 6.15.

The deflection values for different reliability index values are shown in Fig 6.15. The observations are similar to that of compliance values except for problem-4. In problem-4,

for combinations 4, 8, 10, 14, 15, and 16, the deflection values are same for the two reliability indexes. This is attributed to specific physics of the problem and the simply supported plate is stiff compared to the other chosen problems. Hence, its deflection is less sensitive to the input factors. This is the reason why the observed deflection values do not change with respect to the different reliability indexes.
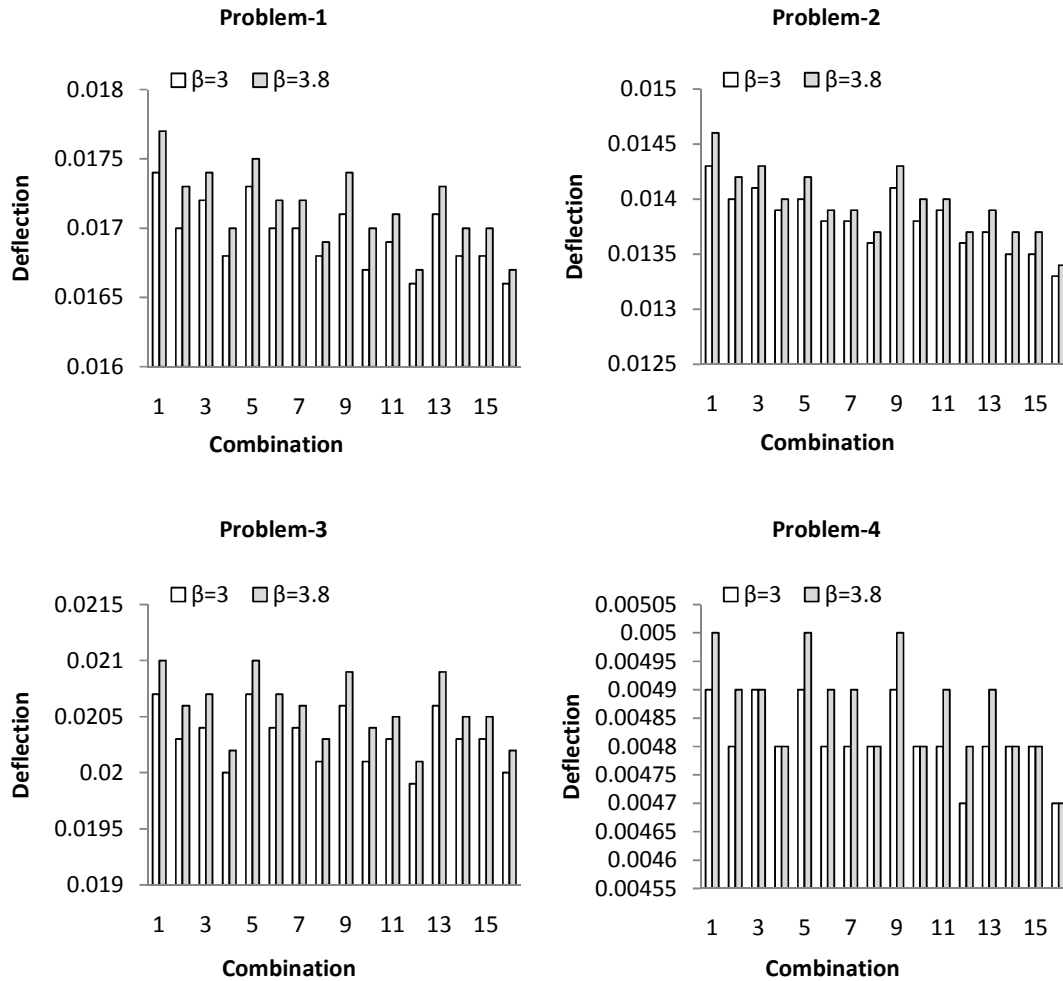


**Fig. 6.15: Deflection values (in mm) for tolerance combinations**

From the presented results of reliability based tolerance range selection, it is observed that the performances values of the combinations are slightly different compared to that of CA-DOE method. Therefore, to achieve a targeted performance in a desired reliable scenario, the above shown results are helpful.

## 6.7    CONCLUSIONS

Current chapter extends the approach discussed in Chapter 5, by incorporating the effect of manufacturing uncertainties for a specific manufacturing process. Here a tolerance-range selection method is proposed, where the optimal topology is manufactured without any further modification. In this process, a methodology to simulate the effect of geometric uncertainties caused by the manufacturing process is developed. This simulation methodology is advantageous to the user in terms of its customization. In present work, an integrated approach is developed, which integrates CA-DOE with proposed method, for the tolerance range selection. The overall methodology was illustrated using benchmark problems. Apart from the tolerance range selection for robust and targeted performance, the results show that the simulations can be performed on coarse mesh, as long as the topology and shape remains unchanged. By the comparison of simulated results, it is observed that the proposed approach is more realistic and accurate to the specific manufacturing process. In addition, a methodology is also presented by integrating the effect of manufacturing uncertainties and RBTO method, for tolerance range selection. The obtained result are based on the reliability index values, and observed to be different from earlier ones. The presented methodology is useful for the development of many critical applications of MEMS structures and the compliant mechanisms.

# CHAPTER 7

## AN INTEGRATIVE APPROACH TO DESIGN A BELL CRANK LEVER FOR FORMULA RACING CAR

### 7.1    INTRODUCTION

The work discussed in the earlier chapters has resulted in development of design methodologies, to ensure the robust and targeted performance of a topologically optimized structural component. During the development and illustration of these methodologies, help of four benchmark problems were taken to maintain consistency. These problems are representative and fundamental to several real life applications. For example, the MBB beam is an example of aircraft platform used by a German aircraft company; and the other benchmark problems i.e. cantilever and simply supported beam/plates, can be found in several structural and machine components. In order to validate the developed methodologies and emphasize its utility, another real life application is considered. This application deal with bell crank lever used in a shock absorber of formula-one racing car. The problem is taken from one of the live projects of Society of Automotive Engineers (SAE) BITS-Pilani, student's chapter (Mehta 2013). In this project, a team of students designed and developed a formula-one racing car to participate in various competitions taking place all over the globe. Through these participations and design exercise, the required knowledge for real time engineering application is imparted to the student community. In this process of application based learning, the design of formula-one vehicle evolves from time to time. In the present chapter, the challenge in weight reduction of the bell crank lever is taken to illustrate the application of developed methodologies. Here the optimal topologies of the bell crank lever are obtained for specified design requirements and weight reduction. Subsequently optimal topologies with robust, reliable, and targeted performance values are obtained

for this component. The systematic ways in which the problem dealt is discussed in next section.

## 7.2    PROBLEM FORMULATION

The bell crank lever is a versatile machine component used in several engineering systems to transfer force from one hinge point to another. In this section, the working principle of bell crank lever, the design parameters, and challenges faced by designer are described.

### 7.2.1    Working principle of bell crank lever

Bell crank levers are very common component in the suspension system of formula-one racing cars. Figure 7.1 shows a typical bell crank lever used in a suspension system of a racing car. In these racing cars, the spring and damper assembly is located within the bodywork due to aerodynamic reasons, which is different from the suspension systems used in standard cars. Apart from the aerodynamic reasons, the use of bell crank lever offers added control over the vehicle's ride height or its location in the suspension stroke via manipulation of the bell crank's geometric parameters.
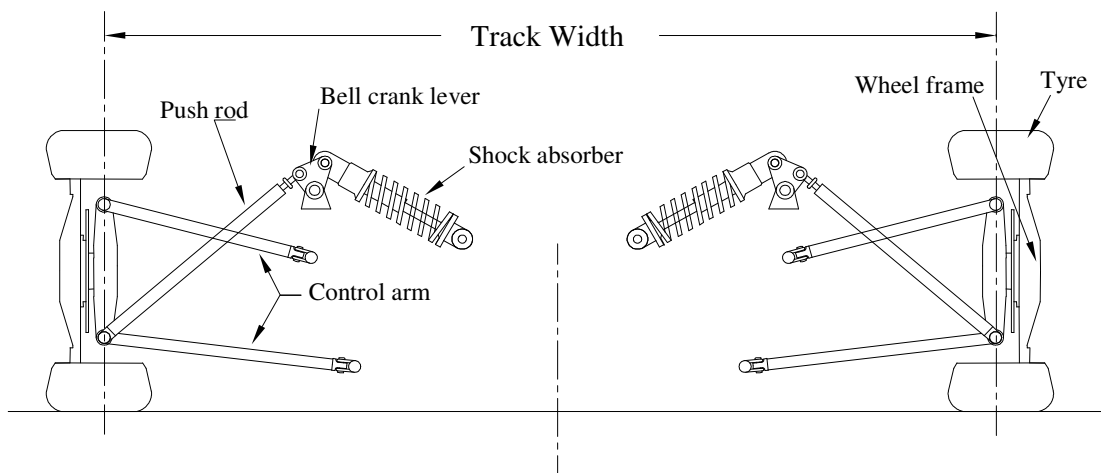


**Fig. 7.1: Bell crank lever in a shock absorber mechanism**

The bell crank lever is part of a shock absorber or suspension mechanism. This mechanism contains control arms to provide the up and down motion to the wheel assembly, and dependent on road conditions and driving skill. The unbalanced forces, which are prominent for this type of motions are exerted by the push rod. These forces from the pushrod are transferred to the shock absorber through the bell crank lever. The Free Body Diagram (FBD) of bell crank lever is shown in Fig. 7.2.
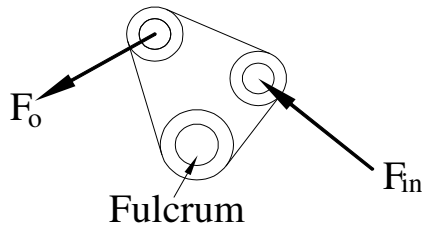
**Fig. 7.2: FBD of bell crank lever**

where, $F_{in}$ is the force acting from the push road and $F_o$ is the force transferred to the shock absorber. In order to transfer the force and motion to the shock absorber, the crank lever rotates by an angle with respect to the fulcrum. The angle of rotation and leverage (mechanical advantage) obtained from the bell crank lever is dependent on several factors such as, the specification of the shock absorber, location of the fulcrum and the other fixed joints in the mechanism, the dynamic loading, material selection for bell crank and chassis, running conditions, etc. In considered bell crank lever, a few design options of the leverage available to the designer, which are detailed in the next section. Subsequently the important design parameters for this component are identified and are presented in next section.

### 7.2.2 Design options for the leverage of bell crank lever

The leverage required from a bell crank lever, is dependent on several aforesaid factors. In the present case, there some design options for leverage are provided to design the lever. These options define the different joint locations on the lever, for the push rod, shock absorber, and fulcrum. For convenience, these design choice are termed as configuration-1, 2, and 3, and shown in Fig. 7.3. This figure shows the joint distances from the fulcrum. Other details of the lever design are discussed next.
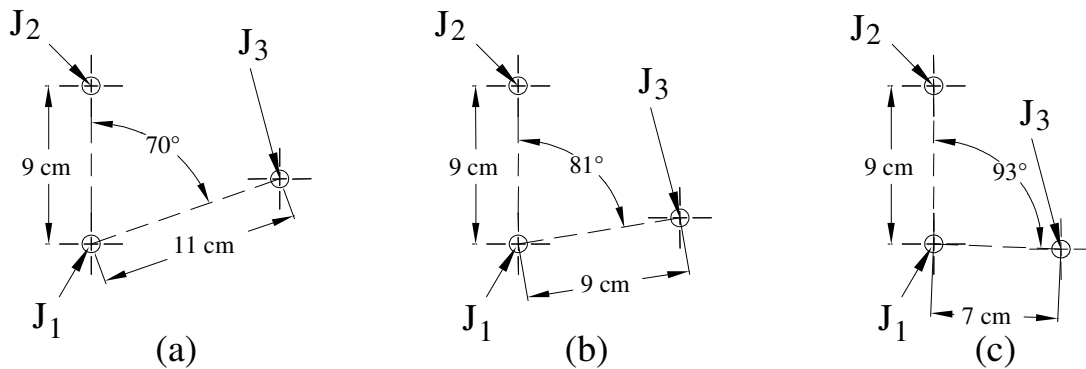


$J_1$: Shock absorber  joint     $J_2$: Pushrod  joint     $J_3$: Fulcrum  joint

**Fig. 7.3: The location of various joints in (a) configuration-1, (b) configuration-2, (c) configuration-3**

### 7.2.3 Loading and material selection

The bell crank lever is an automotive component, which is subjected to dynamic load. To get first cut design of lever and to keep design calculations simple, the design is carried out using maximum static load. The justification behind choosing such load is to take the effects of dynamic loads into account. These effects are incorporated by increasing the value of force to the maximum fluctuating load with a tolerance value. After design calculations, the load acting on pushrod joint is assumed to be 1600N. The joints of bell crank lever are always designed to increase the strength in bearing, bending and shearing. For such condition plates or sheets of bell crank lever is assembled together to provide symmetrical loading, as shown in Fig. 7.4.
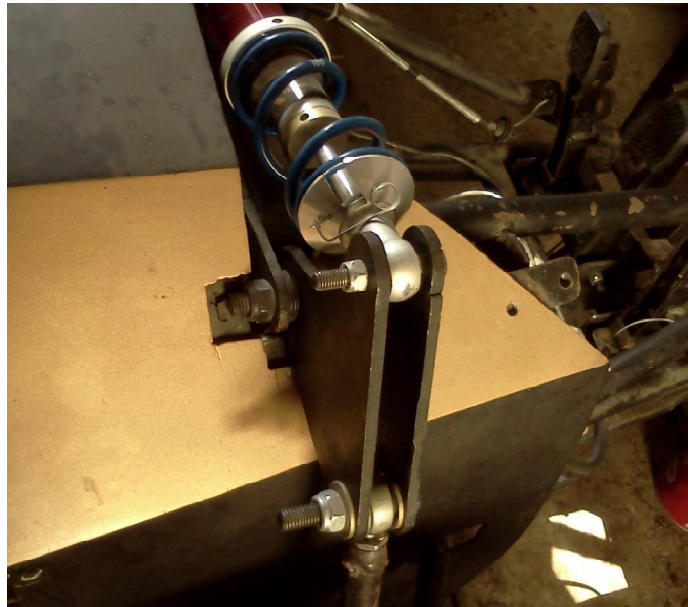


**Fig. 7.4: Bell crank lever Assembly (Mehta 2013)**

From Fig. 7.4, it can be seen that a lever assembly is made using two bell crank lever. Thus, the maximum force acting on a bell crank lever will be 800N. Along with the maximum force values, the direction of the maximum forces on the push rod and shock absorber joint is also specified, for the given configuration, as shown in Fig. 7.5. The stress developed in the lever should be able to withstand the available material strength. There are several options regarding material are available to manufacture the lever. In present case, the available materials are structural steel (ASTM 36), Aluminum alloy 6061 T913, and Aluminum alloy 7075 T6. The engineering properties of these materials are given in Table 7.1

Configuration-1          Configuration-2          Configuration-3
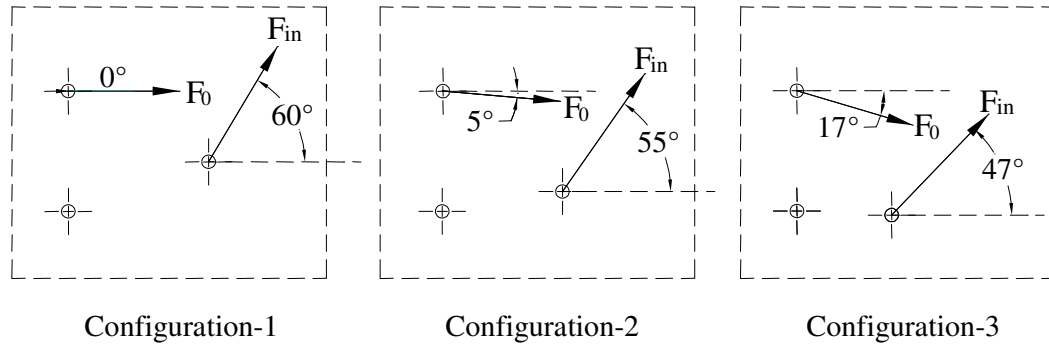
**Fig. 7.5: Direction of forces on the different configurations**

**Table 7.1: Properties of the materials selected to manufacture the bell crank lever**

| Material | Modulus of Elasticity (GPa) | Poison's ratio | Maximum Yield stress (MPa) | Density (gm/cc) |
|---|---|---|---|---|
| Structure steel, ASTM A36 | 200 | 0.26 | 250 | 7.8 |
| Al 6061 T913 | 69 | 0.33 | 455 | 2.7 |
| Al 7075 T6 | 72 | 0.33 | 503 | 2.81 |

With the specified values of forces, materials, and configurations, the important dimensions are provided to the designer and details are discussed in next section.

### 7.2.4   Dimensions of bell crank lever

The dimensions of bell crank lever are given in terms of joint-hole diameter, and thickness, as shown in Fig. 7.7. The radius of joint hole of shock absorber and push rod is provided as 8 mm, the joint hole for fulcrum bearing is provided as 16 mm, and the thickness of the bell crank lever is given as 6 mm, based on the assembly constraints. These dimensions are found to be safe for the materials available for the design. From available initial specifications, the problem for bell crank lever is formulated, and details are discussed below.

### 7.2.5   Problem statement

In the earlier sections 7.2.2 to 7.2.4, the initial geometry, forces, material properties, diameter of holes, and the thickness of the bell crank lever are provided to the designer. The major part of the design that remains unanswered is to give a proper shape or topology to the bell crank lever. Intuitively any shape can be selected for bell crank

lever, which may confirm its strength against the stress developed. However, weight of the component in that case will be higher, and can be lowered by performing shape or topology design in multiple iterations. Instead of doing this manually, topology optimization procedures are adopted, as weight reduction issue is very critical for design of the components of formula one racing cars.

The weight reduction issue, for the 2012 BITS Pilani team is inspired from the competition held in 2005, where the majority of the top ranked vehicles were below 250 kg in weight. While the 2012 BITS Pilani, entry was heavy at 310 kg, thus the primary goal was to achieve weight less than 270 kg. This would represent a weight loss of roughly 13% of the entire vehicle (Mehta 2013). Thus, while designing any component of the 2012 BITS Pilani formula one car, weight reduction was the prime aim along with the other design constraints. It is also evident from the previous discussion that each component should reduce the weight at least by 13%. In fact, a high weight-reduction is desired for most of the components, to compensate the weight of the other components that cannot be lighter more than a limit such as engine, gears, etc. Presently, the BITS Pilani formula one car uses a bell crank lever, shown in Fig. 7.6. This component is an assembly of two levers. The weight of each lever is approximately 425gm, and its weight should be reduced at least by 13%.



**Fig. 7.6: The existing bell crank lever in the BITS Pilani formula car (Mehta 2013)**

Thus, the topology of bell crank lever should be optimized. Application of topology method will provide possible solutions, which have reduced weight, with its strength at the maximum possible value. Being a critical component, the reliability and consistence performance in the realistic scenario is also one of the requirements of the bell crank lever. There are possible variations in the different design constraints such as force, thickness, force-angles, etc. The final design should be robust and reliable enough against these variations. There may be a band of desired performance range, in which the lever has to perform. In case of a topologically optimized machine component, the performance is stated in terms of compliance, deflection, and stress values. The detailed discussion on performance measures is already available in earlier chapters. This performance range, or the targeted performance of the bell crank lever, may change with the design of other components of the formula one racing car. Hence, the issue is to not only provide unique design, but to provide a set of multiple design solutions. This will facilitate to choose a correct design while different parameters are adjusted with other components, and ensure the desired performance. This approach will in fact optimize the overall design and functioning of the BITS-Pilani formula one racing car.

With the earlier stated design parameters, and issues, the problem statement can now be defined as "Generate an optimal topology of the bell crank lever with at least 13% weight reduction, which attains different targeted and robust performance requirements." The methodology used to solve the posed problem is described in the following section.

## 7.3 GENERATION OF OPTIMAL TOPOLOGIES FOR THE BELL CRANK LEVER

Based on the design parameters and conditions discussed in the previous section, the optimal topology is generated using SIMP method. The details of topology optimization method is already discussed and important steps to obtain the optimal topology for the bell crank lever are mentioned sequentially,

### Step 1. Define the initial material domain

In order to apply topology optimization method, a material domain should be defined. The final optimal topology will be obtained within this material domain. Thus, all the design and geometric features must be accommodated in this domain. The initial domain is defined for the specified configurations and shown in Figs. 7.7(a)-(c). In these figures,

notch on the left side is provided, which will avoid the interference of the bell crank lever with the shock absorber as indicated in Fig. 7.6.
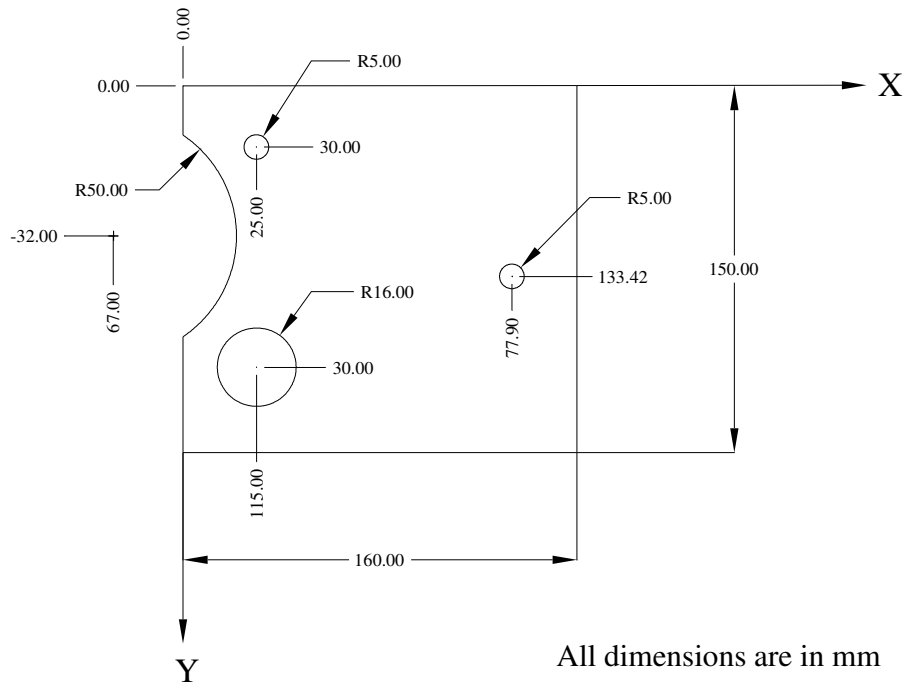
**Fig. 7.7(a): Material domain for the configuration-1**
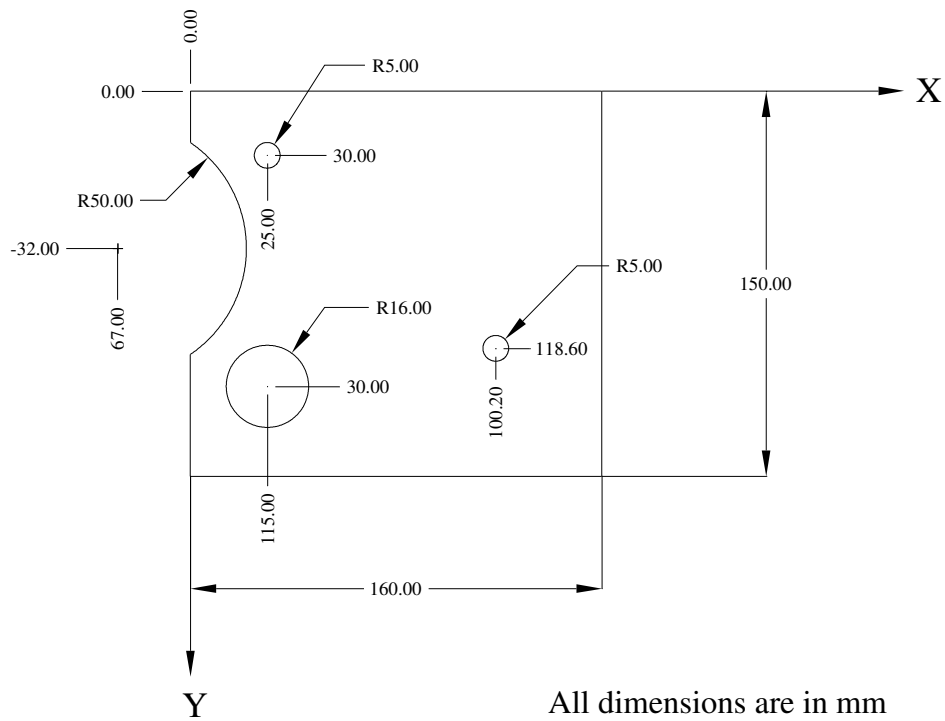
**Fig. 7.7(b): Material domain for the configuration-2**
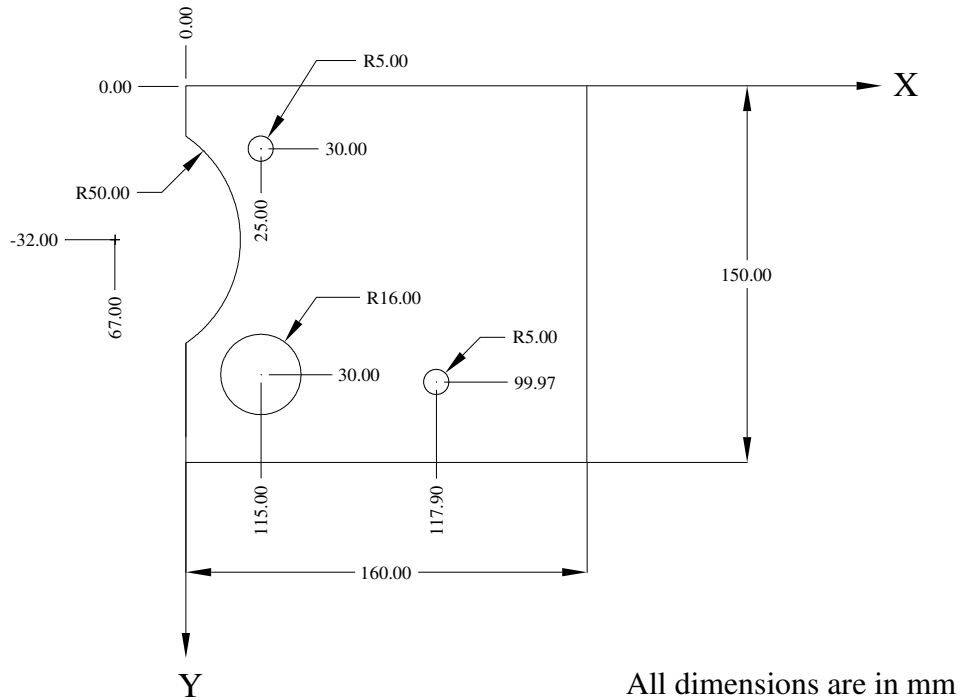
**Fig. 7.7(c): Material domain for the configuration-3**

**Step 2. Define material properties, mesh size, forces, and other boundary conditions**

As discusser earlier, the initial material domain is defined. The materials are selected based on the options available in Table 7.1. Finally, the forces and other boundary conditions are defined to formulate the FE based routine. The boundary conditions including the applied force, fixed and free degrees of freedom at different nodes are defined in parametric form for different element numbers. So that, a changed mesh size can be easily adopted by the FE routine and do not disturb the geometric features and boundary conditions. The developed routine allows generation of the topology at different mesh size without affecting the physics of the problem. Here the mesh size reflects the smoothness of the obtained topology. As it is known already that by increasing the mesh size the computation time increase and vice-versa, hence a proper tradeoff is required and to obtain smoother boundaries, therefore a mesh size of 160×150 is selected in present case.

**Step 3. Set the volume fraction value**

The weight reduction issue is already discussed. At this point, volume fraction value for the material domain should be defined. For the selection of a proper volume fraction

value, the topology is generated at different values. Based on the performance threshold values a particular value or range of volume fraction is selected, and discussed at the end.

**Step 4. Start the iterations of optimization**

After setting all the initial parameters, the topology optimization process is initiated and the procedure is discussed in section 3.3.5.

**Step 5. Application of filter to suppress gray scale**

Since this is a realistic problem, the gray scale or intermediate densities cannot be accepted in the optimal topology. To suppress these grayscale or intermediate densities a Heaviside projection filtration (Guest et al. 2004) method is used to update the density parameters.

**Step 6. Check the termination criterion:**

In each iteration, the values of nodal deflection, compliance, and stress values are computed. The compliance value is compared to check the error tolerance. After achieving the desired tolerance range, the iteration is stopped; otherwise, the steps 4–6 are repeated. At the termination of the optimization process, the final optimal topology with compliance, maximum deflection and maximum Von-Misses stress value are stored for suitable use.

### 7.3.1   Selection of volume fraction value

The upper and lower bound for volume fraction values are obtained by performing following calculations,

Weight of present design (Fig. 7.6) = 425gm

Minimum reduction required = 13% of the present weight

Hence, the maximum allowable weight = 425× (1-0.13) =369.75 gm

The weight of the initial material domain (shown in Fig.7.7), is equivalent to a topology at volume fraction equal to 1.0, and given in Table 7.2.

**Table 7.2: Weight of material domain for the different material options**

| Material | Density (gm/cc) | Wight of material domain (gm) |
|---|---|---|
| Structure steel, ASTM A36 | 7.8 | 1008 |
| Al 6061 T913 | 2.7 | 346 |
| Al 7075 T6 | 2.81 | 360 |

Now, based on the maximum allowable weight (369.75 gm) the maximum volume fraction can be computed for different materials, as below

Max. volume fraction= Max. allowable weight (i.e. 369.75 gm)/total weight of material domain. Hence,

For structural steel (ASTM A36), maximum volume fraction $= \dfrac{369.75}{1008} = 0.37$

For Aluminum alloy (Al 6061 T913), maximum volume fraction $= \dfrac{369.75}{346} = 1.68$

For Aluminum alloy (Al 7075 T6), maximum volume fraction $= \dfrac{369.75}{360} = 1.27$

In order to compare the design obtained by experimental combination set a common volume fraction values is required. Hence, the upper bound for volume fraction can be set as 0.37 for chosen materials.

For the lower bound of volume fraction, the stresses and deflection values are considered in terms of factor of safety. In literature, the minimum factor of safety for bell crank lever and other components of formula-one car is found out to be equal to 2.5 (Bos 2010, FIT-PDR 2008, Fornace 2006). Hence, in the present case the same criterion is followed to decide the lower bound for volume fraction. To observe the values of stress at different volume fractions, various topologies are generated. This process helps in deciding the volume fraction value based on the factor of safety. The optimal topologies with corresponding to different volume fractions are shown in Fig. 7.8.

| Volume fraction & weight (gm) | Configuration-1 | Configuration-2 | Configuration-3 |
|---|---|---|---|
| 0.15 & 151.2 |  |  |  |
| | $C^*$=56.41, $D^*$=0.0771mm, $S^*$=827.3 N/mm$^2$ | C=29.81, D=0.0439mm, S=251.8N/mm$^2$ | C=13.55, D=0.0261mm, S=234.88 N/mm$^2$ |
| | | | **\*C= Compliance, D= Deflection, S= Maximum Von-Mises stress** |

| Volume fraction & weight (gm) | Configuration-1 | Configuration-2 | Configuration-3 |
|---|---|---|---|
| 0.2 & 201.6 |  |  |  |
| | C=21.58, D=0.0251mm, S=133.7 N/mm2 | C=11.56, D=0.0162mm, S=128.9N/mm2 | C=5.53, D=0.0086mm, S=61.2N/mm2 |
| 0.25 & 252 |  |  |  |
| | C=13.72, D=0.0153mm, S=75.3 N/mm2 | C=7.37, D=0.0092mm, S=57.5N/mm2 | C=3.66, D=0.0045mm, S=49.2N/mm2 |
| 0.3 & 302.4 |  |  |  |
| | C=9.50, D=0.0109mm, S=87.8 N/mm2 | C=5.46, D=0.0066m, S=38.1 N/mm2 | C=2.66, D=0.0031mm, S= 36.8N/mm2 |
| 0.35 & 352.8 |  |  |  |
| | C=7.65,D=0.0089mm, S=54.8 N/mm2 | C=4.33,D=0.0054m, S=41.2 N/mm2 | C=2.19,D=0.0024mm, S= 32.1N/mm2 |
| 0.4 & 403.2 |  |  |  |
| | C=7.29,D=0.0074mm, S=48.5 N/mm2 | C=3.59,D=0.0043mm, S=40.3 N/mm2 | C=1.86,D=0.0019mm, S=28.3 N/mm2 |
| | | | **\*C= Compliance, D= Deflection, S= Maximum Von-Mises stress** |
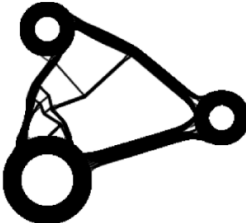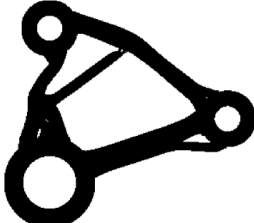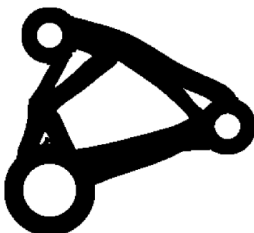
**Fig 7.8 Optimal topologies of the three configurations of bell crank lever, for different volume fractions**

From these results, it can be seen that at the smaller for volume fraction i.e. 0.15 & 0.2, and the factor of safety is lesser than 2.5 for structural steel. However, the other materials are safe, at these values of volume fraction. As discussed earlier, in order to compare the performance of each material at same scale, common values of volume fraction is to be defined. Hence, the lower bound for the volume fraction is selected as 0.25 for all materials. As it can be observed from Fig 7.8, there is a tradeoff is between strength and weight. Hence, the upper bound of volume fraction is taken as 0.35.

It is clear from the given design conditions, i.e. configurations, materials and range of volume fraction that there are several ways by which an optimal topology can be generated. In such scenario, a systematic approach is required to select the required topology for the desired performance values. This type of problems can easily be handled using the DOE approach, where the input factors have certain levels instead of a single value. This approach also provides the opportunity to incorporate the effects of noise factors, thus the solutions become more robust compared to a deterministic case. The details of DOE approach are already mentioned in the earlier chapters. The application of this approach to design a bell crank lever is presented in the next section.

## 7.4    ANALYSIS OF PERFORMANCE MEASURES

In order to analyze the performance of the bell crank lever design and identify the optimal values of the factors, the methodology proposed in Chapter 3 is used here. In this case, available configurations, options for material, and allowable weight reduction for the bell crank lever are treated as the controllable factors. Three level values for volume fraction are selected from the acceptable range of volume fraction. These are 0.25, 0.3, and 0.35. Using selected level values of factors, i.e. $3^3$ factorial designs are obtained. These treatment combinations are shown in Appendix A11.

To simulate realistic scenario, identified effects of uncertainties are included, which are called as noise (non-controllable) factors. These noise factors are: the thickness of the bell crank, force, input force-angle, and output force-angle. The thickness of the bell crank lever is assumed to have a total variation of 10% from its nominal value. Similarly, the variations of force value and its angle of application are considered with 10% and $10^0$ deviations from their nominal value, respectively. The way force is applied to the lever is shown in Fig. 7.4, and simulations are carried out for each controllable factor combination (Appendix A11) and replications are performed using non-controllable factors. As

specified earlier, there are four non-controllable factors, and each of these is has three levels of noise. Thus, the number of replications required will be $3^4$. In this case, the total number of simulations (or experiments) will be very large, as each combination of the controllable factor will undergo $3^4$ replications. Hence, to reduce the total number of simulations, the replications are required to be reduced, without losing the inputs from non-controllable factors. In such case the orthogonal array (OA) suggested by Taguchi is utilized (Sung 1998; Mitra 2008; Montgomery 2007).The column of this OA are assigned to non-controllable factor and the rows correspond to the number of replications. Each row has distinct combination of level of non-controllable factor. A particular Taguchi's array is selected based on the number of non-controllable factors and their levels. In the present case, there are four non-controllable factors with three levels. Hence, Taguchi's $L_9$ OA is selected (Sung 1998; Mitra 2008; Montgomery 2007). The $L_9$ OA for the present case is available in Appendix A12. As per $L_9$ OA, nine replications are generated. By this approach, the number of experiments decreases by nine times. Thus, the worst-case scenarios can be simulated in lesser computation. The optimal topologies of the bell crank lever is generated which gives the performance values. The applied force and the initial material domain are set as shown in Figs. 7.5 and 7.7. The SNR and mean values are obtained after simulation and presented in Figs. 7.9 and 7.10, respectively.

It is observed from these results shown in Figs. 7.9 and 7.10, that the combination number 27 is the best and 1 is the worst in all criterions of mean and SNR of the performances. The other observations made are given below,

➤ In these results, a similar trend is observed, especially in the case of compliance and deflection. The reason for this trend can be understood by referring to the combinations available in Appendix A11. In all the three design configurations, the relative effect of the volume fraction and elasticity values is almost same. That is why when the combinations with same volume fraction and elasticity values are repeated for the three configurations, a similar performance is observed.

➤ From these results, the relative performance with respect to the material type can also be carried out. It is evident from the compliance and deflection results that the increase in elasticity value, leads to increase in structural rigidity. Whereas the stress based performance is not very sensitive to these change. The mean and SNR values of the Von-Mises stress are almost same in the case of different elasticity values, leaving few observations.
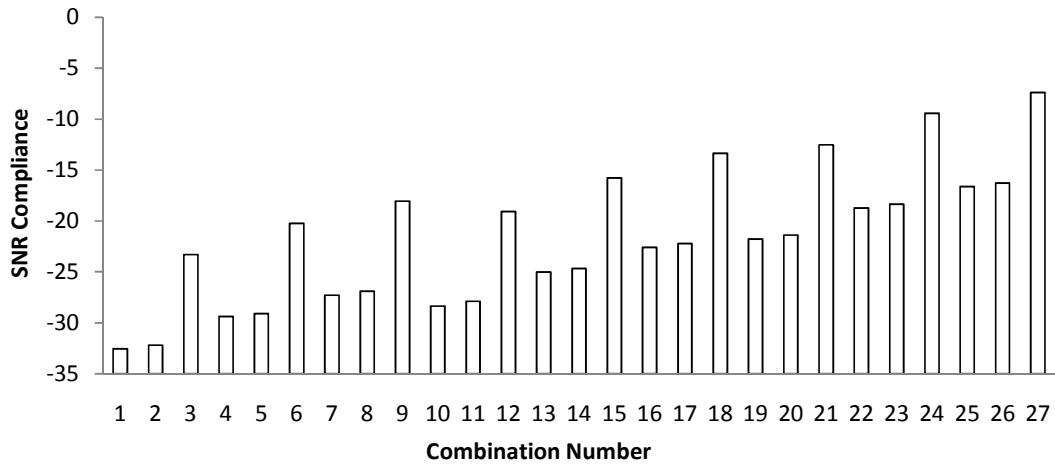
(a)
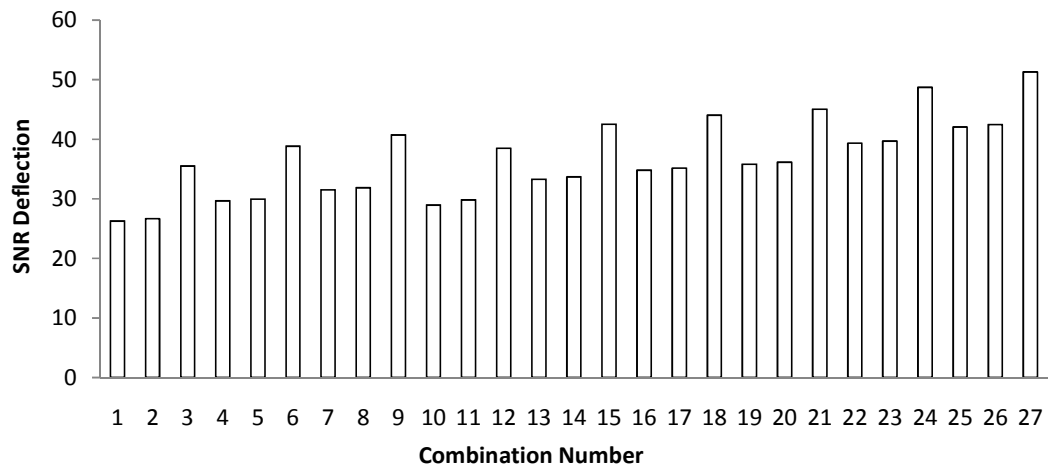


(b)
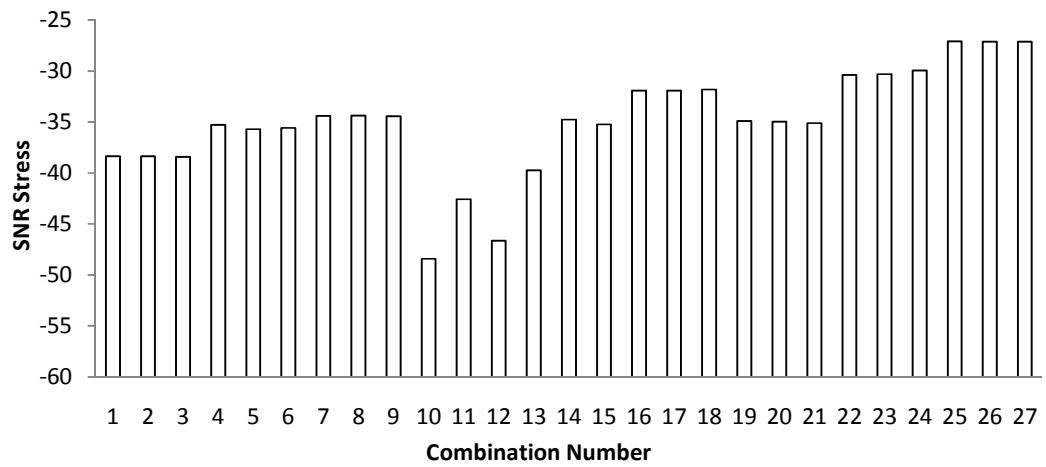


(c)

**Fig. 7.9: Performance values (a) SNR of compliance, (b) SNR of deflection, and (c) SNR of Von-Mises stress, against combination number**
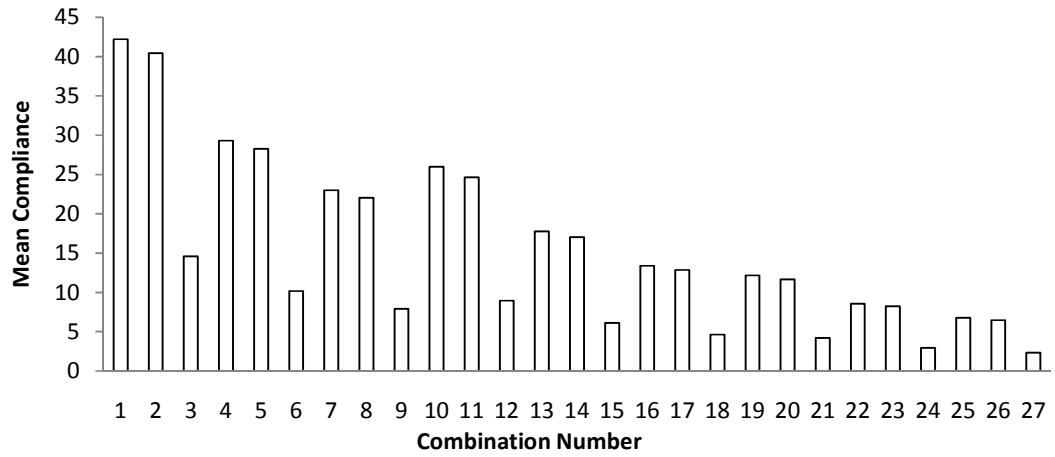
(a)
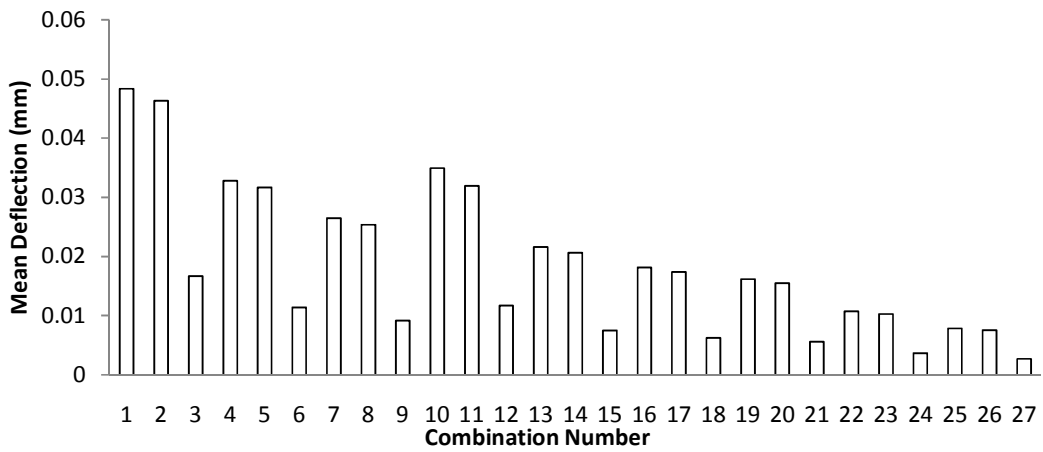


(b)
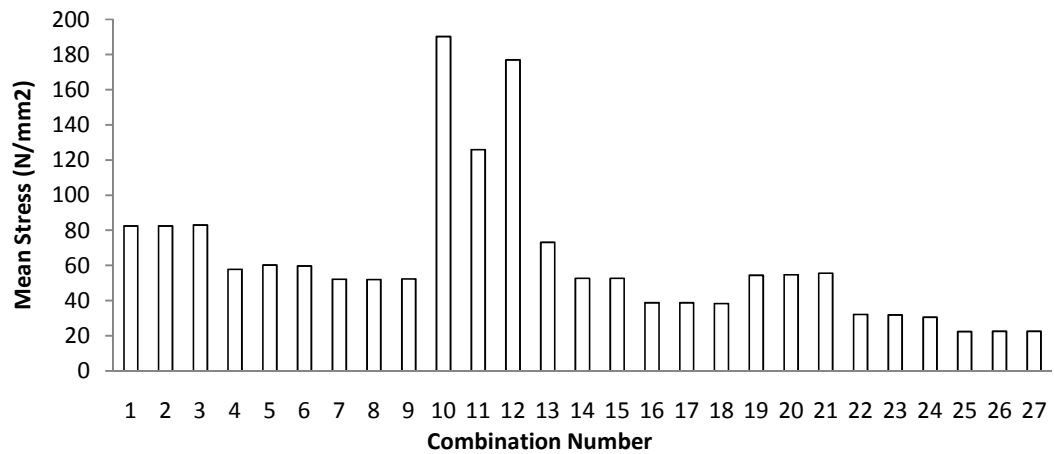


(c)

**Fig. 7.10: Performance values (a) mean compliance, (b) mean deflection, and (c) mean Von-Mises stress, against combination number**

➢ A change in the overall performance can be observed with the shifting of values of volume fraction. Compliance is found to be is highly sensitive, while stress values are least sensitive. Hence, a high value for volume fraction is desirable; at the same time, it should be low to reduce the weight of the component. Therefore, a tradeoff ie required for these two parameters, and selected based on desired values for performance.

➢ The relative performance of the three configurations can also be observed from these results. Based on performances, configuration-3 is observed as the best performer, at the same time configuration-1 is the worst performer. In case of stress values, an abrupt change in the stress values is observed. This is attributed to the physics of the configuration-2. In order to avoid such high stress values, configuration-2 should be avoided.

In order to observe the statistical significance of the controllable factors, ANOVA is performed. Result of ANOVA is summarized in Table 7.3 for the different performance measures. The symbols C, V, and E are used to denote configuration, volume fraction, and elasticity respectively.

**Table 7.3: Statistically significant factors from ANOVA**

| Performance measure | Statistically Significant Input factors |
|---|---|
| Compliance | E, V, C, EV, EC, VC, EVC |
| Deflection | E, V, C, EV, EC, VC |
| Stress | V, C, VC |

As discussed in earlier chapters, one of the main contributions is select alternate combinations of the designs, which delivers desired performance values. From this analysis, the alternatives are identified, which have similar performance as the desired values. In this section, the performance of the bell crank lever was observed by considering the effect of non-controllable factors. In the next section, the same is discussed to incorporate the effect of uncertainties present in the design factors for specified reliability index and spread.

## 7.5    ANALYSIS    OF    PERFORMANCE    MEASURES    BASED    ON RELIABILITY

In this section, the performance of the bell crank lever is simulated by including the effect of uncertainties of the design factors such as, elasticity values, dimensions, and volume fraction. The possible variations of the design factors are selected based on the percentage variation around the nominal values. The variations are considered for the two spread values (S) i.e. 10% and 20% of the nominal values of the factors. The reliability index (β) is taken as 3.8 and 3. For illustration the topologies for β =3.8 and S=10% is shown for different volume fraction values in Fig. 7.11. It can be observed that the topologies are slightly different compared to the deterministic case shown in Fig. 7.8.
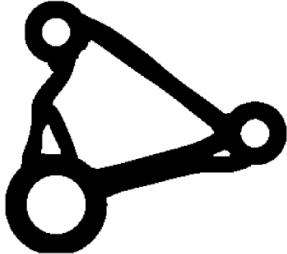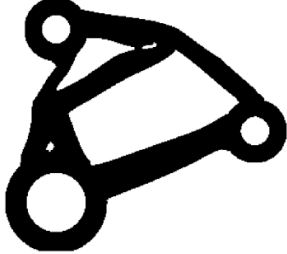
| Volume fraction | Configuration-1 | Configuration-2 | Configuration-3 |
|---|---|---|---|
| 0.25 |  |  |  |
| | *C=18.2353, D=0.0239mm, S=53.31 N/mm2 | C=9.7452,D=0.0125mm, S=43.47N/mm2 | C=4.5915,D=0.0064mm, S=33.60N/mm2 |
| 0.3 |  |  |  |
| | C=13.975,D=0.0177mm, S=70.07N/mm2 | C=7.2584,D=0.01mm, S=31.24N/mm2 | C=3.3979,D=0.0052mm, S=30.73N/mm2 |
| 0.5 |  |  |  |
| | C=5.8829,D=0.0072mm, S=22.8N/mm2 | C=3.3036,D=0.0039mm, S=20.7N/mm2 | C=1.8094,D=0.0015mm, S=17.5N/mm2 |
| | *C= Compliance, D= Deflection, S= Maximum Von-Mises stress | | |

**Fig 7.11: Optimal topologies for the three configurations at different volume fractions, with β =3.8, and S=10%**

As per the methodology detailed in Chapter 4, the performance of the bell crank lever is simulated. The results of this simulation, in terms of mean and SNR of the performances are given in Figs. 7.12 and 7.13 respectively. In these figures, the legends represent the value of reliability index (β)/spread percentage(S).



(a)



(b)



(c)
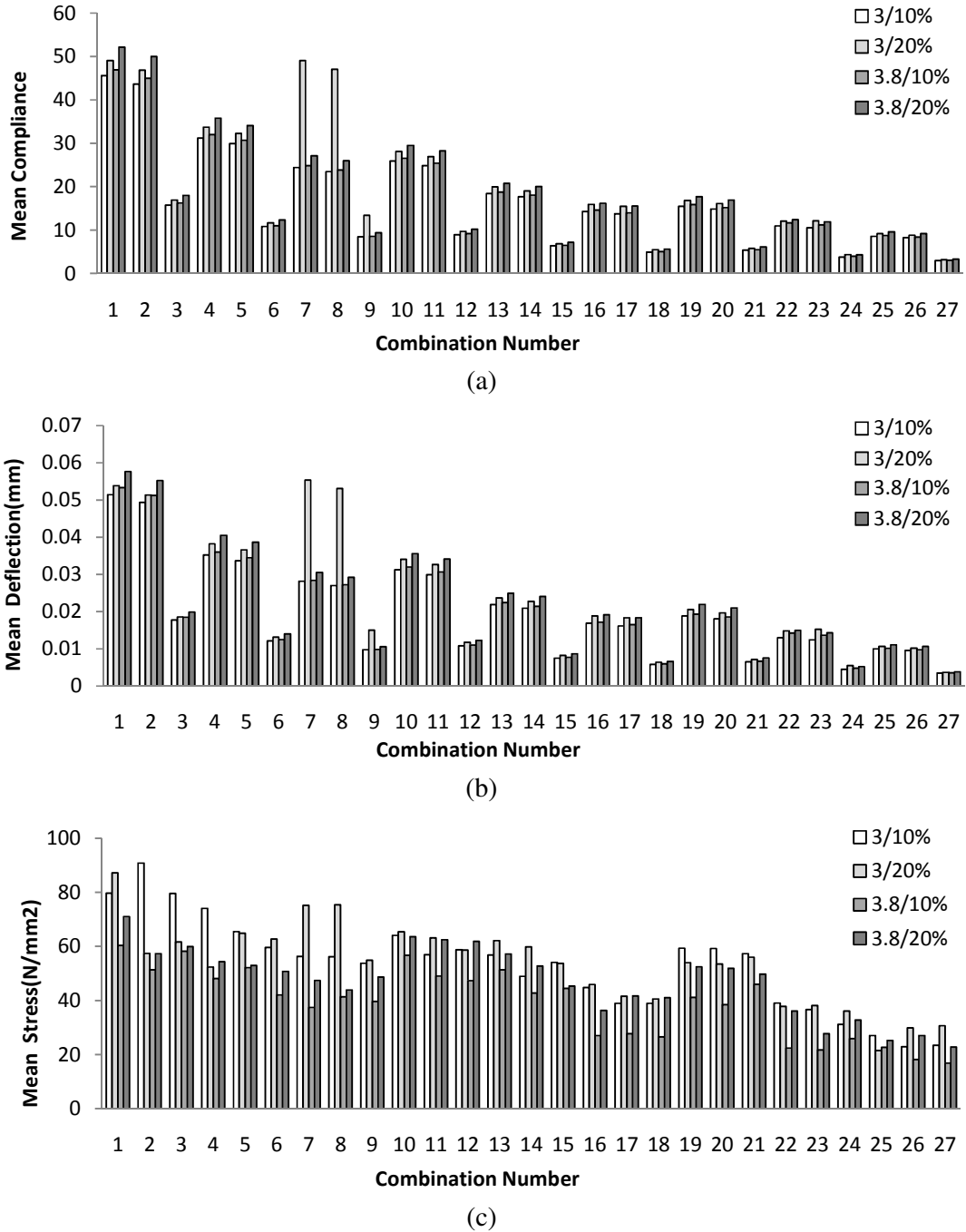
**Fig 7.12: Performance values for (a) mean compliance, (b) mean deflection, and (c) mean Von-Mises stress values, for different values of β and S**

The simulation results for Mean values of performances are show in Fig 7.12. In these figures, the performance values are plotted with respect to different treatment combinations, i.e. reliability index and spread values. The overall variation of performance is similar to the previous result shown in Figs. 7.9 and 7.10. The important observation here is that the mean performance increase when β values increase. Also, an increasing trend is observed with increasing values of spread value. However, the performance values are more sensitive to the spread values compared to the reliability index value. These observations are true for the scenarios when compliance and deflection are the performance. On the contrary to these observations, when the performance measure is mean Von-Mises stress, the increase in reliability index reduces the mean stresses. This indicates that the design is moving into safe region, when there is increase in reliability index. A few combinations i.e. 7th and 8th, show irregularities in the mean stress and this is because of the change of the shape or topology at different reliability index and spread values. Since the topology change for the different combinations, inconsistency in mean stress values are observed here.

Similar to the mean values, the SNR values are plotted for different β, and S values in Fig. 7.13. From Fig 7.13, it is observed that with the change in values of β and S, the SNR values change. The sensitivity of the SNR is high for change in S values compared to β values. The abrupt changes at combination numbers 7 and 8, for β=3 and S=20% are also observed in these results. As discussed earlier, this is because of the change in the topology at these combinations.

The aim of this analysis is to provide alternative options to designer for the selection of affordable combinations of the factor and reliability values in order to achieve the targeted or robust performances. The robustness and targeted values can be improved further by analyzing the tolerance range values of the different factors. The implementation of tolerance range selection methodology for the bell crank problem is discussed in next section.
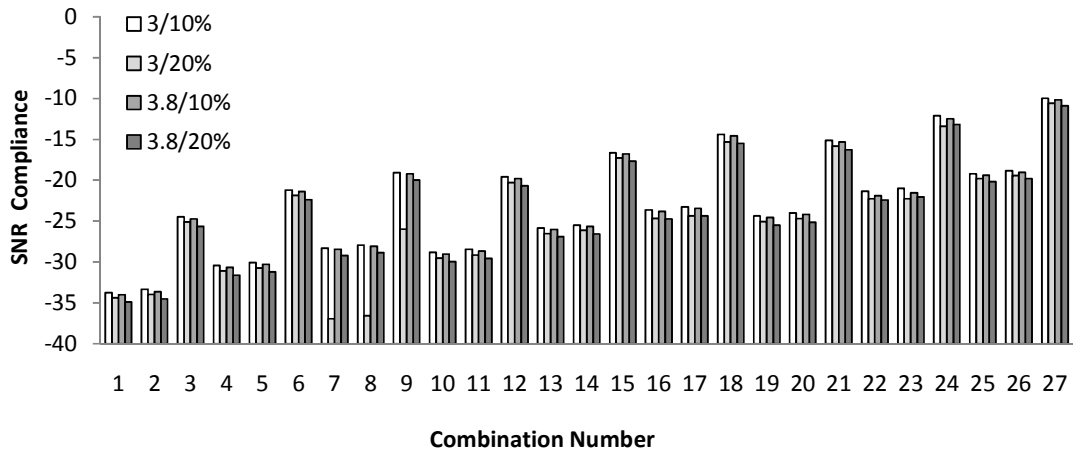
(a)
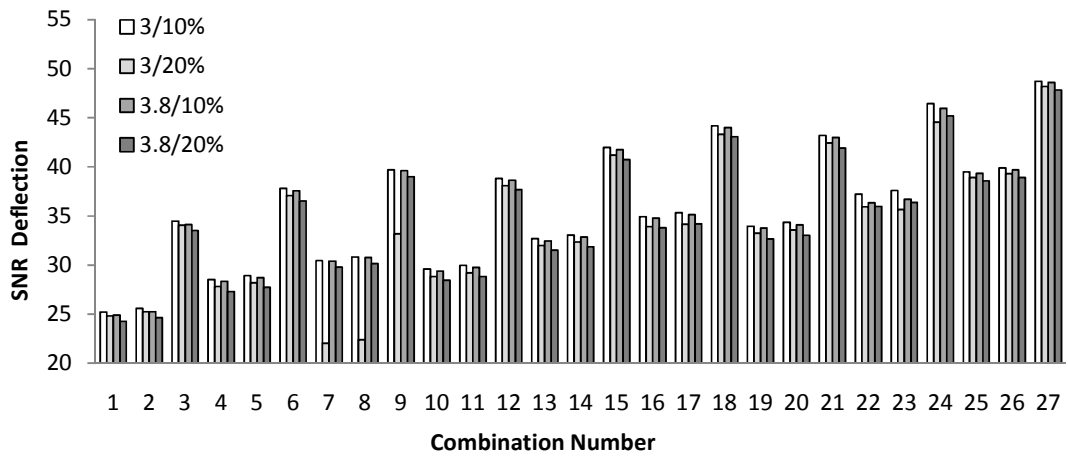


(b)
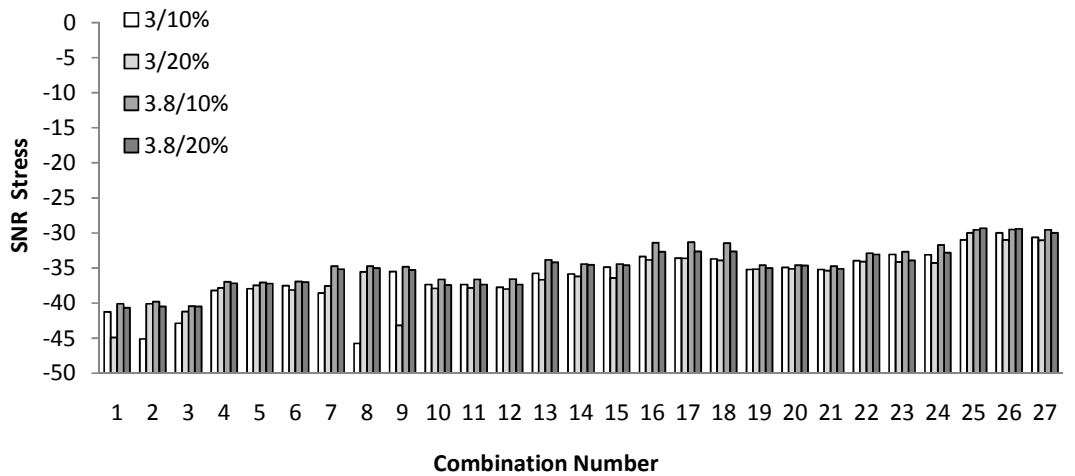


(c)

**Fig 7.13: Performance values for (a) SNR of compliance, (b) SNR of deflection, and (c) SNR of Von-Mises stress values, for different values of β and S**

## 7.6     SELECTION OF TOLERANCE RANGES FOR THE OPTIMAL FACTOR

It can be seen from the previous analysis that the combination number 27 performs best out of the design options. The selection of the combination is entirely dependent on the affordability of the combination, and the combination that gives the best performance in terms of robust and targeted values. In order to achieve targeted and robust performance design, the tolerance ranges are identified. In the present case, for combination number 27 is chosen to extend the analysis for tolerance range selection. The tolerance ranges for each factor is defined in terms of loose and tight tolerance. These values are chosen based on real time application. In the present analysis, the non-controllable factors such as force, thickness and the angles of force are analyzed for its tolerance range. The Figs. 7.8 & 7.11 show that the topologies are complicated to manufacture. Hence, some secondary process is required to simplify the obtained topology. This secondary process may be shape optimization process, or manual correction process, which should be applied on optimal topology to reduce the complexities. Thus, material addition or removal in terms of volume fraction is chosen as secondary process here. This variation in volume fraction is modeled as the tolerance of the volume fraction in the present case. The tight and loose tolerance range is fixed by relaxing the volume fraction from 5% to 10% of its nominal value, respectively. The tolerance values of each of these factors with its nominal values are presented in Table 7.4.

**Table 7.4: Nominal values and loose and tight tolerance limits for the selected factors**

| S. No. | Factor | Nominal Value | Loose tolerance | Tight tolerance |
|:------:|:------:|:-------------:|:---------------:|:---------------:|
| 1 | Thickness(mm) | 6 | ±0.3 | ±0.15 |
| 2 | Elasticity(GPa) | 200 | ±5 | ±2.5 |
| 3 | Volume fraction | 0.35 | ±0.0175 | ±0.00875 |
| 4 | Force(N) | 800 | ±5 | ±2.5 |
| 5 | Input Angle | $47^0$ | $±5^0$ | $±2.5^0$ |
| 6 | Output Angle | $17^0$ | $±5^0$ | $±2.5^0$ |

As already described in section 5.2 (Tolerance-range selection based on CA-DOE method), the inner and outer OAs are utilized to simulated the performances. Hence, based on the two tolerance ranges, i.e. loose and tight, the inner OA is generated. In the present case, there are six factors with two levels of each, therefore 64 (i.e. $2^6$)

combinations are generated, and provided in Appendix A13. In order to incorporate the actual tolerance values, which are treated as noise, an outer OA is selected. In the present case, there are six factors with two levels. Hence, Taguchi's $L_8$ OA is selected to form the outer OA (Appendix A14). The analysis for the tolerance range selection is performed based on the methodology explained in Chapter 5. The results obtained from simulation are given in terms of the mean and SNR values of compliance, deflection and Von-Mises stress. The results corresponding to each combination of inner OA and the performance measures are shown in Figs. 7.14 and 7.15.
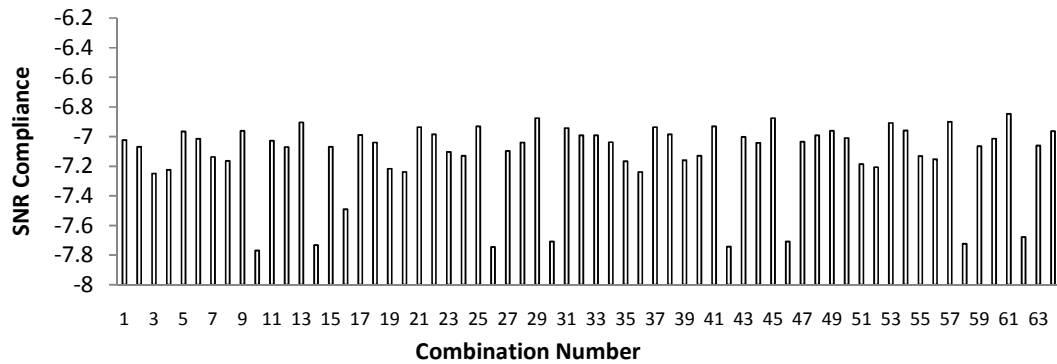


(a)
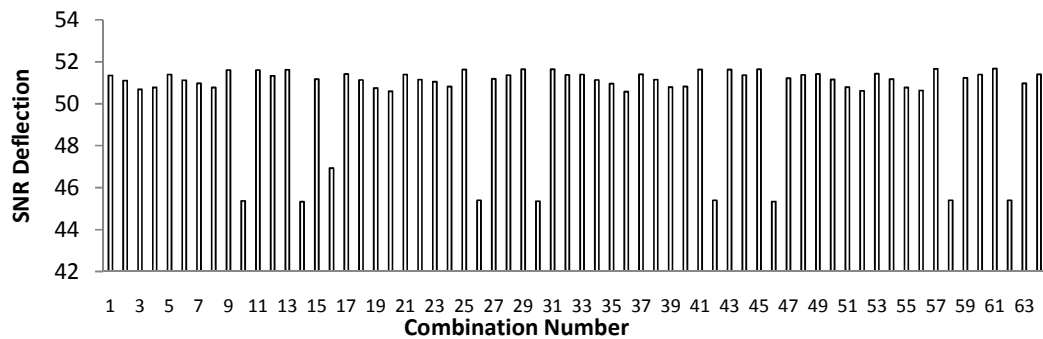


(b)
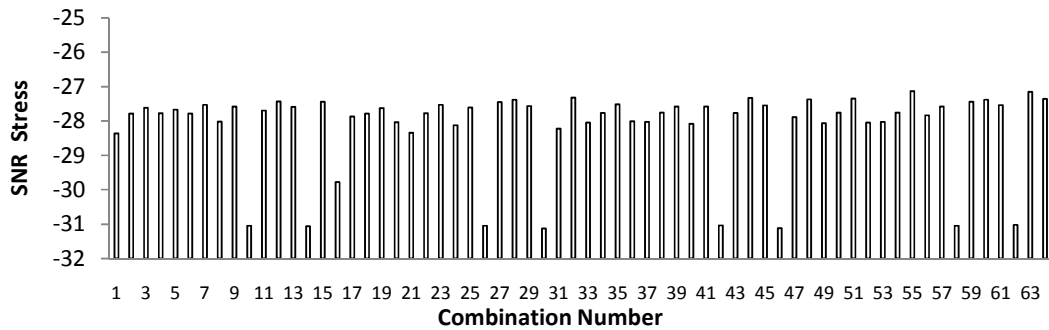


(c)

**Fig. 7.14: Performance values against combination number (a) SNR of compliance, (b) SNR of deflection, and (c) SNR of Von-Mises stress**

From Fig. 7.14 and 7.15, the different tolerance combinations corresponding to the minimum compliance, deflection, and Von-Mises stress are identified. In case of targeted performance problems, the intended performance values should be selected, by referring to possible combinations. Similarly, the robust performance is identified by the SNR values.
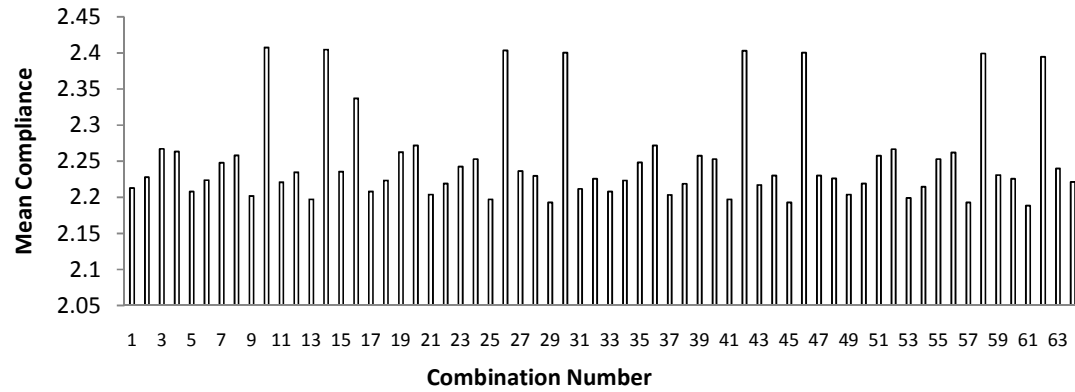


(a)
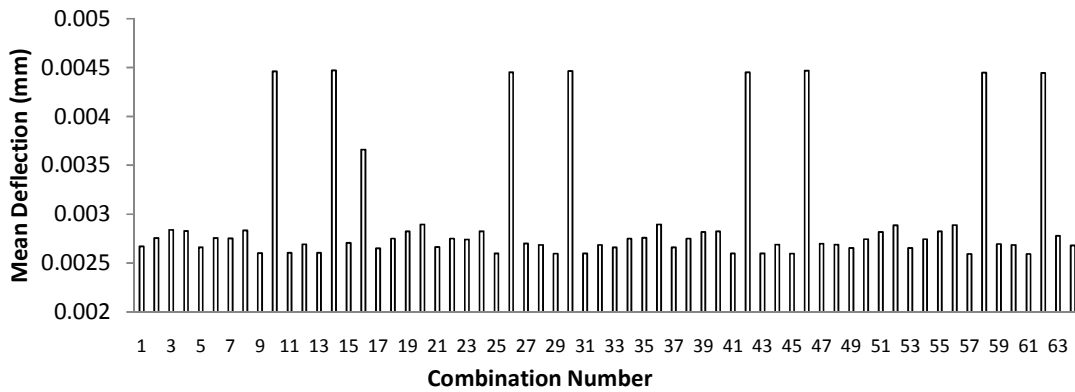


(b)
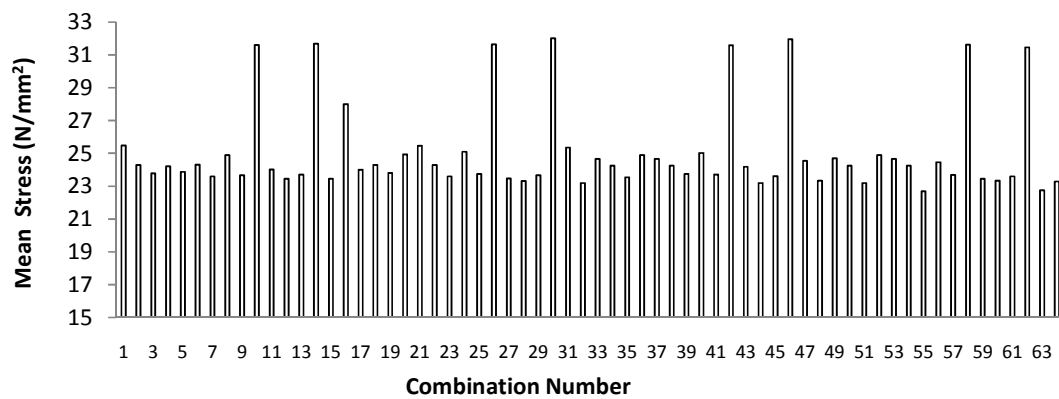


(c)

**Fig. 7.15: Performance values against combination number (a) mean of compliance, (b) mean of deflection, and (c) mean of Von-Mises stress**

It is observed from these results that the combination number corresponding to the SNR and mean of a particular performance is same. Looking at the best three combination numbers, the combination numbers 61, 29 and 45 are the found to be best combination for mean and SNR of the compliance. Combination numbers 61, 57, and 31 are the best for mean and SNR of deflection, while combination number 55, 63, and 44 are the best in mean and SNR of the Von-Mises stress. The actual values of the tolerance range for these combinations can be observed from the Appendix A12. Based on the affordability of the tolerance of factor a suitable combination for best performance/targeted performance can be selected by the designer. In this case, combination number 61 is found to provide the best results for compliance, and deflection; and combination number 55 is the best for Von-Mises stress values. From the present analysis, the effect of each tolerance combination in the three different performances in the realistic scenario is explored. The selection of combination number is dependent on designer's choice and affordability.

## 7.7    CONCLUSIONS

The developed methodologies, discussed in earlier chapters were used to obtain optimal topologies, reliable topologies for targeted compliance, deflection and stress values of a bell crank lever. For this design, static conditions with maximum load during operation were considered. In this case, the problem was formulated to select the configuration, volume fraction, and material that provide the targeted and robust performances in terms of compliance, deflection, and Von-Mises stress. The analysis was carried out in three major steps. By applying the methodology developed in Chapter 3, it was observed that the configuration-3 with volume fraction 0.35 and Structure steel-ASTM A36 gives a robust design. For the RBTO based methodology, same combinations and the performances variation relative to the each combination are found to be robust. By analyzing  the effects of tolerance range of the factors, it was obtained that the values of compliance and deflection at combination number 61 is the best while combination number 55 found to be best for Von-Mises stress based performance. The reason for these combination numbers is explained by the slight non-linear variation in the performance values against the tolerance combinations. The proposed methodology not only gives the design combination and tolerance range but also provides a full range of performance for each combination. The simulated data can be utilized to fine tune the overall performance of the shock absorbers, or the vehicle itself. In this way, the presented work provides an aid to the designer to select the combination of factors and tolerance value.

# CHAPTER 8

## CONCLUSIONS AND FUTURE SCOPE

### 8.1    CONCLUSIONS

Present thesis discusses an integrated approach to select values of controllable factors and their tolerances to achieve the targeted values of performance and robust performance for topologically optimized structural components including effects of uncertainties. The impact of change of factors and its uncertainties on topologically optimized structures are not very much apparent from the physics of the problems. Thus, this thesis provides some worthwhile conclusions based on the investigations carried out in all chapters.

In Chapter 1, the development of topology optimization methods and robust design methods are discussed to provide the necessary foundation. In Chapter 2, the published literature related to effects of uncertainties in the area of topology optimization problems are reviewed. This chapter is organized in two parts. The first part presents the developments on the issue of reliability of the topologically optimized components. The outcome of the RBTO research is explored chronologically and important outcomes are identified. The important outcomes are: FORM is used to approximate the MPP in general; the limit state function is modeled using the maximum allowable deflection values; the uncertainties of applied force, elasticity, and dimension are considered in most of the studies; and in majority of studies, the structural problems are dealt. The second part of the literature review is about the application of robust design methodologies in topology optimization problems. The research in this area is organized in terms of the type of uncertainties and their methods to deal with these uncertainties. From the available literatures, it is evident that the current research focuses more on the uncertainties caused by the manufacturing processes. For this, different methodologies are developed to create the optimal topologies that can be manufactured accurately. From

literature, it is observed that the stochastic methods are utilized in the developed methods and the majority of work use SIMP method. The examples of structural and compliant mechanism problems are used by the researchers in equal proportion.

Based on above reviews the gaps in research are identified. The important findings are, the majority of research is focused on specific applications, rather than providing a generalized methodology; the issues of computational cost, performance analysis, manufacturing, etc. are rarely addressed in detail; there are very limited attempts to incorporate the designer and manufacturer's perspective.

Present thesis is motivated by the above research gaps. In Chapter 3, the analysis of performance of the topologically optimized structures is dealt using DOE approach. In this chapter, the investigation on influence of input factors like force, aspect ratio and volume fraction on performance values is performed. The performance measure is set as compliance and deflection values. The effects of uncertainties are incorporated by considering various loading conditions and material uncertainties. Hence, the results obtained are practical and representative of real life application. To enable this, various performance measures are simulated using combinations generated from DOE approach. The effect of individual factor on performance measure is also obtained to indicate the importance of DOE based methodology. In addition, statistical methods and tools are used to identify the significant input factors and their contributions. The proposed methodology is illustrated using the four benchmark problems. For first three problems, the most and least significant factors are force and aspect ratio, respectively when compliance is the performance measure. For the same performance measure, aspect ratio and force are the most and least significant factor in the fourth problem. For all problems, the most and least significant factors are volume fraction and force, respectively, when deflection is the performance measure. It is found that the seventh ($7^{th}$) combination has highest SNR, with minimum compliance and deflection values. Whereas, twenty first ($21^{st}$) combination has lowest SNR with highest compliance and deflection values. It is also concluded that the combinations of factors, which provide minimum compliance and deflection, are robust compared to others. This analysis is helpful to select the input factor values and their effect on the targeted performance under a specified range, and provides an over-all picture of performance measure behavior to the designers. As an important outcome of this analysis, the suitable nominal

values of the considered factors are found out, which are utilized in the later part of the thesis.

In Chapter 4, the analysis of performance of the topologically optimized structure is carried out using reliability concept. The RBTO method generates reliable optimal topology with its performance values, subject to desired reliability index values and given uncertainties of controllable factors. In this chapter, a methodology based on DOE and RBTO has been integrated to simulate the performance, in a desired range of factors including the effects of uncertainties. This work addresses the issues related to achieving targeted performance for a given structural problem. The methodology has been illustrated using same four benchmark problems available in the literature. The results are analyzed using ANOM, SNR, and ANOVA. The sensitivity and the statistical significance of the factors are obtained. The equivalence equations are generated, which are useful to compute any compliance and deflection values within the selected range of factors. It is again observed that the volume fraction is the most significant factor. The seventh ($7^{th}$) combination performs best for robust design and provides minimum compliance and deflection values. Whereas, twenty first ($21^{st}$) combination provides maximum values of compliance and deflection, and shows minimum robustness. In addition, it is observed that, for the presented methodology a coarse mesh is sufficient, as long as it correctly represents the physics of the problem. The present analysis will be helpful to predict the behavior of performance measures and helps in identifying the relative robustness of the combinations of factor. This analysis can be used to select factor combinations that provide targeted performance measure for topology optimization problems, with reliability considerations. The suitable nominal values of the considered factors are found out using the proposed approach, which is utilized for the selection of tolerance ranges.

In Chapter 5, an approach is proposed to select optimum tolerance of controllable factors for topologically optimized structures. This approach draws inspiration from Taguchi's earlier work on CA-DOE method. Conventionally a CA DOE method is used for the noise analysis, but in the present case, the approach was modified by treating the tolerances as the noise. Such application of CA-DOE to topology optimization problems does not exist in the available literature. This method also explores the possibilities to obtain robust topology using statistical methods. To serve this purpose, four factors, i.e. applied force, volume fraction, aspect ratio, and modulus of elasticity are selected for

their tolerance range selection using CA-DOE approach. The performance measure for this analysis is kept same as discussed earlier. The combinations of the tolerance of factor are identified in which one or few factors are in their loose tolerance limits, though it provides targeted performance or minimum variations of the performance measure. In addition, ANOVA is used for identification of statistically significant tolerances of factors. Summarily, the tolerance of aspect ratio is not significant and tolerance of force is highly significant for the considered problems. In order to integrate the reliability concept in the tolerance range selection, a RBTO based methodology is also proposed in this chapter. From the simulated results, it is concluded that with increased reliability index and spread values, the values of compliance and deflection increases. Also, the performance of each tolerance combination changed from that of previous analysis, because of the RBTO method. Hence, RBTO based method gives results that are for reliability consideration. Apart from tolerance range selection, the whole analysis can be used where the effect of uncertainties of selected factors is required to be investigated. In such case, the tolerances will act as uncertainties. Present analysis provides a comprehensive investigation of the tolerances of factors on different topology optimization problems and offers an offline strategy to the designer. In this chapter, the uncertainty of manufacturing process is considered in a very generic way. The methodology proposed in this chapter, captures the variations in the volume fraction or alteration of shape/size due to any secondary process or manufacturing uncertainties on the optimal topology. However, to observe the effect of a specific manufacturing process, it is necessary to incorporate the uncertainty characteristic of that process. The consideration of the uncertainties specific to a manufacturing process is attempted in Chapter 6.

In Chapter 6, the tolerance range selection of the factors is performed, by incorporating the effects of geometric uncertainties caused by manufacturing process. A methodology is proposed for simulating geometric uncertainties caused by the manufacturing process. This method offers several advantages to the designer in terms of its customization. It is independent of topology optimization method and can be adopted for different type of robust design methodologies. In this chapter, CA-DOE method is integrated with the proposed method for the tolerance range selection. The simulated results are analyzed similar to the previous chapters and compared with earlier results. There are substantial differences observed in this comparison. For all the selected

problems, the mean compliance and deflection values are greater, and SNR of that are lesser, when the effect of uncertainties due to manufacturing process is introduced. However, for problem-4, the mean deflection values are lesser and SNRs of deflection are greater. This indicates that the performance is also dependent on the physics of the problem. During the analysis, a drastic change in the sensitivity of factor is also observed. The most and least significant factors for compliance and deflection are observed to be different when the proposed methodology is applied. Thus, it can be concluded that, the methodology presented in this chapter models the characteristic of manufacturing process more accurately compared the methodology proposed in Chapter 5. However, the methodology proposed in the Chapter 5 can be applied to the problems where the uncertainties of manufacturing processes are very small compared to the uncertainties of other factors. Similar to the previous chapter, a RBTO based tolerance range analysis including the effect of manufacturing uncertainties is also attempted in this chapter. The results obtained from this methodology are influenced by the reliability index and spread of factors. It is observed that the compliance and deflection values are slightly higher compared to results obtained without RBTO. In addition, the performance of each combination of tolerance become more distinct compared to the previous analysis.

In order to substantiate the significance of the developed methodologies, a real time problem is taken from a live project. The problem at hand is to design a bell crank lever used in the BITS-formula one racing car. The process of selecting the different level or options for factors such as volume fraction, material, configurations, and consideration of uncertainties are demonstrated by considering this problem. The various input conditions for this design problem are captured after suitable discussion and analysis, i.e. the applied force, the materials, dimensional or leverage configurations, and the required weight. Being a real life problem the bell crank lever should be designed using factor of safety. Thus, the developed stress is also considered as one of the performance measure. The performance measures of the bell-crank lever are set as the compliance, deflection and the maximum values of Von-Mises stress. The factors considered in this analysis are, type of material, dimensional or leverage configuration, and the volume fraction. The uncertainties involved in the various factors such as, applied force, angle of input and output force, and thickness are also considered here. To simulate the result, a MATLAB code is written based on the developed methodologies in the previous chapters. Based on

simulated performances, it is observed that the third configuration of bell crank lever shows best values for robust and targeted performances. According to materials used for investigation, structural steel ASTM A36 shows best results for robust and targeted performance. Although the weight of bell crank lever can further be minimized by selecting the design combinations comprising other lighter materials i.e. Aluminum alloys. For such selection, simulated performance measure values can be compared, and for the desired performance, lighter designs can be selected. In the next step of design, the performance of the bell crank lever is observed by including the effect of uncertainties of the controllable factors such as, elasticity values, dimensions, and volume fraction. From the simulated results, it is found that by increasing the reliability index and spread values, the compliance and deflection values increase. Here, these performance measures are observed to be more sensitive to the spread values compared to the change in reliability index values. However, in case of Von-Mises stress, it is found that the values are less with increased values of reliability index, which is the indication of increased reliability. From the results, it is observed that by applying the reliability method, the deflection and compliance value increased, at the same time the developed Von-Mises stress is decreased compare to an earlier DOE based approach. Such analysis helps the designer to make a proper tradeoff between the performance and safety.

In order to illustrate the tolerance range selection of this problem, one of the optimal designs is selected. In this analysis, the tolerance of the factors such as, thickness, elasticity, volume fraction, applied force, input and output angles of the applied force are considered. From the simulated results, the combination numbers 61, 29 and 45 are the found to be best combination for mean and SNR of the compliance. Combination numbers 61, 57, and 31 are found to be the best for mean and SNR of deflection, while combination number 55, 63, and 44 are found to be the best for mean and SNR of the Von-Mises stress. Based on the developed methodologies a range of performances for the different tolerance combinations including effect of uncertainties/noise, are generated. This performance range provides a simpler approach to designers to select tolerances of factors based on their requirements. Presented performance behavior is also helpful to tune the overall performance of the racing car, while designing or selecting the other components connected to bell crank-lever.

From the simulation results it is found that, the optimal topologies are very sensitive to the selected factors and types of uncertainties. Therefore, with the change in values of factor, the optimal topologies change drastically. Here, each factor combination provides a family of optimal topologies. Above observations with respect to considered problem was an eye opener, and illustrates the utility and significance of the application of DOE and CA-DOE methods, which helps in simulation of the performance values at each factor levels, considering the effect of various uncertainties independently. It is also observed from above example, that the developed methodologies are well suited even if the factors, performance measures, and type of uncertainties changes according to the analysis requirement.

The performance of each problem is simulated at each possible factor levels, and uncertainties, with or without the consideration of reliability values. It is concluded that the performance behavior is dependent on physics of the problem. The methodology explores all possible performance measure of the structure, in terms of targeted values and robustness. Thus proposed methods are very handy and useful for many realistic applications like various structural elements; micro cantilever, micro levers, force amplifier, etc.

## 8.2    FUTURE SCOPE

The presented work provides methodologies for the robust and targeted performance of the topologically optimized structures. On similar line, above work can be extended in the following directions;

**Implementation for three-dimensional system:** The presented work in this thesis deals with the two-dimensional (2-D) problems. The methodologies developed were illustrated using the 2-D benchmark problems because it is easy to visualize and present the changes in 2-D topology, and relate it with performance behavior. Illustration of these methodologies can also be applied to three-dimensional (3-D) problems as a future scope. It requires the improvements in topology optimization methods that handle the non-convergence and numerical instability of problems, with refined FE routine for 3-D solution. Another requirement in such implementation will be to identify the real time factors and effect of uncertainties during the manufacturing of 3-D systems. However, all other steps used in developed methodologies will remain unchanged.

**Topology optimization for an integrated engineering system:** In Chapter 7, the proposed methodologies are illustrated using a bell crank lever design. While this component is treated individually**.** However, engineering system such as large structural systems or mechanisms can also be analyzed, where multiple components are assembled to achieve a desired performance. The performance analysis of such systems will involve the preparation of topology optimization method for multiple loading of components with interconnected input and outputs in terms of deflection and loading values. Along with this, the objective function should minimize compliance for the whole system instead of each component. In such problems, the identification of system performance, factors, and noise will be different from that of individual components.

**Application area:** Current thesis deals with only structural problems. The obvious extension is possible to deal different problem domain, where the objective function for topology optimization may attempt to maximize force, displacement, heat flux, fluid flow, fundamental eigen frequency that are effected by material distribution. For example, this work can be extended for the robust and targeted synthesis of compliant mechanisms. These problems require modification of the basic optimization problem. In case of structural problems, the objective of the optimization is to minimize the compliance value subject to the constraint of volume fraction. While in the case of complaint mechanisms, the objective function will be to maximize the compliance value, or the ratio of deflection values at output to input points of the mechanism. Thus, the methodologies required for the compliant mechanisms will be different compared to the structural problems. However the used of methods i.e., DOE, RBTO, and CA-DOE require same or little modifications.

**Software development:** The overall methodology from the optimal factor to tolerance selection is coded in MATLAB. The codes are compatible for the change in different grid size, rectangular elements, and local minima, etc. These codes can be used simultaneously in a single routine and a Graphical User Interface can be developed to obtain optimal parameters for robust performance. Presently, commercial software packages available for topology optimization with the use of deterministic method and these software packages do not consider any type of uncertainty of factors, tolerance, or reliability concepts. Even these software packages do not have capability to handle manufacturing perspective. Hence, development of user friendly software for these considerations will help the designer community.

# REFERENCES

Albert, A., & Etman, L. (2009). A simple heuristic for gray-scale suppression in optimality criterion-based topology optimization. *Structural and Multidisciplinary Optimization, 39*, 217-225.

Allaire, G., Jouve, F., & Toader, A. M. (2004). Structural optimization using sensitivity analysis and a level-set method. *Journal of Computational Physics, 194*, 363-393.

Amir, O., Sigmund, O., Lazarov, B., & Schevenels, M. (2012). Efficient reanalysis techniques for robust topology optimization. *Computer Methods in Applied Mechanics and Engineering, 245-246*, 217-231.

Ananthasuresh, G. K., & Kota, S. (1995). Designing compliant mechanisms. *ASME Mechanical Engineering, 117*, 93-96.

Ananthasuresh, G., Kota, S., & Gianchandan, Y. (1994). A methodical approach to design of compliant micro-mechanisms, (pp. 189-192). Hilton Head Island, SC.

Andreassen E., Clausen A., Schevenels M. Lazarov B. S. & Sigmund O. (2011). Efficient topology optimization in MATLAB using 88 lines of code. *Structural and Multidisciplinary Optimization*, 43, 1–16.

Bae, K., Wang, S., & Choi, K. (2002). Reliability-based topology optimization. *In proceedings of 9th AIAA/ISSMO Symposium on Multidisciplinary Analysis and Optimization*, (pp. 2002-5542). Atlanta, Georgia.

Band, S., & Min, S. (2006). Reliability-based topology optimization using single-loop single-vector approach. *Journal of KSME, 20*, 889-896.

Bendsøe, M. P. (1989). Optimal shape design as a material distribution problem. *Structural and Multidisciplinary Optimization, 1*, 193-202.

Bendsøe, M. P. (1995). *Optimization of structural topology: shape and material* (1 ed.). Berlin: Springer.

Bendsøe, M. P., & Kikuchi, N. (1988). Generating optimal topologies in structural design using a homogenization method. *Computer Methods in Applied Mechanics and Engineering, 71*, 197-224.

Bendsøe, M. P., & Sigmund., O. (2003). *Topology optimization: theory, methods and applications* (2 ed.). Berlin: Springer.

Beyer, H., & Sendhoff, B. (2007). Robust optimization - A comprehensive survey. *Computer Methods in Applied Mechanics and Engineering, 33-34*, 3190-3218.

Blaise, B. (2001). Filters in topology optimization. *International Journal for Numerical Methods in Engineering, 50*, 2143-2158.

Bos, P. (2010). *Design of a formula student race car spring-damper system.* M.S. theis, Technische Universiteit Eindhoven, Department of Mechanical Engineering, Eindhoven.

Bruns, T. (2005). A re-evaluation of the SIMP method with filtering and an alternative formulation for solid-void topology optimization. *Structural and Multidisciplinary Optimization, 30*, 428-436.

Buhl, T. (2002). Simultaneous topology optimization of structure and supports. *Structural and Multidisciplinary Optimization, 23*, 223-346.

Chen, S., & Chen, W. (2011). A new level-set based approach to shape and topology optimization under geometric uncertainty. *Structural and Multidisciplinary Optimization, 44*, 1-18.

Chen, S., Chen, W., & Lee, S. (2010). Level set based robust shape and topology optimization under random field uncertainties. *Structural and Multidisciplinary Optimization, 41*, 507-524.

Cherkaev, A., & Cherkaeva, E. (1999). Stable optimal design for uncertain loading condition. *Series on Advances in Mathematics for Applied Sciences: Homogenization, 50*, 193-213.

Design-Expert software. (cited 2011 Oct 15). *Available from: http://www.statease.com.*

Diaz, A. R., & Kikuchi, N. (1992). Solution to shape and topology eigenvalue optimization problems using a homogenization method. *International Journal for Numerical Methods in Engineering, 35*, 1487-1502.

Diaz, R., & Sigmund, O. (1995). Checkerboards patterns in layout optimization. *Structural and Multidisciplinary Optimization, 10*, 10-45.

Dongbin, X. (2010). *Numerical methods for stochastic computations: a spectral method approach.* New Jersey: Princeton University Press.

Dunning, P. D., Kim, H., & Mullineux, G. (2011). Introducing loading uncertainty in topology optimization. *AIAA Journal, 49*, 760-768.

Duysinx, P., & Bendsøe, M. P. (1998). Topolgy optimization of continuum structures with local stress constraints. *International Journal for Numerical Methods in Engineering, 43*, 1453-1478.

Elesin, Y., Lazarov, B., Jensen, J., & Sigmund, O. (2012). Design of robust and efficient photonic switches using topology optimization. *Photonics and Nanostructures - Fundamentals and Applications, 10*, 153-165.

Eom, Y. S., Yoo, K. S., Park, J. Y., & Han, S. Y. (2010). Reliability-based topology optimization using a standard response surface method for three-dimensional structures. *Structural and Multidisciplinary Optimization, 43*, 287-295.

Fatma, Y. K., Colby, C. S., & Jasbir, S. A. (1999). Comparison of continuum and ground structure topology optimization methods for concept design of structures. *Presented in ASCE/SEI Structures Congress*, New Orleans, LA.

FIT-PDR. (2008). Florida Tech Motorsports 98: Preliminary Design Report. Florida Institute of Technology, College of Engineering, Florida.

Folgado, J., & Rodrigues, H. C. (1997). Topology optimization methods applied to the design of orthopaedics implants. *Second World Congress of Structural and Multidisciplinary Optimization*, (pp. 563-568). Warsaw.

Fornace, L. (2006). *Weight reduction rechniques applied to eormula SAE vehicle design: An investigation in topology optimization.* M.S. thesis, University of California, Mechanical Engineering Department, San Diego.

Frecker, M. I., Ananthasuresh, G., Nishiwaki, S., Kikuchi, N., & Kota, S. (1997). Topological synthesis of compliant mechanisms using multi-criteria optimization. *Transactions of the ASME, 119*, 238-245.

Guo, X., Zhang, W., & Zhang, L. (2013). Robust structural topology optimization considering boundary uncertainties. *Computer Methods in Applied Mechanics and Engineering, 253,* 356-368.

Gournay, F., Allaire, G., & Jouve, F. (2008). Shape and topology optimization of the robust compliance via the level set method. *ESAIM: Control, Optimization and Calculus of Variations, 14*, 43-70.

Guest, J., Prevost, J., & Belytschko, T. (2004). Achieving minimum length scale in topology optimization using nodal design variables and projection functions. *International Journal of Numerical Methods in Engineering, 61*, 238-254.

Hasofer, A. M., & Lind, N. C. (1974). Exact and invariant second-moment code format. *Journal of the Engineering Mechanics Division, 100*, 111-121.

Herskovits, J. (1995). *Advances in structural optimization.* Massachusetts, USA: Kluwer Academic Publishers.

Howell, L. (2001). *Compliant Mechanisms.* New York: John Wiley & Sons Inc.

Huang, X., & Xie, Y. (2007). Bidirectional evolutionary topology optimization for structures with geometrical and material nonlinearities. *AIAA Journal, 45*, 308-313.

Jang, G.W., Dijk, P.N., & Keulen, F. (2012). Topology optimization of MEMS considering etching uncertainties using the level-set method. *International Journal for Numerical Methods in Engineering, 92,* 571-588.

Jansen, M., Lombaert, G., Diehl, M., Lazarov, B.S., & Sigmund, O. (2013). Robust topology optimization accounting for misplacement of material. *Structural and Multidisciplinary Optimization, 47*, 317-333.

Javed, A., Rout, B. K., & Mittal, R. K. (2007). A review on design and synthesis of compliant mechanism for micro actuation. *Presented in 2nd ISSS National Conference on MEMS, Microsensors, Smart Materials, Structures and Systems,* CEERI-BITS, (pp. 1-10). Pilani, India.

Javed, A., Safal, M., & Rout, B. K. (2011). Numerical simulation of compliance variation for a topology-optimized structure. *In Proceedings of Numerical simulation of compliance variation for a topology-optimized structure*, (pp. 1-5). Coimbatore, India.

Javed, A., & Rout, B. K. (2012). Tolerance range section of topologically optimized structure using combined array design of experiments approach. *Proceedings of the Institution of Mechanical Engineers, Part C: Journal of Mechanical Engineering Science*, *227*, 2023-2038.

Javed, A, & Rout, B. K. (2014). Tolerance range selection of topologically optimized structures with the effects of uncertainties of manufacturing process. *Proceedings of the Institution of Mechanical Engineers, Part C: Journal of Mechanical Engineering Science*. Online published on April 11, 2014 as doi:10.1177/0954406214528484

Jung, H. S., & Cho, S. (2004). Reliability-based topology optimization of geometrically nonlinear structures with loading and material uncertainties. *Finite Element in Analysis and Design, 43*, 311-331.

Kang, J., Kim, C., & Wang, S. (2004). Reliability-based topology optimization for electromagnetic systems. *International Journal for Computation and Mathematics in Electrical and Electronic Engineering, 23*, 715-723.

Kang, Z., & Luo, Y. (2009). Non-probabilistic reliability-based topology optimization of geometrically nonlinear structures using convex models. *Computer Methods in Applied Mechanics and Engineering, 198*, 3228-3238.

Kang, Z., & Luo, Y. (2009). Reliability-based structural optimization with probability and convex set hybrid models. *Structural and Multidisciplinary Optimization, 42*, 89-102.

Kharmanda, G., & Olhoff, N. (2002). Reliability-based topology optimization as a new strategy to generate different structural topologies. *In 15th Nordic Seminar on Computational Mechanics.* Aalborg, Denmark.

Kharmanda, G., Olhohoff, N., Mohamed, A., & Lemaire, M. (2004). Reliability-based topology optimization. *Structural and Multidisciplinary Optimization, 26*, 295-307.

Kim, C., Wang, S. Y., Bae, K. R., Moon, H., & Choi, K. K. (2006). Reliability-based topology optimization with uncertainties. *Journal of Mechanical Science and Technology, 20*, 494-504.

Kim, C., Wang, S., Kang, E., & Lee, K. (2006). New design process for reliability-based topology optimization of a laser scanned model. *Mechanics Based Design of Structures and Machines, 34*, 325-347.

Kim, S. R., Lee, W. G., Park, J. Y., Yu, J. S., & Han, S. Y. (2008). Reliability-based topology optimization using reliability index approach. *In Proceedings of International Conference on Experimental Mechanics*, *7375.* Nanjing, China.

Kim, S. R., Park, J. Y., Lee, W., Yu, J. S., & Han, S. Y. (2007). Reliability-based topology optimization based on evolutionary structural optimization. *Proceedings of World Academy of Science: Engineering & Technology, 36*, 168-172.

Kim, C., Wang, S., Hwang, I., & Lee, J. (2005). Parallel computed reliability-based topology optimization using response surface method. *In Proceedings of 6th World Congresses of Structural and Multidisciplinary Optimization.* Rio de Janeiro, Brazil.

Kogiso, N., Ahn, W., Nishiwaki, S., Izui, K., & Yoshimura, M. (2008). Robust topology optimization for compliant mechanisms considering uncertainty of applied loads. *Journal of Advanced Mechanical Design, Systems, and Manufacturing, 2*, 96-107.

Kota, S., Joo, J., Li, Z., Rodgers, S. M., & Sniegowski, J. (2001). Design of compliant mechanisms: applications to MEMS. *Analog Integrated Circuits and Signal Processing, 29*, 7-15.

Lau, G. K., Du, H., & Lim, M.K. (2001). Techniques to suppress intermediate density in topology optimization of compliant mechanisms. *Computational Mechanics, 27,* 426-435.

Lazarov, B.S., Schevenels, M., & Sigmund, O. (2011). Robust design of large-displacement compliant mechanisms. *Mechanical Sciences, 2*, 175-182.

Lazarov, B.S., Schevenels, M., & Sigmund, O. (2012a). Topology optimization considering material and geometric uncertainties using stochastic collocation methods. *Structural and Multidisciplinary Optimization, 46*, 597–612

Lazarov, B.S., Schevenels, M., & Sigmund, O. (2012b). Topology optimization with geometric uncertainties by perturbation techniques. *International Journal for Numerical Methods in Engineering, 90*, 1321-1336.

Lee, J. O., Yang, Y. S., & Ruy, W. S. (2002). A comparative study on reliability and target-performance-based probabilistic structural design optimization. *Computers and Structures, 80*, 257-269.

Lee, K., Shin, J. K., Song, S., Yoo, Y., & Park, G. (2003). Automotive door design using structural optimization and design of experiments. *Proceedings of the Institution of Mechanical Engineers,, Part D: Journal of Automobile Engineering, 217*, 855-865.

Logo, J. (2007). New type of optimality criteria method in case of probabilistic loading conditions. *Mechanics Based Design of Structures and Machines, 35*, 147-162.

Logo, J., Ghaemi, M., & Rad, M. (2009). Optimal topologies in case of probabilistic loading: the influence of load correlation,. *Mechanics Based Design of Structures and Machines, 37*, 327-348.

Luo, Y., Kang, Z., Luo, Z., & Li, A. (2009). Continuum topology optimization with non-probabilistic reliability constraints based on multi-ellipsoid convex model. *Structural and Multidisciplinary Optimization, 39*, 297-310.

Li, M., Tang, W., & Yuan, M. (2014). Structural dynamic topology optimization based on dynamic reliability using equivalent static loads. *Structural and Multidisciplinary Optimization*, *49*, 121-129.

Matlab Optimization Tool box. (2013, December). Retrieved from Math Works Documentation: *http://www.mathworks.in/help/optim/ug/fsolve.html*

Maute, K., & Frangopol, D. M. (2003). Reliability-based design of MEMS mechanisms by topology optimization. *Computers and Structures, 81*, 8-11.

Mayer, R. R., Kikuchi, N., & Scott, R. A. (1996). Application of topological optimization techniques to structural crashworthiness. *International Journal for Numerical Methods in Engineering, 39*, 1383-1404.

Mehta, V. (2013). *Topology optimization of the rear bell crank of an FSAE car.* Study Oriented Project Report, Department of Mechanical Engineering, BITS-Pilani, Pilani, Rajasthan.

Michell, A. G. (1904). The limit of economy of material in frame structures. *Philosophical Magazine, 8*, 589-597.

Mijar, A. R., Swan, C. C., Arora, J. S., & Kosaka, I. (1998). Continuum topology optimization for concept design of frame bracing systems. *Journal of Structural Engineering - Reston, 124*, 541-550.

Mitra, A. (2008). *Fundamentals of quality control and improvement* (3 ed.). New Jersy: John Wiley & Sons Inc.

Mohsine, A., Kharmanda, G., & El-Hami, A. (2006). Improved hybrid method as a robust tool for reliability-based design optimization. *Structural and Multidisciplinary Optimization, 32*, 203-213.

Montgomery, D. C. (2007). *Design and analysis of experiments* (5 ed.). Wiley, Aisa.

Mozumder, C. K., Patel, N. M., Tillotson, D., & Renaud, J. E. (2006). An investigation of reliability-based topology optimization techniques. *In Proceedings of the 11th AIAA/ISSMO Multidisciplinary Analysis and Optimization Conference*, (pp. 1-11). Portsmouth, Virginia.

Neves, N. M., Rodrigues, H. C., & Guedes, J. M. (1995). Generalized topology design of structures with a buckling load criterion. *Structural Optimization, 10*, 71-78.

Nguyen, T. H., Song, J., & Paulino, G. H. (2011). Single-loop system reliability-based topology optimization considering statistical dependence between limit-states. *Structure and Multidisciplinary Optimization, 44*. 593–611.

Osher, S., & Fedkiw, R. P. (2001). Level set methods: An overview and some recent results. *Journal of Computational Physics, 169*, 475-502.

Osher, S., & Sethian, J. (1988). Front propagating with curvature-dependent speed: Algorithms based on Hamilton-Jacobi formulations. *Journal of Computational Physics, 78*, 12-49.

Ouyang, G., Zhang, X., & Kuang, Y. (2008). Reliability-based topology optimization of continuous structures. *In Proceedings of the 7$^{th}$ World Congress on Intelligent Control and Automation.* Chongqing, China.

Park, G. (2010). *Analytic methods for design practice.* London: Springer-Verlag.

Patel, N., Renaud, J., Agarwal, H., & Tovar, A. (2005). Reliability based topology optimization using the hybrid cellular automaton method. *In Proceedings of 46th AIAA/ASCE/AHS/ASC Structurs, Structural Dynamics & Materials Conference*, (pp. 1-13). Austin, Texas.

Pedersen, C. B. (2004). Crashworthiness design of transient frame structures using topology optimization. *Computer Methods in Applied Mechanics and Engineering, 193*, 653-678.

Petersson, J. (1999). Some convergence results in perimeter controlled topology optimization. *Computer Methods in Applied Mechanics and Engineering, 171*, 123-140.

Querin, O., Steven, G., & Xie, Y. (1998). Evolutionary structural optimisation (ESO) using a bidirectional algorithm. *Engineering Computations, 15*, 1031-48.

Reihl, K., Meier, K., Grubesich, J., Carelli, G., Candarli, M., Allenbaugh, J., Agou, J., Zahlan, J., Almoayed, T., Agou, J., Griveau, S. (2009). *Florida Tech. Motorsports PDR Report.* Florida Institute of Technology, Formula SAE Team, Melbourne.

Richardson, J.N., Coelho R.F., & Adriaenssens, S. (2013). Robust topology optimization of 2D and 3D continuum and truss structures using a spectral stochastic fnite element method. *In proceedings of 10th World Congress on Structural and Multidisciplinary Optimization*, (pp. 1-11). Orlando, Florida, USA.

Rietz, A. (2001). Sufficiency of a finite exponent in SIMP (power law) methods. *Structural and Multidisciplinary Optimization, 21*, 159-163.

Roger, G., & Pol, D. (1991). *Stochastic finite elements: a spectral approach.* New York: Springer-Verlag.

Rozvany, G. I. (1998). Exact analytical solutions for some popular benchmark problems in topology optimization. *Structural and Multidisciplinary Optimization, 15*, 42-48.

Rozvany, G. I. (2009). A critical review of established methods of structural topology optimization. *Structural and Multidisciplinary Optimization, 37*, 217-237.

Rozvany, G. I., & Zhou, M. (1990). Applications of the COC method in layout optimization. *In Proceedings of International Conference on Engineering Optimization in Design Processes* (pp. 59-70). Karlsruhe: Springer, Berlin.

Rozvany, G. I., Zhou, M., & Birker, T. (1992). Generalized shape optimization without homogenisation. *Structural and Multidisciplinary Optimization, 4*, 250-254.

Ryu, J., Park, F., & Kim, Y. (2012). Mobile robot path planning algorithm by equivalent conduction heat flow topology optimization. *Structural and Multidisciplinary Optimization, 45*, 703-715.

Schevenels, M., Lazarov, B., & Sigmund, O. (2011). Robust topology optimization accounting for spatially varying manufacturing errors. *Computer Methods in Applied Mechanics and Engineering, 200*, 3613-3627.

Seepersad, C., Alien, J., Mcdowell, D., & Mistree, F. (2006). Robust design of cellular materials with topological and dimensional imperfections. *ASME Journal of Mechanical Design, 128*, 1285-1297.

Sethian, J. A., & Wiegmann, A. (2000). Structural boundary design via level set and immersed interface methods. *Journal of Computational Physics, 163*, 489-528.

Sigmund, O. (1994a). Materials with prescribed constitutive parameters: An inverse homogenization problem. *International Journal of Solids and Structures, 31*, 2313-2329.

Sigmund, O. (1994b). *Design of material structures using topology optimization.* Ph.D. Thesis, Technical University of Denmark, Department of Solid Mechanics.

Sigmund, O. (1995). Tailoring materials with prescribed elastic properties. *Mechanics of Materials, 20*, 351-368.

Sigmund, O. (1997). On the design of compliant mechanisms using topology optimization. *Mechanics of Structures and Machines, 25*, 493-524.

Sigmund, O. (2001). A 99 line topology optimization code written in Matlab. *Structural and Multidisciplinary Optimization*, 21, 120–127.

Sigmund, O. (2007). Morphology-based black and white filters for topology optimization. *Structural and Multidisciplinary Optimization, 33*, 401-424.

Sigmund, O. (2009). Manufacturing tolerant topology optimization. *Acta Mechanica Sinica, 25*, 227-239.

Sigmund, O., & Jensen, J. (2003). Systematic design of phononic band-gap materials and structures by topology optimization. *Philosophical Transactions: Mathematical, Physical and Engineering Sciences, 361*, 1009-1019.

Sigmund, O., & Petersson, J. (1998). Numerical instabilities in topology optimization: a survey on procedures dealing with checkerboards, mesh-dependencies and local minima. *Structural and Multidisciplinary Optimization, 16*, 68-75.

Sigmund, O., & Torquato, S. (1997). Design of materials with extreme thermal expansion using a three-phase topology optimization method. *Journal of Mechanics and Physics of Solids, 45*, 1037-1067.

Sigmund, O., & Torquato, S. (1999). Design of smart composite materials using topology optimization. *Smart Materials and Structures, 8*, 365-379.

Sigmund, O., Torquato, S., & Aksay, I. (1998). On the design of 1-3 piezocomposites using topology optimization. *Journal of Materials Research, 13*, 1038-1048.

Silva, M., Tortorelli, D. A., Norato, J. A., Ha, C., & Bae, H. R. (2010). Component and system reliability-based topology optimization using a single-loop method. *Structural and Multidisciplinary Optimization, 41*, 87-106.

Sung, H. P. (1998). *Robust design and analysis for quality engineering.* London: Chapman & Hall Publication.

Svanberg, K. (1987). The method of moving asymptotes - a new method for structural optimization. *International Journal of Numerical Methods in Engineering, 24*, 359-373.

Svanberg, K., & Svard, H. (2013). Density filters for topology optimization based on the geometric and harmonic means. *In Proceedings of 10th World Congress on Structural and Multidisciplinary Optimization*, (pp. 1-10). Orlando, Florida, USA.

Svanberg, K., & Werme, M. (2005). A hierarchical neighborhood search method for topology optimization. *Structural and Multidisciplinary Optimization, 29*, 325-340.

Takezawa, A., Nii, S., Kitamura, M., & Kogiso, N. (2011). Topology optimization for worst load conditions based on the eigenvalue analysis of an aggregated linear system. *Computer Methods in Applied Mechanics and Engineering, 200*, 2268-2281.

Tcherniak, D. (2002). Topology optimization of resonating structures using SIMP method. *International Journal for Numerical Methods in Engineering, 54*, 1605-1622.

Tootkaboni, M., Asadpoure, A., & Guest, J. K. (2012). Topology optimization of continuum structures under uncertainty - a polynomial chaos approach. *Computer Methods in Applied Mechanics and Engineering, 201-204*, 263-275.

Tsompanakis, Y. L., & Papadrakakis, M. (2008). *Structural design optimization considering uncertainties* (Vol. 1). London, UK: Taylor & Francis.

Tu, J., Choi, K. K. & Park, Y. H. (1999). A new study on reliability-based design optimization. *ASME Journal of Mechanical Design, 121*, 557-564.

Wang, F., Lazarov, B., & Sigmund, O. (2011a). On projection methods, convergence and robust formulations in topology optimization. *Structural and Multidisciplinary Optimization, 43*, 767-784.

Wang, F., Lazarov, B., & Sigmund, O. (2011b). Robust topology optimization of photonic crystal waveguides with tailored dispersion properties. *Journal of the Optical Society of America B, 28*, 387-397.

Wang, S., Moon, H., Kim, C., Kang, J., & Choi, K. K. (2006). Reliability-based topology optimization (RBTO). *In Proceedings of the IUTAM Symposium on Topological Design Optimization of Structures, Machines and Materials: Status and Perspective. 137,* (pp.493-504), Copenhagen, Denmark: Springer.

Wang, M., Wang, X. M., & Guo, D. M. (2003). A level set method for structural topology optimization. *Computer Methods in Applied Mechanics and Engineering, 192*, 227-246.

Xie, Y., & Steven, G. (1993). A simple evolutionary procedure for structural optimisation. *Computers and Structures, 49*, 885-896.

Xie, Y., & Steven, G. (1994). Optimal design of multiple loaf case structures using an evolutionary procedure. *Engineering Computations, 11*, 295-302.

Xie, Y., & Steven, G. (1997). *Evolutionary Structural Optimization.* Berlin: Springer-Verlag.

Yang, X., Xie, Y., Steven, G., & Querin, O. (1999). Bidirectional evolutionary method for stiffness optimization. *AIAA Journal, 37*, 1483-1488.

Yin, L., & Yang, W. (2000). Topology optimization for tunnel support in layered geological structures. *International Journal for Numerical Methods in Engineering, 47*, 1983-1996.

Yoo, J., & Soh, H. (2005). An optimal design of magnetic actuators using topology optimization and the response surface method. *Microsystem Technologies, 11*, 1252-1261.

Yoo, K. S., Eom, Y. S., Park, J. Y., Han, S. Y., & Im, M. G. (2011). Reliability-based topology optimization using successive standard response surface method. *Finite Elements in Analysis and Design, 47*, 843-849.

Yoon, B. D., & Choi, K. K. (2004). A new response surface methodology for reliability-based design optimization. *Computers and Structures, 82,* 241-256.

Young, V., Querin, O., Steven, G., & Xie, Y. (1999). 3D and multiple load case bi-directional evolutionary structural optimization (BESO). *Structural Optimization, 18*, 183-192.

Zhou, M., & Rozvany, G. (1991). The COC algorithm, part II:topological, geometry and generalized shape optimization. *Computer Methods in Applied Mechanics and Engineering, 89*, 197-224.

# APPENDIX

**Table A1: Combinations of the factors generated by $3^3$ full factorial design**

| Combination number | Aspect Ratio Length/Width A | Volume fraction V | Force Applied F(N) |
|---|---|---|---|
| 1 | 1.2 | 0.4 | 100 |
| 2 | 1.4 | 0.4 | 100 |
| 3 | 1.6 | 0.4 | 100 |
| 4 | 1.2 | 0.5 | 100 |
| 5 | 1.4 | 0.5 | 100 |
| 6 | 1.6 | 0.5 | 100 |
| 7 | 1.2 | 0.6 | 100 |
| 8 | 1.4 | 0.6 | 100 |
| 9 | 1.6 | 0.6 | 100 |
| 10 | 1.2 | 0.4 | 120 |
| 11 | 1.4 | 0.4 | 120 |
| 12 | 1.6 | 0.4 | 120 |
| 13 | 1.2 | 0.5 | 120 |
| 14 | 1.4 | 0.5 | 120 |
| 15 | 1.6 | 0.5 | 120 |
| 16 | 1.2 | 0.6 | 120 |
| 17 | 1.4 | 0.6 | 120 |
| 18 | 1.6 | 0.6 | 120 |
| 19 | 1.2 | 0.4 | 140 |
| 20 | 1.4 | 0.4 | 140 |
| 21 | 1.6 | 0.4 | 140 |
| 22 | 1.2 | 0.5 | 140 |
| 23 | 1.4 | 0.5 | 140 |
| 24 | 1.6 | 0.5 | 140 |
| 25 | 1.2 | 0.6 | 140 |
| 26 | 1.4 | 0.6 | 140 |
| 27 | 1.6 | 0.6 | 140 |

**Table A2: Compliance data for bench mark problems for $3^3$ factorial design**

| S.N. | Combinations | | | Problem-1, MBB | | | | Problem-2, Cantilever | | | | Problem-3, Cantilever with hole | | | | Problem-3, Simply supported | | | |
|---|---|---|---|---|---|---|---|---|---|---|---|---|---|---|---|---|---|---|---|
| | A | V | F | MEAN | RANGE | SNR | SD | MEAN | MAX | SNR | SD | MEAN | RANGE | SNR | SD | MEAN | RANGE | SNR | SD |
| 1 | 1.2 | 0.4 | 100 | 2.4084 | 0.3613 | -7.6462 | 0.1367 | 2.0779 | 1.1426 | -6.4905 | 0.4092 | 3.2681 | 1.3307 | -10.3652 | 0.4858 | 0.5555 | 0.1431 | 8.0681 | 0.0725 |
| 2 | 1.4 | 0.4 | 100 | 3.2051 | 0.3298 | -10.1240 | 0.1421 | 2.8786 | 1.4267 | -9.2951 | 0.5086 | 4.3294 | 1.6125 | -12.7937 | 0.5829 | 0.7392 | 0.1734 | 5.5947 | 0.0875 |
| 3 | 1.6 | 0.4 | 100 | 4.3689 | 1.2507 | -12.8734 | 0.5926 | 3.4503 | 2.5446 | -11.0571 | 1.0107 | 4.7749 | 2.5782 | -13.7309 | 0.9860 | 0.9542 | 0.2063 | 3.3835 | 0.1032 |
| 4 | 1.2 | 0.5 | 100 | 1.6358 | 0.2743 | -4.2923 | 0.1141 | 1.4040 | 0.8150 | -3.0985 | 0.2895 | 2.5350 | 0.9028 | -8.1473 | 0.3479 | 0.4009 | 0.0990 | 10.9043 | 0.0499 |
| 5 | 1.4 | 0.5 | 100 | 2.1882 | 0.3128 | -6.8114 | 0.1130 | 1.9228 | 0.9126 | -5.7830 | 0.3281 | 3.0989 | 1.0836 | -9.8801 | 0.3863 | 0.4886 | 0.1285 | 9.1820 | 0.0643 |
| 6 | 1.6 | 0.5 | 100 | 2.9386 | 0.7537 | -9.4139 | 0.3502 | 2.3246 | 1.5950 | -7.5940 | 0.6412 | 3.5051 | 1.6206 | -11.0103 | 0.6324 | 0.6078 | 0.1391 | 7.2977 | 0.0696 |
| 7 | 1.2 | 0.6 | 100 | 1.3181 | 0.1391 | -2.4064 | 0.0610 | 1.0674 | 0.6167 | -0.7225 | 0.2239 | 2.2324 | 0.6364 | -7.0215 | 0.2521 | 0.3304 | 0.0799 | 12.5873 | 0.0400 |
| 8 | 1.4 | 0.6 | 100 | 1.7810 | 0.2262 | -5.0215 | 0.0853 | 1.4588 | 0.7291 | -3.3912 | 0.2578 | 2.6380 | 0.7741 | -8.4676 | 0.2849 | 0.3945 | 0.0954 | 11.0479 | 0.0477 |
| 9 | 1.6 | 0.6 | 100 | 2.2540 | 0.4014 | -7.0808 | 0.1747 | 1.7573 | 1.2071 | -5.1500 | 0.4717 | 3.0425 | 1.3373 | -9.7657 | 0.5118 | 0.4678 | 0.1152 | 9.5647 | 0.0577 |
| 10 | 1.2 | 0.4 | 120 | 3.4692 | 0.4260 | -10.8139 | 0.1752 | 2.9961 | 1.4707 | -9.6540 | 0.5562 | 4.6661 | 1.7744 | -13.4538 | 0.6740 | 0.7904 | 0.1847 | 5.0136 | 0.0924 |
| 11 | 1.4 | 0.4 | 120 | 4.5979 | 0.5686 | -13.2584 | 0.2051 | 4.1058 | 2.1041 | -12.3875 | 0.7510 | 6.2234 | 2.2673 | -15.9439 | 0.8265 | 1.0592 | 0.2395 | 2.4733 | 0.1207 |
| 12 | 1.6 | 0.4 | 120 | 6.2782 | 1.8416 | -16.0180 | 0.8199 | 4.9524 | 3.5836 | -14.2037 | 1.4694 | 6.8223 | 3.6494 | -16.8281 | 1.3989 | 1.3702 | 0.2690 | 0.2466 | 0.1354 |
| 13 | 1.2 | 0.5 | 120 | 2.3640 | 0.3201 | -7.4842 | 0.1322 | 2.0158 | 1.0432 | -6.2168 | 0.3820 | 3.6436 | 1.2726 | -11.2923 | 0.4770 | 0.5724 | 0.1351 | 7.8165 | 0.0677 |
| 14 | 1.4 | 0.5 | 120 | 3.1720 | 0.3364 | -10.0327 | 0.1310 | 2.7519 | 1.4276 | -8.9083 | 0.4952 | 4.4457 | 1.5783 | -13.0220 | 0.5895 | 0.7090 | 0.1729 | 5.9540 | 0.0866 |
| 15 | 1.6 | 0.5 | 120 | 4.2605 | 1.0794 | -12.6319 | 0.4643 | 3.3778 | 2.3882 | -10.8438 | 0.9391 | 5.0277 | 2.5016 | -14.1550 | 0.9513 | 0.8753 | 0.2101 | 4.1256 | 0.1052 |
| 16 | 1.2 | 0.6 | 120 | 1.9052 | 0.2758 | -5.6118 | 0.1134 | 1.5313 | 0.8589 | -3.8482 | 0.3110 | 3.1782 | 0.8436 | -10.0838 | 0.3355 | 0.4876 | 0.1127 | 9.2102 | 0.0570 |
| 17 | 1.4 | 0.6 | 120 | 2.5576 | 0.3272 | -8.1641 | 0.1171 | 2.0984 | 1.0819 | -6.5593 | 0.3873 | 3.7904 | 1.1456 | -11.6196 | 0.4285 | 0.5568 | 0.1316 | 8.0555 | 0.0659 |
| 18 | 1.6 | 0.6 | 120 | 3.2656 | 0.6624 | -10.3028 | 0.2636 | 2.5296 | 1.7277 | -8.3084 | 0.6707 | 4.3207 | 1.7852 | -12.8049 | 0.6997 | 0.6658 | 0.1815 | 6.4897 | 0.0910 |
| 19 | 1.2 | 0.4 | 140 | 4.7214 | 0.6038 | -13.4913 | 0.2459 | 4.1362 | 2.3042 | -12.4808 | 0.8460 | 6.3898 | 2.3843 | -16.1784 | 0.8836 | 1.0916 | 0.2694 | 2.2049 | 0.1348 |
| 20 | 1.4 | 0.4 | 140 | 6.3371 | 0.7214 | -16.0461 | 0.3032 | 5.6453 | 2.9902 | -15.1596 | 1.0606 | 8.4436 | 3.0300 | -18.5929 | 1.1128 | 1.4305 | 0.3150 | -0.1346 | 0.1584 |
| 21 | 1.6 | 0.4 | 140 | 8.5773 | 2.6930 | -18.7379 | 1.2052 | 6.7100 | 4.8076 | -16.8349 | 1.9671 | 9.3319 | 4.7828 | -19.5469 | 1.9006 | 1.8794 | 0.4120 | -2.5049 | 0.2062 |
| 22 | 1.2 | 0.5 | 140 | 3.2238 | 0.4238 | -10.1771 | 0.1685 | 2.7611 | 1.4515 | -8.9529 | 0.5300 | 4.9489 | 1.5923 | -13.9445 | 0.6085 | 0.7888 | 0.1998 | 5.0251 | 0.1000 |
| 23 | 1.4 | 0.5 | 140 | 4.2824 | 0.4898 | -12.6415 | 0.1977 | 3.7669 | 1.7002 | -11.6127 | 0.6070 | 6.0788 | 2.2109 | -15.7366 | 0.7866 | 0.9693 | 0.2282 | 3.2405 | 0.1147 |
| 24 | 1.6 | 0.5 | 140 | 5.7075 | 1.5268 | -15.1784 | 0.6689 | 4.5628 | 3.1821 | -13.4566 | 1.2708 | 6.8698 | 3.1178 | -16.8551 | 1.2390 | 1.1966 | 0.3272 | 1.3977 | 0.1638 |
| 25 | 1.2 | 0.6 | 140 | 2.5942 | 0.3432 | -8.2906 | 0.1398 | 2.0793 | 1.1454 | -6.5010 | 0.4162 | 4.3312 | 1.2407 | -12.7740 | 0.4663 | 0.6486 | 0.1567 | 6.7283 | 0.0784 |
| 26 | 1.4 | 0.6 | 140 | 3.4748 | 0.4812 | -10.8287 | 0.1839 | 2.8523 | 1.4808 | -9.2266 | 0.5286 | 5.1729 | 1.4026 | -14.3115 | 0.5234 | 0.7654 | 0.1925 | 5.2866 | 0.0963 |
| 27 | 1.6 | 0.6 | 140 | 4.4314 | 0.8298 | -12.9497 | 0.3198 | 3.4594 | 2.4242 | -11.0321 | 0.9263 | 5.9077 | 2.3884 | -15.5167 | 0.9275 | 0.9105 | 0.2457 | 3.7722 | 0.1229 |

A= Aspect Ratio, V=Volume Fraction, F=Force

**Table A3: Deflection data for bench mark problems for $3^3$ factorial design**

| S.N. | Combinations | | | Problem-1, MBB | | | | Problem-2, Cantilever | | | | Problem-3, Cantilever with hole | | | | Problem-3, Simply supported | | | |
|---|---|---|---|---|---|---|---|---|---|---|---|---|---|---|---|---|---|---|---|
| | A | V | F | MEAN | RANGE | SNR | SD | MEAN | RANGE | SNR | SD | MEAN | RANGE | SNR | SD | MEAN | RANGE | SNR | SD |
| 1 | 1.2 | 0.4 | 100 | 0.0245 | 0.0027 | 32.2269 | 0.0011 | 0.0218 | 0.0072 | 33.1921 | 0.0026 | 0.0335 | 0.0103 | 29.4589 | 0.0037 | 0.0055 | 0.0007 | 48.1906 | 0.0004 |
| 2 | 1.4 | 0.4 | 100 | 0.0327 | 0.0026 | 29.7136 | 0.0011 | 0.0299 | 0.0090 | 30.4396 | 0.0032 | 0.0449 | 0.0106 | 26.9223 | 0.0038 | 0.0074 | 0.0009 | 45.6146 | 0.0005 |
| 3 | 1.6 | 0.4 | 100 | 0.0448 | 0.0100 | 26.9322 | 0.0050 | 0.0370 | 0.0173 | 28.5169 | 0.0071 | 0.0507 | 0.0167 | 25.8441 | 0.0066 | 0.0097 | 0.0006 | 43.3019 | 0.0003 |
| 4 | 1.2 | 0.5 | 100 | 0.0166 | 0.0020 | 35.6131 | 0.0009 | 0.0145 | 0.0054 | 36.7126 | 0.0020 | 0.0256 | 0.0073 | 31.8013 | 0.0029 | 0.0040 | 0.0005 | 51.0301 | 0.0003 |
| 5 | 1.4 | 0.5 | 100 | 0.0223 | 0.0022 | 33.0412 | 0.0009 | 0.0199 | 0.0059 | 33.9777 | 0.0022 | 0.0318 | 0.0078 | 29.9218 | 0.0029 | 0.0049 | 0.0007 | 49.2506 | 0.0004 |
| 6 | 1.6 | 0.5 | 100 | 0.0301 | 0.0058 | 30.4084 | 0.0029 | 0.0249 | 0.0109 | 31.9727 | 0.0046 | 0.0369 | 0.0112 | 28.6030 | 0.0045 | 0.0061 | 0.0007 | 47.3416 | 0.0004 |
| 7 | 1.2 | 0.6 | 100 | 0.0133 | 0.0014 | 37.5471 | 0.0006 | 0.0109 | 0.0044 | 39.1784 | 0.0017 | 0.0225 | 0.0049 | 32.9139 | 0.0020 | 0.0033 | 0.0005 | 52.7111 | 0.0003 |
| 8 | 1.4 | 0.6 | 100 | 0.0179 | 0.0019 | 34.9280 | 0.0008 | 0.0150 | 0.0049 | 36.4343 | 0.0018 | 0.0268 | 0.0058 | 31.4021 | 0.0022 | 0.0039 | 0.0005 | 51.2513 | 0.0003 |
| 9 | 1.6 | 0.6 | 100 | 0.0230 | 0.0031 | 32.7453 | 0.0014 | 0.0186 | 0.0083 | 34.4836 | 0.0034 | 0.0316 | 0.0096 | 29.9665 | 0.0037 | 0.0046 | 0.0006 | 49.6799 | 0.0003 |
| 10 | 1.2 | 0.4 | 120 | 0.0293 | 0.0027 | 30.6513 | 0.0012 | 0.0262 | 0.0081 | 31.5954 | 0.0031 | 0.0399 | 0.0118 | 27.9292 | 0.0044 | 0.0066 | 0.0008 | 46.5649 | 0.0004 |
| 11 | 1.4 | 0.4 | 120 | 0.0391 | 0.0035 | 28.1448 | 0.0013 | 0.0357 | 0.0112 | 28.9008 | 0.0040 | 0.0537 | 0.0128 | 25.3710 | 0.0046 | 0.0089 | 0.0010 | 44.0454 | 0.0005 |
| 12 | 1.6 | 0.4 | 120 | 0.0536 | 0.0125 | 25.3722 | 0.0060 | 0.0443 | 0.0204 | 26.9414 | 0.0085 | 0.0605 | 0.0196 | 24.3045 | 0.0077 | 0.0116 | 0.0006 | 41.7441 | 0.0003 |
| 13 | 1.2 | 0.5 | 120 | 0.0199 | 0.0023 | 34.0211 | 0.0010 | 0.0174 | 0.0059 | 35.1274 | 0.0023 | 0.0306 | 0.0086 | 30.2338 | 0.0033 | 0.0047 | 0.0006 | 49.4949 | 0.0003 |
| 14 | 1.4 | 0.5 | 120 | 0.0268 | 0.0021 | 31.4384 | 0.0009 | 0.0238 | 0.0077 | 32.4084 | 0.0028 | 0.0381 | 0.0093 | 28.3581 | 0.0035 | 0.0059 | 0.0007 | 47.5825 | 0.0004 |
| 15 | 1.6 | 0.5 | 120 | 0.0362 | 0.0073 | 28.7984 | 0.0034 | 0.0300 | 0.0134 | 30.3415 | 0.0055 | 0.0441 | 0.0139 | 27.0494 | 0.0055 | 0.0073 | 0.0008 | 45.6955 | 0.0004 |
| 16 | 1.2 | 0.6 | 120 | 0.0159 | 0.0019 | 35.9435 | 0.0009 | 0.0131 | 0.0051 | 37.6059 | 0.0020 | 0.0269 | 0.0056 | 31.3880 | 0.0024 | 0.0040 | 0.0005 | 50.9565 | 0.0003 |
| 17 | 1.4 | 0.6 | 120 | 0.0215 | 0.0022 | 33.3517 | 0.0009 | 0.0180 | 0.0060 | 34.8446 | 0.0023 | 0.0322 | 0.0071 | 29.8256 | 0.0027 | 0.0046 | 0.0006 | 49.6799 | 0.0003 |
| 18 | 1.6 | 0.6 | 120 | 0.0277 | 0.0041 | 31.1253 | 0.0018 | 0.0223 | 0.0098 | 32.9118 | 0.0040 | 0.0376 | 0.0108 | 28.4424 | 0.0043 | 0.0055 | 0.0008 | 48.1878 | 0.0004 |
| 19 | 1.2 | 0.4 | 140 | 0.0342 | 0.0034 | 29.3124 | 0.0015 | 0.0307 | 0.0104 | 30.2050 | 0.0039 | 0.0469 | 0.0137 | 26.5448 | 0.0050 | 0.0077 | 0.0010 | 45.2307 | 0.0005 |
| 20 | 1.4 | 0.4 | 140 | 0.0460 | 0.0037 | 26.7461 | 0.0017 | 0.0419 | 0.0133 | 27.5079 | 0.0048 | 0.0628 | 0.0144 | 24.0199 | 0.0053 | 0.0103 | 0.0012 | 42.7715 | 0.0006 |
| 21 | 1.6 | 0.4 | 140 | 0.0628 | 0.0154 | 23.9963 | 0.0073 | 0.0516 | 0.0234 | 25.6266 | 0.0098 | 0.0709 | 0.0223 | 22.9274 | 0.0091 | 0.0135 | 0.0009 | 40.3784 | 0.0005 |
| 22 | 1.2 | 0.5 | 140 | 0.0233 | 0.0026 | 32.6628 | 0.0011 | 0.0204 | 0.0071 | 33.7566 | 0.0027 | 0.0357 | 0.0095 | 28.8998 | 0.0037 | 0.0056 | 0.0007 | 48.0869 | 0.0004 |
| 23 | 1.4 | 0.5 | 140 | 0.0311 | 0.0027 | 30.1306 | 0.0012 | 0.0279 | 0.0079 | 31.0415 | 0.0030 | 0.0445 | 0.0110 | 27.0002 | 0.0040 | 0.0069 | 0.0008 | 46.2648 | 0.0004 |
| 24 | 1.6 | 0.5 | 140 | 0.0418 | 0.0084 | 27.5426 | 0.0041 | 0.0349 | 0.0156 | 29.0334 | 0.0065 | 0.0516 | 0.0152 | 25.6979 | 0.0062 | 0.0085 | 0.0012 | 44.3735 | 0.0006 |
| 25 | 1.2 | 0.6 | 140 | 0.0186 | 0.0021 | 34.6001 | 0.0010 | 0.0152 | 0.0059 | 36.2828 | 0.0023 | 0.0314 | 0.0068 | 30.0385 | 0.0027 | 0.0046 | 0.0005 | 49.8095 | 0.0003 |
| 26 | 1.4 | 0.6 | 140 | 0.0250 | 0.0027 | 32.0222 | 0.0011 | 0.0209 | 0.0071 | 33.5249 | 0.0027 | 0.0376 | 0.0077 | 28.4772 | 0.0030 | 0.0054 | 0.0007 | 48.3495 | 0.0004 |
| 27 | 1.6 | 0.6 | 140 | 0.0323 | 0.0045 | 29.8037 | 0.0019 | 0.0261 | 0.0118 | 31.5485 | 0.0048 | 0.0440 | 0.0125 | 27.0831 | 0.0049 | 0.0065 | 0.0009 | 46.7826 | 0.0005 |

A= Aspect Ratio, V=Volume Fraction, F=Force

**Table A4: Mean values of compliance for Problem-1**

| Problem-1 Compliance | | | β → | 2 | | | 2.5 | | | 3 | | | 3.8 | | |
|---|---|---|---|---|---|---|---|---|---|---|---|---|---|---|---|
| | | | S (%) → | 10 | 20 | 30 | 10 | 20 | 30 | 10 | 20 | 30 | 10 | 20 | 30 |
| C. No. | A | V | F | | | | | | | | | | | | |
| 1 | 1.2 | 0.4 | 100 | 2.634 | 2.881 | 3.223 | 2.708 | 3.035 | 3.605 | 2.760 | 3.241 | 4.438 | 2.848 | 3.600 | 5.306 |
| 2 | 1.4 | 0.4 | 100 | 3.546 | 3.896 | 4.328 | 3.641 | 4.075 | 5.243 | 3.715 | 4.346 | 6.241 | 3.885 | 5.364 | 7.323 |
| 3 | 1.6 | 0.4 | 100 | 4.759 | 5.249 | 6.549 | 4.843 | 6.104 | 7.994 | 4.942 | 6.548 | 9.246 | 5.203 | 8.169 | 10.965 |
| 4 | 1.2 | 0.5 | 100 | 1.780 | 1.958 | 2.202 | 1.824 | 2.037 | 2.465 | 1.874 | 2.180 | 3.027 | 1.936 | 2.445 | 3.596 |
| 5 | 1.4 | 0.5 | 100 | 2.392 | 2.635 | 3.040 | 2.449 | 2.832 | 3.555 | 2.514 | 3.029 | 4.228 | 2.629 | 3.671 | 5.005 |
| 6 | 1.6 | 0.5 | 100 | 3.206 | 3.499 | 4.239 | 3.286 | 3.966 | 5.159 | 3.368 | 4.264 | 5.981 | 3.450 | 5.218 | 7.056 |
| 7 | 1.2 | 0.6 | 100 | 1.422 | 1.542 | 1.736 | 1.441 | 1.595 | 1.879 | 1.479 | 1.741 | 2.237 | 1.529 | 1.879 | 2.663 |
| 8 | 1.4 | 0.6 | 100 | 1.936 | 2.086 | 2.338 | 1.953 | 2.188 | 2.624 | 2.000 | 2.334 | 3.097 | 2.065 | 2.698 | 3.609 |
| 9 | 1.6 | 0.6 | 100 | 2.467 | 2.662 | 3.132 | 2.509 | 2.947 | 3.706 | 2.557 | 3.140 | 4.244 | 2.647 | 3.758 | 4.946 |
| 10 | 1.2 | 0.4 | 120 | 3.795 | 4.127 | 4.690 | 3.912 | 4.355 | 5.213 | 3.964 | 4.703 | 6.350 | 4.124 | 5.218 | 7.605 |
| 11 | 1.4 | 0.4 | 120 | 5.118 | 5.589 | 6.320 | 5.205 | 5.828 | 7.405 | 5.340 | 6.312 | 9.050 | 5.533 | 7.714 | 10.523 |
| 12 | 1.6 | 0.4 | 120 | 6.872 | 7.369 | 9.382 | 7.026 | 8.823 | 11.614 | 7.238 | 9.358 | 13.423 | 7.334 | 11.740 | 15.869 |
| 13 | 1.2 | 0.5 | 120 | 2.569 | 2.827 | 3.134 | 2.636 | 2.964 | 3.513 | 2.698 | 3.164 | 4.357 | 2.796 | 3.537 | 5.151 |
| 14 | 1.4 | 0.5 | 120 | 3.462 | 3.816 | 4.425 | 3.561 | 4.072 | 5.088 | 3.625 | 4.398 | 6.128 | 3.744 | 5.258 | 7.201 |
| 15 | 1.6 | 0.5 | 120 | 4.573 | 5.071 | 6.114 | 4.758 | 5.671 | 7.384 | 4.859 | 6.112 | 8.663 | 5.024 | 7.469 | 10.195 |
| 16 | 1.2 | 0.6 | 120 | 2.063 | 2.203 | 2.487 | 2.056 | 2.308 | 2.714 | 2.117 | 2.526 | 3.255 | 2.189 | 2.722 | 3.811 |
| 17 | 1.4 | 0.6 | 120 | 2.775 | 3.000 | 3.404 | 2.813 | 3.151 | 3.798 | 2.869 | 3.394 | 4.445 | 2.978 | 3.865 | 5.192 |
| 18 | 1.6 | 0.6 | 120 | 3.550 | 3.829 | 4.536 | 3.636 | 4.279 | 5.314 | 3.692 | 4.527 | 6.154 | 3.803 | 5.377 | 7.133 |
| 19 | 1.2 | 0.4 | 140 | 5.161 | 5.671 | 6.393 | 5.302 | 5.918 | 7.071 | 5.419 | 6.277 | 8.632 | 5.593 | 7.076 | 10.357 |
| 20 | 1.4 | 0.4 | 140 | 6.951 | 7.663 | 8.568 | 7.114 | 7.909 | 10.362 | 7.272 | 8.563 | 12.352 | 7.554 | 10.511 | 14.457 |
| 21 | 1.6 | 0.4 | 140 | 9.409 | 10.010 | 12.841 | 9.616 | 11.959 | 15.851 | 9.491 | 12.767 | 18.190 | 10.175 | 16.056 | 21.534 |
| 22 | 1.2 | 0.5 | 140 | 3.520 | 3.835 | 4.267 | 3.582 | 4.025 | 4.817 | 3.659 | 4.327 | 5.873 | 3.761 | 4.804 | 7.083 |
| 23 | 1.4 | 0.5 | 140 | 4.728 | 5.109 | 5.958 | 4.787 | 5.548 | 6.856 | 4.909 | 5.980 | 8.231 | 5.109 | 7.089 | 9.837 |
| 24 | 1.6 | 0.5 | 140 | 6.231 | 6.876 | 8.359 | 6.388 | 7.796 | 10.103 | 6.577 | 8.274 | 11.698 | 6.807 | 10.209 | 13.775 |
| 25 | 1.2 | 0.6 | 140 | 2.774 | 3.011 | 3.397 | 2.839 | 3.130 | 3.672 | 2.889 | 3.373 | 4.422 | 3.001 | 3.710 | 5.239 |
| 26 | 1.4 | 0.6 | 140 | 3.754 | 4.067 | 4.593 | 3.832 | 4.304 | 5.139 | 3.923 | 4.571 | 6.032 | 4.086 | 5.236 | 7.174 |
| 27 | 1.6 | 0.6 | 140 | 4.799 | 5.213 | 6.175 | 4.949 | 5.797 | 7.252 | 5.049 | 6.200 | 8.285 | 5.168 | 7.345 | 9.673 |

A= Aspect Ratio, V=Volume Fraction, F=Force

**Table A5: Mean values of deflection (in mm) for Problem-1**

| Problem-1 Deflection | | | β → | 2 | | | 2.5 | | | 3 | | | 3.8 | | |
|---|---|---|---|---|---|---|---|---|---|---|---|---|---|---|---|
| | | | S (%) → | 10 | 20 | 30 | 10 | 20 | 30 | 10 | 20 | 30 | 10 | 20 | 30 |
| C. No. | A | V | F | | | | | | | | | | | | |
| 1 | 1.2 | 0.4 | 100 | 0.026 | 0.028 | 0.032 | 0.027 | 0.029 | 0.037 | 0.027 | 0.032 | 0.043 | 0.028 | 0.037 | 0.050 |
| 2 | 1.4 | 0.4 | 100 | 0.036 | 0.038 | 0.043 | 0.036 | 0.041 | 0.054 | 0.037 | 0.043 | 0.062 | 0.038 | 0.054 | 0.070 |
| 3 | 1.6 | 0.4 | 100 | 0.048 | 0.050 | 0.064 | 0.049 | 0.061 | 0.081 | 0.050 | 0.064 | 0.091 | 0.051 | 0.081 | 0.104 |
| 4 | 1.2 | 0.5 | 100 | 0.018 | 0.019 | 0.022 | 0.018 | 0.020 | 0.025 | 0.018 | 0.022 | 0.029 | 0.019 | 0.025 | 0.034 |
| 5 | 1.4 | 0.5 | 100 | 0.024 | 0.026 | 0.030 | 0.024 | 0.028 | 0.036 | 0.025 | 0.030 | 0.041 | 0.025 | 0.037 | 0.047 |
| 6 | 1.6 | 0.5 | 100 | 0.032 | 0.035 | 0.041 | 0.033 | 0.039 | 0.051 | 0.033 | 0.042 | 0.058 | 0.034 | 0.052 | 0.067 |
| 7 | 1.2 | 0.6 | 100 | 0.014 | 0.015 | 0.017 | 0.014 | 0.015 | 0.019 | 0.014 | 0.017 | 0.022 | 0.015 | 0.019 | 0.025 |
| 8 | 1.4 | 0.6 | 100 | 0.019 | 0.020 | 0.023 | 0.019 | 0.022 | 0.026 | 0.020 | 0.023 | 0.030 | 0.020 | 0.027 | 0.034 |
| 9 | 1.6 | 0.6 | 100 | 0.025 | 0.026 | 0.031 | 0.025 | 0.029 | 0.037 | 0.025 | 0.031 | 0.041 | 0.026 | 0.037 | 0.047 |
| 10 | 1.2 | 0.4 | 120 | 0.031 | 0.034 | 0.038 | 0.032 | 0.035 | 0.044 | 0.033 | 0.038 | 0.052 | 0.034 | 0.044 | 0.059 |
| 11 | 1.4 | 0.4 | 120 | 0.042 | 0.046 | 0.052 | 0.043 | 0.049 | 0.063 | 0.044 | 0.052 | 0.074 | 0.046 | 0.066 | 0.084 |
| 12 | 1.6 | 0.4 | 120 | 0.058 | 0.061 | 0.077 | 0.059 | 0.074 | 0.097 | 0.060 | 0.077 | 0.109 | 0.061 | 0.098 | 0.125 |
| 13 | 1.2 | 0.5 | 120 | 0.021 | 0.023 | 0.026 | 0.022 | 0.024 | 0.030 | 0.022 | 0.026 | 0.035 | 0.023 | 0.030 | 0.041 |
| 14 | 1.4 | 0.5 | 120 | 0.029 | 0.031 | 0.036 | 0.029 | 0.034 | 0.043 | 0.030 | 0.036 | 0.050 | 0.030 | 0.044 | 0.057 |
| 15 | 1.6 | 0.5 | 120 | 0.039 | 0.041 | 0.050 | 0.039 | 0.047 | 0.062 | 0.040 | 0.050 | 0.070 | 0.041 | 0.062 | 0.080 |
| 16 | 1.2 | 0.6 | 120 | 0.017 | 0.018 | 0.020 | 0.017 | 0.019 | 0.023 | 0.017 | 0.020 | 0.026 | 0.018 | 0.023 | 0.030 |
| 17 | 1.4 | 0.6 | 120 | 0.023 | 0.024 | 0.027 | 0.023 | 0.026 | 0.032 | 0.024 | 0.027 | 0.036 | 0.024 | 0.032 | 0.041 |
| 18 | 1.6 | 0.6 | 120 | 0.030 | 0.031 | 0.037 | 0.030 | 0.035 | 0.044 | 0.031 | 0.037 | 0.049 | 0.031 | 0.045 | 0.056 |
| 19 | 1.2 | 0.4 | 140 | 0.037 | 0.039 | 0.045 | 0.037 | 0.041 | 0.051 | 0.038 | 0.045 | 0.061 | 0.039 | 0.052 | 0.069 |
| 20 | 1.4 | 0.4 | 140 | 0.050 | 0.053 | 0.060 | 0.051 | 0.057 | 0.074 | 0.051 | 0.060 | 0.086 | 0.053 | 0.077 | 0.099 |
| 21 | 1.6 | 0.4 | 140 | 0.067 | 0.072 | 0.090 | 0.068 | 0.086 | 0.114 | 0.070 | 0.090 | 0.127 | 0.071 | 0.114 | 0.146 |
| 22 | 1.2 | 0.5 | 140 | 0.025 | 0.027 | 0.030 | 0.025 | 0.027 | 0.035 | 0.026 | 0.030 | 0.041 | 0.026 | 0.035 | 0.048 |
| 23 | 1.4 | 0.5 | 140 | 0.033 | 0.036 | 0.042 | 0.034 | 0.040 | 0.050 | 0.035 | 0.042 | 0.058 | 0.036 | 0.051 | 0.066 |
| 24 | 1.6 | 0.5 | 140 | 0.045 | 0.048 | 0.058 | 0.046 | 0.055 | 0.072 | 0.047 | 0.058 | 0.081 | 0.048 | 0.073 | 0.093 |
| 25 | 1.2 | 0.6 | 140 | 0.020 | 0.021 | 0.024 | 0.020 | 0.022 | 0.027 | 0.020 | 0.024 | 0.031 | 0.021 | 0.027 | 0.035 |
| 26 | 1.4 | 0.6 | 140 | 0.027 | 0.028 | 0.032 | 0.027 | 0.031 | 0.037 | 0.028 | 0.032 | 0.042 | 0.028 | 0.038 | 0.048 |
| 27 | 1.6 | 0.6 | 140 | 0.035 | 0.037 | 0.043 | 0.035 | 0.041 | 0.052 | 0.036 | 0.043 | 0.058 | 0.037 | 0.052 | 0.066 |

A= Aspect Ratio, V=Volume Fraction, F=Force

**Table A6: Inner array of the tolerance combination of the factors**

| Combination no. | Aspect ratio $\sigma_A$ | Elasticity (GPa) $\sigma_E$ | Volume fraction $\sigma_V$ | Force (N) $\sigma_F$ |
|---|---|---|---|---|
| 1 | 0.01 | 3.3333 | 0.01 | 1.6667 |
| 2 | 0.01 | 3.3333 | 0.01 | 0.8333 |
| 3 | 0.01 | 3.3333 | 0.005 | 1.6667 |
| 4 | 0.01 | 3.3333 | 0.005 | 0.8333 |
| 5 | 0.01 | 1.6667 | 0.01 | 1.6667 |
| 6 | 0.01 | 1.6667 | 0.01 | 0.8333 |
| 7 | 0.01 | 1.6667 | 0.005 | 1.6667 |
| 8 | 0.01 | 1.6667 | 0.005 | 0.8333 |
| 9 | 0.002 | 3.3333 | 0.01 | 1.6667 |
| 10 | 0.002 | 3.3333 | 0.01 | 0.8333 |
| 11 | 0.002 | 3.3333 | 0.005 | 1.6667 |
| 12 | 0.002 | 3.3333 | 0.005 | 0.8333 |
| 13 | 0.002 | 1.6667 | 0.01 | 1.6667 |
| 14 | 0.002 | 1.6667 | 0.01 | 0.8333 |
| 15 | 0.002 | 1.6667 | 0.005 | 1.6667 |
| 16 | 0.002 | 1.6667 | 0.005 | 0.8333 |

**Table A7: Outer array, based on $L_8$ OA for a particular Inner array combination**

| Run no. | Column number | | | |
|---|---|---|---|---|
| | 1 (Aspect ratio) | 2 (Elasticity) | 3 (Volume fraction) | 4 (Force) |
| 1 | $A - 3\sigma_A$ | $E - 3\sigma_E$ | $V - 3\sigma_V$ | $F - 3\sigma_F$ |
| 2 | $A - 3\sigma_A$ | $E - 3\sigma_E$ | $V - 3\sigma_V$ | $F + 3\sigma_F$ |
| 3 | $A - 3\sigma_A$ | $E + 3\sigma_E$ | $V + 3\sigma_V$ | $F - 3\sigma_F$ |
| 4 | $A - 3\sigma_A$ | $E + 3\sigma_E$ | $V + 3\sigma_V$ | $F + 3\sigma_F$ |
| 5 | $A + 3\sigma_A$ | $E - 3\sigma_E$ | $V + 3\sigma_V$ | $F - 3\sigma_F$ |
| 6 | $A + 3\sigma_A$ | $E - 3\sigma_E$ | $V + 3\sigma_V$ | $F + 3\sigma_F$ |
| 7 | $A + 3\sigma_A$ | $E + 3\sigma_E$ | $V - 3\sigma_V$ | $F - 3\sigma_F$ |
| 8 | $A + 3\sigma_A$ | $E + 3\sigma_E$ | $V - 3\sigma_V$ | $F + 3\sigma_F$ |
| A, E, V & F represents the nominal value of Aspect ratio, Elasticity, Volume fraction and Force respectively | | | | |

**Table A8: Inner OA of factors**

| Combination No. | Aspect ratio $\sigma_A$ | Elasticity (Pa) $\sigma_E$ | Force (N) $\sigma_F$ |
|---|---|---|---|
| 1 | 0.01 | 3333.33 | 1.6667 |
| 2 | 0.01 | 3333.33 | 0.8333 |
| 3 | 0.01 | 1666.67 | 1.6667 |
| 4 | 0.01 | 1666.67 | 0.8333 |
| 5 | 0.002 | 3333.33 | 1.6667 |
| 6 | 0.002 | 3333.33 | 0.8333 |
| 7 | 0.002 | 1666.67 | 1.6667 |
| 8 | 0.002 | 1666.67 | 0.8333 |

**Table A9: Outer OA of factors tolerance based on Taguchi's $L_4$ OA**

| Run No. | Aspect ratio | Elasticity (Pa) | Force (N) |
|---|---|---|---|
| 1 | $\square$ 3 $\sigma_A$ | $\square$ 3$\sigma_E$ | $\square$ 3$\sigma_F$ |
| 2 | $\square$ 3 $\sigma_A$ | + 3$\sigma_E$ | + 3$\sigma_F$ |
| 3 | + 3 $\sigma_A$ | $\square$ 3$\sigma_E$ | + 3$\sigma_F$ |
| 4 | + 3 $\sigma_A$ | + 3$\sigma_E$ | $\square$ 3$\sigma_F$ |

**Table A10: The combination of factor-tolerances including volume fraction**

| Combination No. | Volume fraction $\sigma_V$ | Aspect ratio $\sigma_A$ | Elasticity (Pa) $\sigma_E$ | Force (N) $\sigma_F$ |
|---|---|---|---|---|
| 1 | | 0.01 | 3333.33 | 1.6667 |
| 2 | | 0.01 | 3333.33 | 0.8333 |
| 3 | | 0.01 | 1666.67 | 1.6667 |
| 4 | 0.0250 | 0.01 | 1666.67 | 0.8333 |
| 5 | | 0.002 | 3333.33 | 1.6667 |
| 6 | | 0.002 | 3333.33 | 0.8333 |
| 7 | | 0.002 | 1666.67 | 1.6667 |
| 8 | | 0.002 | 1666.67 | 0.8333 |
| 9 | | 0.01 | 3333.33 | 1.6667 |
| 10 | | 0.01 | 3333.33 | 0.8333 |
| 11 | | 0.01 | 1666.67 | 1.6667 |
| 12 | 0.0150 | 0.01 | 1666.67 | 0.8333 |
| 13 | | 0.002 | 3333.33 | 1.6667 |
| 14 | | 0.002 | 3333.33 | 0.8333 |
| 15 | | 0.002 | 1666.67 | 1.6667 |
| 16 | | 0.002 | 1666.67 | 0.8333 |

**Table A11: The combinations of the factors based on factorial DOE**

| Combination No. | Configuration | Volume fraction, V | Modulus of Elasticity, E (GPa) |
|---|---|---|---|
| 1 | | 0.25 | 69 |
| 2 | | 0.25 | 72 |
| 3 | | 0.25 | 200 |
| 4 | | 0.3 | 69 |
| 5 | Con1 | 0.3 | 72 |
| 6 | | 0.3 | 200 |
| 7 | | 0.35 | 69 |
| 8 | | 0.35 | 72 |
| 9 | | 0.35 | 200 |
| 10 | | 0.25 | 69 |
| 11 | | 0.25 | 72 |
| 12 | | 0.25 | 200 |
| 13 | | 0.3 | 69 |
| 14 | Con2 | 0.3 | 72 |
| 15 | | 0.3 | 200 |
| 16 | | 0.35 | 69 |
| 17 | | 0.35 | 72 |
| 18 | | 0.35 | 200 |
| 19 | | 0.25 | 69 |
| 20 | | 0.25 | 72 |
| 21 | | 0.25 | 200 |
| 22 | | 0.3 | 69 |
| 23 | Con3 | 0.3 | 72 |
| 24 | | 0.3 | 200 |
| 25 | | 0.35 | 69 |
| 26 | | 0.35 | 72 |
| 27 | | 0.35 | 200 |

**Table A12: Taguchi's $L_9$ array corresponding to noise**

| Experiment no. | Force F(N) | Change in input Force angle $A_i$ (degree) | Change in output Force angle $A_o$ (degree) | Thickness T(mm) |
|---|---|---|---|---|
| 1 | 840 | 5 | 5 | 6.3 |
| 2 | 840 | 0 | 0 | 6 |
| 3 | 840 | -5 | -5 | 5.7 |
| 4 | 800 | 5 | 0 | 5.7 |
| 5 | 800 | 0 | -5 | 6.3 |
| 6 | 800 | -5 | 5 | 6 |
| 7 | 760 | 5 | -5 | 6 |
| 8 | 760 | 0 | 5 | 5.7 |
| 9 | 760 | -5 | 0 | 6.3 |

**Table A13: Inner OA of factors tolerances**

| Combination No. | $\sigma_T$ | $\sigma_E$ | $\sigma_V$ | $\sigma_F$ | $\sigma_{Ai}$ | $\sigma_{Ao}$ |
|---|---|---|---|---|---|---|
| 1 | 0.1 | 3.333 | 0.0058 | 13.33 | 0.7833 | -0.2833 |
| 2 | 0.1 | 3.333 | 0.0058 | 13.33 | 0.7833 | -0.14167 |
| 3 | 0.1 | 3.333 | 0.0058 | 13.33 | 0.39167 | -0.2833 |
| 4 | 0.1 | 3.333 | 0.0058 | 13.33 | 0.39167 | -0.14167 |
| 5 | 0.1 | 3.333 | 0.0058 | 6.667 | 0.7833 | -0.2833 |
| 6 | 0.1 | 3.333 | 0.0058 | 6.667 | 0.7833 | -0.14167 |
| 7 | 0.1 | 3.333 | 0.0058 | 6.667 | 0.39167 | -0.2833 |
| 8 | 0.1 | 3.333 | 0.0058 | 6.667 | 0.39167 | -0.14167 |
| 9 | 0.1 | 3.333 | 0.0029 | 13.33 | 0.7833 | -0.2833 |
| 10 | 0.1 | 3.333 | 0.0029 | 13.33 | 0.7833 | -0.14167 |
| 11 | 0.1 | 3.333 | 0.0029 | 13.33 | 0.39167 | -0.2833 |
| 12 | 0.1 | 3.333 | 0.0029 | 13.33 | 0.39167 | -0.14167 |
| 13 | 0.1 | 3.333 | 0.0029 | 6.667 | 0.7833 | -0.2833 |
| 14 | 0.1 | 3.333 | 0.0029 | 6.667 | 0.7833 | -0.14167 |
| 15 | 0.1 | 3.333 | 0.0029 | 6.667 | 0.39167 | -0.2833 |
| 16 | 0.1 | 3.333 | 0.0029 | 6.667 | 0.39167 | -0.14167 |
| 17 | 0.1 | 1.667 | 0.0058 | 13.33 | 0.7833 | -0.2833 |
| 18 | 0.1 | 1.667 | 0.0058 | 13.33 | 0.7833 | -0.14167 |
| 19 | 0.1 | 1.667 | 0.0058 | 13.33 | 0.39167 | -0.2833 |
| 20 | 0.1 | 1.667 | 0.0058 | 13.33 | 0.39167 | -0.14167 |
| 21 | 0.1 | 1.667 | 0.0058 | 6.667 | 0.7833 | -0.2833 |
| 22 | 0.1 | 1.667 | 0.0058 | 6.667 | 0.7833 | -0.14167 |
| 23 | 0.1 | 1.667 | 0.0058 | 6.667 | 0.39167 | -0.2833 |
| 24 | 0.1 | 1.667 | 0.0058 | 6.667 | 0.39167 | -0.14167 |
| 25 | 0.1 | 1.667 | 0.0029 | 13.33 | 0.7833 | -0.2833 |
| 26 | 0.1 | 1.667 | 0.0029 | 13.33 | 0.7833 | -0.14167 |
| 27 | 0.1 | 1.667 | 0.0029 | 13.33 | 0.39167 | -0.2833 |
| 28 | 0.1 | 1.667 | 0.0029 | 13.33 | 0.39167 | -0.14167 |
| 29 | 0.1 | 1.667 | 0.0029 | 6.667 | 0.7833 | -0.2833 |
| 30 | 0.1 | 1.667 | 0.0029 | 6.667 | 0.7833 | -0.14167 |
| 31 | 0.1 | 1.667 | 0.0029 | 6.667 | 0.39167 | -0.2833 |
| 32 | 0.1 | 1.667 | 0.0029 | 6.667 | 0.39167 | -0.14167 |
| 33 | 0.05 | 3.333 | 0.0058 | 13.33 | 0.7833 | -0.2833 |
| 34 | 0.05 | 3.333 | 0.0058 | 13.33 | 0.7833 | -0.14167 |
| 35 | 0.05 | 3.333 | 0.0058 | 13.33 | 0.39167 | -0.2833 |
| 36 | 0.05 | 3.333 | 0.0058 | 13.33 | 0.39167 | -0.14167 |
| 37 | 0.05 | 3.333 | 0.0058 | 6.667 | 0.7833 | -0.2833 |
| 38 | 0.05 | 3.333 | 0.0058 | 6.667 | 0.7833 | -0.14167 |
| 39 | 0.05 | 3.333 | 0.0058 | 6.667 | 0.39167 | -0.2833 |
| 40 | 0.05 | 3.333 | 0.0058 | 6.667 | 0.39167 | -0.14167 |
| 41 | 0.05 | 3.333 | 0.0029 | 13.33 | 0.7833 | -0.2833 |

| Combination No. | $\sigma_T$ | $\sigma_E$ | $\sigma_V$ | $\sigma_F$ | $\sigma_{Ai}$ | $\sigma_{Ao}$ |
|---|---|---|---|---|---|---|
| 42 | 0.05 | 3.333 | 0.0029 | 13.33 | 0.7833 | -0.14167 |
| 43 | 0.05 | 3.333 | 0.0029 | 13.33 | 0.39167 | -0.2833 |
| 44 | 0.05 | 3.333 | 0.0029 | 13.33 | 0.39167 | -0.14167 |
| 45 | 0.05 | 3.333 | 0.0029 | 6.667 | 0.7833 | -0.2833 |
| 46 | 0.05 | 3.333 | 0.0029 | 6.667 | 0.7833 | -0.14167 |
| 47 | 0.05 | 3.333 | 0.0029 | 6.667 | 0.39167 | -0.2833 |
| 48 | 0.05 | 3.333 | 0.0029 | 6.667 | 0.39167 | -0.14167 |
| 49 | 0.05 | 1.667 | 0.0058 | 13.33 | 0.7833 | -0.2833 |
| 50 | 0.05 | 1.667 | 0.0058 | 13.33 | 0.7833 | -0.14167 |
| 51 | 0.05 | 1.667 | 0.0058 | 13.33 | 0.39167 | -0.2833 |
| 52 | 0.05 | 1.667 | 0.0058 | 13.33 | 0.39167 | -0.14167 |
| 53 | 0.05 | 1.667 | 0.0058 | 6.667 | 0.7833 | -0.2833 |
| 54 | 0.05 | 1.667 | 0.0058 | 6.667 | 0.7833 | -0.14167 |
| 55 | 0.05 | 1.667 | 0.0058 | 6.667 | 0.39167 | -0.2833 |
| 56 | 0.05 | 1.667 | 0.0058 | 6.667 | 0.39167 | -0.14167 |
| 57 | 0.05 | 1.667 | 0.0029 | 13.33 | 0.7833 | -0.2833 |
| 58 | 0.05 | 1.667 | 0.0029 | 13.33 | 0.7833 | -0.14167 |
| 59 | 0.05 | 1.667 | 0.0029 | 13.33 | 0.39167 | -0.2833 |
| 60 | 0.05 | 1.667 | 0.0029 | 13.33 | 0.39167 | -0.14167 |
| 61 | 0.05 | 1.667 | 0.0029 | 6.667 | 0.7833 | -0.2833 |
| 62 | 0.05 | 1.667 | 0.0029 | 6.667 | 0.7833 | -0.14167 |
| 63 | 0.05 | 1.667 | 0.0029 | 6.667 | 0.39167 | -0.2833 |
| 64 | 0.05 | 1.667 | 0.0029 | 6.667 | 0.39167 | -0.14167 |

**Table A14: Outer OA of factors tolerance based on Taguchi's $L_8$ OA**

| Run no. | T | E | V | F | $A_i$ | $A_o$ |
|---|---|---|---|---|---|---|
| 1 | $\square$ 3 $\sigma_T$ | $\square$ 3 $\sigma_E$ | $\square$ 3 $\sigma_V$ | $\square$ 3 $\sigma_F$ | $\square$ 3 $\sigma_{Ai}$ | $\square$ 3 $\sigma_{Ao}$ |
| 2 | $\square$ 3 $\sigma_T$ | $\square$ 3 $\sigma_E$ | $\square$ 3 $\sigma_V$ | + 3 $\sigma_F$ | + 3 $\sigma_{Ai}$ | + 3 $\sigma_{Ao}$ |
| 3 | $\square$ 3 $\sigma_T$ | + 3 $\sigma_E$ | + 3 $\sigma_V$ | $\square$ 3 $\sigma_F$ | $\square$ 3 $\sigma_{Ai}$ | + 3 $\sigma_{Ao}$ |
| 4 | $\square$ 3 $\sigma_T$ | + 3 $\sigma_E$ | + 3 $\sigma_V$ | + 3 $\sigma_F$ | + 3 $\sigma_{Ai}$ | $\square$ 3 $\sigma_{Ao}$ |
| **5** | + 3 $\sigma_T$ | $\square$ 3 $\sigma_E$ | + 3 $\sigma_V$ | $\square$ 3 $\sigma_F$ | + 3 $\sigma_{Ai}$ | $\square$ 3 $\sigma_{Ao}$ |
| 6 | + 3 $\sigma_T$ | $\square$ 3 $\sigma_E$ | + 3 $\sigma_V$ | + 3 $\sigma_F$ | $\square$ 3 $\sigma_{Ai}$ | + 3 $\sigma_{Ao}$ |
| 7 | + 3 $\sigma_T$ | + 3 $\sigma_E$ | $\square$ 3 $\sigma_V$ | $\square$ 3 $\sigma_F$ | + 3 $\sigma_{Ai}$ | + 3 $\sigma_{Ao}$ |
| 8 | + 3 $\sigma_T$ | + 3 $\sigma_E$ | $\square$ 3 $\sigma_V$ | + 3 $\sigma_F$ | $\square$ 3 $\sigma_{Ai}$ | $\square$ 3 $\sigma_{Ao}$ |
| T: Thickness, E: Elasticity, V: Volume fraction, F: Force, Ai: Input force angle, Ao: output force angle | | | | | | |

# LIST OF PUBLICATIONS AND PRESENTATIONS

**International journal publications:**

1. Arshad Javed and B.K. Rout, "Investigation on parametric sensitivity of topologically optimized structures", *Proceedings of the Institution of Mechanical Engineers, Part C: Journal of Mechanical Engineering Science*, 2012, 226(11), pp. 2791-2804, DOI: 10.1177/0954406212437513.

2. Arshad Javed and B.K. Rout, "Tolerance range section of topologically optimized structure using combined array design of experiments approach", *Proceedings of the Institution of Mechanical Engineers, Part C: Journal of Mechanical Engineering Science*, 2012, 227(9), pp. 2023-2038, DOI:10.1177/0954406212468652.

3. Arshad Javed and B.K. Rout, "Tolerance range selection of topologically optimized structures with the effects of uncertainties of manufacturing process", *Proceedings of the Institution of Mechanical Engineers, Part C: Journal of Mechanical Engineering Science*. Online published on April 11, 2014 as doi:10.1177/0954406214528484

4. Arshad Javed and B.K. Rout, "Reliability based performance analysis of topologically optimized structures", *Journal of Mechanical Science and Technology*, Springer. (Communicated)

**International/National conference publications and presentation:**

1. Arshad Javed and B.K. Rout, "Parametric sensitivity of topologically optimized structures using RBTO technique", *In Proceedings of Third Asian Conference on Mechanics of Functional Materials and Structures (ACMFMS 2012),* Indian Institute of Technology, Delhi, India, December 5-8, 2012, pp. 252-255.

2. Arshad Javed, A.K. Sengar, and B.K. Rout, "A FEM and image processing based method for simulation of manufacturing imperfections", *In Proceedings of International Conference on Advancements and Futuristic Trends in Mechanical and Materials Engineering,* Punjab Technical University, Kapurthala, India, October 5-7, 2012, pp. 255-229.

3. Arshad Javed and B.K. Rout, "Issues in design for manufacturing using topology optimization method", *Presented in National Conference on Modeling,*

*Computational Fluid Dynamics & Operations Research Under UGC-SAP, DRS-I,* Birla Institute of Technology & Science, Pilani, Rajasthan, February 4-5, 2012.

4. Arshad Javed, M. Safal, and B.K. Rout, "Numerical simulation of compliance variation for a topology-optimized structure", *In Proceedings of IEEE international conference on Process Automation, Control and Computing (PACC)*, Coimbatore, Tamilnadu, India, July 20-22, 2011, pp. 1-5, DOI:10.1109/PACC.2011.5978893.

5. Arshad Javed, B.K. Rout and R.K. Mittal, "A review on compliant mechanisms for MEMS applications", *Presented in 2nd ISSS National Conference on MEMS, Microsensors, Smart Materials, Structures and Systems,* CEERI-BITS, Pilani, India, November 15-17, 2007.

# BRIEF BIOGRAPHY OF THE CANDIDATE

**Mr. Arshad Javed** did his B.Tech. in Mechanical Engineering from Bundelkahnd Institute of Engineering and Technology (BIET), Jhansi (U.P.) and M.E. from Birla Institute of Technology & Science (BITS) Pilani, Pilani Campus (Rajasthan) in Mechanical Engineering. He is presently pursuing Ph.D. at BITS-Pilani, and working as a Lecturer with Department of Mechanical Engineering, BITS-Pilani, Pilani campus. He has eight years teaching experience at under graduate and postgraduate levels. His areas of research interest are Topology optimization, Mechatronics, and Robotic systems.

# BRIEF BIOGRAPHY OF THE SUPERVISOR

**Dr. B.K. Rout** is presently working as Associate Professor in the Department of Mechanical Engineering as well as Coordinator of Centre for Robotics and Intelligent Systems (CRIS) of Birla Institute of Technology and Science (BITS) Pilani, Rajasthan. He has been working with BITS Pilani for last fifteen years in various capacities and has total of eighteen years of experience in academics and three years of experience in industry. He has published several papers in various national and international journals, and conferences. His current research interest is in the area of rehabilitation robotics; industrial robotics and the use of statistical techniques to model, synthesize, and optimize complex dynamic systems; statistical methods for system design, parameter design and tolerance design of mechanical equipment. He has been guiding research students in mobile robotics, robust design of manipulators, topologically optimized compliant structure, and mechanism areas. He is actively involved in teaching and consultancy of subjects related to robotics, mechatronics, quality engineering and operations research. He is a fellow of professional bodies like Institution of Engineers (IE), Indian Institute of Industrial Engineers (IIIE), and member of Indian Society for Theoretical and Applied Mechanics (ISTAM).